Development of Novel Enantioselective Diazepane Carboxylate Catalysts for the Diels-Alder Reaction of α-Substituted Enals and Studies Investigating Urea Hydrogen Bonding

BY

Nicklas O. Häggman

Department of Chemistry, McGill University, Montreal

November 2018

A thesis submitted to McGill University in partial fulfillment of the requirements of the degree of Doctor of Philosophy

Abstract

Green chemistry has become an important topic due to current environmental concerns. Green chemistry is a broad term which generally refers to the development of chemical processes that are less toxic and more environmentally friendly. One important field of green chemistry, that has rapidly grown the last 20 years is organocatalysis, wherein the catalyst for a given chemical transformation is an organic molecule. This thesis describes two projects which have focused on organocatalysis and green chemistry. Part A involves investigations into urea hydrogen bond catalysis while Part B describes the development of a new type of enantioselective iminium ion organocatalyst for the Diels-Alder reaction.

The first part describes our efforts into investigating optimal parameters for hydrogen bond catalyst systems that resulted from failed attempts to develop a new peptide coupling catalyst. It was hypothesized that a system capable of both activation of a carboxylate, through hydrogen bonding, and activation of an amine, via proximity to the carboxylate, might be competent in furnishing the desired bond. The screening for catalytic activity was unsuccessful and it was unknown what was limiting activity. A significant unknown was the optimal position of the nucleophile relative to the urea and we accordingly undertook investigations to probe this key parameter. A catalogue of general scaffolds consisting of a urea and linker to a hydroxyl nucleophile were synthesized and screened for their activity towards additions to an electrophile. Close proximity to the urea was found to be key and two acyl transfer agents were designed based on the results with one successfully employed as an additive in peptide coupling, affording activity equal to or slightly better than that of the current standard HOAt in combination with a coupling reagent.

In the second part, we describe the development of an organocatalytic Diels-Alder cycloaddition using an achiral ethyl diazepane carboxylate catalyst developed in our lab. The catalyst showed good reactivity for α-substituted enals, a substrate class typically incompatible with iminium ion catalysts. We set out to investigate the reactivity and mechanism of this achiral diazepane for these challenging alpha-substituted enals, showing it was compatible with a wide range of enals which showed no activity with contemporary secondary amine catalysts. Efforts to reach high enantioselectivity proved challenging for this scaffold. The efforts focused on three

areas: installation of bulky substituents on the ring, tuning the electron withdrawing group (including employing chiral electron withdrawing groups), and computational studies to provide insight into the origins of the selectivity. The conclusions of these studies led to a final diazepane carboxylate catalyst containing stereogenic centers on both the ring and electron withdrawing group. This catalyst displayed good reactivity and moderate to excellent *exo*-, regio- and enantioselectivity for a wide range of alpha-substituted alpha,beta-unsaturated aldehydes for the Diels-Alder cycloaddition.

Résumé

La Chimie Verte est devenue un domaine important de la chimie du fait des problèmes environnementaux actuels. Le terme Chimie Verte est large et renvoie généralement au développement de procédés chimiques peu toxiques et éco-compatibles. L'un des champs les plus importants de la Chimie Verte et qui a rapidement progressé au court des 20 dernières années, est l'organocatalyse, dans laquelle le catalyseur d'une transformation chimique donnée est une molécule organique. La présente thèse décrit deux projets portant sur l'organocatalyse et la Chimie Verte. La partie A examine la catalyse par des dérivés d'urée par formation de liaison hydrogène tandis que le partie B décrit le développement d'un nouveau organocatalyseur de type iminium énantiosélectif pour la réaction de Diels-Alder.

Nous allons décrire nos efforts pour déterminer les paramètres optimaux des systèmes de catalyseurs par liaison hydrogène résultants d'essais infructueux pour le développement d'un nouveau catalyseur de formation de liaison peptidique. Nous avons fait l'hypothèse qu'un système capable d'activer, par liaison hydrogène, à la fois un carboxylate et une amine par effet de proximité serait également capable de créer la liaison désirée. La position optimale du nucléophile relativement à l'urée étant inconnue, nous avons étudié en détail ce paramètre clé. Une bibliothèque de structures reliant une urée à un nucléophile hydroxylé a été synthétisée et l'activité de chacune a été testée dans le cadre d'une addition à un électrophile. La proximité à l'urée s'est révélée primordiale et deux agents de transfert de groupe acyle ont été conçus en se basant sur ces résultats. L'un d'entre eux a été utilisé avec succès en tant qu'additif lors d'un couplage peptidique et a montré une activité équivalente voir légèrement supérieure à un agent standard.

Dans la partie B, nous décrivons le développement d'une cyclo-addition de Diels-Alder organocatalysée, utilisant un carboxylate d'éthyl diazépane achiral développé au laboratoire en tant que catalyseur. Le catalyseur montre une haute réactivité pour les énals alpha-substitués, substrats typiquement incompatibles avec les catalyseurs de type iminium. Nous avons étudié la réactivité et le mécanisme de ce diazépane achiral pour ces susbtrats, montrant qu'il est compatible avec un grand nombre d'énals inertes en présence catalyseurs aminés classiques. Les efforts pour obtenir une haute énantiosélectivité se sont portés sur trois aspects : l'installation de groupes

encombrants sur le cycle, la variation du groupe électro-attracteur (incluant l'emploi de groupes chiraux) et des études computationnelles procurant des indices sur l'origine de la sélectivité. Les conclusions de ces différentes études ont conduits à la synthèse d'un catalyseur final portant des centres stéréogènes à la fois sur le cycle et le groupe électro-attracteur. Ce catalyseur a montré une bonne réactivité et des *exo*-, régio- et énantiosélectivités moyennes à excellentes dans le cadre de la cycloaddition de Diels-Alder face à une large gamme d'aldéhydes alpha-substitués et alpha,beta-insaturés.

Acknowledgement

I want to start by thanking my supervisor Dr Jim Gleason who has been a great mentor and teacher. He gave me the opportunity to come to Montreal and conduct my graduate work and provided me with the resources and knowledge to perform it. He has not just provided me with expert synthetic advice and training to be an excellent chemist, but has also been performing all the DFT calculations and helping me put together this thesis. His contributions throughout the years have been priceless.

I am grateful to McGill University and especially the people from the department of chemistry who have made the last 6 years an amazing experience. A special mention to Chantal Marotte and Sandra Aerssen who have helped me with all kinds of bureaucratic items necessary to keep me at McGill University and importantly, in the country. Special thanks to the professors of my courses who taught me advanced chemistry subjects, Dr. J-P. Lumb, Dr. N. Moitessier, Dr. J. L. Gleason and Dr. C-J. Li to give me the fundamental knowledge of chemistry that I have today.

For all the technical assistance throughout my PhD degree, many thanks to Dr. Fred Morin (NMR) for running ^{1}H-^{31}P HMBC and succeeded by Dr. Robin Stein (NMR) for running the NMR facility and skillfully answering all my silly questions. Thank you to Nadim Saade and Dr. Alexander Sean Wahba for their help in the mass spectrometry facility and to share of their knowledge and spending countless hours performing my experiments and explaining the procedures and results.

I want to highlight my friend Dainis Kaldre who started the iminium ion project and introduced me to it and was a great co-worker at the beginning of the enantioselective development, and more importantly, thank you for being a great friend and roommate and teaching me to play ultimate frisbee. Second to none, Adam Elmehriki who provided great moral support throughout the last 4 years and has given great advice, listening to my rants and been a formable opponent for the most ridiculous debates. I want to thank Adam again together with Dainis, Jon Hughes and Sam Plamondon who have proof-read different sections of this thesis and have helped a poor foreigner by correcting spelling, grammar, and content. I want to again mention Samuel Plamondon, who has also worked on the iminium ion project, for fruitful discussions and importantly of figuring out how to recrystallize the final diazepane to afford enantiopure material.

He abandoned the diazepane in favour the piperazines for his polyene cyclization project but has still been a great co-worker on the hydrazide project. A special mention to my undergrad Ben Zank who ran the first Diels-Alder reactions with the diazepane carboxylate catalyst. I'm very grateful to my friend Fabien Hammerer for both translating my abstract into French and being a great hockey coach and wine connoisseur. There have been many more great coworkers in our group that all deserves great appreciation for helping maintain a functional, smooth running lab to work in. Some special shout-outs, not just in my lab or chemistry, to my friends who have kept me sane, entertained, and happy during my time in Montreal, Adam, Jon Hughes-Johnson, Lindsey Hughes-Johnson Josie Warnica, Fabien, Nicole Fu, Tim Mack, Daniel Rivalti, Rodrigo Sanches, Michelle Bezanson, Chris Doyle, Angel Gopal, Dainis and Yiram Kim and also my entourage back in Sweden, Marcus Ljungberg, Pontus Jahder, Johan Landgren and Henrik Nilsson who have supported me through the interwebs and brief visits. There are many more, especially on the intramural hockey, frisbee, waterpolo, dodgeball, softball, volleyball, and soccer teams that deserves thanks for making my time at McGill amazing. These teams and the games followed by beers after have been an amazing break from the lab.

Finally, I must thank my parents Olle and Birgitta who have always encouraged and supported me to do what I want in life. My sister Alexandra, who is probably the most important person in my life and has always been there for me. Words can't describe what she means for me. Especially now nearing the end, I'm really excited to spend more time with my niece and nephew who are growing up quicker than I ever could have imagined.

Contributions of Authors

- Dainis Kaldre developed the achiral ethyl diazepane carboxylate catalyst and was first to synthesize both the chiral C3 and C7 phenyl substituted diazepane and the synthetic routes have been repeated by me for this thesis. He was also first to synthesize menthol diazepane carboxylate **271** and bicyclic carbamate diazepane **218**, both of which were repeated by me for this thesis.
- Preliminary results for the Diels-Alder were performed by Mr Benjamin Zank with the diazepane carboxylate showed good reactivity for several different α-substituted enals. All those Diels-Alder reactions have been repeated by me for this thesis under optimized conditions.
- Samuel Plamondon developed a crystallization method to obtain the final catalyst **281** with high enantiopurity and repeated synthesis of the achiral 5, 6 and 7 membered rings.
- Chiral 6 membered rings were synthesized by Adamo Sulpizi and Samuel Plamondon.
- All DFT calculations have been performed by J. L. Gleason.
- The abstract was translated from English to French by Fabien Hammerer.

List of Contents

List of Figures

List of Schemes

List of Tables

List of abbreviations

Ac	acetyl
aq.	Aqueous
Bn	benzyl
Boc	*t*-Butyloxycarbonyl
bs	broad singlet
CBMIT	1,1'-carbonylbis(3-methylimidazolium)triflate
Cbz	carboxybenzyl
CDI	Carbonyldiimidazole
COSY	homonuclear correlation spectroscopy
d	doublet
dd	doublet of doublets
DCM	dichloromethane
ddd	doublet of doublet of doublets
DFT	density functional theory
DIPEA	*N,N*'-diisopropylethylamine
DMAP	4-(dimethylamino)pyridine
DMF	*N*,*N*-dimethylformamide
DMP	Dess-Martin periodinane
DMSO	dimethylsulfoxide

dr	diasteromeric ratio
ee	enantiomeric excess
EDC	1-Ethyl-3-(3-dimethylaminopropyl)carbodiimide
er	enantiomeric ratio
equiv.	equivalent
ESI	electron spray ionization
Et	ethyl
EtOAc	ethyl acetate
Et_2O	diethyl ether
EWG	electron withdrawing group
g	grams(s)
GC (GLC)	gas liquid chromatography
h	hour(s)
HATU	1-[Bis(dimethylamino)methylene]-1H-1,2,3-triazolo[4,5-b]pyridinium 3-oxid hexafluorophosphate
HMBC	Heteronuclear Multiple Bond Correlation
HPLC	high-performance liquid chromatography
HRMS	high-resolution mass spectrometry
HOAt	1-Hydroxy-7-azabenzotriazole
HOBt	1-Hydroxybenzotriazole
HOMO	Highest occupied molecular orbital

HSQC	Heteronuclear single quantum coherence spectroscopy
Hz	hertz
i	iso
IBX	2-iodoxybenzoic acid
ISC	intersystem crossing
J	coupling constant
L	litre
LA	Lewis acid
LUMO	lowest unoccupied molecular orbital
m	multiplet
M	moles per liter
m	meta
m/z	mass to charge ratio
m-CPBA	*meta*-chloroperbenzoic acid
Me	methyl
MeOH	methanol
mL	milliliter
mmol	millimole
mol	mole
MS	mass spectrometry; molecular sieves
Ms	mesyl, methanesulfonyl

n	normal
N.R.	no reaction
NMR	nuclear magnetic resonance
Ph	phenyl
Pr	propyl
PyBOP	Tripyrrolidinophosphonium hexafluorophosphate
RBF	round bottom flask
rt	room temperature
s	singlet
sat.	saturated
SM	starting material
t	tertiary
t	triplet
TBAF	tetrabutylamonium fluoride
TBS	*tert*-butyldimethylsilyl
Tf	triflyl
TFA	trifluoroacetic acid
THF	tetrahydrofurane
TIPS	triisopropylsilyl
TLC	thin layer chromatography
TMS	trimethylsilyl

TS	transition state
μg	microgram
°C	degree Celsius
Δ	heat

Chapter 1

Organocatalysis Its Potential Towards Amide Bond Formation and the Diels-Alder Reaction

1.1 Organocatalysis

As with most sectors of our society and economy, synthetic chemistry is undergoing a transformation towards employing more environmentally sustainable practices. This acceptance of responsibility is exemplified by the rapid adoption of green chemistry and its accompanying strategies, as indicated by the plethora of articles published in which it is a core theme.[1] Considering the scope and magnitude of issues being addressed, the exact boundaries of green chemistry are understandably ill-defined, but as a general guideline, a reaction abiding any of the 12 principles green chemistry[2], may be considered green. The 12 principles of green chemistry were introduced by P. Anastas and J. Warner and are not intended to be strict rules, but instead to act as guidelines for conducting more environmentally conscious and sustainable chemistry. The principles outline several key considerations, for example developing safer and less toxic chemicals, more energy efficient processes, reactions of higher atom economy and methods to limit produced waste. One of the 12 principle central to reaction design is that of catalysis, with it having received a large portion of the academic community's attention. In examining the field of green chemistry, it is critical to appreciate that no reaction can ever be considered completely environmentally benign or "green". However, modifications and improvements, e.g. replacing stoichiometric reagents with catalysts, reducing or eliminating the use of solvents, or using more abundant elements leading to more efficient processes are all positive steps towards a greener future.[3,4]

One field that has gained traction within this green chemistry movement is organocatalysis. Broadly defined it is the acceleration of chemical reactions with a sub stoichiometric amount of an organic compound.[5] In relation to metal catalysis, it is a comparatively new concept in organic chemistry as metals have a long history of performing reactions of impressive variety, complete with high yields and selectivity. However, the use of metals has several drawbacks as they are often toxic, expensive, and many of the most synthetically useful metals have low abundancy in the Earth's crust. These realities have enormous environmental consequences for their extraction and purification. These features make the field of organocatalysis very attractive, both for academia and industry.[6]

As will be described in this chapter, organocatalysis has the capacity to perform a wide variety of reactions complete with several different modes of activity. This chapter will begin with

describing different types of hydrogen bond catalysis. The chapter will continue with the problems involved with amide bond formation and the current solutions, including the few organocatalytic options which have been developed. This chapter will end with a discussion of the Diels-Alder reaction and the impact that iminium ion organocatalysis had on the reaction, focusing on α-substituted enals and hydrazides as organocatalysts.

1.2 Hydrogen bond organocatalysis

A major subfield of organocatalysis is hydrogen bond catalysis.[7] It acts in a similar fashion as classic Brønsted acid, a proton donor, which transfers a proton onto a substrate with a basic functional group. One of the earliest and simplest proton catalyzed reactions is the classic Fischer esterification which was discovered over 100 years ago (Scheme 1.1).[8] The first step in the Fischer esterification mechanism is the protonation of the carbonyl of the carboxylic acid (**I**) to form **II** which has two resonance forms. The alcohol (**III**) attacks the activated carbonyl and forms the tetrahedral intermediate **IV**. After proton transfer to form **V**, water is eliminated, and oxonium ion **VI** is formed. Deprotonation reforms the proton catalyst and yields ester **VII**. Although this is a simple, old reaction, the general principal behind proton catalysis is consistent.

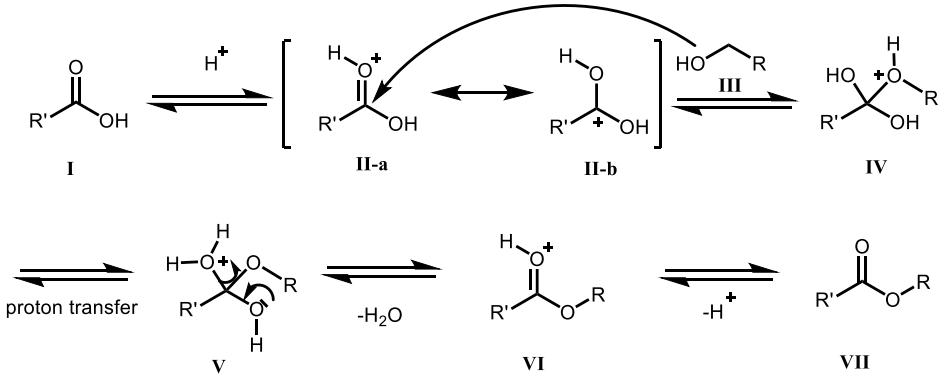

Scheme 1.1 Fischer esterification mechanism

The advances in acid catalyzed reactions have continued over the last century and a plethora of different types of organic and inorganic acids have been employed. In the last 20 years chiral organic acids have shown great success in a variety of different reactions.[9] In particular, chiral phosphoric acids have seen a rapid development after publications by Akiyama[10] and

Terada[11] in 2004. One illustrative recent example from Yamamoto's group is a kinetic resolution of 2-pyridyl esters that is achieved via an amide bond formation catalyzed by BINOL derived phosphoric acid **1** (Scheme 1.2).[12] Moderate to good selectivity factors were achieved for a limited scope of 2-pyridyl esters and *p*-toluidine. Pyridyl esters are often used as activated esters, but this is the first example of their application in asymmetric synthesis. The mechanism proceeds through protonation/activation of the pyridyl ester while the coordinating phosphonate dictates the nucleophilic attack by blocking one face. The activity of the BINOL phosphoric acids and phosphate derivatives have been improved by changing the pKa through changing the type of phosphate. Stereoselectivity was improved by changing the *ortho* aryl groups to more bulky and electron withdrawing aryls and by modifying the phosphate group. To date there have been several hundreds of publications employing this privileged scaffold.[13]

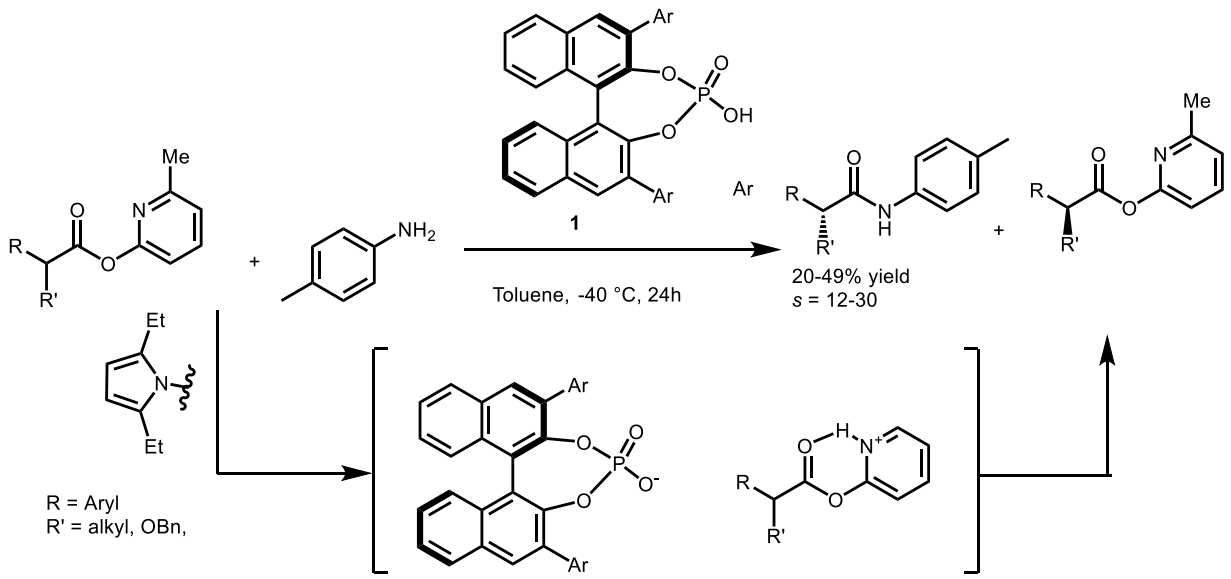

Scheme 1.2 Phosphoric acid catalyzed kinetic resolution of 2-pyridyl esters

The general concept in Brønsted acid to transfer a proton which interacts with an electrophile to lower the energy of its LUMO to promote reactivity towards nucleophiles. For chiral catalysis, the chiral conjugate base, phosphonate in the example above, dictates the stereochemical outcome of the reaction. Hydrogen bond donor catalysis works in a similar fashion by lowering the LUMO, but instead of proton transfer to form the salt, it works through hydrogen

bonding between the catalyst and the substrate. In the example illustrated in Figure 1.1, hydrogen bonding between the carbonyl and the proton or a urea removes electron density from the carbonyl lowering the energy of the LUMO and imposes an ordered geometry on the now activated carbonyl. This two-point, equal hydrogen bonding is a simplified model which is proposed for the reactions in this chapter but in chapter 2 we will see examples of exceptions.

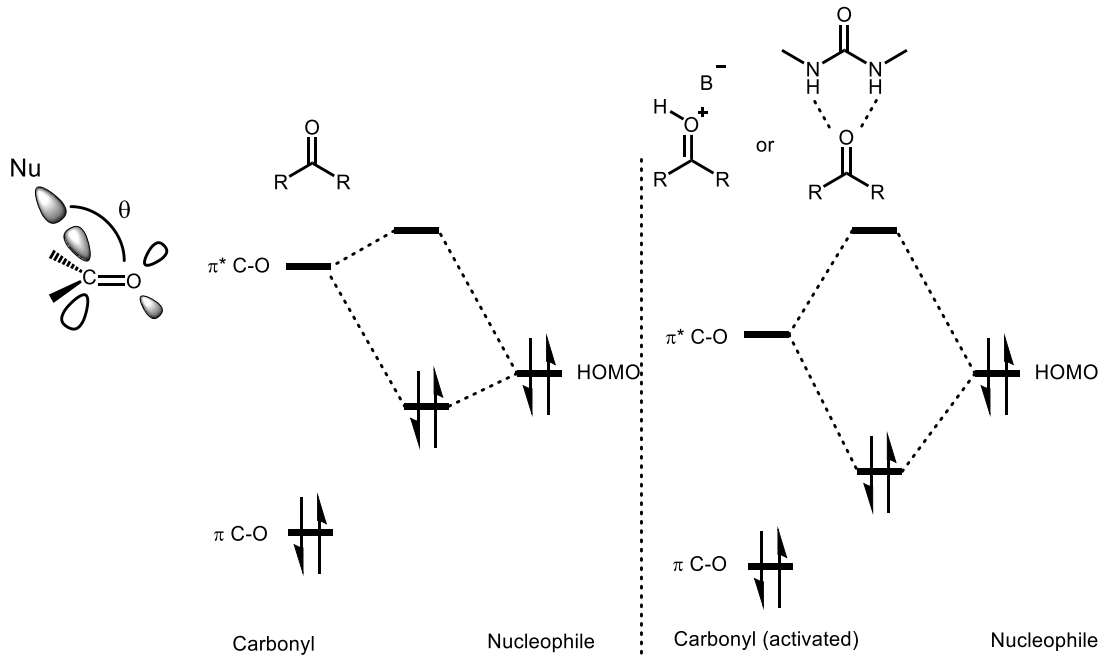

Figure 1.1 Molecular orbital diagram of nucleophile HOMO and the π-system of carbonyl

Many types of hydrogen bond donors have been developed such as diols, (thio)ureas, guanidines and squaramides.[7, 14] For some of the catalysts like phosphoric acid described above, it is at times argued whether catalysis is induced by hydrogen bonding or simple protonation by a Brønsted acid.[15, 16] One of the early examples of proposed hydrogen bond catalysis came from Hine's group who showed enhanced acceleration of epoxide opening using 1,8-biphenylenediol **2** relative to simple phenols (Scheme 1.3).[17] The article suggests that the higher activity observed with bis-phenol **2** relative to cases where **2** is absent was due to dual hydrogen bond donation to the epoxide oxygen.

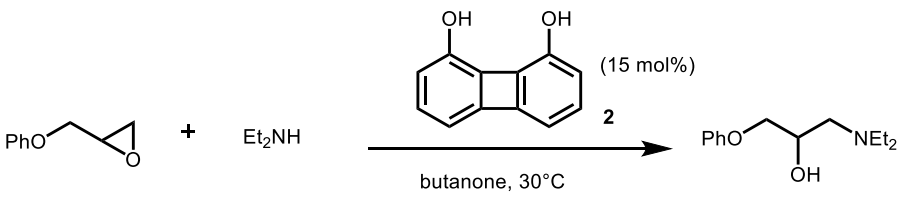

Scheme 1.3 Hydrogen bond catalyzed epoxide opening

The first example of urea catalysis was reported by Curran's group who reported an allylation reaction of cyclic α-sulfinyl radicals with allyltributylstannane, achieving higher yield and better retention of diastereoselectivity when employing urea **3** (Scheme 1.4 a) relative reactions without **3**.[18] Urea **3** is proposed to coordinate to the oxygen through hydrogen bonding and thus adding more steric bulk in the top face to improve the diastereoselectivity. Curran's group also showed that catalyst **3** could also accelerate the Claisen rearrangement by coordinating to the oxygen at the 3-position (Scheme 1.4 b).[19]

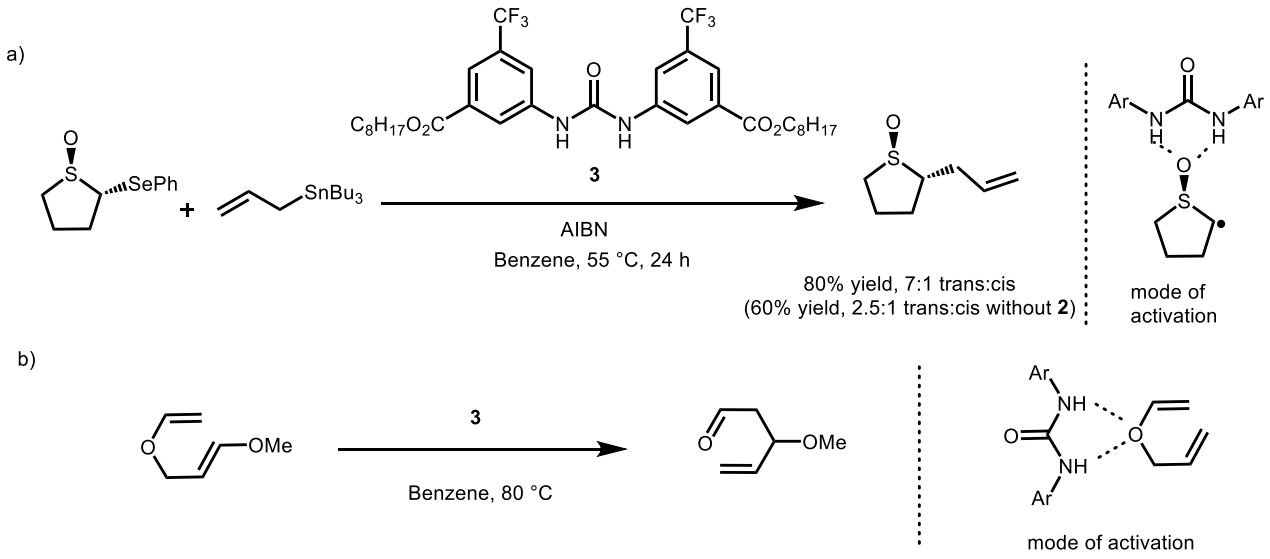

Scheme 1.4 a) Urea catalyzed allylation of α-sulfinyl radical b) urea catalyzed Claisen rearrangement

The field of asymmetric hydrogen bond catalysis emerged after a seminal paper by Jacobsen and co-workers where a chiral bifunctional scaffold was used to perform a Strecker reaction (Scheme 1.5).[20] They employed combinatorial chemistry where they synthesized three libraries to screen for Strecker like reactivity between TBSCN and *N*-allylbenzaldimine. In the first library, they screened several metals in combination with a urea-alcohol (structure **5**) attached

to solid support. The system without a metal coordinating to the urea-alcohol afforded the highest enantioselectivity (19% ee). Therefore, the next library screened excluded the use of a metal and 48 structures based on sub-structure **6** were synthesized and screened. The key structural features responsible for higher enantioselectivity were found to be a thiourea and a 3-*t*-butyl substituted salicylaldehyde. The third library included the structure of these leads and found a catalyst which gave the highest enantioselectivity (80% ee). Based on the best result, solvent phase catalyst **7** was synthesized and screened for activity using both the model system and 6 other allyl imines with HCN as the nucleophile where it achieved good to high enantioselectivity for all examples.

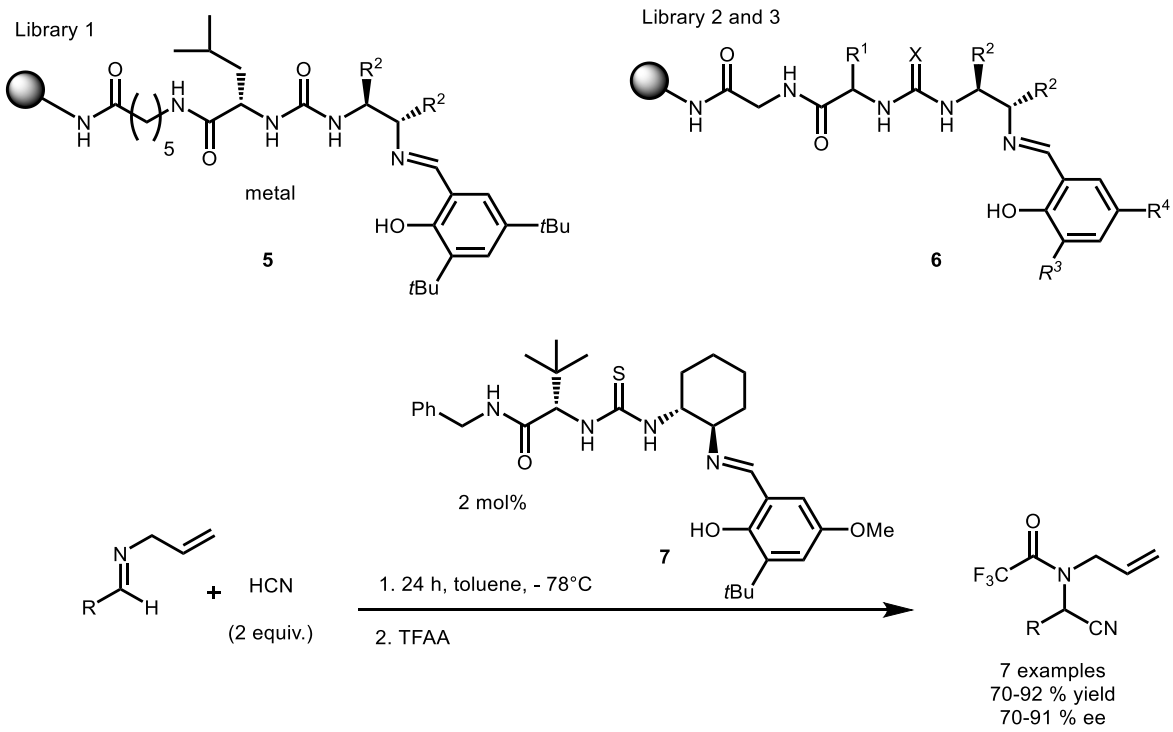

Scheme 1.5 Thiourea catalyzed Strecker reaction

Takemoto's group subsequently developed the bifunctional catalyst **8** for Michael additions of malonates to nitroolefins.[21] The catalyst scaffold consisted of a thiourea for activation of the nitroolefin (**8a**) and an amine for directing a nucleophile (Scheme 1.6 a). Good yields and high enantioselectivities were achieved for a wide range of substrates. The same catalyst was used for an aza-Henry reaction with moderate success (Figure 1.6 b), but importantly showed that the same catalyst can activate both imine and nitro groups which is significant because one is dual bonding to two oxygens (nitro) and the other is dual bonding to one nitrogen (**8b**).[22] In the original

article it was only proposed that the thiourea-amine was to activate nitromethane (**8c**). These are very simplified models and later studies have suggested more complex modes of activation (Figure 1.6 c).[23] Takemoto and coworkers proposed complex **8d** for the Michael addition of diethyl malonates with nitroolefin, where the thiourea activates and directs the nitroalkane and the amine activates and directs the malonate.[24] Pápai and coworkers proposed complex **8e** for the identical reaction where the thiourea activates and directs the malonate while the amine activates and directs the nitroalkane.[25] To date, there is still no prevailing mode of activation for this specific reaction and in general, every different reaction and catalyst have several potential activation modes.

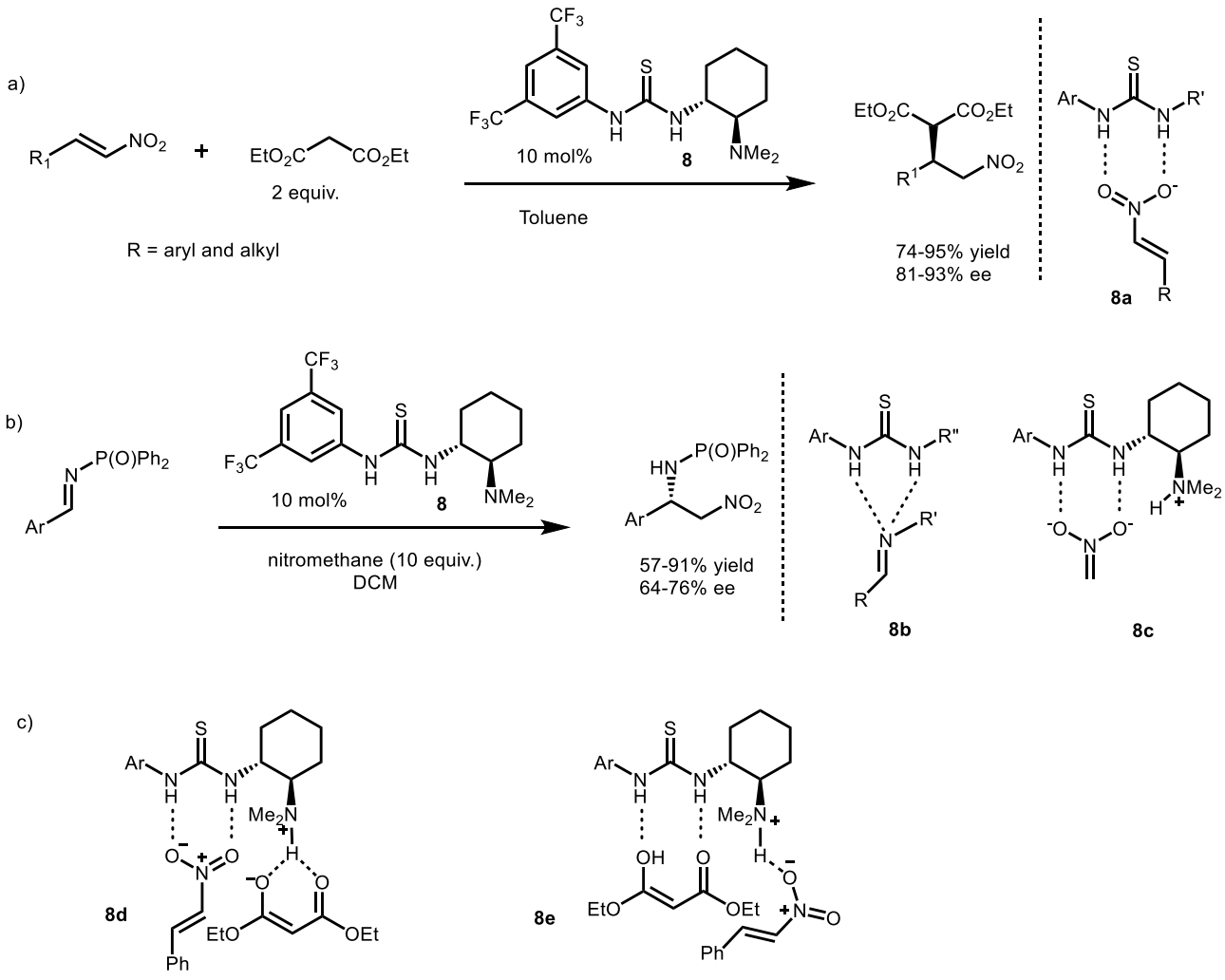

Scheme 1.6 a) Thiourea catalyzed Michael addition, b) aza-Henry reaction c) proposed activation modes

Berkessel and coworkers used urea-amine catalyst **9**, the urea version of Takemoto's thiourea **8**, for kinetic dynamic resolution of (4H)-oxazolone which would racemize in solution (Scheme 1.7).[26] Simple (thio)ureas without the basic dimethylamine had no activity, proving that the directing group is not only important for enantioselectivity but also reactivity. Moderate to good yields and high enantioselectivities were achieved for attack by allyl alcohol on oxazolones derived from phenylalanine, alanine, valine, leucine and *tert*-leucine. Second generation catalysts replaced the bis-3,5(trifluoromethyl)phenyl group with a chiral group (**10**) which extended the nucleophile scope and gave better enantioselectivity.[27]

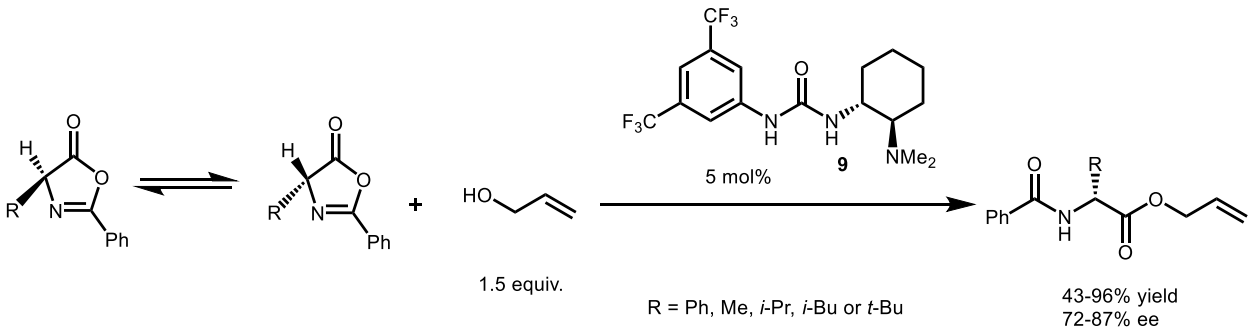

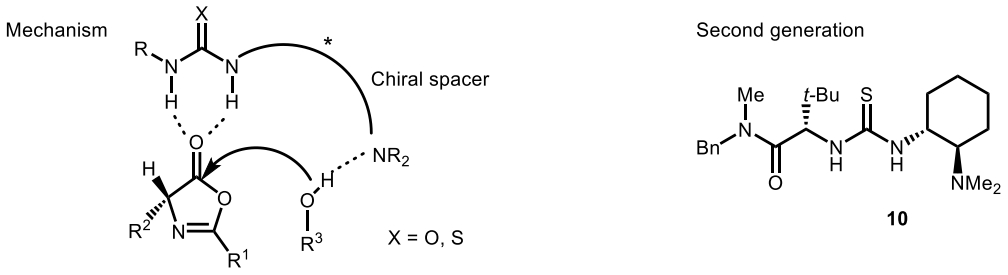

Scheme 1.7 Dynamic kinetic resolution of oxazolone

Jacobsen's group found that guanidinium ions can catalyze the Claisen rearrangement through hydrogen bond donor catalysis (Scheme 1.8).[28] The article claims this was bioinspired by the enzyme *chorismate mutase* which is proposed to utilize hydrogen bonding to perform the [3,3]-sigmatropic rearrangement of chorismate to prephenate. The first generation catalyst guanidinium ion **11** was able to achieve good conversion for a variety of substituted allyl vinyl ethers relative the thermal background reaction. An enantioselective version using the C2-symmetrical catalyst **12** provided good to excellent enantioselectivity and high diastereomeric ratios to provide synthetically interesting α-keto esters at ambient temperatures in 5-14 days. The scope was limited due to complexity of the starting materials which required the ester group on the 1' position and

only low or insignificant stereoselectivities were achieved on other types of allyl vinyl ethers. For catalyst **12**, the mechanism is proposed to be hydrogen bond activation of the ether oxygen, similar to what Curran proposed above in Scheme 1.2. In the case of the enantioselective reaction, a more complex activation by hydrogen bonding from **12** to both the ether oxygen and ester carbonyl is proposed in a later publication supported by DFT calculations.[29] The enantioselectivity is induced by favouring one chair-like transition state over the other.

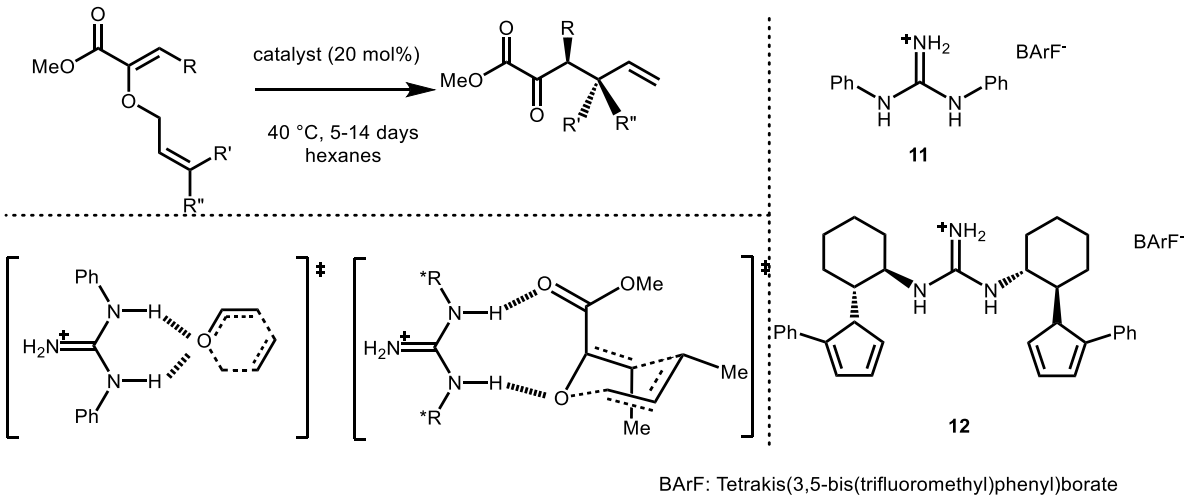

Scheme 1.8 Guanidine catalyzed Claisen rearrangement

Different types of alcohols have also been utilized for asymmetric hydrogen bond catalysis. The first example using a chiral diol was published in 2004 by Rawal and coworkers where TADDOL was found to catalyze a Diels-Alder reaction in good yield and enantioselectivity (Scheme 1.9).[30] They propose a single hydrogen bond to activate the carbonyl from one hydroxyl of the TADDOL which is activated into a stronger hydrogen bond donor by hydrogen bonding with the other hydroxyl group.

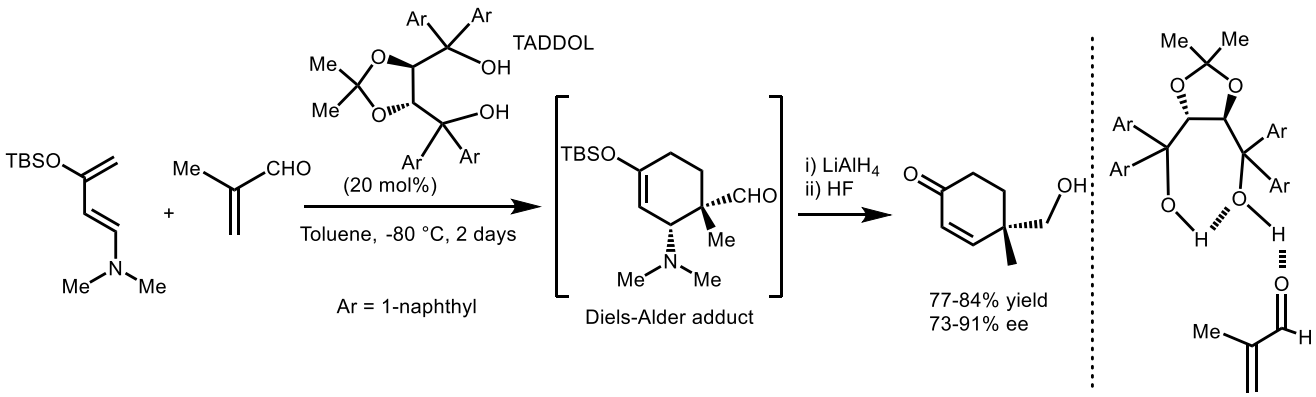

Scheme 1.9 TADDOL catalyzed Diels-Alder reaction

Schaus and coworkers showed early on that biaryl **13** in combination with triethylphosphine catalyzes the asymmetric Morita-Baylis-Hillman reaction, achieving high enantioselectivity and moderate to good yields (Scheme 1.10).[31] The diols are proposed to function in a similar fashion as in Scheme 1.9 where hydrogen bonding activates the carbonyl while the biaryl scaffold hinders one facial approach on the aldehyde.

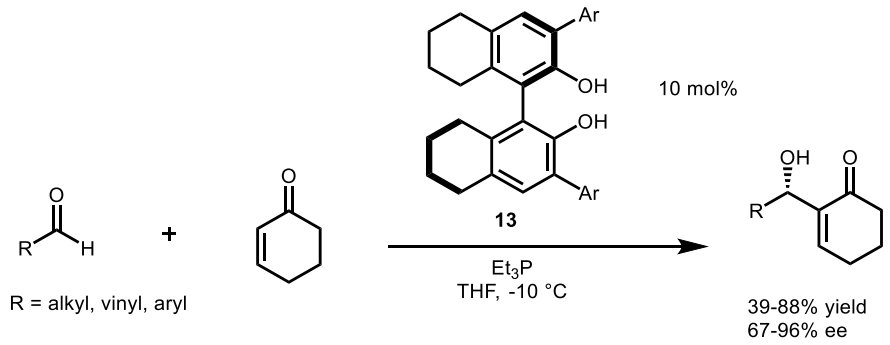

Scheme 1.10 Binaphthol catalyzed Morita-Baylis-Hillman reaction

A more complex version of the BINOL hydrogen bond catalyst was developed for the aza-Morita-Baylis-Hillman by Shi's group (Scheme 1.11).[32] Thiourea-phosphine **14** includes a stronger hydrogen bond donor (thiourea) in combination with an intramolecular phosphine nucleophile. The bifunctional catalyst gave enantioselectivity up to 97% ee with good to high yields for a large scope *N*-sulfonated arylimines and a few different α,β-unsaturated ketones.

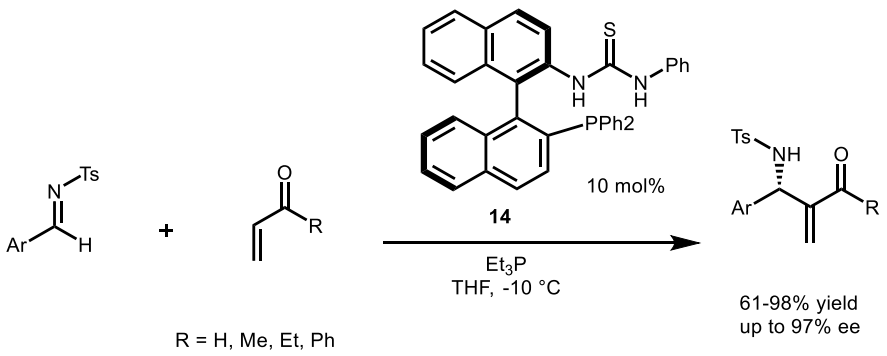

Scheme 1.11 BINOL thiourea-phosphine catalyzed aza-Morita-Baylis-Hillman

One of the impressive abilities of these hydrogen bond catalysts is that they can be utilized in combination with several different modes of activation and can perform asymmetric catalysis on increasingly inert bonds, which is well described in a recently published review by Qin *et al*.[33] A recent example from Melchiorre and coworkers combined the chiral cinchona-based hydrogen bonding thiourea **15** with photochemistry to perform a Diels-Alder (Scheme 1.12).[34] This is a classical photoenolization/Diels-Alder reaction (PEDA) of 2-methylbenzophenone which in situ forms a diene and the dienophile maleimide,[35] and in Melchiorie's work this PEDA reaction was for the first time combined with the use of substoichiometric chiral catalysts. The dual modes of reactivity provided good enantioselectivity and yields with a wide scope. However lower enantioselectivity was achieved if R" on maleimide is not a *t*-butyl or diphenylmethyl group. The mechanism starts with the carbonyl absorbing light to form a singlet excited diradical state (S_1) which decays to the triplet excited state (T_1) through intersystem crossing (ISC). The T_1 diradical undergoes 1,5 hydrogen shift followed by rotation to form a very reactive enol. The urea activates the maleimide while the chiral backbone blocks one facial approach of the enol. This is just one example of organocatalytic Diels-Alder reaction. Many other modes of activation have been developed for the Diels-Alder reaction,[36] some of which will be presented later in this chapter when addressing Lewis acid catalysis and iminium ion catalysis. Generally, this is a state of the art example combining hydrogen bond activation with another hot topic in synthetic chemistry while highlighting the compatibility and functional group tolerance of hydrogen bond activation.

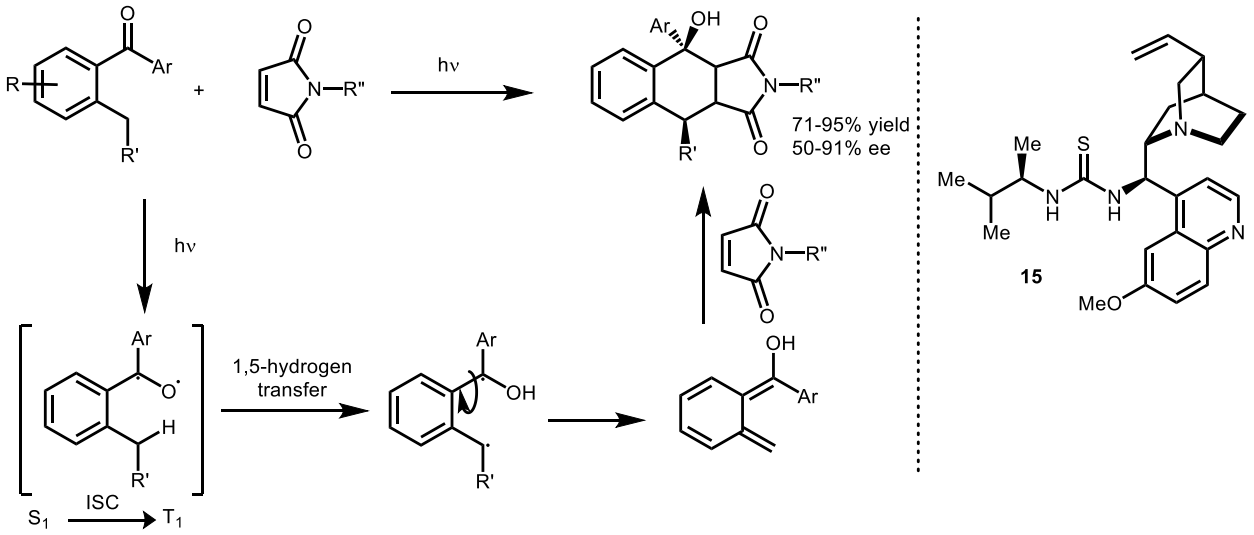

Scheme 1.12 Combined photoenolization and thiourea catalysis

All examples above are versions of direct activation, where the hydrogen bond donor interacts directly with either the electrophile to activate it for nucleophilic attack or lowers the LUMO for pericyclic reactions. A more complex mode of activation is chiral ion-pairing in which the hydrogen bond donor performs an anion abstraction from the substrate to form an electrophilic cation and a chiral hydrogen bonded counterion which dictates the stereochemical outcome of the attack by a nucleophile.[37]

One of the first examples of utilizing a dual hydrogen bond in asymmetric ion-pairing organocatalysis donor was presented by Seidel and co-workers (Scheme 1.13).[38] They employed thiourea **16** in combination with DMAP derivative for the kinetic resolution of amines to form amides using benzoic anhydride. After only achieving moderate selectivity of their first generation which was based on a C2-symmetric di-thiourea and DMAP,[39] it was discovered that the non-chiral DMAP derived *N,N*-dipropylaminopyridine co-catalyst was essential to achieve high *s*-factor. However, no explanation to why these was selective was given.

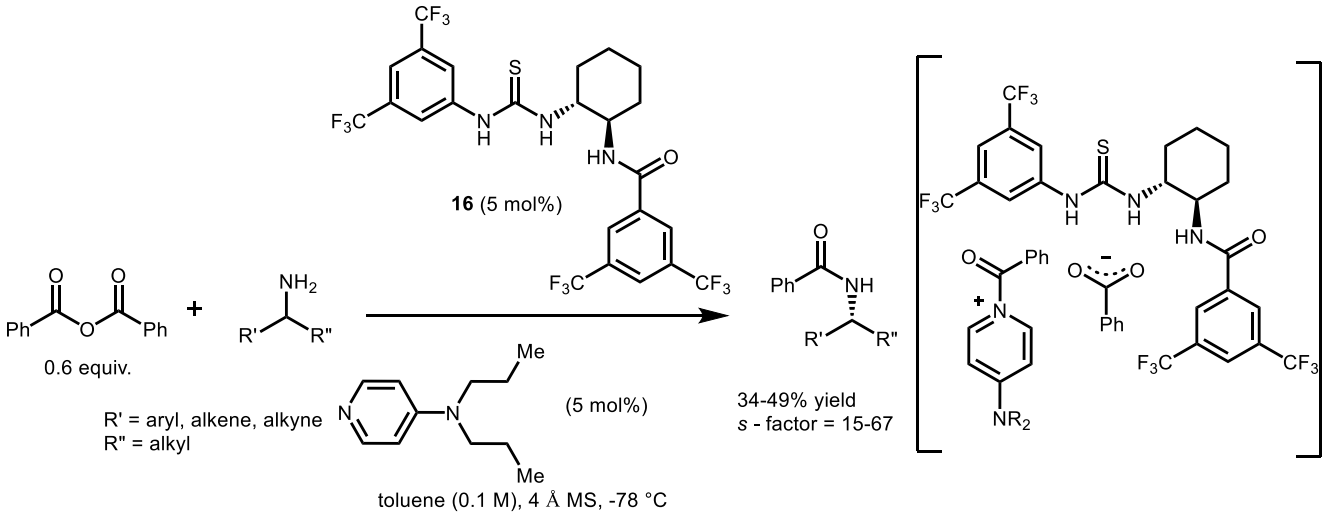

Scheme 1.13 Kinetic resolution of amines with ion-pairing catalysis

A new mode of chiral ion-paring catalysis was recently published by Jacobsen's group where they used the chiral squaramide **17** to enhance the reactivity of a silyl triflate through hydrogen bonding to the triflate (Scheme 1.14).[40] The Lewis acid-squaramide system was employed to catalyze the 4 + 3 cycloaddition between 3-substituted furans and oxyallyl cation formed *in situ* by the catalytic system and achieved high yield and enantioselectivity. The reaction initiates with formation of a silyl triflate-squaramide complex which promotes acetal ionization to form oxyallyl cation/triflate-squaramide complex. This complex undergoes the 4 + 3 cycloaddition with furan to form the desired bridged [3,2,1] bicyclo compound. Squaramides have higher binding affinity that other bidentate hydrogen bond donors due to its aromaticity, the dual effect from two electron withdrawing carbonyls and rigidity.[41, 42]

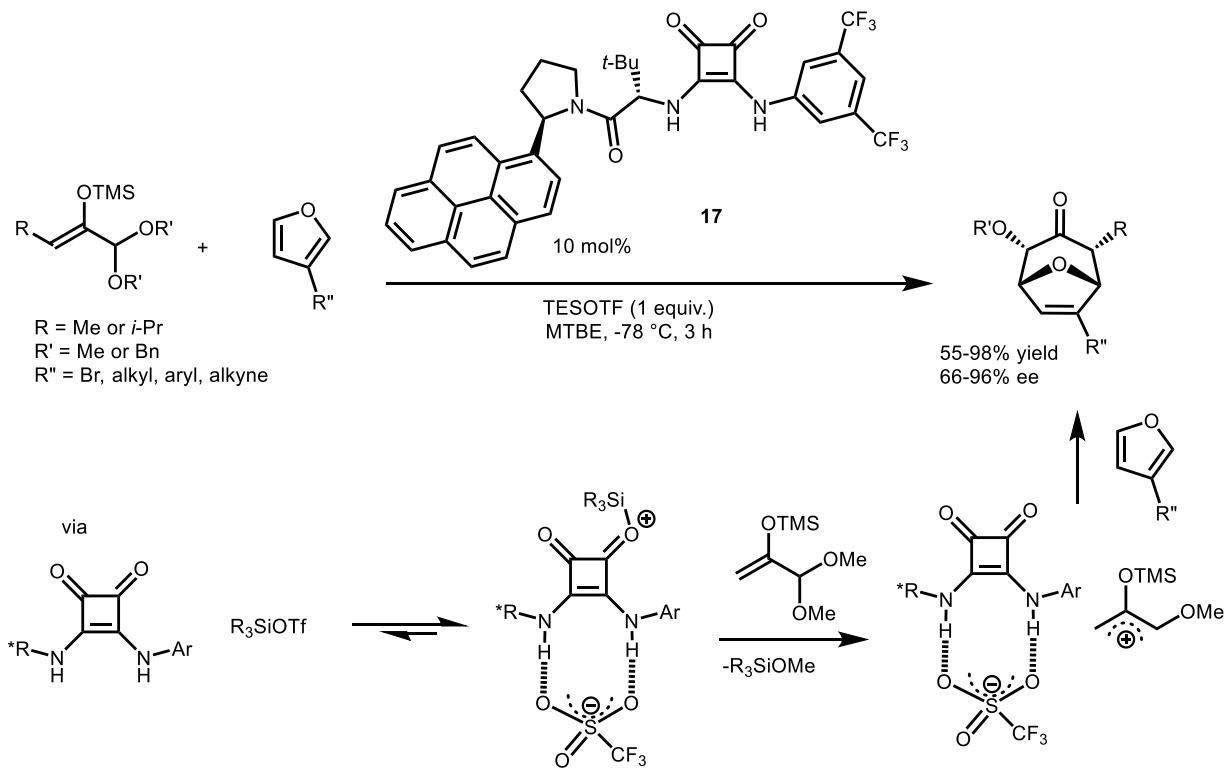

Scheme 1.14 Combined Lewis acid-squaramide catalysis

The above selection of seminal articles and recent publications highlights the potential and varied uses of hydrogen bond catalysis. The success of combining a hydrogen bond donor with other modes of activation has shown huge potential in expanding the field of hydrogen bond organocatalysis into new and unexplored modes of activation. The major successes of hydrogen bonding organocatalysis have been achieved by combining a hydrogen bond donor with a chiral spacer.[43] The chiral spacer mainly functions through either containing a hydrogen bond donor/acceptor which directs a nucleophile onto the hydrogen bonded electrophile with stereocontrol or impacts as steric hindrance on the hydrogen bonded electrophile, favouring one facial approach of the nucleophile. Given the success and interest in the field, we envisioned an extension of hydrogen bond organocatalysis strategy apply in the realm of amide bond formation and our efforts are presented in chapter 2.

1.3 Amide bond formation

Amide bond formation is one of the most important reactions in organic chemistry. It is essential both in nature, where it constructs the bonds connecting amino acids in peptides, and in organic synthesis, where it is one of the most heavily utilized reactions, particularly in medicinal chemistry.[44] This is due to several advantageous characteristics of the amide bond such as its high stability, polarity and conformational diversity.[45] A survey from three leading pharmaceutical companies (AstraZeneca, Pfizer and GlaxoSmithKlyne) found that amide bond formation was used in the syntheses of 84 (66%) out of 128 drug candidates.[46] There are several potential starting materials to form an amide but the direct bond formation through the condensation of a carboxylic acid and an amine is the conceptually most logical one and the method nature employs. Upon inspection, one might imagine such a condensation should follow the same principle as that of a Fischer esterification. However, direct amidation does not proceed under such mild conditions. The fundamental problem arises from the amine and carboxylic acid rapidly forming a stable ammonium carboxylate salt though instantaneous acid base chemistry (Scheme 1.15). This acid base chemistry prevents direct amide bond formation at ambient temperatures because the lone pair on the nitrogen is protonated and is no longer nucleophilic and the resonance stabilized, anionic carboxylate is not a competent electrophile.[47] To achieve direct condensation from the ammonium carboxylate salt, very high temperatures (160-200 °C) are required which are typically proven incompatible with other functional groups.[48]

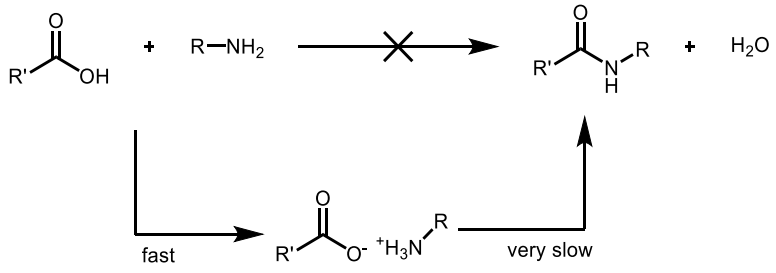

Scheme 1.15 Direct thermal amide bond formation

1.3.1 Peptide Coupling

To circumvent salt formation, several methodologies have been developed. Pre-transforming the carboxylic acid to an acyl chloride eliminates the acidic proton and generates a superior electrophile (Scheme 1.16). Acyl chlorides are typically generated using oxalyl chloride or thionyl chloride, generating moderately benign side-products (CO_2, CO and HCl or SO_2 and HCl). This approach constitutes 44% of the peptide forming reactions surveyed (*vide supra*) but is not always a viable option due to functional group incompatibility.[49]

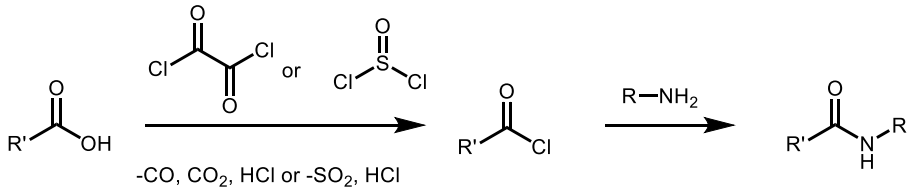

Scheme 1.16 Amide bond formation from acyl chloride and amine

One of the standard methods of synthesizing peptides, particularly on smaller laboratory scale, is the use of peptide coupling reagents, where a stoichiometric amount of a coupling reagent is used in the presence of a base (Scheme 1.17). Some of the most common and widely used simple coupling reagents are carbodiimides (e.g. DCC, EDC•HCl). Using a coupling reagent circumvents the acid base chemistry as the carboxylate is able to react with the coupling reagent under the basic conditions necessary to prevent protonation of the amine, allowing the amine to remain nucleophilic. However, coupling reagents are used stoichiometrically and are not reusable making their application expensive and resulting in the production of a stoichiometric amount of waste which must be removed during purification and then properly disposed of. The choice of base has an impact on both the reactivity and the stereochemical integrity of the starting materials and products. Tertiary amines and pyridines such as diisopropylethylamine (DIPEA), *N*-methylmorpholine (NMM) and 4-(dimethylamino)pyridine (DMAP) have been the most fruitful in the development of these conditions. All of these features result in an arguably highly useful, but flawed synthetic technique which suffers from negative characteristics making it a less than elegant synthetic method.

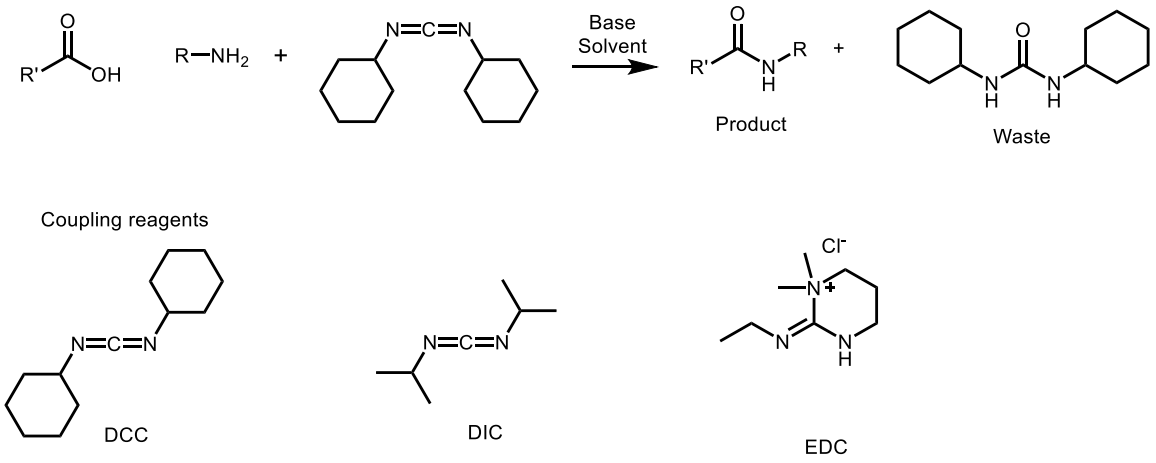

Scheme 1.17 Peptide coupling reagents

Two more subtle problems associated with using these coupling reagents are low reactivity of the carboxylate adduct and racemization/epimerization of α-stereogenic centers. Racemization/epimerization takes place via three potential mechanisms: 1) elimination of the α-proton; 2) reversible β-elimination; and 3) formation of a reactive 5-(4H)-oxazolone, with this being the most significant source of racemization/epimerization.[50] To minimize these problems, coupling reagents are commonly used in combination with acyl transfer agents such as 1-hydroxybenzotriazole (HOBt), which was first introduced by Koenig and Geiger (Figure 1.2).[51] Carpino and co-workers have performed extensive research showing higher rates and critically lower racemization during amide bond formation when using acyl transfer agents, mainly HOAt.[52] DMAP and its derivatives have occasionally been employed both as a base and an acyl transfer agent.

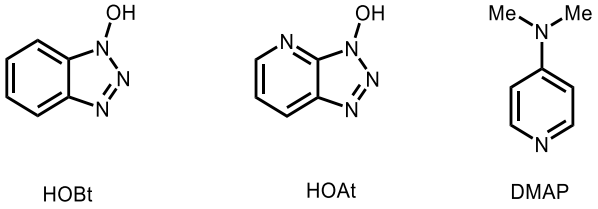

Figure 1.2 Peptide coupling additives

More advanced coupling reagents have combined the coupling reagent and the acyl transfer reagent into a salt with a weak, non-coordinated counterion. The most common types of these advanced coupling agents are phosphonium salts (e.g. PyBOP), uronium/aminium salts (e.g.

HATU), immonium salts (e.g. BOMI), or imidazolium salts (e.g. CBMIT) (Figure 1.3). These have good reactivity, affording high yield and lower epimerisation, but due to their stoichiometric use are usually expensive in addition to often being toxic. Several other, more exotic and unique, coupling agents have also been developed.[53]

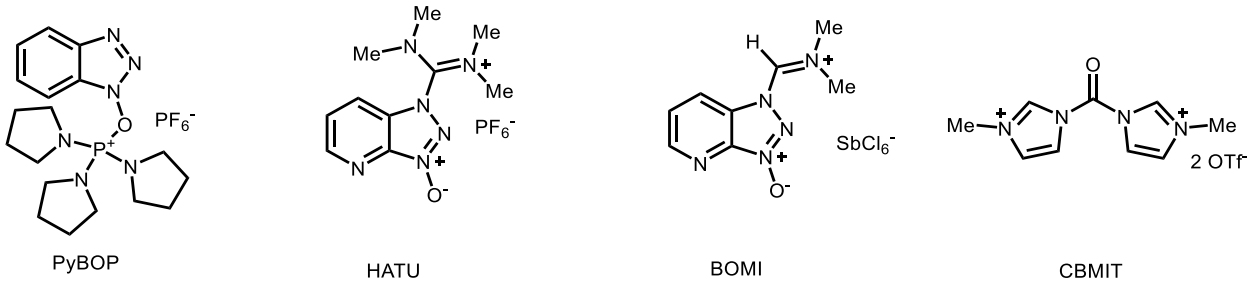

Figure 1.3 Coupling reagents

Despite the incredible range of coupling reagents and additives, the peptide coupling reaction follows the same general mechanism in the large majority of cases. Scheme 1.18 illustrates the established mechanism for amide bond formation using HATU as the coupling reagent. After initial deprotonation of the carboxylic acid, nucleophilic attack of the carboxylate on to the uronium electrophile initiates the reaction. Tetrahedral intermediate **A** then collapses and forms acyl uronium **B** and OAt anion. The nucleophilic $^{-}$OAt attacks the acyl group on intermediate **B** forming the activated intermediate **C** and urea by-product **D**. The amine then participates in an acyl transfer event form amide **E** and liberating HOAt.

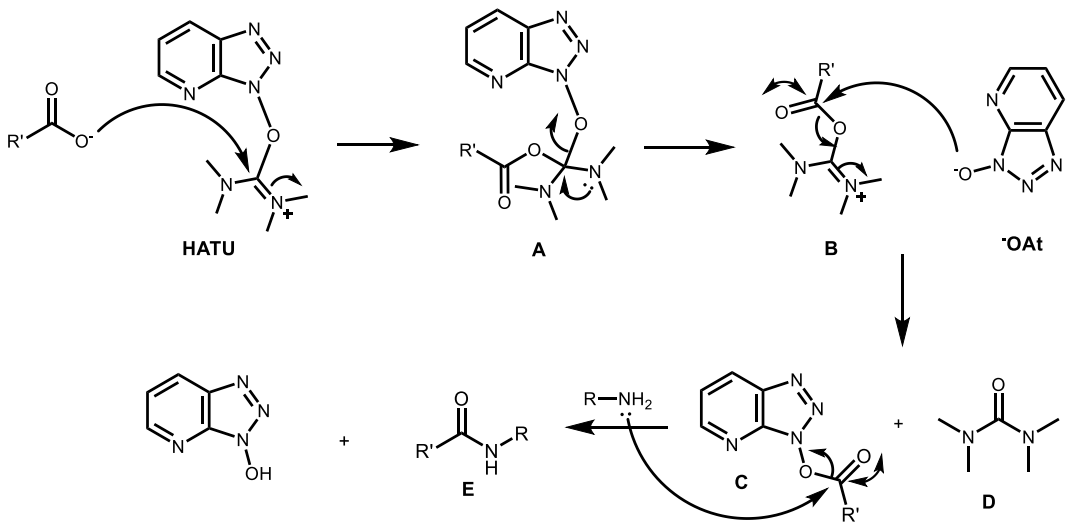

Scheme 1.18 Mechanism of peptide coupling using HATU

1.3.2 Catalytic amide bond formation from carboxylic acids and amines

In 2005, The American Chemical Society (ACS), Green Chemistry Institute (GCI) Pharmaceutical Roundtable (PR), comprised of members from major pharmaceutical institutes, voted "amide formation avoiding poor atom economy reagents" as the top challenge for organic chemistry.[54] A few catalytic methods for amide bond formation from carboxylic acid and amine were subsequently developed.

Williams and co-workers screened an extensive list of metal salts for direct amide bond formation between a carboxylic acid and amine (Scheme 1.19). Several metal salts, such as CuBr, $ZrCl_4$, $Ni(NO_3)_2$, $TiCl_4$ and $ZrCp_2Cl_2$, gave good to excellent conversion of the model system at 110 °C and 20 mol% catalyst loading.[55] Notably, the thermal background reaction gave 20% conversion and some salts resulted in lowering the conversion. When the catalyst loading was dropped to 5 mol%, $ZrCp_2Cl_2$ or $ZrCl_4$ still gave complete conversion for the amide bond formation for 3-phenylpropionic acid and benzylamine. The study included one example of a chiral carboxylic acid, Boc protected proline, and displayed full retention of enantiomeric excess. Several catalytic amide bond formations using metals but not originating from carboxylic acids and amines have also been developed.[56]

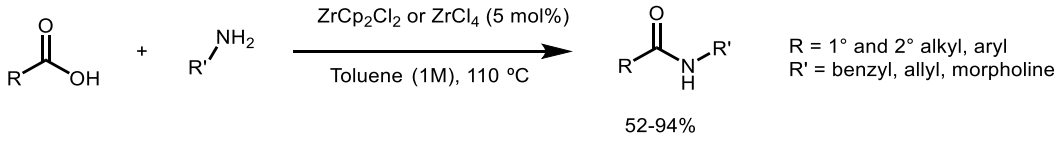

Scheme 1.19 Zirconium catalyzed amide bond formation

1.3.3 Organocatalytic amide bond formation

One very interesting result in the article by the Williams group,[55] see above, was that *N*,*N*-diphenylurea (**20**) gave 51% conversion in the model system of 3-phenylpropionic acid and benzylamine (Scheme 1.20). The article concluded that the catalytic effect was presumably from the urea acting as a hydrogen bond donor but did not continue to investigate hydrogen bond donors. However, this shows potential to create a catalyst for amide bond formation utilizing hydrogen bond catalysis.

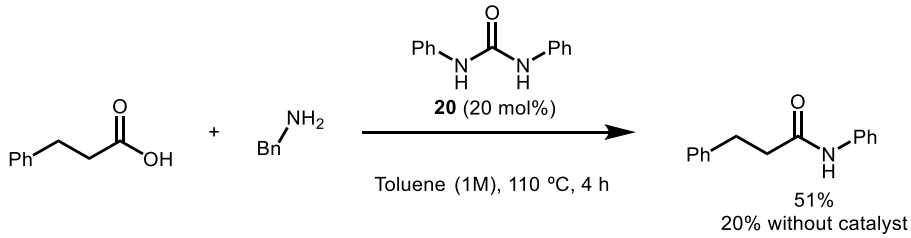

Scheme 1.20 Urea catalyzed amide bond formation

One of the more successful approaches has been boron based catalysis which falls under the field of organocatalysis. The first report was from Yamamoto and co-workers where they showed that electron deficient aromatic boronic acids such as 3,4,5-trifluorophenylboronic acid (**21**) could catalyze amide bond formation (Scheme 1.21).[57] The boronic acid activates the carboxylate by forming the acylborate **22**. The reaction conditions were harsh and required temperatures over 110 °C, providing poor functional group compatibility. Other groups have developed different boronic acid derivatives but these methods also suffer the requirement of elevated temperatures.[58]

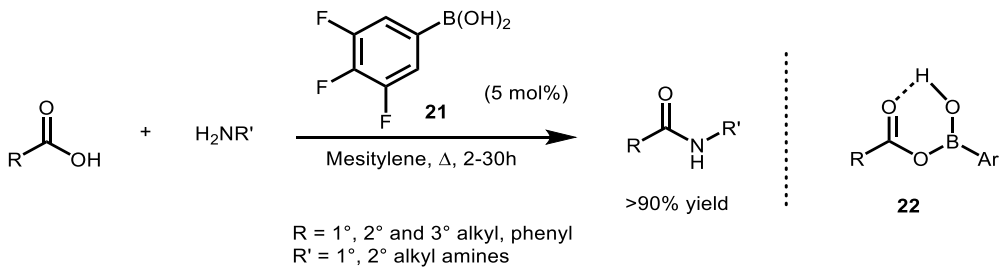

Scheme 1.21 Borane mediated amide bond formation

Hall and coworkers have expanded the work on boronic acid catalysis by developing ortho halo boronic acid catalysts which catalyzed the amidation between a variety of different amines and carboxylic acids at room temperature in 48 h (Scheme 1.22).[59] They discovered catalyst **24** after screening a library of 45 *ortho*-substituted boronic acids (**23**) and found that having a ortho bromide or iodide positively influenced the reaction, giving moderate to high yields for a variety of starting materials. Adding a para-methoxy group relative to the halide increased the reactivity of the catalyst and extended the scope.[60] The ortho halide is essential for high activity and is proposed to have a significant halogen-hydrogen bond in the transition state (**TS 24**) as demonstrated by DFT calculations. This promotes the elimination of water to regenerate the catalyst and yield the amide in the proposed rate determining step.[61] This is to date the most benign and environmentally friendly catalyst developed, being inexpensive, easy to prepare, and recyclable. The catalyst is effective with a variety of both primary and secondary carboxylic acids and amines with good functional group compatibility, including nucleophilic hydroxyl groups and unprotected indoles. Sterically hindered carboxylic acids required higher catalyst loading (20 mol%) and slightly elevated temperatures (50 °C). The catalyst also demonstrated low levels of racemization for a select substrate. Boronic acids together with one example of a urea are to our knowledge the only organic catalysts for the amide bond formation from carboxylic acids and amines.

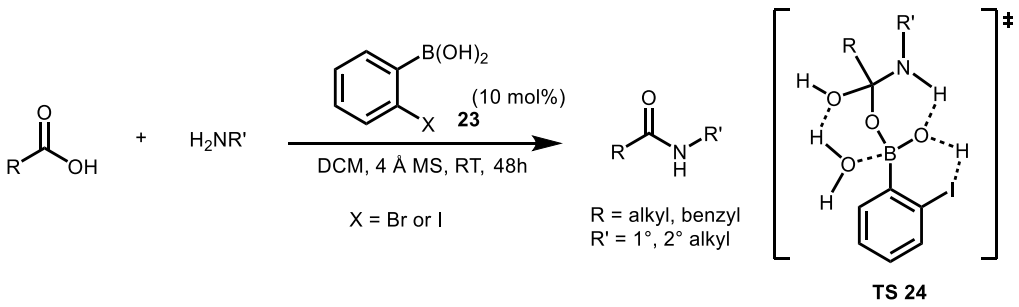

Scheme 1.22 *ortho*-halogen boronic acid catalyzed amide bond formation

1.4 Diels-Alder cycloaddition

The Diels-Alder cycloaddition is one of the most powerful reactions in synthesis. It has been argued that the reaction has shaped the art and science of total synthesis.[62] The Diels-Alder reaction was first observed by Euler in 1920 between para-quinone (**25**) and isoprene.[63] Otto Diels and his graduate student Kurt Alder published their initial work in 1928[64] and throughout a span of 10 years, the Diels group published an impressive amount of work on what became known as the Diels-Alder reaction. They were rewarded for their work in 1950 with the Nobel prize. The fundamental process is the reaction of a 1,3-diene with an alkene, also known as a dienophile to afford a cyclohexene (Figure 1.4). The first reaction reported by Diels and Alder was the reaction between cyclopentadiene (CpH) and para-quinone **25**. It afforded first the mono-adduct **26** which continued to give the di-adduct **27** in good yield. The stereochemistry of the product will be explained later.

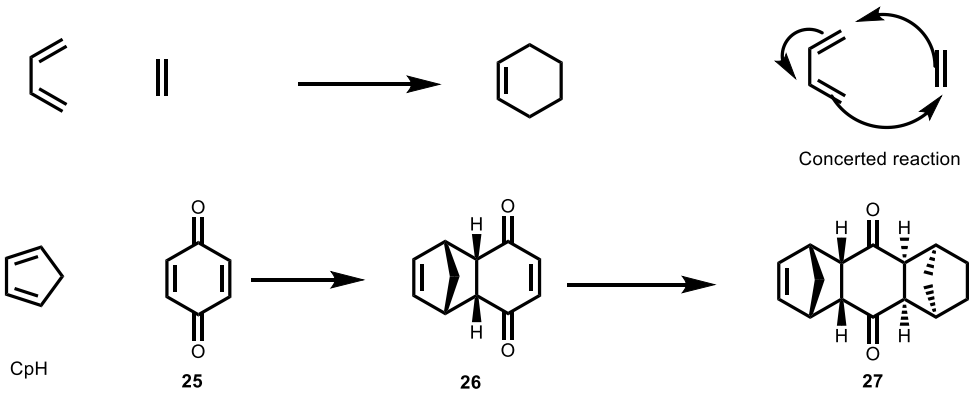

Figure 1.4 The Diels-Alder reaction

The Diels-Alder reaction normally proceeds through a concerted cyclic transition state and is classified as a pericyclic reaction. Pericyclic reactions follow the Woodward Hoffmann rules which state that if the total number of (4n + 2) antarafacial (opposite face) and (4n) suprafacial (same face) components is an odd value, the reaction is thermally allowed. There is only one $(4n + 2)_s$ component, from the dienophile, and no $(4n)_a$ component so the reaction is allowed because the total number is 1. The 4π electrons from the diene are reacting in a suprafacial fashion in the reaction and are not considered in the equation.

As a bimolecular reaction, the Diels-Alder reaction takes place when a dienophile and a diene collide with enough energy to overcome the activation barrier. Following standard FMO theory, the key interactions that determine the fate of the collision is the interaction of the filled HOMO orbital of one reaction partner with the empty LUMO orbital of the other one. There are two types of Diels-Alder cycloadditions, normal electron demand where the key interaction is the HOMO of the diene and the LUMO of the dienophile and inverse electron demand (IED) where the opposite occurs (Figure 1.5). The driving force is the formation of a lower energy product originating from breaking 2π-bonds in favour to form two stable σ-bonds.

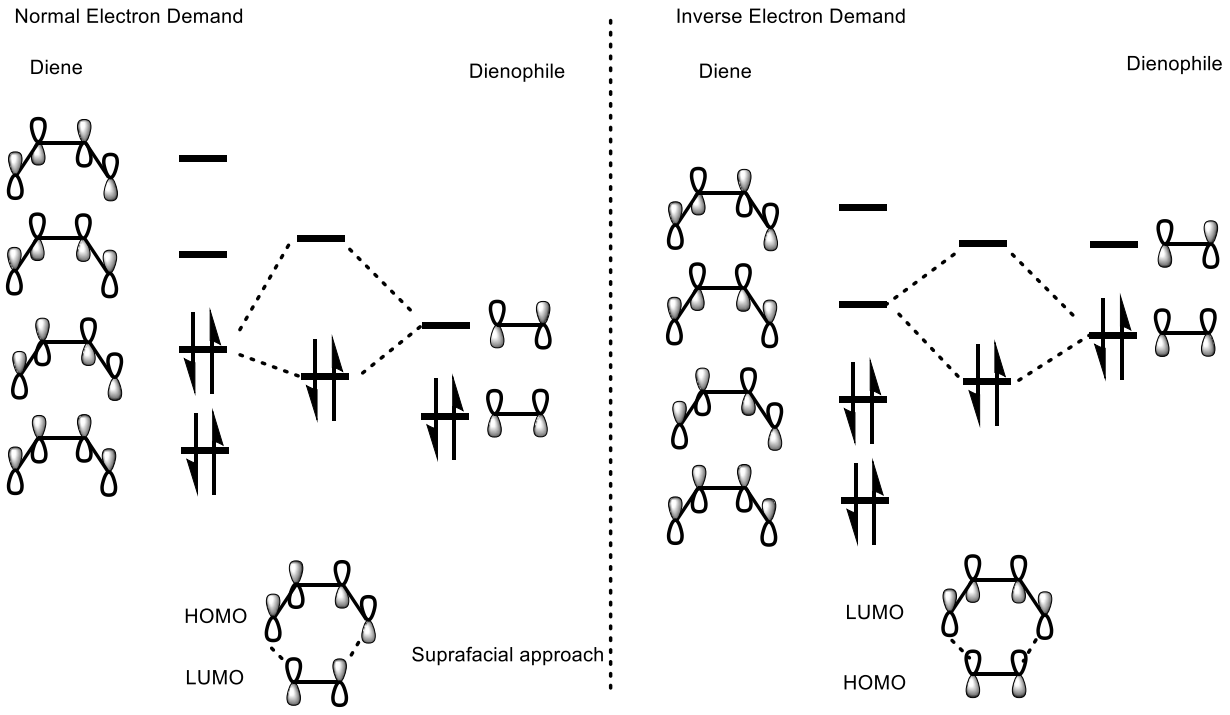

Figure 1.5 Molecular orbital diagram for normal electron demand and inverse electron demand.

The rates of normal electron demand cycloadditions can be increased when the energy of the diene's HOMO is raised or the energy of the dienophile's LUMO is lowered, ultimately bringing these pairs of orbitals closer in energy. The closer the orbitals are, the more energy stabilization will be obtained from their interactions. Adding an electron withdrawing group to the dienophile significantly lowers the LUMO and slightly lowers the HOMO. An electron donating group will substantially raise the energy of the HOMO and slightly raise the energy of LUMO. This trend is observed for the diene as well, and thus the combination of electron poor dienophile and electron rich diene reacts more quickly. The opposite is true for inverse electron demand DA where an EDG would benefit the dienophile and an EWG would benefit the diene (Figure 1.6).[65]

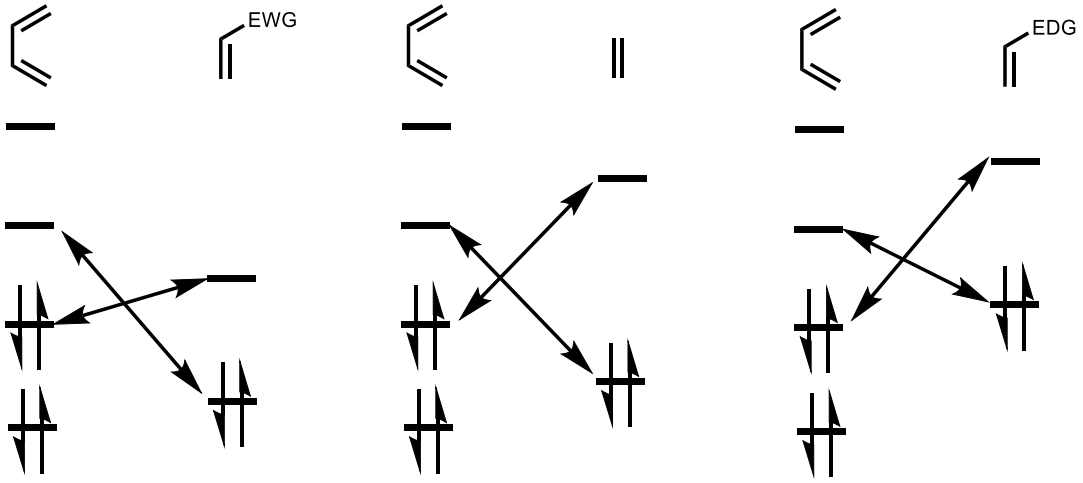

Figure 1.6 Molecular orbital diagram for dienophile with EWG, unsubstituted and EDG

To get the required geometrical alignment, the diene must be in a s-*cis* conformation rather than the s-*trans*. Certain privileged dienes such as cyclopentadiene are already locked into the reactive s-*cis* conformation and other dienes are prevented or restricted from forming the s-*cis* conformation due to geometrical constraint or high conformational strain. For example, for butadiene, the conformational energy between s-*cis* and s-*trans* is 3.5 kcal/mol in favour of s-*trans* which means fewer reactive species in the reaction mixture (Figure 1.7).

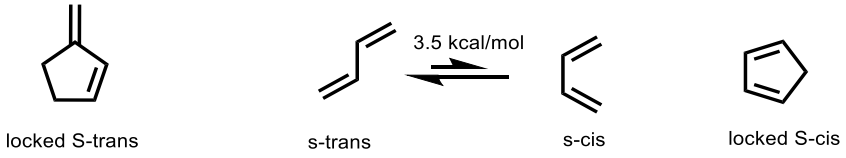

Figure 1.7 Conformations of dienes

In Figure 1.4, products **26** and **27** are displayed with specific relative stereochemistry. This selectivity arises from the fact that dienophiles with extended π-systems, such as acrolein, will have a favourable interaction between the extended π-system and the π-systems of the diene (Figure 1.8). These attractive interactions are termed secondary orbital effects and the resulting selectivity for the endo product is known as the *endo* rule.

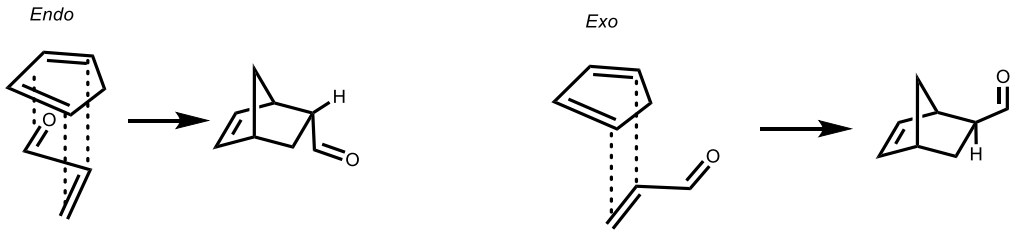

Figure 1.8 Endo and Exo adducts

1.4.1 Lewis acid catalysis

Lewis acid coordination to an EWG lowers the energy of the LUMO orbitals. This has spurred the use of Lewis acids in a whole array of reactions. For example, Lewis acids have catalyzed cycloadditions, including both the Diels-Alder reaction[66] and 1,3-dipolar cycloaddition[67], Mukaiyama aldol[68] and 1,4-addition reactions of α,β-unsaturated carbonyls[69] (Figure 1.9).

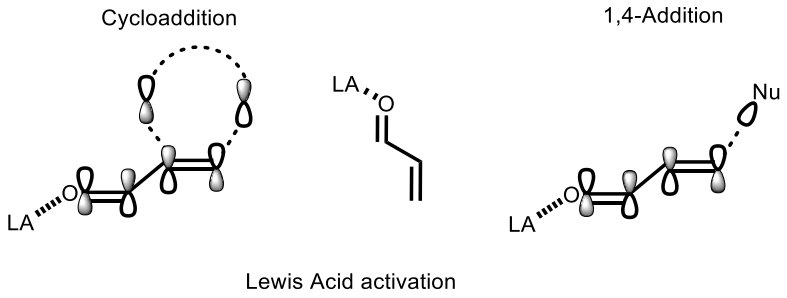

Figure 1.9 Lewis acid activation of acrolein

There has been a plethora of chiral Lewis acids developed for the use in the Diels-Alder reaction.[70] In one early example, Corey and co-workers developed oxazaborolidines (**28**) for the highly selective reaction between α-bromoacrolein and CpH (Scheme 1.23 a).[71] Several versions

of the oxazaborolidines have been developed since then to perform the Diels-Alder reaction with a large scope of dienes and dienophiles.[72] The Evans group developed chiral bis(oxazoline)copper(II) complexes (**29**) as Lewis acid catalysts for the enantioselective Diels-Alder reaction giving high enantioselectivity and yields between acrylate imides and cyclopentadiene (Scheme 1.23 b).[73] The copper is able to coordinate to both carbonyls forming a square planer catalyst-substrate complex and the C2-symmetric bisoxazoline dictates the facial approach of the diene. These are but two examples among numerous other Lewis acid catalyzed Diels-Alder reactions.

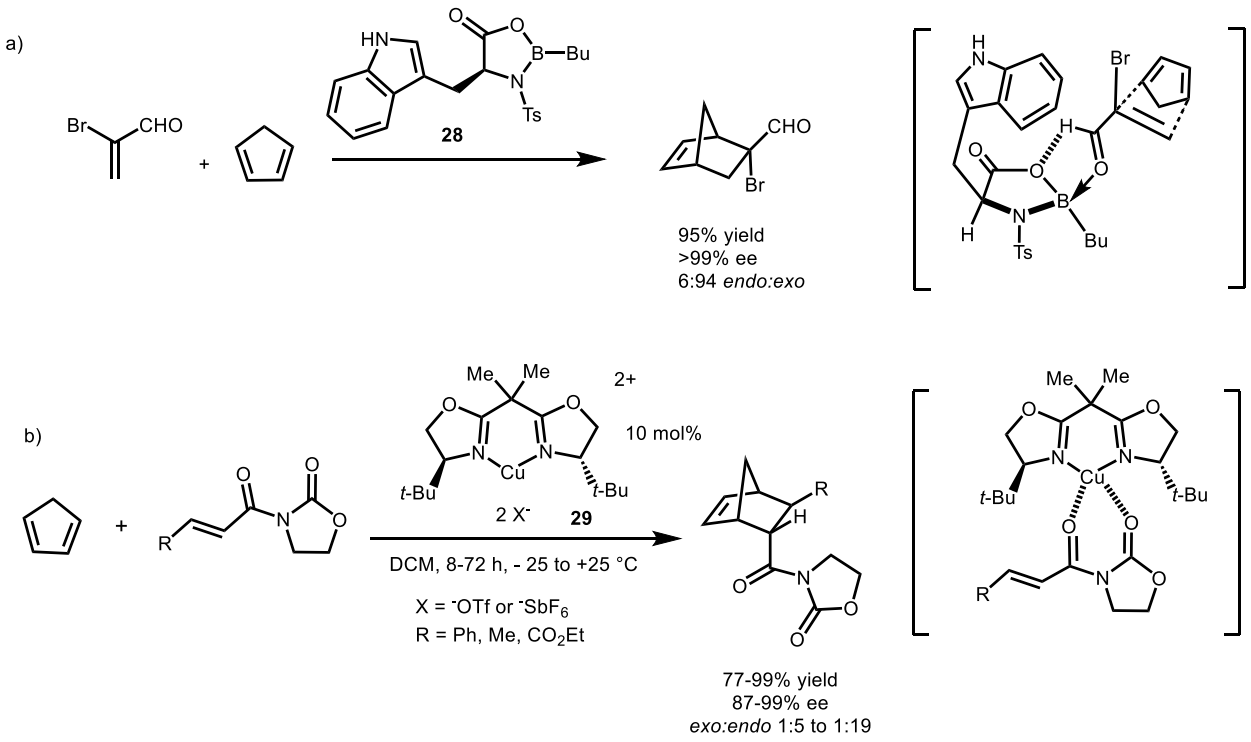

Scheme 1.23 Lewis acid catalyzed Diels-Alder reactions

The advantages of Lewis acid catalyzed Diels-Alder reaction are high reactivity, high yields and great regio- and enantio-selectivity. The disadvantages associated with Lewis acid catalysis are similar to that discussed in the introduction such as financial and environmental drawbacks, sensitivity to oxygen and water and difficulties in preparation and handling.[74] Many Lewis acid activated complexes also do not display reversible formation, and thus, are employed stoichiometrically.

1.4.2 Iminium ion catalysis

An alternative to Lewis acid catalysis is iminium ion catalysis where an iminium ion is formed between an amine and an aldehyde or a ketone to catalyze a reaction of that carbonyl compound. The first organocatalytic reaction was a piperidine (**30**) catalyzed Knoevenagel reaction between malonic acid (**31**) and benzaldehyde (**32**) to form cinnamic acid (**33**) (Scheme 1.24).[75] Knoevenagel didn't explicitly propose the iminium ion intermediate but suggested that the condensation between the secondary amine and aldehyde played a part in the reaction.[76] Today it is established that this reaction is iminium ion catalyzed.

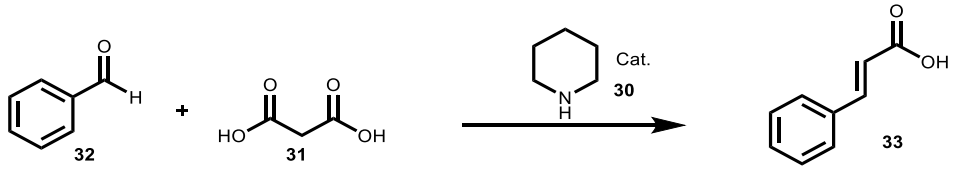

Scheme 1.24 The first organocatalytic reaction by Knoevenagel

The general reaction mechanism of acid catalyzed iminium ion formation begins with protonation of the carbonyl **34** and then nucleophilic attack by amine to give the tetrahedral intermediate **36** (Figure 1.10). Proton transfer between ammonium and hydroxyl gives water as a good leaving group, forming the imine **38** after elimination. The entire process is reversible and depending on the carbonyl, amine and water, the equilibrium can favour either the starting material or the iminium ion product.

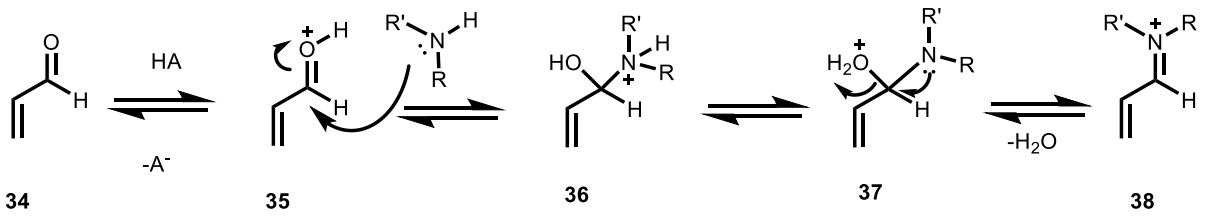

Figure 1.10 Iminium ion formation mechanism

1.4.3 Iminium ion catalyzed Diels alder reaction

Arguably the most important use of iminium ion catalysis has been its applications to the Diels-Alder reaction, which has become one of the most powerful reactions in synthesis.[77] The iminium ion acts in an analogous way to Lewis acid catalysis, by drawing electron density away from the dienophile olefin, lowering the energy of LUMO orbital, bringing it closer in energy to the HOMO orbitals of the diene (Figure 1.11).

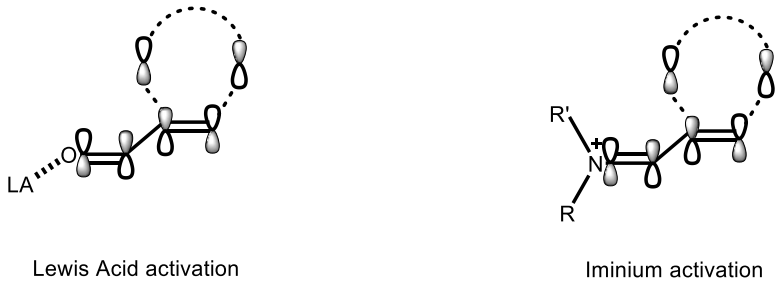

Figure 1.11 Similarity between Lewis acid catalysis and iminium ion catalysis

In 2000, David MacMillan's group published a seminal paper in which they developed the first highly enantioselective organocatalytic Diels-Alder reaction based on iminium ion catalysis (Scheme 1.25).[78] The reaction worked for a wide scope of both dienes and enal dienophiles with moderate *exo*-selectivity and good to excellent yield and enantioselectivity. This imidazolidinone catalyst (**39**) has established itself as the benchmark standard for iminium ion and also enamine catalysis, with new applications still being developed.[79] A second generation imidazolidinone replaced the gem-dimethyl with a *t*-butyl syn to the benzyl (**40**). This still favoured the E-geometry for the iminium ion, while being slightly less sterically encumbering around the reacting nitrogen, creating a more reactive catalyst.[80]

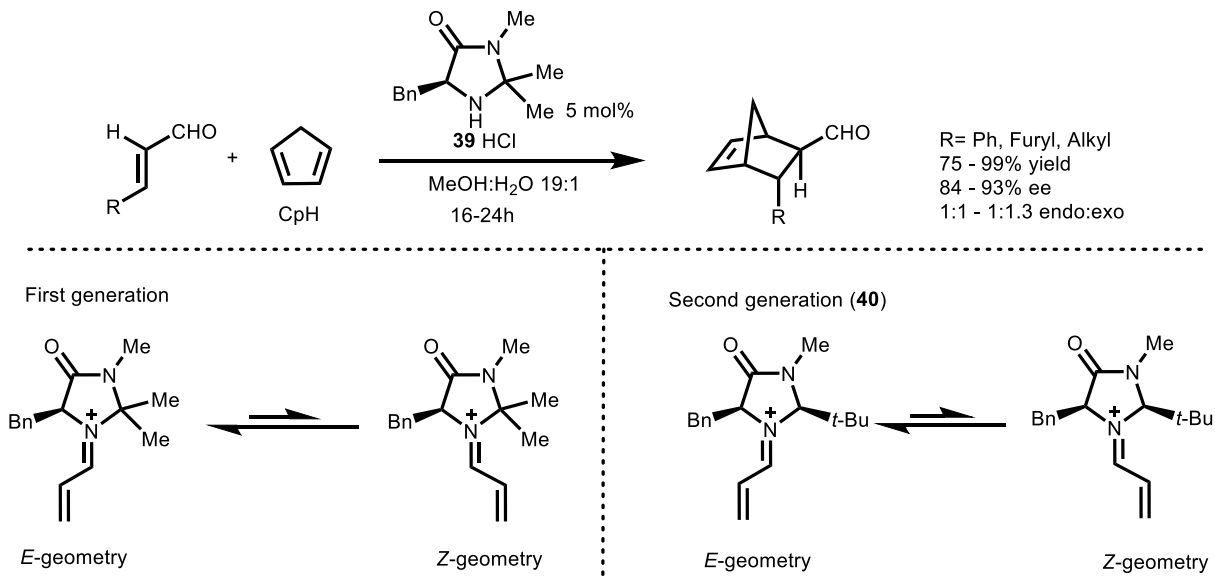

Scheme 1.25 MacMillan's imidazolidinone catalysts

Since the MacMillan imidazolidinone catalysts (**111** and **112**) were developed, the field of iminium ion catalysis has exploded. The Diels-Alder reaction itself is among the most common reactions for catalyst development and to date a huge catalogue of catalysts have been examined. Select catalysts are displayed in Figure 1.12 and include everything from natural proline (**113**) to proline derivatives like **114** and other pyrrolidine derivatives such as **115** and Jorgensen's diaryl prolinols **116** and **117**.[81]

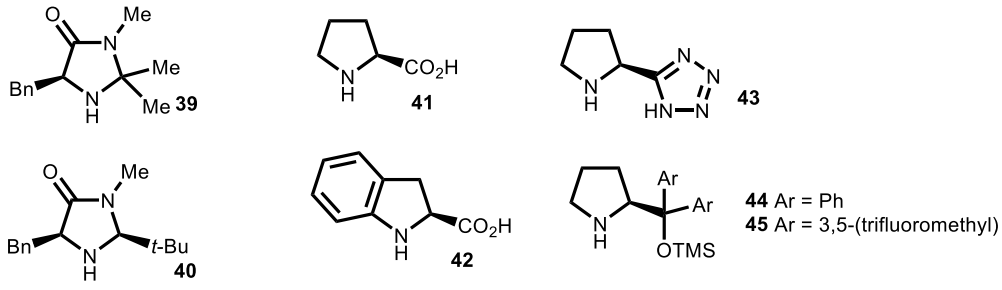

Figure 1.12 Types of secondary amine catalysts

1.4.4 Hydrazides in iminium ion catalysis

In 2003, Tomkinson and co-workers proposed that the α-effect can be utilized in the iminium ion catalyzed Diels-Alder reaction.[82] The α-effect is the increased nucleophilicity of a heteroatom, arising from interactions with a neighboring heteroatom. The interactions originate from orbital overlap between the lone pair of the nucleophilic heteroatom with the lone pair of its neighbor, raising the energy of the HOMO orbitals of both lone pairs.[65] The effect was established in Jecks *et al* in 1962,[83] however, there have been studies questioning and partially disproving the α-effect.[84] Mayr's group has performed experiments where they studied reactivity of benzhydrylium ions with amines, hydrazines and hydroxylamines.[85] In the study, no enhanced nucleophilicity, α-effect, was observed for either hydrazines or hydroxylamines relative alkylamines.

In Tomkinson's initial study, they screened simple hydroxylamine, hydrazine and hydrazide derivatives and found enhanced acceleration for the Diels-Alder reaction, postulating that the higher rates are related to the α-effect. Later studies explored more complex hydrazides, which turned out to have greater reactivity (Figure 1.13).[86,] They didn't develop an enantioselective version but they did prove the hydrazides are more active than simple hydrazines and secondary amines. In contrast to conventional secondary amine catalysis where the 5-membered pyrrolidine is more reactive than the 6-membered piperidine, the larger ring 6-membered hydrazide (**51**) was found to be more active than the 5-membered hydrazide (**50**). The carbonyl was important not only for LUMO lowering properties, but also participated directly in iminium ion formation by acting as a proton shuttle and/or lowering the basicity of the catalyst. They later proposed that proton affinity rather than enhanced nucleophilicity is the key parameter for the higher activity, where less basic amines, more acidic iminium ions, displayed higher reactivity.[87]

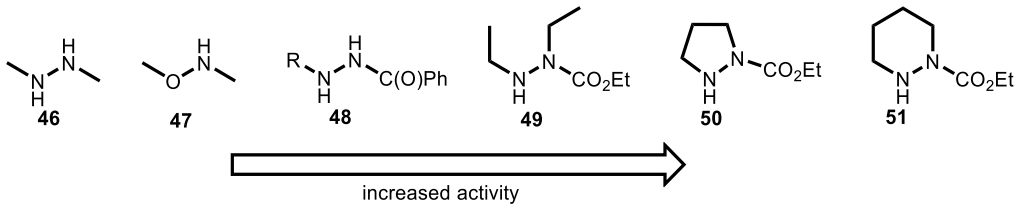

Figure 1.13 Activity of secondary amines with an α-heteroatom

Ogilvie *et al.* developed a related asymmetric hydrazide catalyst for the Diels-Alder reaction.[88] Their bicyclic catalyst **52** contained the electron withdrawing carbonyl within the ring and possessed chirality derived from camphor. Moderate *exo*-selectivity was achieved with high to excellent enantioselectivity for a series of cinnamaldehydes reacting with cyclopentadiene (CpH). Other acyclic dienes gave slightly lower enantioselectivity and yield (Scheme 1.26). They conducted a NMR study of the iminium ion formation between cinnamaldehyde with hydrazine **52** and compared it with imidazolidinone **39** and discovered that iminium ion formation was more rapid for hydrazine **52**; full conversion was observed in 1 h while the imidazolidinone barely reached 10% iminium ion formation. More extensive mechanistic studies suggested that the cycloaddition is the rate-determining step after concluding that both iminium ion formation and hydrolysis after the cycloaddition to release product and catalyst were rapid.[89]

Similar catalysts have been developed by Lee's group where the first generation included a sulfonyl in the 6-membered ring (**53**) rather than a carbonyl and the second generation catalyst utilized a 5-membered ring sulfonyl hydrazine (**54**) with a free amine outside of the ring which gave slightly better enantioselectivity.[90, 91] Finally, Suzuki's group developed a C2-symmetric hydrazide (**55**) for the Diels-Alder reaction with moderate to good results.[92] These hydrazine catalysts clearly demonstrated the potential of utilizing hydrazines for iminium ion catalysis.

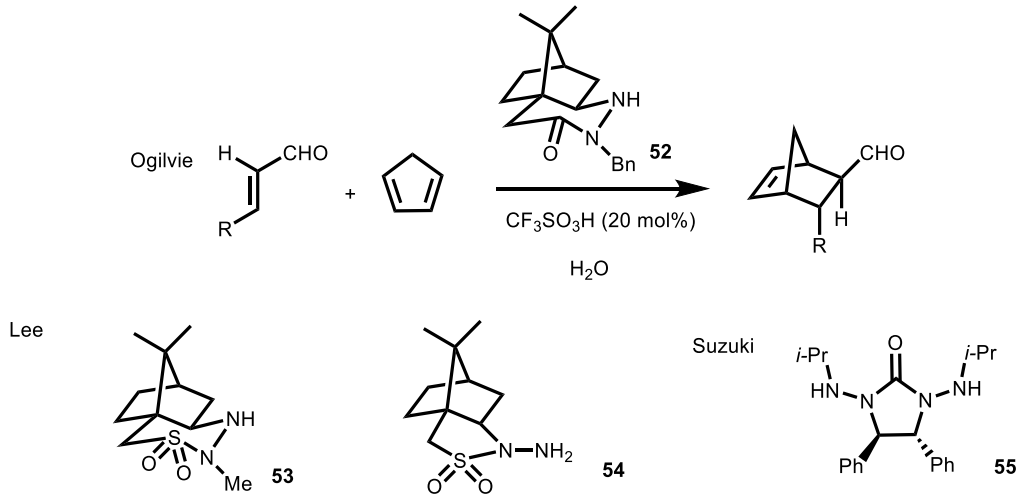

Scheme 1.26 Ogilvie's camphor hydrazide and other chiral hydrazine motifs

1.4.5 Diels-Alder cycloadditions with α-substituted acroleins

While there is generally a wide scope in iminium ion catalyzed reactions, only a select few secondary amine catalysts are able to form iminium ions with α-substituted enals.[93] The problem with forming the iminium ion of an α-substituted enals with a secondary amine catalyst is the significant A-1,3 strain in the formed iminium ion, which raises the energy of the iminium ion (Figure 1.14). The higher strain causes a higher energy barrier to form the iminium ion, pushing the equilibrium towards starting materials. This leads to lower concentrations of reactive iminium ion, effectively limiting the reaction rate. The A-1,3 strain in these systems is so great that the few examples that do exist are generally limited to α-methyl substitution, with the notable exceptions by Hayashi (Scheme 1.25) and Champagne.[94]

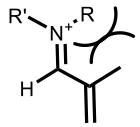

Significant A-1,3 strain

Figure 1.14 A-1,3 strain in an iminium ion of a secondary amine catalyst

In late 2016, Hayashi showed that the Jorgensen/Hayashi prolinol catalyst **56** could catalyze the Diels-Alder reaction of some α-substituted acroleins with CpH, obtaining moderate to good yields in 72-96 h and achieving good to high *exo* and enantioselectivity.[95] The catalyst also performed well with a select scope of acyclic dienes (isoprene and 2,3-dimethylbutadiene) with α-acyloxy enals to provide products with good yields and selectivities (Scheme 1.27). They have previously published extensive studies of this and similar catalysts showing that the trifluoromethyl groups on the aromatic rings have significant effects on the catalytic properties by withdrawing electron density through the system, which strongly influences the iminium ion and lowers the energy of the LUMO.[96]

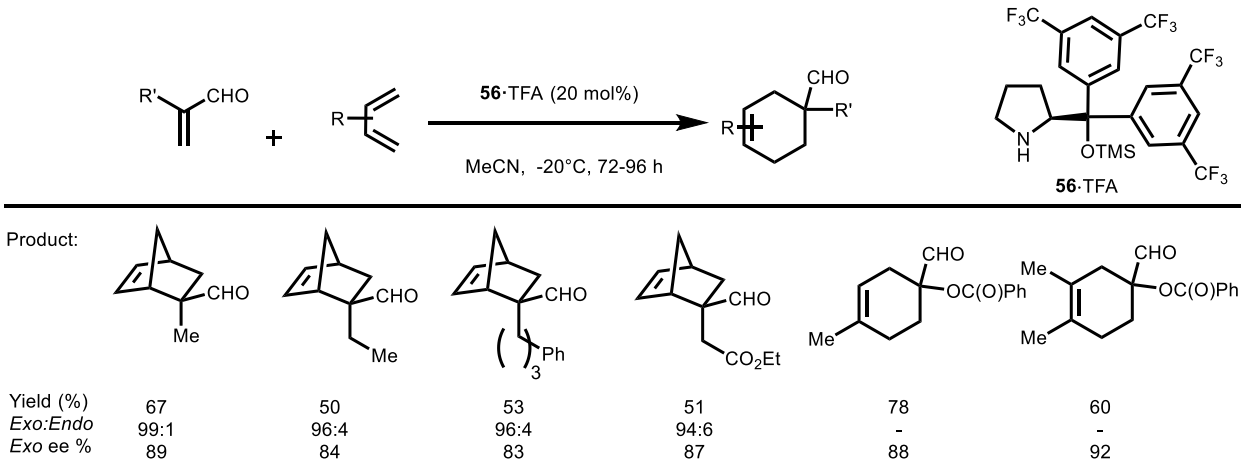

Scheme 1.27 Jorgensen/Hayashi prolinol catalysis of α-substituted enals

1.4.6 Diels-Alder reaction catalysis with primary amines

To circumvent the A-1,3 strain incurred with secondary amines, primary amines have been explored. These experience less strain in the iminium ion due to one R group from the catalyst being replaced with a proton (Figure 1.15). The challenge in this approach is that they must remain protonated to allow for LUMO-lowering catalysis.

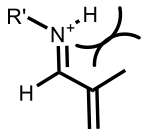

Less A-1,3 strain

Figure 1.15 A-1,3 strain with primary amine catalyst

Several groups have reported examples of primary amine catalysis for the Diels-Alder reaction. Ishihara's group developed a diamine and eventually the triamine **57** to perform the Diels-Alder reaction with α-substituted acroleins (Scheme 1.28).[97] The pyrrolidine was added to the tri-amine generation to increase the steric bulk, together with counterions, favouring Z-geometry for iminium ion **58** while the benzyl group blocks one face of the diene approach. The triamine gave moderate enantioselectivity for α-methylacrolein but high to excellent enantioselectivity for α-

arylacyloxy substrates. One could argue based on their presented mechanism, that it is not a proper iminium ion but a hydrogen bond activated Schiff base.

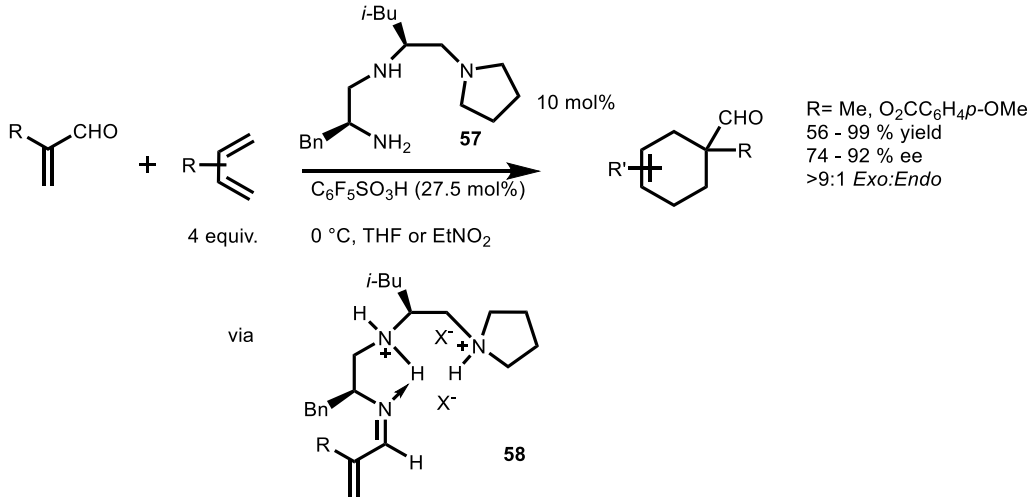

Scheme 1.28 Triamine catalyzed Diels-Alder cycloadditions including iminium/imine

Ishihara's group also developed a binaphthyl based primary amine catalyst **59** for the Diels-Alder reaction of α-substituted enals (Scheme 1.29).[98,99] Maruoka's group improved upon this catalyst by adding an aryl group (**60**) to improve the steric shielding of the dienophile, which was essential to get enantioselectivity over 62% for α-substituents other than α-acyloxyacroleins, which were used in the Ishihara study.[100] Interestingly, Maruoka observed higher enantioselectivity for acyclic butadienes and cyclohexa-1,3-diene rather than CpH, which is opposite to most methods in literature.

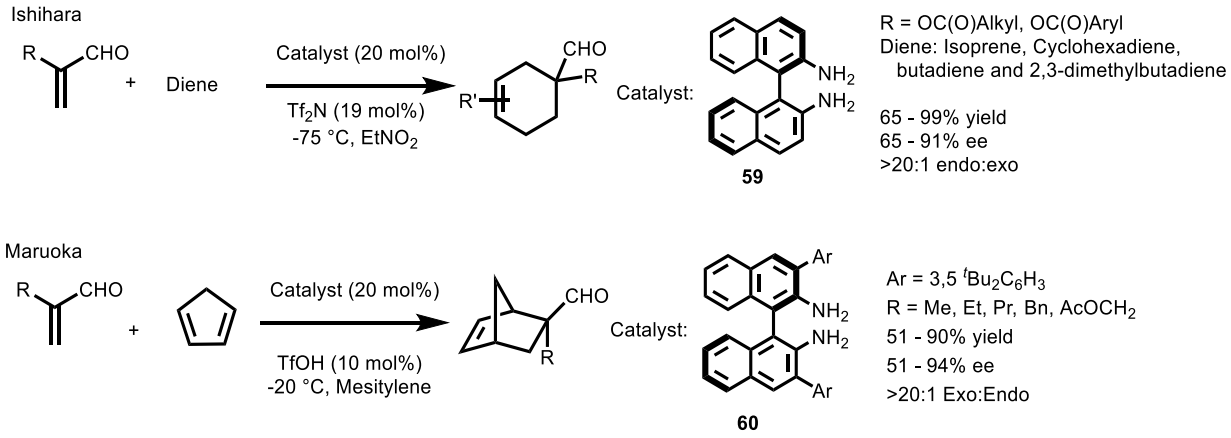

Scheme 1.29 Aromatic amine derive catalyst

The groups of Cheng[101] and Melchiorre[102] have developed other amino acid or cinchona base primary amine catalysts for cyclopropanation and Friedel-Crafts addition. A vast amount of work has been performed[103] but there is still need for improvement of both enantioselectivity and reactivity to extend the scope.

1.5 Iminium ion catalyzed Cope rearrangement

Our group became interested in catalyzing the Cope rearrangement, a classic reaction in organic synthesis with a notoriously high activation barrier.[104] To achieve good conversion of this [3,3]-sigmatropic rearrangement, elevated temperatures and long reaction times are usually required. Overman and coworkers have previously used Pd(II) to accelerate the reaction by coordinating to the double bonds (Scheme 1.30).[105] The reaction is suggested to proceed stepwise though a chair like transition state via a tertiary cation intermediate which then opens up to the product. Gagne developed the first enantioselective catalyst for the Cope rearrangement of vinyl cyclopropane using a gold catalyst with chiral ligand.[106] The gold catalyst is believed to follow the same mechanism as the palladium example. At that time, there were no examples of organocatalytic cope rearrangements.

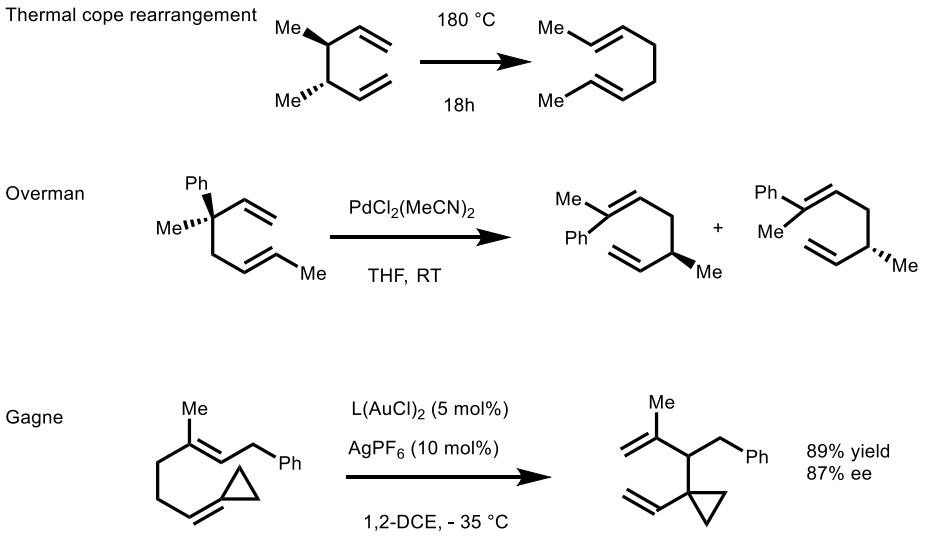

Scheme 1.30 Thermal and metal catalyzed Cope Rearrangement.

Our group envisioned that by installing an electron withdrawing group at the 2-position of a 1,5-diene, the transition state energy should be lowered via a LUMO lowering effect. DFT calculations (by J. L. Gleason) supported the lowering of the transition state energy, dropping from 36 kcal/mol (**61**) to 31 kcal/mol by just installing an aldehyde (**62**). DFT calculations for an iminium ion (**63**) of the aldehyde **62**, showed the calculated transition state energy was lowered to 12 kcal/mol (Figure 1.16). This substantially lower transition state energy indicated the possibility of using iminium ion catalysis for the Cope rearrangement in this system. If successful, this would be the first organocatalytic cope rearrangement.

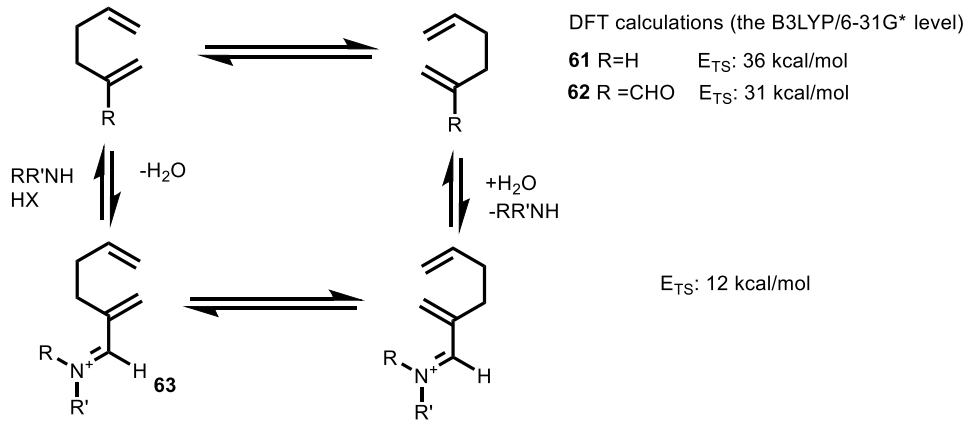

Figure 1.16 Proposed iminium ion catalyzed Cope rearrangement

1.5.1 Development of catalyst

A former graduate student in our lab, Dr. Dainis Kaldre, who performed all the synthetic work in the Cope project, started with synthesizing model substrate **62** (Figure 1.17). Screening standard amine catalysts such as MacMillan's 2nd generation imidazolidinone (**40**)[80] and proline gave no conversion at r.t., even when 50 mol% of catalyst and 50 mol% HCl co-catalyst were employed. Simple primary amines like methoxyamine (**66**), aniline (**67**) and benzyl amine (**68**) also gave no conversion under these conditions. The inability of these amines to catalyze the reaction is not too surprising considering that the 2-carboxaldehyde-1,5-diene is an α-substituted enal with high A-1,3 strain. Based on work previously reported by Tomkinson and Ogilvie that

hydrazides have higher propensity to form iminiums, hydrazides **49**, **50** and **51** were prepared and screened.[82] With acyclic hydrazide **49**, 13% conversion was observed after 24 h. The 5-membered hydrazide **50** gave small amount of product (6% conversion, 24 h) while a jump in activity was observed for the 6-membered hydrazide **51** (28% conversion, 24 h), the same trend that was observed for Tomkinson *et al.* in the Diels-Alder reaction. Intrigued by whether the correlation of ring size versus reactivity would continue, the 7-membered ring catalyst **69** and the 8-membered ring catalyst **70** were synthesized and tested in the reaction of 1,5-diene **64**. High conversions were achieved using both catalyst **69** (83%) and catalyst **70** (89%) after 24 h.

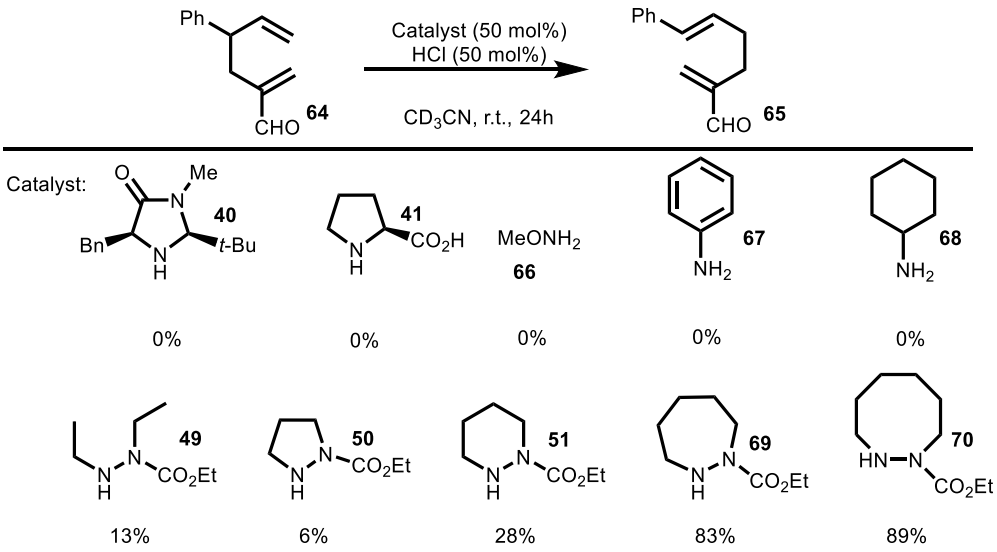

Figure 1.17 Catalyst screening for the Cope rearrangement

Even though the 8-membered ring **70** had a slight edge on diazepane **69** in conversion, they chose to proceed with ethyl diazepane carboxylate **69** as the preferred catalyst due to the more accessible chemistry to synthesize 7-membered rings. The 8-membered ring **70** required a slow and low yielding olefin metathesis to form the ring while the **69** can readily be synthesized from *t*-butyl ethyl hydrazine dicarboxylate and 1,5-dibromopentane with NaH followed by deprotection. The catalyst loading could be lowered after an acid optimization found that a stronger acid like TfOH was far superior. A series of 2-carboxaldehyde-1,5-hexadienes were synthesized and a selection of the scope is shown in Figure 1.18. Notably, products **74** and **75** were formed from very sterically encumbered aldehydes, bearing all-carbon quaternary centers on the α-position of

the enal in the starting material, which is highly unusual for on catalysis. This shows potential for a scope which is usually not compatible with iminium ion catalysis.

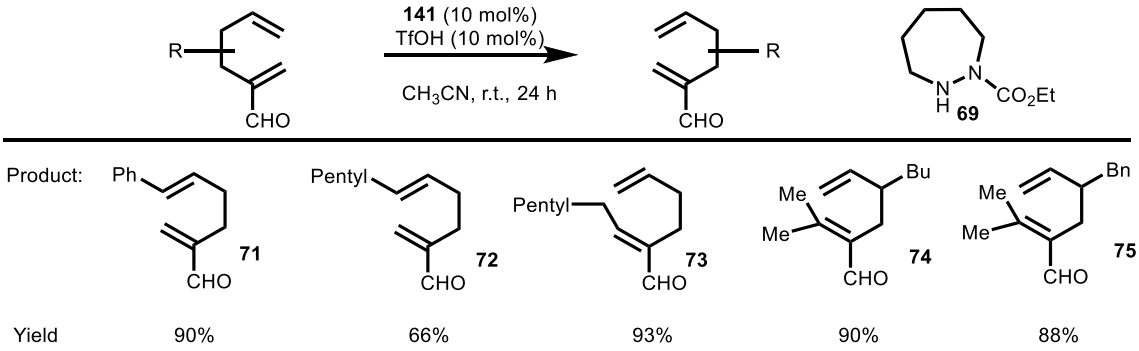

Figure 1.18 Organocatalytic Cope rearrangement

This was the first example of an organocatalytic Cope rearrangement and ethyl diazepane carboxylate **69** has been proven to have enhanced reactivity in iminium ion formation with sterically hindered substrates like α-branched α,β-unsaturated aldehydes.[107] Products **74** and **75** are particularly interesting because they contain a stereogenic centre, but each was produced as a racemic mixture using achiral diazepane carboxylate. We envisioned that we could develop an enantioselective catalyst by adding substituents onto the 7-membered ring. Catalyst **77** and **78** with ethyl or phenyl substituents adjacent to the nucleophilic nitrogen afforded low enantioselectivity (9% ee for **77** and 10% ee for **78**, Figure 1.19). Remarkably, introducing the stereogenic centre adjacent to the carbamate achieved modest enantioselectivity, with catalyst **80**, bearing a phenyl substituent on the diazepane ring adjacent to the carbamate, provided 47% ee for the model substrate.

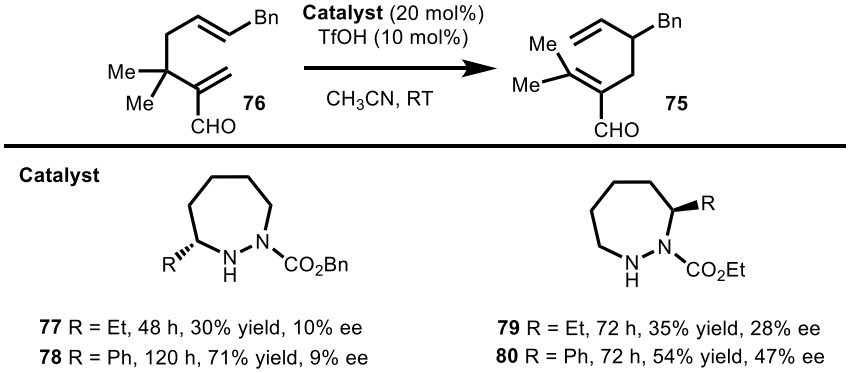

Figure 1.19 Screening of asymmetric catalysis

1.6 Conclusion

There has been significant effort towards improving techniques for amide bond formation, both through stoichiometric coupling reagents and catalysts. The best option remains the development of a catalytic method, ideally with an organocatalyst, that would be able to perform the direct amide bond formation of unreactive and sterically hindered carboxylic acids and amines without epimerization. Boronic acids have achieved great success but there is room for improvement and in chapter 2, we describe our efforts to use ureas as amide bond formation catalysts.

Given our interest in the application of organocatalysis to meet unmet synthetic challenges, this thesis also details contributions we have made to the use of organocatalysis in facilitating the Diels-Alder reaction. The ethyl diazepane carboxylate is an unprecedented scaffold in catalysis and has the potential for breaking new grounds in iminium ion catalysis of α-substituted enals. In chapter 3 we describe its utility towards the achiral Diels-Alder reaction. The preliminary results for the Cope rearrangement are very promising considering the new stereocenters on the product is remote from the catalyst. The possibility of incorporating different stereogenic centers on the scaffold (chapter 4) could yield an enantioselective catalyst with enhanced reactivity relative to other secondary amine catalysts.

1.7 References

[1] Horvath, I. T.; Anastas, P. T. *Chem. Rev.,* **2007**, 107, 2167.

[2] Anastas, P. T.; Warner, J. C. *Green Chemistry: Theory and Practice*, Oxford University Press: New York, **1998**.

[3] Horvath, I. T.; Anastas, P. T. *Chem. Rev.* **2007**, 107, 2169.

[4] Walsh, P. J.; Li, H.; Anaya de Parrodi, C. *Chem. Rev.* **2007**, 107, 2503.

[5] Dalko, P. I.; Moisan, L. *Angew. Chem. Int. Ed.* **2004**, 43, 5138.

[6] Horvath, I. T. Acc. Chem. Res. **2002**, 35, 685.

[7] Doyle, A. G.; Jacobsen, E. N.; *Chem. Rev.* **2007,** 107, 5713.

[8] Fischer, E.; Speier, A.; *Chemische Berichte* **1895**, 28, 3252.

[9] Min. C.; Seidel, D.; *Chem. Soc. Rev.* **2017**, 46, 5889.

[10] Akiyama, T.; Itoh, J.; Yokota, K.; Fuchibe, K.; *Angew. Chem., Int. Ed.,* **2004**, 43, 1566.

[11] Uraguchi D.; Terada, M.; *J. Am. Chem. Soc.,* **2004**, 126, 5356.

[12] Shimode, S.; Yamamoto, H.; *J. Am. Chem. Soc.* **2017**, 139, 6855.

[13] Parmar, D.; Sugiono, E.; Raja, S.; Reuping, M. *Chem. Rev*. **2014**, 114, 9047.

[14] Connon, S. J. *Chem. Commun*. **2008**, 2499.

[15] Parmar, D. Sugiono, E.; Raja, S.; Rueping, M. *Chem*. Rev. **2014**, 114, 9047.

[16] Connon, S. J. *Angew. Chem. Int. Ed.* **2006**, 45, 3909.

[17] Hine, J.; Linden, S.-M.; Kanagasabapathy, V. M. *J. Am. Chem. Soc*. **1985**, 107, 1082.

[18] Curran, D. P.; Kuo, L. H.; *J. Org. Chem*. **1994**, 59, 3259.

[19] Curran, D. P.; Kuo, L. H.; *Tetrahedron Lett.* **1995**, 36, 6647.

[20] Sigman, M. S.; Jacobsen, E. N.; *J. Am. Chem. Soc.* **1998,** *120,* 4901.

[21] Okino, T.; Y. Hoashi, Y.; Y. Takemoto, Y.; *J. Am. Chem. Soc*. **2003**, 125, 12672.

[22] Okino, T.; Nakamura, S.; Furukawa, T.; Takemoto, Y.; *Org. Lett.* **2004**, 6, 625.

[23] Zhang, Z.; Schreiner, P. R.; *Chem. Soc. Rev.* **2009**, 38, 1187.

[24] Okino, T.; Hoashi, Y.; Furukawa, T.; Xu, X. N.; Takemoto, Y.; *J. Am. Chem. Soc.* **2005**, 127, 119.

[25] Hamza, A.; Schubert, G.; Soo´s, T.; Papai, I.; *J. Am. Chem. Soc.,* **2006**, 128, 13151.

[26] Berkessel, A.; Cleemann, F.; Mukherjee, S.; Muller, T. N.; Lex, L.; *Angew.Chem.* **2005**, 117, 817.

Berkessel, A.; Cleemann, F., Mukherjee, S. Muller, T. N., Lex, L.; *Angew.Chem. Int. Ed.* **2005**, 44, 807.

[27] Berkessel, A.; Mukherjee, S.; Cleemann, F.; Muller, T. N.; Lex, L.; *Chem. Commun.* **2005**, 1898.

Berkessel, A.; Mukherjee, S.; Cleemann, F.; Muller, T. N.; Roland, K.; Brandenburg, M.,; Neudorfl, J-M.; Lex, L.; *Org. Biomol. Chem.* **2006**, 4, 4319.

[28] Uyeda, C.; Jacobsen, E. N.; *J; Am. Chem. Soc.* **2008**, 130, 9228.

[29] Uyeda, C.; Jacobsen, E. N.; *J. Am. Chem. Soc.* **2011**, 133, 5062.

[30] Thadani, A. N.; Stankovic, A. R.; Rawal, V. H.; *Proc. Natl. Acad. Sci. USA* **2004**, 101, 5846.

[31] McDougal, N. T.; Schaus, S. E.; *J. Am. Chem. Soc.* **2003**, 125, 12094.

[32] Shi, Y-L.; Shi, M.; *Adv. Synth. Catal.* **2007**, 349, 2129.

[33] Qin, Y.; Lihui Zhu, L.; Sanzhong Luo, S.; *Chem. Rev.* **2017**, 117, 9433.

[34] Dell'Amico, L.; Vega-Penaloza, A.; Cuadros, S.; Melchiorre, P. E.; *Angew. Chem., Int. Ed.* **2016**, 55, 3313.

[35] Yang, N. C.; Rivas*,* C. *J. Am. Chem. Soc.* **1961**, 83, 2213.

[36] Merino*, P.;* Marques-Lopez*, E.;* Tejero*, T.;* Herrera*,* R. P. *Synthesis* **2010**, 1.

[37] Brak, K.; Jacobsen, E. N. *Angew. Chem. Int. Ed.* **2013**, 52, 534.

[38] Mittal, N.; Sun, D. X.; Seidel, D. *Org. Lett.* **2012**, 14, 3084.

[39] De, K. C.; Klauber, E. G.; Seidel, D. *J. Am. Chem. Soc*. **2009**, 131, 17060.

[40] Banik, S. M.; Levina, A.; Hyde, A. M.; Jacobsen, E. N. *Science* **2017**, 761.

[41] Storer, I. R. Aciro, C. Jones, L. H. *Chem. Soc. Rev*., **2011**, 40, 2330.

[42] Ni, X.; Li, X.; Wang, Z.; Cheng, J-P. *Org. Lett.* **2014**, 16, 1786.

[43] Schreiner, P. R. *Chem. Soc. Rev.,* **2003**, 32, 289.

[44] Valeur, E.; Bradley, M.; *Chem. Soc. Rev.* **2009**, 38, 608.

[45] Pattabiraman, V. R., Bode, J. W.; *Nature* **2011**, 480, 471.

[46] Carey, J. S.; Laffan, D.; Thomson, C.; Williams, M. T.; *Org. Biomol. Chem.* **2006**, 4, 2337.
Dugger, R. W.; Ragan, J. A.; Ripin, D. H. B.; *Org. Process Res. Dev.* **2005**, 9, 253.

[47] Beckwith, A. L. J. *The Chemistry of Amides*; Zabicky, J., Ed.; Interscience: London, **1970**; pp 105–109.

[48] Montalbetti, C. A. G. N.; Falque, V.; *Tetrahedron,* **2005**, 61, 10827.

[49] Carey, J. S.; Laffan, D.; Thomson, C.; Williams, M. T.; *Org. Biomol. Chem.* **2006**, 4, 2337.

[50] Kemp, D. S. *In The Peptides;* (Ed: Gross, E., Meienhofer, J).; Academic Press: New York, **1979**; pp 317-378.

[51] Koenig W. Geiger, R. *Chem. Ber.,* **1970**, 103, 788.

Koenig W. Geiger, R. *Chem. Ber.,* **1970**, 103, 2024.

[52] Carpino, L. A. *J. Am. Chem. Soc.* **1993**, 115*,* 4397,

[53] Han, S-Y.; Kim, Y-A.; *Tetrahedron* **2004**, 60, 2447.

[54] Constable, D. J. C.; Dunn, P. J.; Hayler, J. D.; Humphrey, G. R.; Leazer, J. L.; Linderman, R. J.; Lorenz, K.; Manley, J.; Pearlman, B. A.;Wells, A.; Zaks, A.; Zhang, T. Y.; *Green Chem.* **2007**, 9, 411.

[55] Allen, C. L. Chatwal, R.; Williams, J. M. J.; *Chem. Comm.* **2012**, 48, 666.

[56] Allen C. L.; Williams J. M. J.; *Chem. Soc. Rev*., **2011**, 40, 3405.

[57] Ishihara, K.; Ohara, S.; Yamamoto, H.; *J. Org. Chem.* **1996,** *61,* 4196.

[58] Latta, R.; Springsteen, G.; Wang, B.; *Synthesis* **2001**, 1611.

Arnold, K.; Davies, B.; Giles, R. L.; Grojean, C.; Smith, G. E.; Whiting, A.; *Adv. Synth. Catal.* **2006**, 348, 813.

[59] Al-Zoubi, R. M.; Hall, D. G.; *Angew. Chem. Int. Ed.* **2008**, 47, 2876.

[60] Gernigon, N.; Al-Zoubi, R. M.; Hall, D. G.; *J. Org. Chem.* **2012**, 77, 8386.

[61] Marcelli, T.; *Angew. Chem. Int. Ed.* **2010**, 49, 6840.

[62] Nicolaou, K. C.; Snyder, S. C.; Montagnon, T.; Vassilikogiannakis, G. *Angew. Chem. Int. Ed.* **2002**, 41, 1668.

[63] von Euler, H.; Josephson, K. O.; *Ber. Dtsch. Chem. Ges. B* **1920** , 53 , 822.

[64] Diels, O.; Alder, K.; *Synthesen in der hydroaromatischen Reihe, I.* Justus Liebigs Annalen der Chemie*.* **1928***:* pp 98–122.

[65] Fleming, I. *Molecular Orbitals and Organic Chemical Reactions*: *Reference Edition*. John Wiley & Sons, Chichester, **2010**. pp. 1 - 528.

[66] Fringuelli, F., Piermatti, 0., Pizzo, F., and Vaccaro, L., *Eur. J. Org. Chem.,* **2001**, 439.

[67] Gothelf, K. V.; Jorgensen, K. A. *Chem. Rev.* **1998**, 98, 863.

[68] Palomo, C.; Oiarbide, M.; García, J. M. *Chem. Soc. Rev.,* **2004**, 33, 65.

[69] Csµkÿ, A.; de la Herrµn, G.; Murcia, M. C. *Chem. Soc. Rev.* **2010**, 39, 4080.

[70] Du, H.; Ding, K.; *Handbook of Cyclization Reactions* (Ed.: S. Ma), Wiley-VCH, Weinheim, **2010**, pp. 1 – 57.

[71] Corey, E. J.; Loh, T-P.; *J. Am. Chem. SOC.* **1991,** 113**,** 8966.

[72] Corey, E. J.; *Angew. Chem. Int. Ed*. **2002**, 41, 1650.

[73] Evans*, D. A.;* Miller*, S. J.;* Lectka*, T.*; von Matt, P.; *J. Am*. *Chem*. *Soc*. **1999**, 121, 7559.

[74] Kobayashi. S.; Manabe, K.; *Acc. Chem. Res*. **2002**, 35, 209.

[75] Knoevenagel, E.; *Chem. Ber.* **1894**, *27*, 2345.

Knoevenagel, E.; *Chem. Ber.* **1898**, *31*, 2596.

[76] Erkkila, A.; Majander, I.; Pihko, P. M.; *Chem. Rev.* **2007,** 107, 5416.

[77] Bertelsen, S.; Jorgensen, K. A.; *Chem.Soc.Rev.,* **2009**, 38, 2178.

[78] Ahrendt, K. A.; Borths, C. J.; MacMillan, D. W. C. *J. Am. Chem. Soc.* **2000**, 122, 4243.

[79] Nicewicz, D. A.; MacMillan, D. W. C.; *Science* **2008**, 322, 77.

[80] Austin, J. F.; MacMillan, D. W.; *J. Am. Chem. Soc.* **2002**, 124, 1172.

[81] Brazier, J. B.; Tomkinson, N. C. *Topics in current chemistry,* Springer Link, **2010**, 291, 281.

[82] Cavill, J. L.; Peters, J. U.; Tomkinson, N. C. O.; *Chem. Commun.* **2003**, 728.

[83] Jencks, W. P.; Carriuolo, J.; *J. Am. Chem. Soc.* **1960**, 82, 675.

[84] Villano, S. M.; Eyet, N.; Lineberger, W. C.; Bierbaum, V. M.; *J. Am. Chem. Soc.* **2009**, 131, 8227−8233.

[85] Nigst, T. A.; Antipova, A.; Mayr, H.; *J. Org. Chem.* **2012**, 77, 8142.

[86] Cavill, J. L.; Elliott, R. L.; Evans, G.; Jones, I. L.; Platts, J. A.; Ruda, A. M.; Tomkinson, N. C. O.; *Tetrahedron* **2006**, *62*, 410.

[87] Brazier, J. B.; Cavill, J. L.; Elliott, R. L.; Evans, G.; Gibbs, T. J. K.; Jones, I. L.; Platts, J. A.; Tomkinson, N. C. O.; *Tetrahedron* **2009**, *65*, 9961.

[88] Lemay, M.; Ogilvie, W. W.; *Org. Lett.* **2005**, *7*, 4141.

[89] Lemay, M.; Ogilvie, W. W.; *J. Org. Chem.* **2006**, 71, 4663.

Lemay, M. Aumand, L.; Ogilvie, W. W.; *Adv. Synth. Catal.* **2007**, 349, 441.

[90] He, H.; Pei, B. J.; Chou, H. H.; Tian, T.; Chan, W. H.; Lee, A. W.; *Org. let.* **2008**, 10, 2421.

[91] Li, Q. H.; Wong, W. Y.; Chan, W. H.; Lee, A. W. M.; *Adv. Synth. Catal.* **2010**, 352, 2142.

[92] Suzuki, I.; Ando, M.; Shimabara, R.; Hirata, A.; Takeda, K.; *Organic & biomolecular chemistry* **2011**, *9*, 3033.

[93] a) Bondzic, B. P.; Urushima, T.; Ishikawa, H.; Hayashi, Y.; *Org. Lett.* **2010**, 12, 5434.

b) Quintard, A.; Lefranc, A.; Alexakis, A.; *Org. Lett.* **2011**, 13, 1540.

c) Kemppainen, E.K.; Sahoo, G.; Valkonen, A.; Pihko, P. M.; *Org. Lett.* **2012**, 14, 1086.

d) Wei, Y.; Yoshikai, N.; *J. Am. Chem. Soc.* **2013**, 135, 3756.

[94] Terrasson, V.; van der Lee, A.; Marcia de Figueiredo, R.; Campagne, J. M.; *Chem. Eur. J.* **2010**, 16, 7875.

[95] Hayashi, Y.; Bondzic, B.P.; Yamazaki, T.; Gupta, Y.; Ogasawara, S.; Taniguchi, T.; Monde, K.; *Chem. Eur. J.*, **2016**, 22, 15874.

[96] Gotoh, H.; Uchimaru, T.; Hayashi, Y.; *Chem. Eur. J.*, **2015**, 12337.

[97] Ishihara, K.; Nakano, K.; *J. Am. Chem. Soc.* **2005**, 127, 10504.

[98] Sakakura, A.; Suzuki, K.; Ishiharaa, K.; *Adv. Synth. Catal.* **2006**, 348, 2457.

[99] Sakakura, A.; Suzuki, K.; Nakano, K.; Ishihara, K.; *Organic letters* **2006**, *8*, 2229.

[100] Kano, T.; Tanaka, Y.; Osawa, K.; Yurino, T.; Maruoka, K.; *Chem. Comm.*, **2009**, 1956.

[101] Fu, N.; Zhang, L.; Li, J.; Luo, S.; Cheng, J. P.; *Angewandte Chemie Int. Edit.* **2011**, *50*, 11451.

[102] Galzerano, P.; Pesciaioli, F.; Mazzanti, A.; Bartoli, G.; Melchiorre, P.; *Angew. Chem. Int. Edit.* **2009**, *48*, 7892.

[103] Brazier J. B., Tomkinson N. C. O. *Secondary and Primary Amine Catalysts for Iminium Catalysis. In: List B. (eds) Asymmetric Organocatalysis. Topics in Current Chemistry*, Springer, Berlin, Heidelberg, **2010**.

[104] Kaldre, D. **2015**, *Development of Hybrid Drugs for Cancer Treatment and Studies in Asymmetric Organocatalysis*, Doctorial dissertation, McGill University, Department of Chemistry, Montreal, Canada.

[105] Overman, L.E.; Jacobsen, E. J.; *J. Am. Chem. Soc.* **1982**, 104, 7225.

[106] Felix, R. J.; Weber, D.; Gutierrez, O.; Tantillo, D. J.; Gagné, M. R.; *Nature Chem.* **2012**, 4, 405.

[107] Kalde, D.; Gleason J. L.; *Angew. Chem. Int. Ed.* **2016**, 55, 11557.

Chapter 2

Study of urea hydrogen bonding and development of acyl transfer agent

2.1 Introduction

This chapter will describe our effort to investigate optimal parameters for hydrogen bonding catalysts systems after failed attempts to develop a new type of peptide coupling catalyst. We hypothesized that a system capable of both activation of the carboxylate, through hydrogen bonding, and activation of an amine via proximity to the carboxylate, might be competent in furnishing the desired bond. The screening for catalytic activity was unsuccessful and it was unknown what was limiting activity. In attempting to ascertain the issues associated with the system it became clear that there were too many variables to be optimized in a traditional systematic fashion. One significant unknown, was the optimal position of a nucleophile for reactivity, relative to the urea. After an extensive literature search, we discovered that this was a general gap in the understanding of the field. We therefore decided to investigate what this optimal position may be for systems of this general structure and not immediately focus on catalyst development. A catalogue of general scaffolds consisting of a urea and linker to a hydroxyl nucleophile were synthesized and screened for their activity towards additions to an electrophile. Closer proximity of the hydroxyl group to the urea (i.e. shorter linker) was optimal for higher reactivity and two acyl transfer agents were designed based on the results with one successfully employed as an additive in peptide coupling, affording activity equal to or slightly better than that of the current standard HOAt in combination with a coupling reagent.

2.1.1 Peptide synthesis catalyst design and mechanism

As noted above, we envisaged the design of a new peptide coupling catalyst comprised of two functional groups which were each envisioned to activate one component, i.e. amine (ammonium) and carboxylic acid (carboxylate). We envisaged a hydrogen bond donor (e.g. (thio)urea or guanidine) to coordinate and activate the carboxylate and an aldehyde to condense with the amine to form an imine which would be held in proximity to the carboxylate (Figure 2.1). As discussed in Chapter 1, the main problem in direct amide bond formation is the acid base equilibrium favouring the less reactive carboxylate and ammonium ions. Hydrogen bonding between the urea and the carboxylate could reduce the charge of the carboxylate, making it more electrophilic. Ureas are known to be strong receptors for carboxylates though a bidentate binding

motif.[108] In forming the imine, we were hoping to overcome the inherent lack of nucleophilicity of the imine by bringing the nitrogen into proximity with the carboxylate. However, by forming the imine the basicity of the nitrogen is reduced providing the neutral imine rather than the protonated, less nucleophilic, ammonium. This would produce a quasi-intramolecular reaction which could provide the necessary reactivity. We imagined connecting the aldehyde to the urea via a biaryl scaffold. The biaryl linker was selected as it would afford a rigid non-planar structure, possessing a twist of about 30 degrees. It was thought this would be advantageous for the system by potentially aligning the imine for nucleophilic attack on the carboxylate along the Bürgi-Dunitz trajectory. The carboxylate is assumed to bind to the urea through a two-point hydrogen bonding that have been seen in crystals by Berkessel's group.[109] The *meta* substitution of the aldehyde was thought to give free rotation around the bi-aryl bond while preventing the formation of a stable 5-membered ring hemiaminal between the urea and the aldehyde which would be possible with the *ortho* substituted aldehyde (Scheme 2.5 c). This would be the first bifunctional organocatalyst for amide bond formation of carboxylic acid and amine. Only one reported hydrogen bond organocatalyst is known for the amide bond formation (diphenylurea, Scheme 1.19). However, it was reported to operate under harsh conditions and provided only 2.5 turnovers.[55]

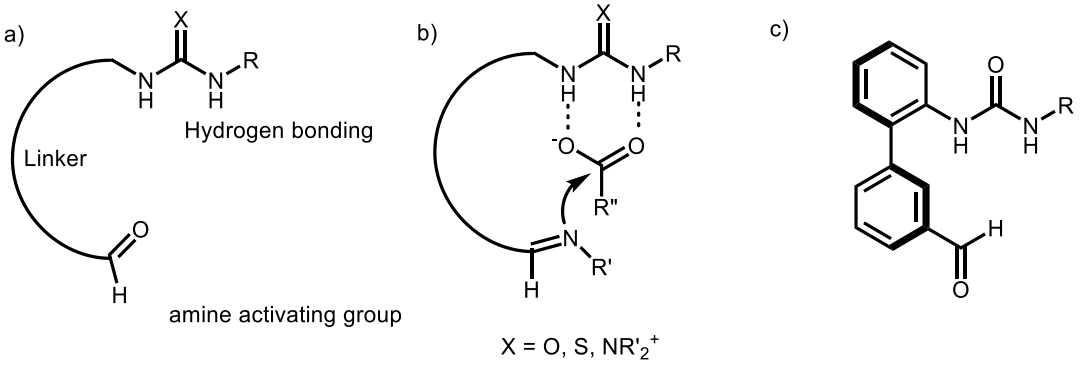

Figure 2.1 a) General design, b) summarized mechanism and c) proposed scaffold

The proposed mechanism initiates with amine condensation onto aldehyde **I** to give imine **II** (Scheme 2.1). The carboxylate coordinates to the urea dual hydrogen bond donor which both coordinates the carboxylate to hold it in place, and delocalize the charge of the carboxylate. The attack on the carboxylate would give a high energy tetrahedral intermediate **IV** which could be protonated by ammonium or water present in the reaction mixture, facilitating collapse to complex

V. Complex **V** undergoes a 1,2-addition to afford hemiaminal **VI** followed by protonation, releasing the amide and regenerating the catalyst.

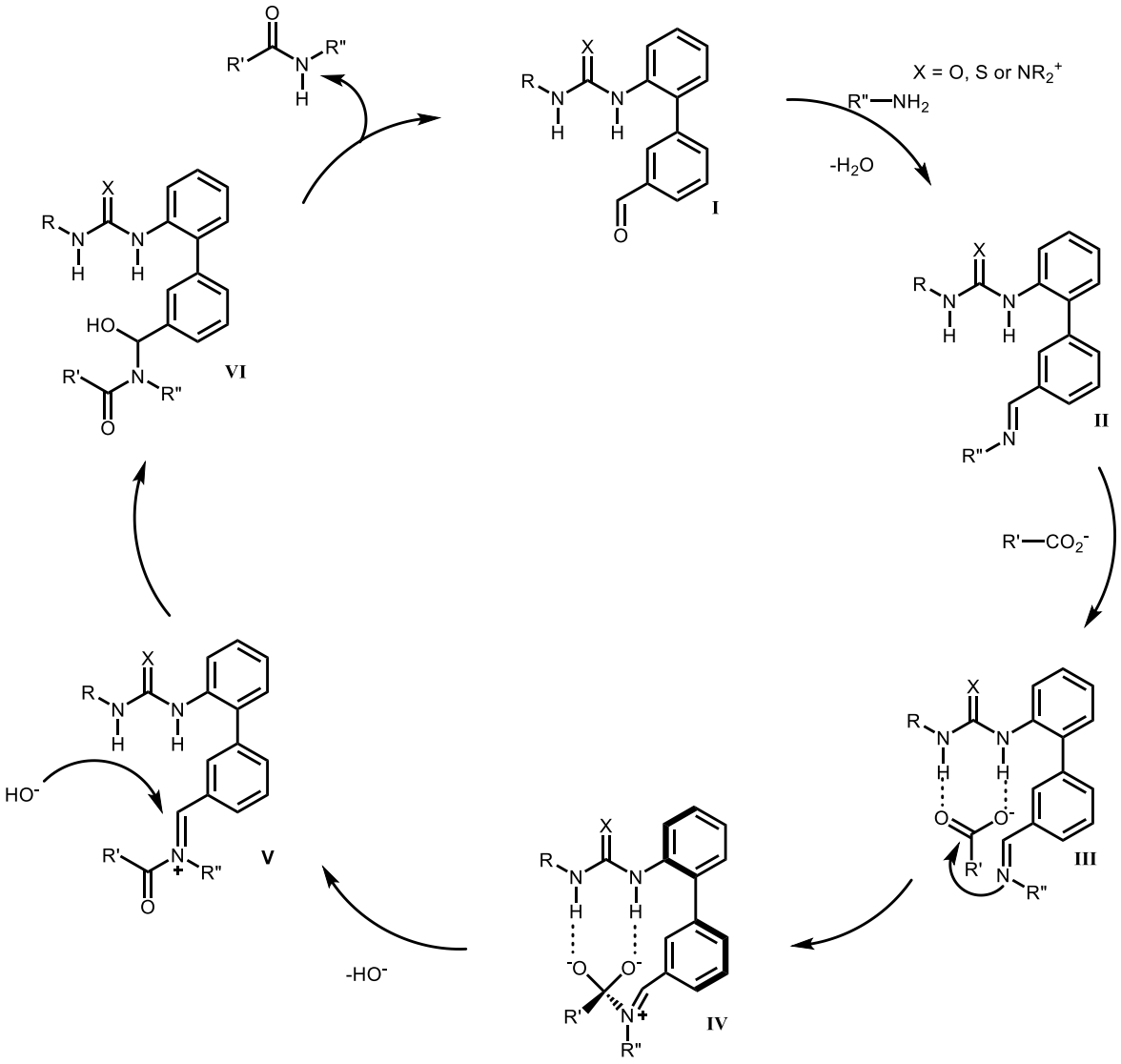

Scheme 2.1 Proposed mechanistic cycle

To test our hypothesis, we designed urea-aldehyde **84** to be our model system (Figure 2.2). Our retrosynthetic analysis suggested, the scaffold could readily be assembled through palladium cross coupling reaction and urea formation.

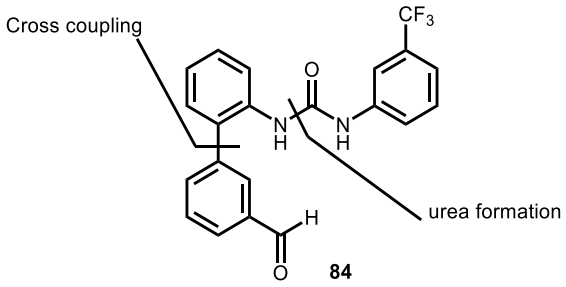

Figure 2.2 Proposed catalyst with retrosynthesis

2.1.2 Syntheses of 84

The synthesis of urea-aldehyde **84** started from 3-iodobenzoic acid (**85**) with borane reduction of the carboxylic acid and subsequent TBS protection affording TBS protected alcohol **86** (Scheme 2.2) in 94% yield. Boronic acid **87** was prepared in 86% yield by adding *n*-BuLi to a solution of halide **86** and triisopropyl borate. This provided higher yields than the conventional addition of the borate to the preformed aryl lithium. Urea **89** was synthesized in 50% yield through a Curtius rearrangement of 2-bromobenzoic acid followed by condensation of the intermediate isocyanate with 3-(trifluoromethyl)-aniline. Halide **89** and boronic acid **87** underwent palladium catalyzed Suzuki cross-coupling and subsequent TBAF deprotection of the TBS group afforded alcohol **90** (76%, two steps). Alcohol **90** was oxidized with IBX to desired aldehyde **84** in 97% yield.

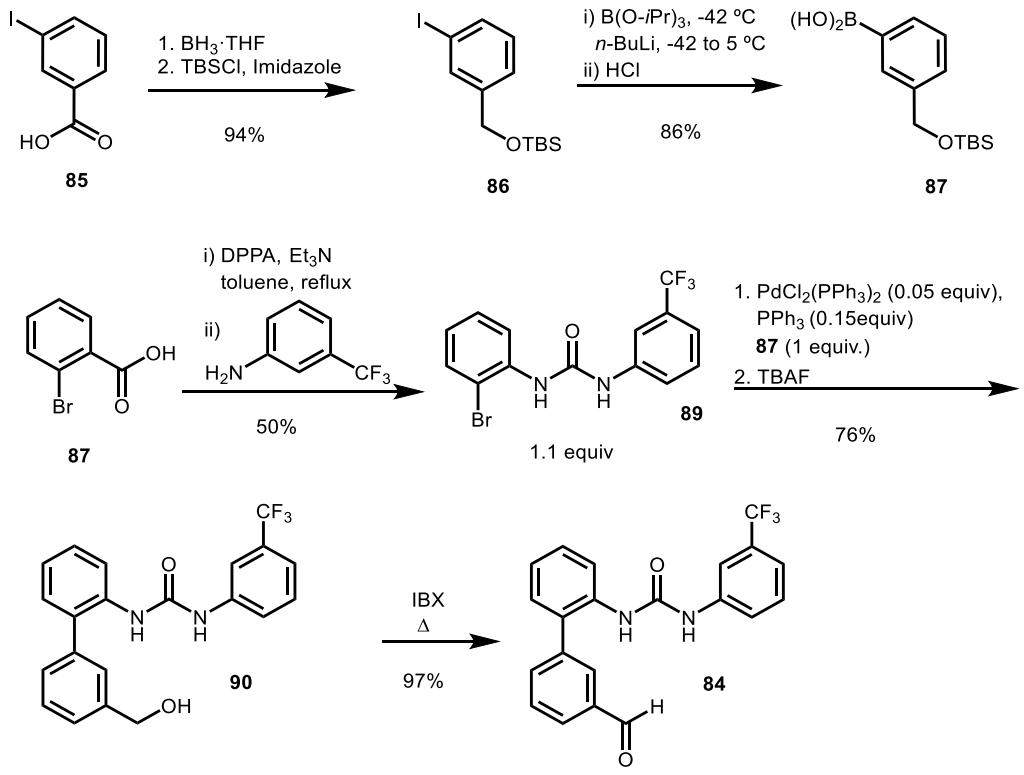

Scheme 2.2 Synthesis of 84

2.1.3 Screening of urea-aldehyde for catalytic activity

Screening catalyst **84** for catalytic activity in peptide coupling was unfruitful. Benzyl amine and propionic acid were used in combination with catalyst **84**, initially employed in catalytic amounts and later stoichiometrically (Scheme 2.3). No activity was observed under mild conditions and decomposition of the urea was observed at higher temperature with no enhanced product formation relative the thermal background reaction. The use of dehydrating agents such as molecular sieves also provided no improvement. Preforming the imine by condensing it on the aldehyde followed by combination with the carboxylic acid or carboxylate also gave no amide formation.

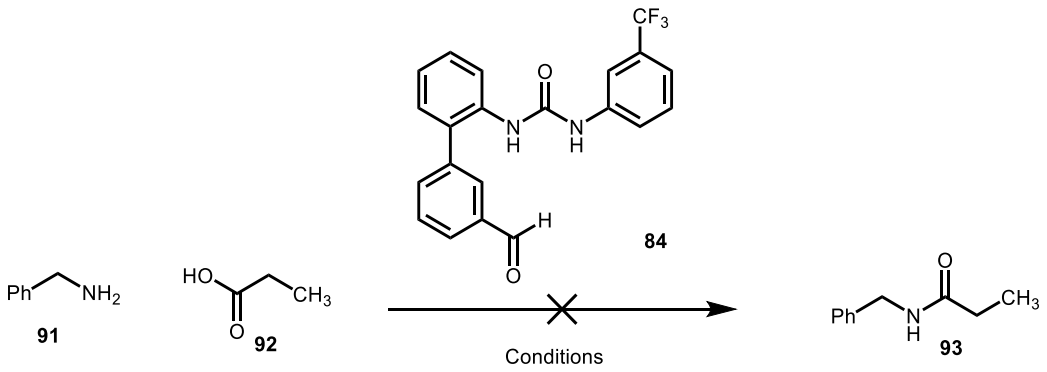

Scheme 2.3 General scheme for peptide coupling catalysis

We envisioned that there were potentially three major issues which may have prevented catalysis occurring with urea **84**: 1) poor nucleophilicity of the imine, 2) insufficient activation of the carboxylate, and 3) incorrect positioning of the nucleophile relative to the urea/coordinated carboxylate.

To address the first issue, we considered that the benefit of having an intramolecular nucleophile did not compensate for the low nucleophilicity of the imines. Imines are generally not considered good nucleophiles and reactions that rely on imine nucleophiles utilize highly reactive electrophiles (e.g. ketene in the Staudinger synthesis). But to achieve reactivity for our system, we needed to evaluate the positioning first before we could evaluate the nucleophilicity.

In regard to our second concern, modifications to the scaffold by adding additional electron withdrawing groups could provide a stronger hydrogen bond donor but this would potentially only have a moderate effect. A bigger impact could be achieved by changing the type of hydrogen bond donor to a stronger hydrogen bond donor (e.g. thiourea, guanidine or urea-boronate developed by Smith's group[110]).[111]

Finally, in addressing the position of the nucleophile, we assessed that the general scaffold, and particularly the position of the nucleophile, would be a key parameter for achieving the desired reactivity and is also a parameter we readily could change. After an extensive literature search it became clear that there are no studies which investigated the position systematically and as such, no clear conclusions have been established to help provide a rational for an improved scaffold design.

To date, a vast variety of urea hydrogen bond catalysts have been developed.[18] However, very few studies have been performed studying the hydrogen bonding system and if they do, they usually focus on the strength of the hydrogen bond donor. The strength of hydrogen bond donors has been attributed both to pKa of the catalyst[112] and the change of pKa when coordinating to substrate[113]. These studies do not take into account secondary interactions such as sterics, dual interactions and binding geometry. Kozlowski's group proposed to instead use an organic molecule as spectrophotometric sensor to measure LUMO lowering properties of the hydrogen bonding organocatalysts.[114] The greater the blue shift measured, when combining the hydrogen bond donor with the molecular sensor, the stronger (more LUMO lowering) the hydrogen bond donor was expected to be. The strength of the hydrogen bond donors based on the sensor correlated well to experimental results for their model Diels-Alder reaction and Friedel-Crafts reactions.

2.2 Investigation of position of nucleophile relative to the urea

As the positioning of the nucleophile in urea based electrophile activation was the most poorly explored element of our system we endeavoured to investigate factors leading to optimal nucleophile orientation. Without proper positioning of the nucleophile, activation of the nucleophile and electrophile is irrelevant. Accordingly, we suspended attempts towards the development of a functional catalyst, and directed our attention to studying the optimal position of the nucleophile. Simultaneously, we took the opportunity to briefly investigate the effect on the system from the electron withdrawing properties of the aryl ring.

2.2.1 Synthesis of test substrates

The general design for this investigation was a biaryl urea linked to a nucleophilic hydroxyl group (Figure 2.3). The relative rate of nucleophilic addition of the hydroxyl group to an electrophile known to react with a hydroxyl group by urea activation, (e.g. an oxazolone, used by Berkessel's group, Scheme 1.7)[26] would allow us to systematically study the reactivity of the system. Replacing the imine with a hydroxyl group which has rotation around the C-O bond relative the rigid C=N bond would improve the number of conformations which can reach the

Bürgi-Dunitz trajectory. However, this advantage for the hydroxyl is believed to be constant for all different linker so the general trend should be accurate for the imine nucleophile too. The synthetic routes to these substrates were designed around the same modular steps discussed above, with the key connections being urea formation and cross coupling. The sequence of these steps has been modified depending on the desired substitution and accessible starting materials.

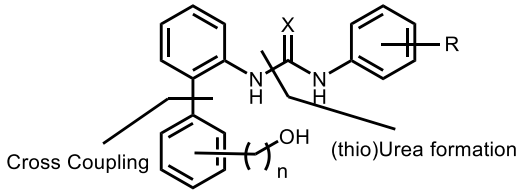

Figure 2.3 First generation of test substrate

Nine different compounds with the tri-aryl scaffold presented in Figure 2.3 were synthesized, including urea **90** which was synthesized previously. 2-phenyl-4-isopropyl-5(4H)-oxazolone (**94**) is known to be activated by ureas for nucleophilic attack by alcohols (Berkessel *et al*.)[26] and was chosen as the model substrate. We employed **94** as the electrophile in the presence of base (1.5 equiv. Et_3N) in $CDCl_3$ using anisole as internal standard (Scheme 2.4).

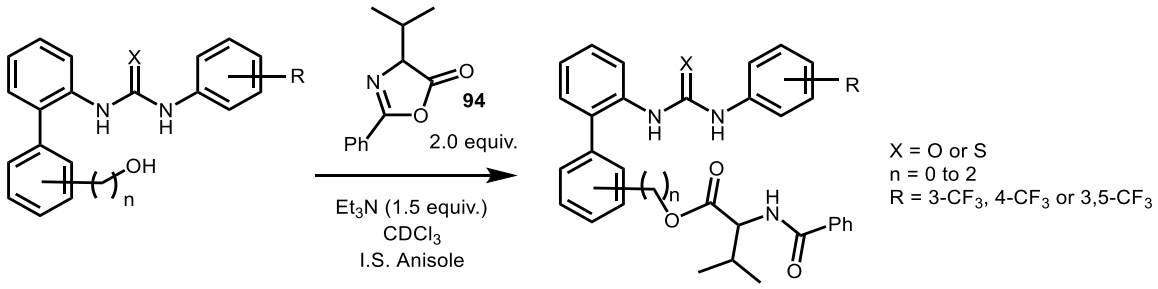

Scheme 2.4 General screening reaction for acylation

The scaffolds synthesized showed poor solubility and required testing at dilute conditions which produced slow rates and unreasonable reaction times (over a week). Thus, this gave inconsistent results and required us to revisit the design to increase solubility before continuing with reactivity screening. The syntheses of these urea-alcohol test substrates are not included here but were performed in analogy to the compounds in section 2.2.2.

2.2.2 Modified scaffold with a *t*-butyl group

To address to the solubility issue, a second generation was designed bearing a *t*-butyl group to improve solubility by preventing π-stacking and increasing lipophilicity (Figure 2.4). The same modular robust synthesis could be applied as above, simply by changing the aniline starting material.

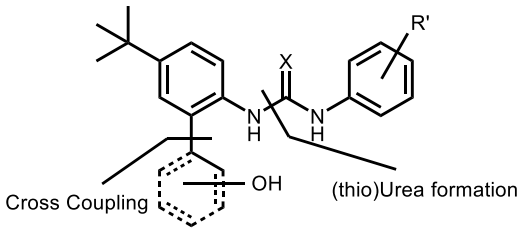

Figure 2.4 Second generation Urea-Alcohols

2.2.3 Synthesis of second generation scaffolds

Several urea-alcohol scaffolds could be reached through the modular route as described for urea **84** in Scheme 2.2. Four boronic acids were made efficiently from the commercially available carboxylic acids in an identical sequence of borane reduction, TBS protection and boronic acid formation, affording boronic acids **95-97** and **85** in overall yields of 60% and above (Scheme 2.5). The halide coupling partner **105** was obtained in 66% yield through ortho iodination of 4-*t*-butylaniline with KI and hydrogen peroxide under acidic conditions. The isocyanates **108** and **109** came from Curtius rearrangement from the corresponding carboxylic acid (**106** and **107**, respectively). The reaction of isocyanates **108** and **109** with aniline **105** yielded ureas **110** and **111**, in moderate yields (44% and 55%, respectively). For the Suzuki cross coupling, the standard conditions employed were 7 mol% $Pd(OAc)_2$ and PPh_3. Higher catalyst loadings were used for the ortho substituted boronic acid but yields for **112** (27%) and **117** (16%) remained low. For non-*ortho* substituted substrates in the series, the cross coupling, followed by TBS deprotection was generally high yielding (50-90%) and proved to be a smooth and efficient synthesis of seven different substrates.

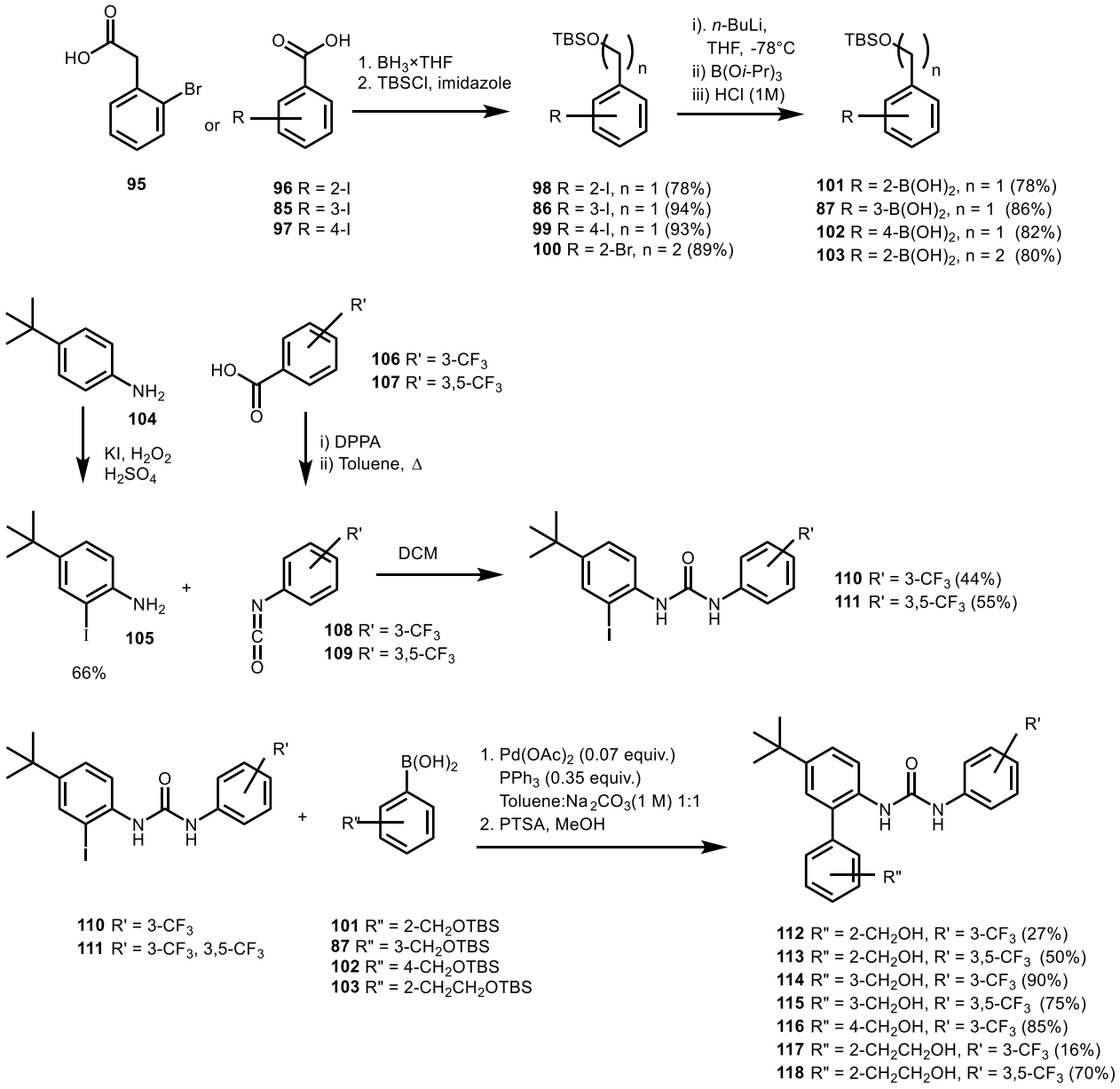

Scheme 2.5 Syntheses of a series of compounds (112-118)

As will be seen below, a general trend indicated that closer proximity to the urea was beneficial. Investigation of a more flexible chain rather than the biaryl was of interest considering the biaryl scaffold would have either partially or completely restricted rotation that could affect reactivity. The non-biaryl urea-alcohols **121** and **122** were proposed to both be more flexible and bring the nucleophile closer to the urea (Scheme 2.6). Syntheses began with a Suzuki coupling to install the vinyl group on halide **111** using vinyl boronic acid pinacol ester affording styrene **120** in 90% yield. The primary alcohol **121** was a minor product (29%) in the hydroboration oxidation

of styrene **120** and the secondary alcohol was isolated as the major product (40%). However, a bulkier borane, such as 9-BBN, would presumably have been beneficial in this case to drive selectivity towards the primary alcohol. However, sufficient supplies of urea-alcohol **121** were obtained in our first reaction and optimization was not attempted. Ozonolysis of olefin **120**, followed by immediate reduction of the trioxolane yielded alcohol **122** in 33% yield.

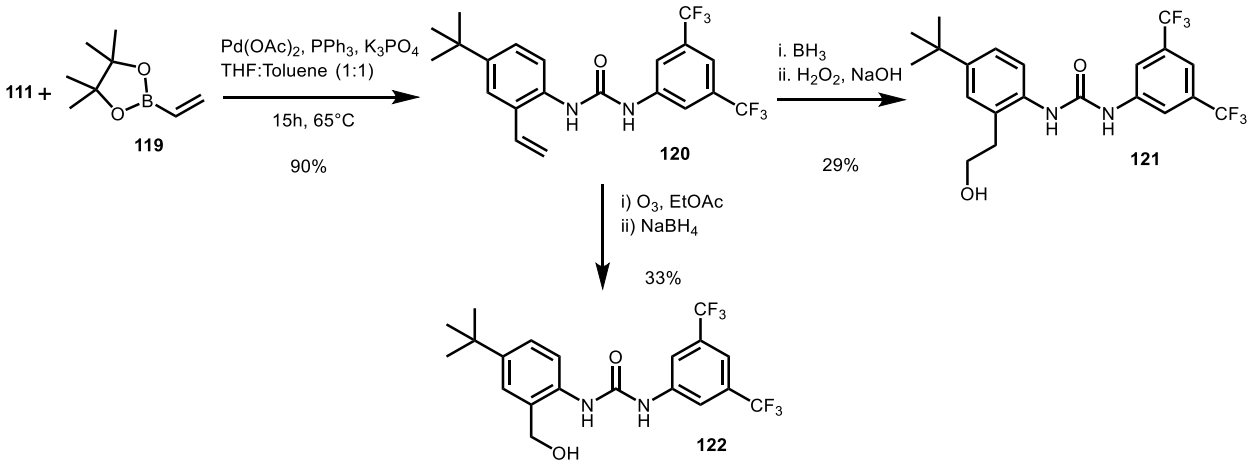

Scheme 2.6 Syntheses of 121 and 122

To investigate a slightly different type of nucleophile, phenol **128** was synthesized (Scheme 2.7). The synthesis started with 2-iodo-4-*t*-butylaniline (**105**), which underwent palladium catalyzed borylation with pinacol borane (**125)** to afford boronic ester **126** (53% yield). Alternatively, Miyaura borylation[115] using $B_2(pin)_2$ instead of pinacol borane gave higher borylation yields (82%). Suzuki reaction between boronic ester **126** and 2-iodophenol, gave the biaryl scaffold **127** in 60% yield. Urea formation with **68** gave a poor yield (30%) of phenol **128**, due to purification issues involving removal of an impurity. Fortunately, a sufficient amount of phenol **128** was still isolated for our experiments.

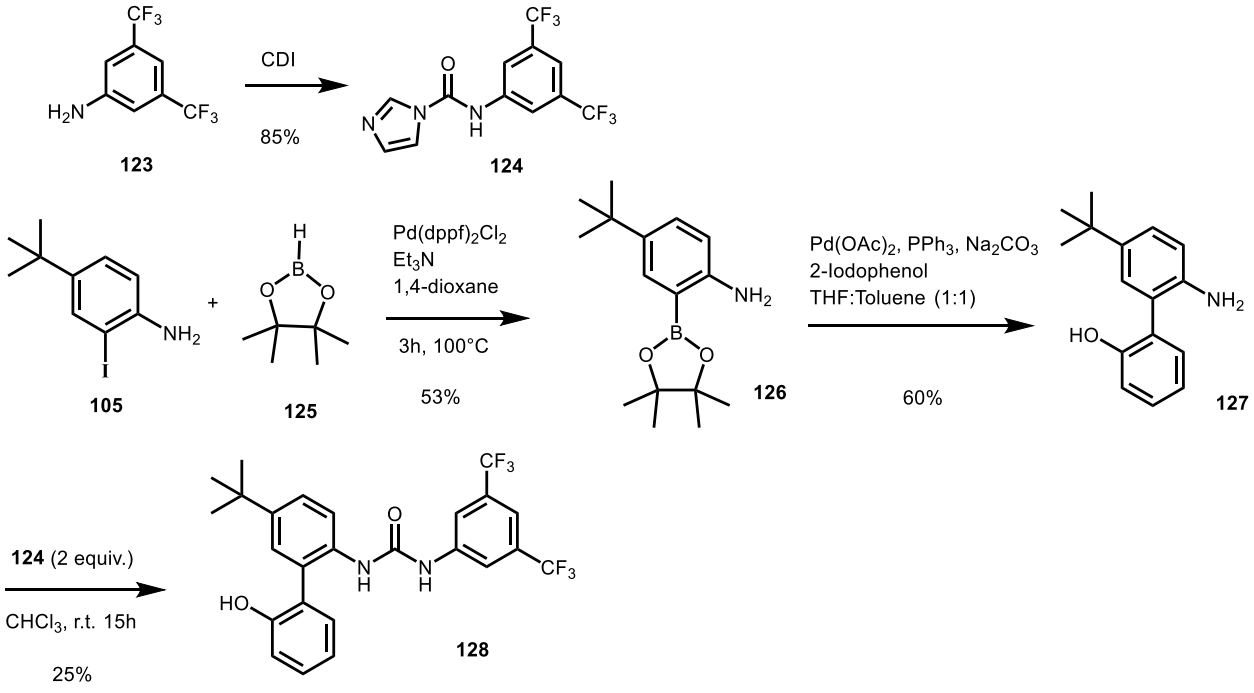

Scheme 2.7 Synthesis of 128

2.2.4 Screening of the synthesized urea-alcohols

We screened all synthesized urea-alcohols under identical conditions (Scheme 2.8). The *t*-butyl group enabled testing of the acylation at higher concentrations, allowing for faster acylation rates that could be measured over the course of 1-24 h. The reactions were monitored with ^{1}H-NMR at regular intervals. 2-Phenyl-4-isopropyl-5(4H)-oxazolone **94** was used as electrophile and the reactions were performed in the presence of base (Et_3N 1.5 equiv.) in $CDCl_3$ (0.2 M based on urea-alcohols) at room temperature.

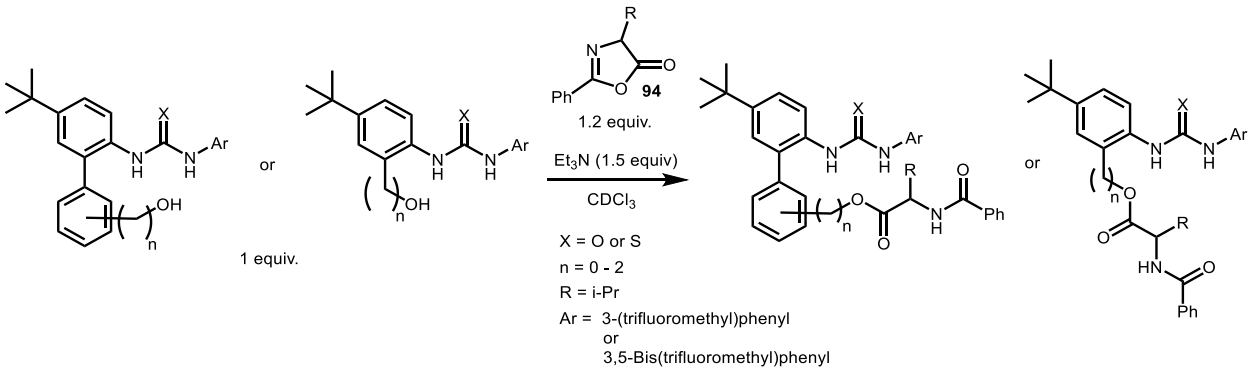

Scheme 2.8 General reaction scheme for testing

Our studies began with the screening of *ortho*-, *meta*- and *para*-substituted benzyl alcohols **112**, **114** and **116** under standard conditions for acylation with oxazolone **94** (Figure 2.5). The ortho-substituted benzyl alcohol **112** was more reactive than meta substituted benzyl alcohol **114**. As expected, the para substituted **116** had no activity, providing evidence for the absence of an intermolecular background reaction. Benzyl alcohol together with 1,3-bis(3,5-bis(trifluoromethyl)phenyl)urea also underwent no acylation confirming the lack of any background reactivity.

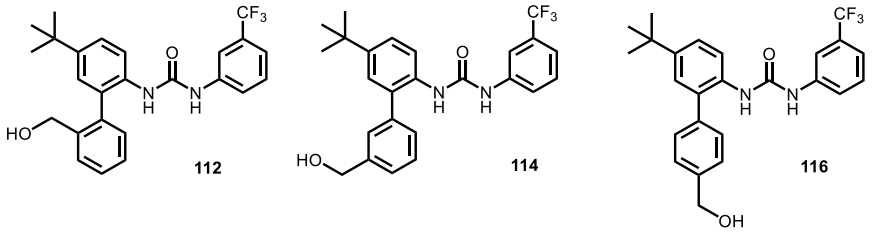

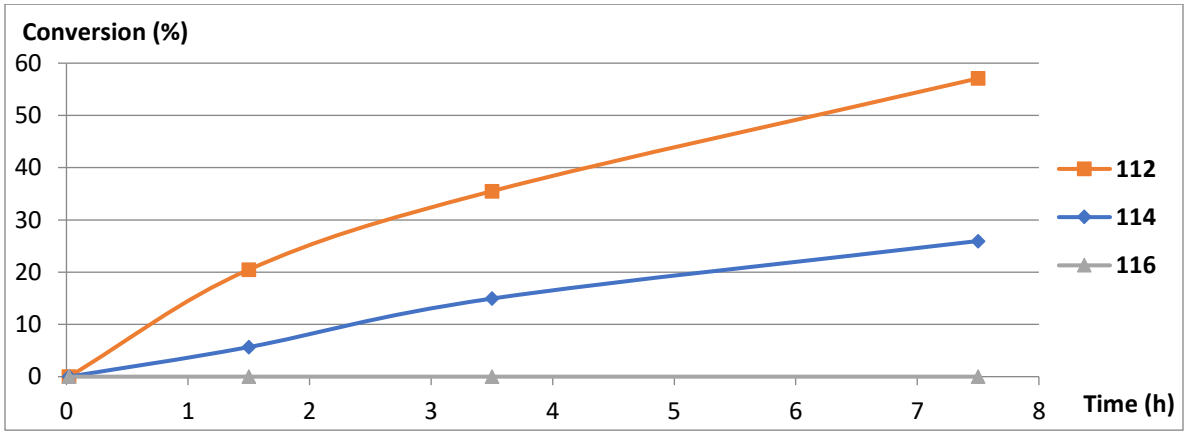

Figure 2.5 Acylation of 112, 114, 116

We sought to compare how the electron withdrawing properties on the urea would influence the activity of these structures (Figure 2.6). For both *ortho* and *meta* substituted benzyl alcohols, we observed a slight improvement in activity for ureas bearing a 3,5-bis(trifluoromethyl)phenyl group (ortho **113** and meta **115**) relative to their analogue with one electron withdrawing group (ortho **112** and meta **114**). This is not surprising considering electron poor ureas are known to be stronger hydrogen bond donors. The strength of the hydrogen bond is directly related to its pK_a value and Schreiner and coworkers have measured that the pK_a value of a urea could decrease more that 1-2 pK_a units by adding one trifluoromethyl group to the meta position of an attached aryl ring.[116] Importantly, the effect on activity is more substantial by changing position, going from meta substituted alcohols **114** and **115** to ortho substituted alcohols **112** and **113**, than adding electron withdrawing group.

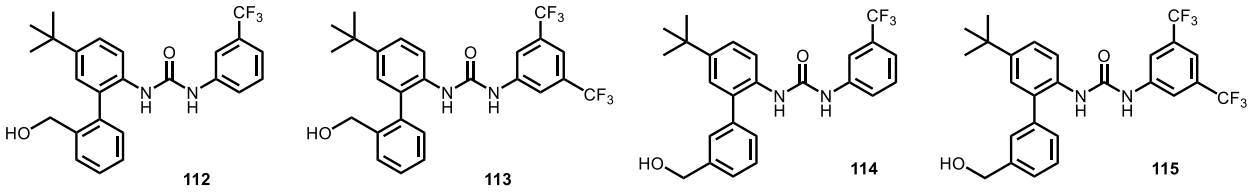

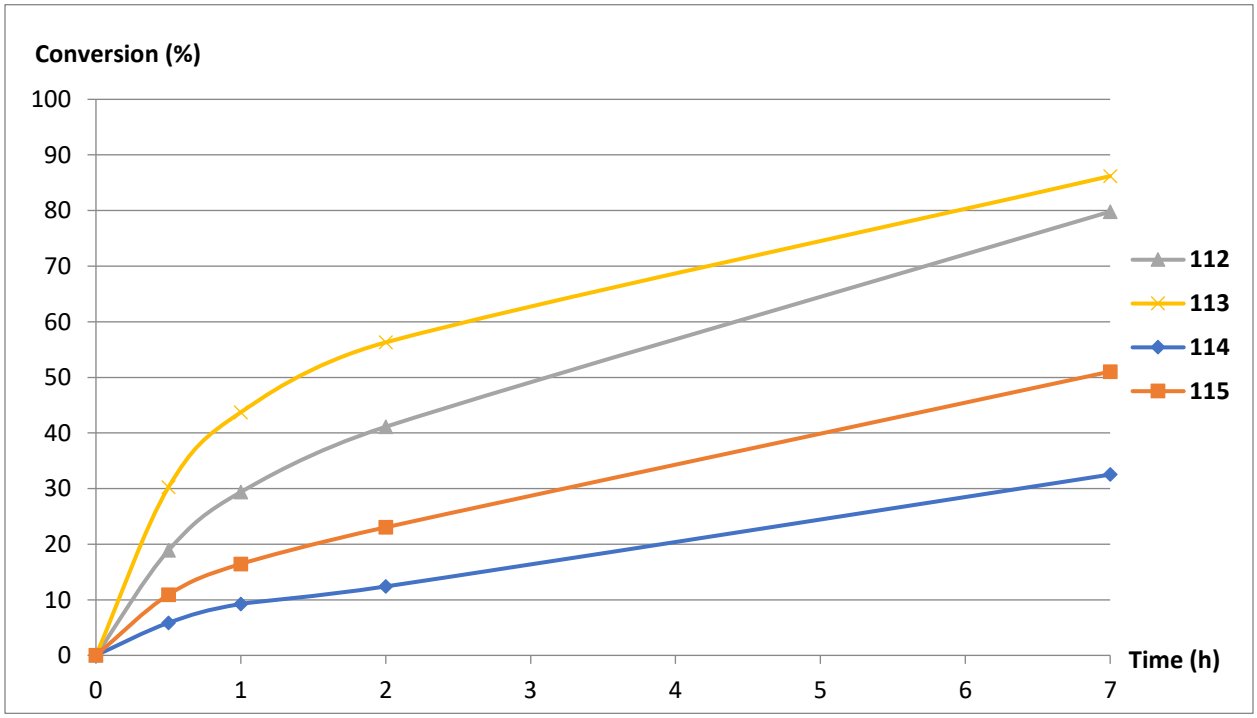

Figure 2.6 Acylation of 112-115

We screened longer alkyl chain derivatives under our standard acylation conditions (Figure 2.7). Alcohols **114**, **115**, **117** and **118** have the same number if intramolecular carbons, similar length, from the nucleophile to the urea. Interestingly, hydroxymethyl substituted **114** and the longer hydroxyethyl substituted **117** and **118** have similar activities. This might be due to *ortho* ethyl alcohol **117** (also *ortho* ethyl alcohol **118**) suffering from limited rotation due to steric restrictions, which might direct the alkyl alcohol chain away from the urea. *meta*-Substituted hydroxymethyl **115** was significantly faster than all others in this series and reached 86% conversion in 24 h.

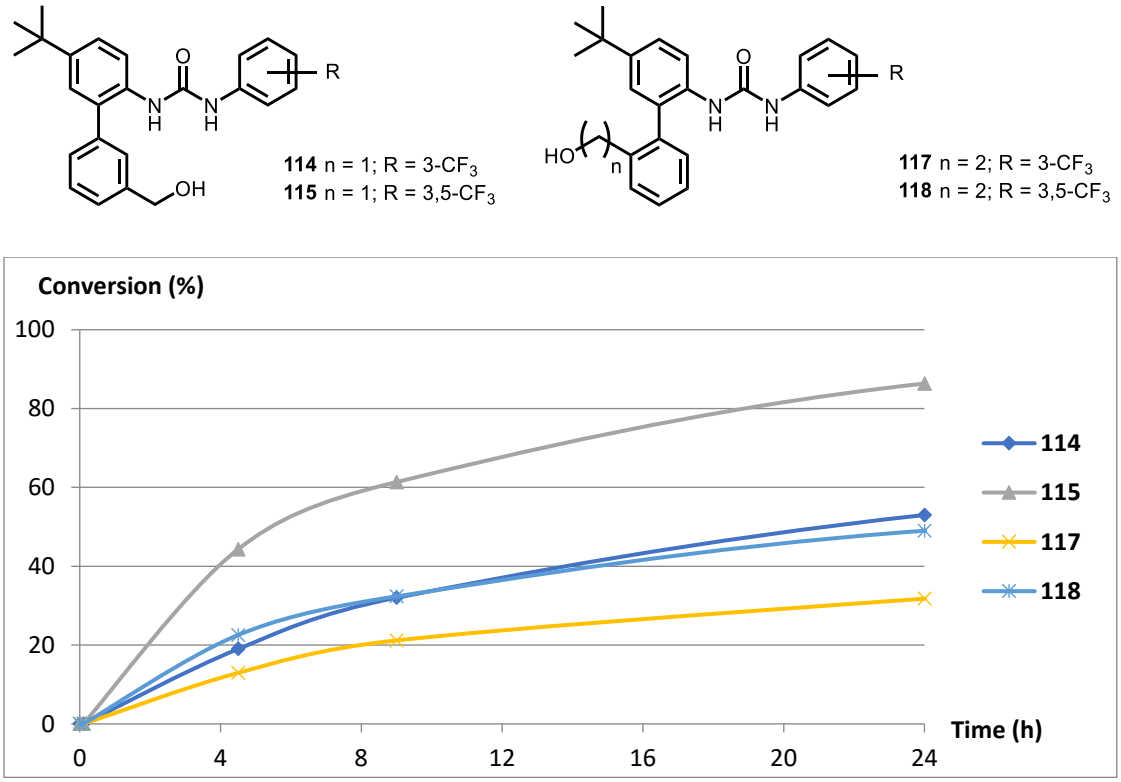

Figure 2.7 Acylation of 114, 115, 117 and 118

At this point, a trend of higher reactivity for acylation with increased proximity to the urea had been observed. We screened the three urea-alcohols that have the nucleophile in the closest proximity to the urea and compared them with benzyl alcohol **113** which has been the most reactive so far (Figure 2.8). Phenol **128** and ethyl alcohol **121** have nearly identical acylation rates, both reached completion in 4.5 h. They also have their hydroxyl nucleophile the same number of carbons away from the urea, and are hence of similar distance, indication that the nature of

hydroxyl nucleophile, alkyl alcohol and phenol, plays only a minor role. Importantly, compound **122** reached full completion in less than 1 h which was significantly faster than all other substrates that was evaluated.

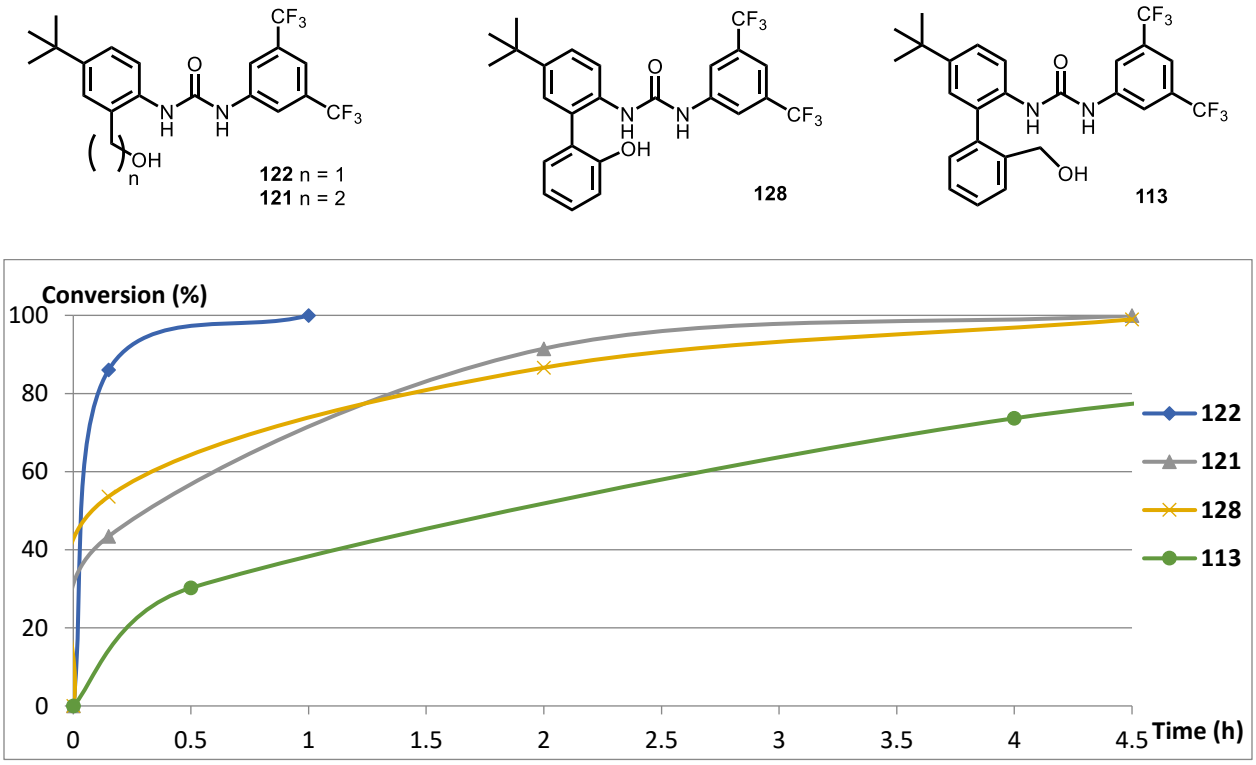

Figure 2.8 Acylation of 113, 121, 122 and 128

2.2.5 Screening of thiourea

Of interest was to compare urea **114** with thioureas which are known to be better hydrogen bond donors.[117, 118] First, Suzuki reaction between boronic acid **87** and halide **105**, prepared previously, afforded biaryl **130** in 69% yield (Scheme 2.9). Synthesis of thiourea **132** was low-yielding and only 21% was isolated after thiourea formation from aniline **130** with isothiocyanate **108** followed by TBS deprotection. Surprisingly, thiourea **132** only achieved 3% conversion under our standard acylation conditions after 24 h which contradicts the trend observed above that stronger hydrogen bonding donors are more efficient. Reasons for the lack of activity have not been identified. Attempts were made to synthesize an *ortho* substituted arylthiourea but it was isolated in combination with urea **112**. Further column chromatography gave complete conversion

from thiourea to urea **112**, indicating inherent instability of the thiourea to hydrolysis, potentially meditated by the intramolecular hydroxyl group.

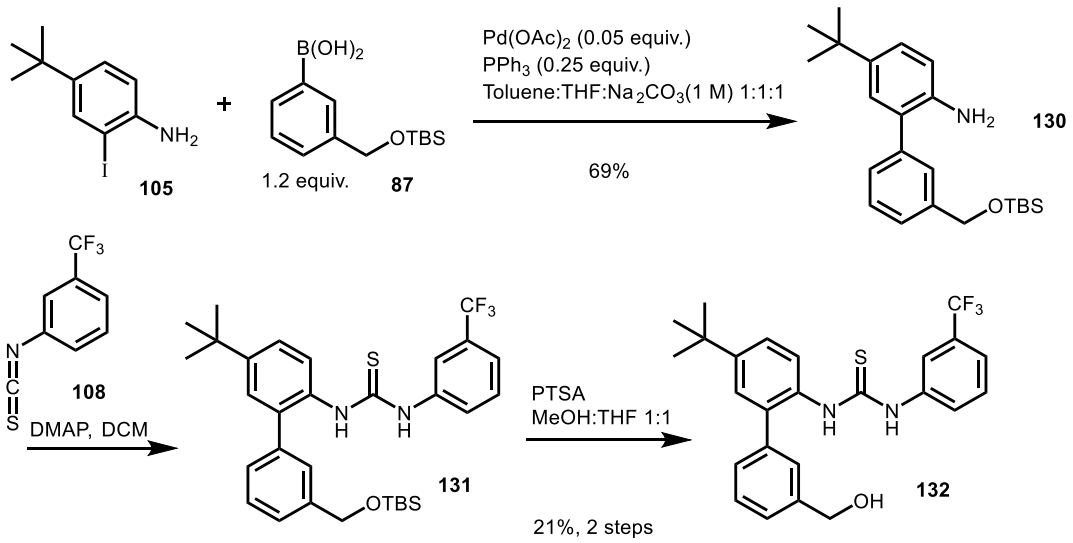

Scheme 2.9 Synthesis of thiourea 132

2.3.1 Mechanistic support for dual hydrogen bonding

To support that dual hydrogen bonding is important for reactivity, both mono *N*-methyl versions of benzyl alcohol **114** were synthesized using a single reaction starting from TBS protected **133** using NaH and MeI (Scheme 2.10). The compounds displayed, unsurprisingly, similar R_f but after several, slow gradient, flash chromatography columns, enough material of both *N*-methyl **134** and *N*-methyl **135** were isolated for characterization and screening. Neither **134** or **135** displayed any acylating properties (0% conversion at 48 h for both) supporting the contention that dual two-point hydrogen bonding is essential for activity. An argument that the introduced steric encumbrance of the neighboring methyl group prevents the required hydrogen bonding can be made. However, methyl is arguable the smallest substituent that could be installed to selectively remove a hydrogen bonding site.

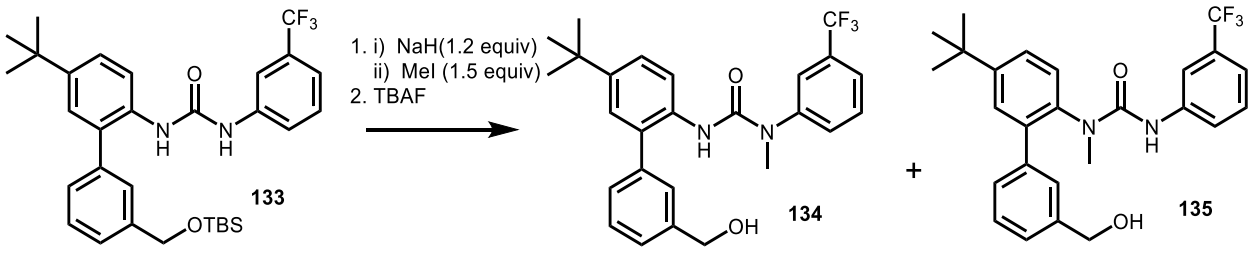

Scheme 2.10 Syntheses of *N*-Methyl 134 and 135

To further support strong intramolecular hydrogen bonding, we synthesized phosphonate **136** from **114** by allowing alcohol **114** react with methyl methylphosphonium chloride in the presence of excess base (Scheme 2.11). Methyl methylphosphonium chloride was synthesized from dimethyl methyl phosphonate and oxalyl chloride. A clear ^{1}H-^{31}P HMBC correlation was observed between the N-H proton at 9.3 ppm and the only phosphorous peak at 32 ppm. The protons in phosphonate **136** were assigned based on COSY, ^{1}H-^{13}C HSQC, ^{1}H-^{13}C HMBC correlations and the N-H proton at 9.3 ppm showed strong ^{1}H-^{13}C-HMBC correlation to the carbon ortho to the trifluoromethyl group. The other N-H was more upfield (7.4 ppm) and 5 bonds away from that carbon making it unlikely to display such correlation.

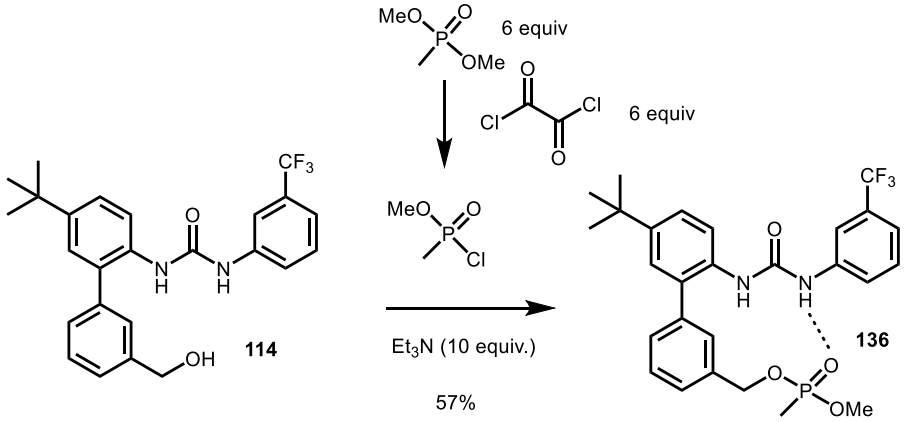

Scheme 2.11 Synthesis of phosphonate and ^{1}H-^{31}P-HMBC correlation

2.3.2 Structural evaluation of urea alcohol substrates

The proximity of the nucleophile to the urea appeared to be the essential feature for activity. More electron withdrawing groups provided only slight enhancements but moving the nucleophile

3 atoms closer decreased reaction time for full acylation from over 48 h to less than 1h. These results could partially explain why we observed no activity for our original catalyst **84** for amide bond formation.

To explain why we observe this trend in activity, we need to reconsider the simple dual hydrogen bond model where both urea nitrogen hydrogens bond to the carbonyl in straight, equal, planar fashion. Quickly observing the 2D drawing in Figure 2.9, one could easily argue that the length of the linker in **122** would be insufficient to react with the oxazolone. (Figure 2.9 a). NMR studies by Berkessel and coworkers showed that forming the oxazolone-catalyst **8** complex in toluene-d_8 showed a significantly higher downfield shift for one of the urea protons indicating a much stronger, and maybe closer, hydrogen bond by one of the urea protons (adjacent to $(CF_3)_2Ar$; $\Delta\delta = 0.7$ vs 0.2 ppm), but both are lowered supporting dual hydrogen bonding.[26] A NOE correlation between an *ortho* proton on the electron withdrawing ring and the 4-H proton on oxazolone suggests the orientation of the oxazolone and supports that it is coordinated to the urea rather than the amine.

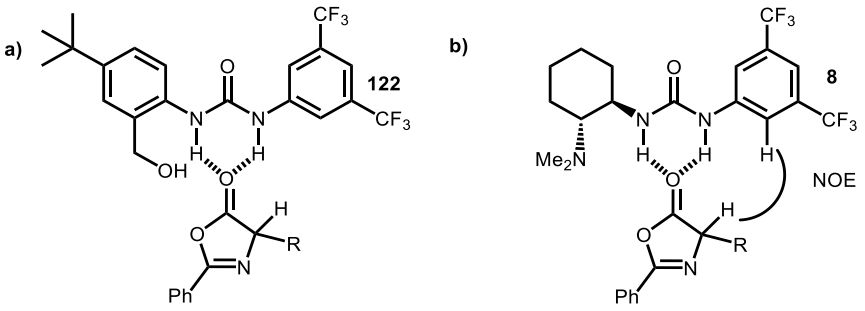

Figure 2.9 Simple dual hydrogen bond model for a) our substrate and b) Berkessel catalyst

Although, as discussed above, the urea protons are parallel in crystal structures, this is not necessarily true for the reactive conformation of the catalyst in solution. Calculations by Pihko and coworkers on their biaryl-thiourea catalyst **137**, showed that the lowest energy in activating the nitroolefin was a complex structure where the urea protons are antiparallel to each other.[119] This is just one example of many proposed activation confirmations. However, it suggests that the planar dual hydrogen bond donor by (thio)urea is not always the active conformation.

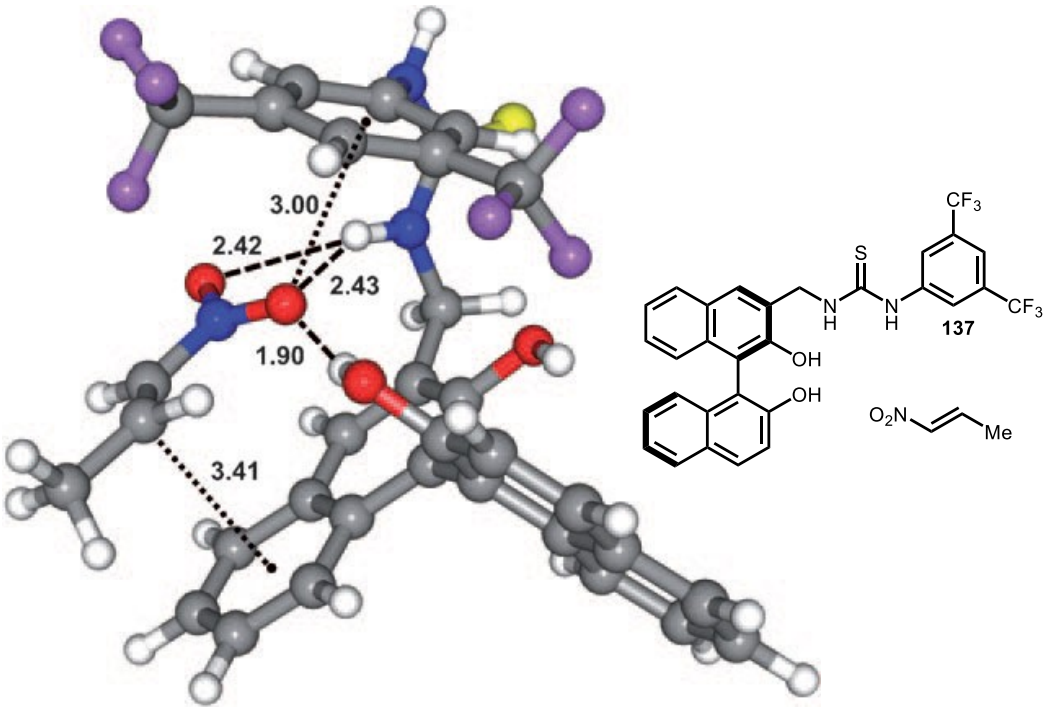

Figure 2.10 Calculated activation mode for catalyst 137. Picture copied from Pihko *et al.*[119]

In our system, there are several parameters which could make the shortest linker the most reactive, such as the rotation of the N-Ar bonds, the angle of the hydrogen bond, entropy and whether dual hydrogen bonding is taking place. Starting with the first option, a slight rotation is likely favoured between the urea-nitrogen and the aryl group containing the nucleophilic group due to strain arising from the *ortho* substituent (Figure 2.11 a). Thomas Steiner has analyzed the Cambridge Structural Database for structural aspects of hydrogen bonding in organic crystals and showed variety in the X─H···X hydrogen bond angle (X = O or N), from 0 degrees (linear) to over 90 degrees angle.[120] If our activation was in a non-linear hydrogen bond, it would bring the oxazolone electrophile into a better position for nucleophilic attack (Figure 2.11 b). Applying these features to our original imine nucleophile, this simple model suggests that the imine lone pair should be able to reach the Bürgi-Dunitz trajectory (Figure 2.11 c). Another important feature is that the shorter linker length has fewer possible conformations, hence, it is more entropically favoured to react to a hydrogen bonded substrate. Even if having a non-linear hydrogen bond ($\theta>0$) would not yield the optimal activation strength, that in combination with entropy and rotation of the N-Ar bond could explain why urea-alcohol **122** showed the highest reactivity. This is plain speculation and other, more complex, conformations of the activation complex can not be ruled

out. Proper computational calculations could bring more insight into the actual active conformation of the oxazolone urea-alcohol complex. However, those calculations have not been performed.

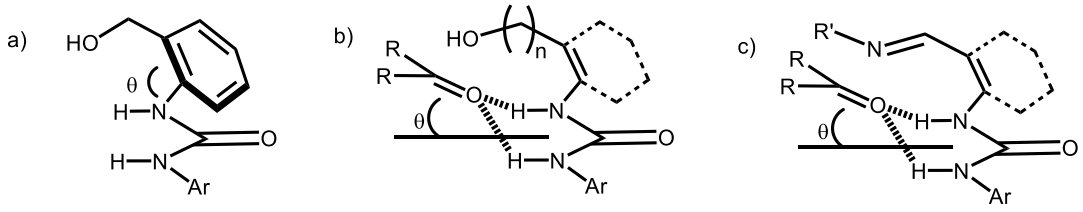

Figure 2.11 Geometrical analysis of urea-alcohol system and urea-imine

2.4 Acyl transfer agent

We wished to implement these results into a functional system and see if it still followed the same trend. We envisioned the creation of a new type of acyl transfer agent and designed 1-hydroxy-7-azabenzotriazole derivatives **138** and **139**, based on **113** and **121**, respectively (Figure 2.12). We also designed a triazole (**140**) based on our most active urea-alcohol (**122**) but we were unable to produce a reasonable synthesis to access it. We hypothesized that hydrogen bonding from the urea will accelerate the acylation of the triazole and subsequently the acyl transfer from the triazole to the nucleophile.

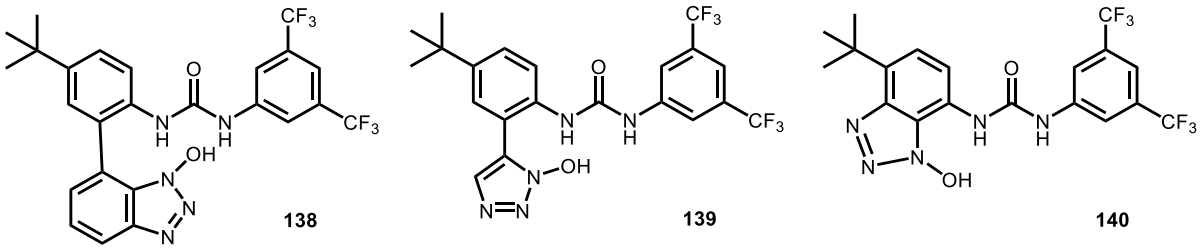

Figure 2.12 Proposed acyl transfer agent

2.4.1 Synthesis of acyl transfer agent

A similar modular synthetic route as we have employed so far (*vide supra*) was employed to synthesize triazoles **138** and **139**. The route was adjusted by preparing the triazoles as the halide

coupling partner for the Suzuki reaction. In the forward direction, hydrogen peroxide oxidation of 2,6-dichloroaniline under acidic conditions gave 2,6-dichloronitrobenzene **141** in 50% yield (Scheme 2.12). Triazole formation by heating **141** with hydrazine yielded benzyl protected benzotriazole **142** in 41% yield after subsequent benzyl protection. Suzuki reaction between sterically hindered chloride **142** and pinacol boronic ester **126** did not give any desired product under our standard conditions. Switching the ligand from PPh_3 to SPhos and performing the reaction in a Schlenk bomb yielded the cross coupling adduct **143** in 61% yield. The final urea-benzotriazole **138** was synthesized by urea formation with activated aniline **124** and deprotection of the benzyl group (89% yield).

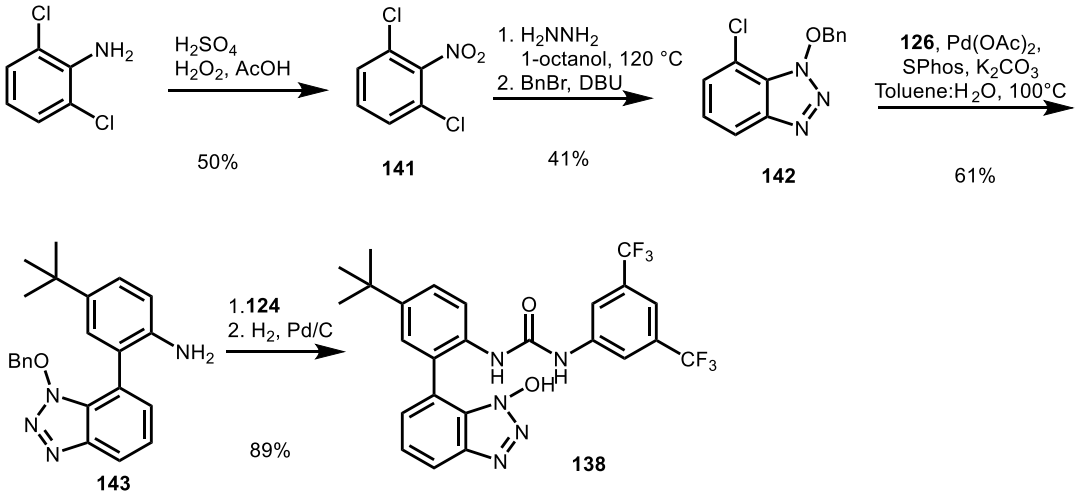

Scheme 2.12 Synthesis of 138

The synthesis of **139** used the same two common intermediates as for **138**, carbonylimidazole activated aniline **124** and pinacol boronic ester **126**. The coupling partner 5-iodo-triazole **147** was synthesized according to a literature[121] procedure by two subsequent condensations on glyoxal (**144**), first with O-benzylhydroxylamine followed by hydrazine to give the bis-hydrazone species **145** (Scheme 2.13). Intermediate **145** underwent radical closure to the benzyl protected 1,2,3-triazole **146** in 58% yield. Directed ortho metalation enabled installation of an iodo group at the 5-position and Suzuki coupling with pinacol boronic ester **126** afforded biaryl **148** (57% yield). The synthesis of the final acyl transfer agent was completed after urea formation with activated aniline **124** followed by benzyl deprotection to yield triazole **139** (80% yield). In

both benzyl hydrogenation deprotections, a slight amount of the deoxygenation product was observed which was confirmed by ^{1}H and ^{13}C NMR (very similar) and HRMS (loss of m/z 16, loss of one oxygen, relative **138** and **139**).

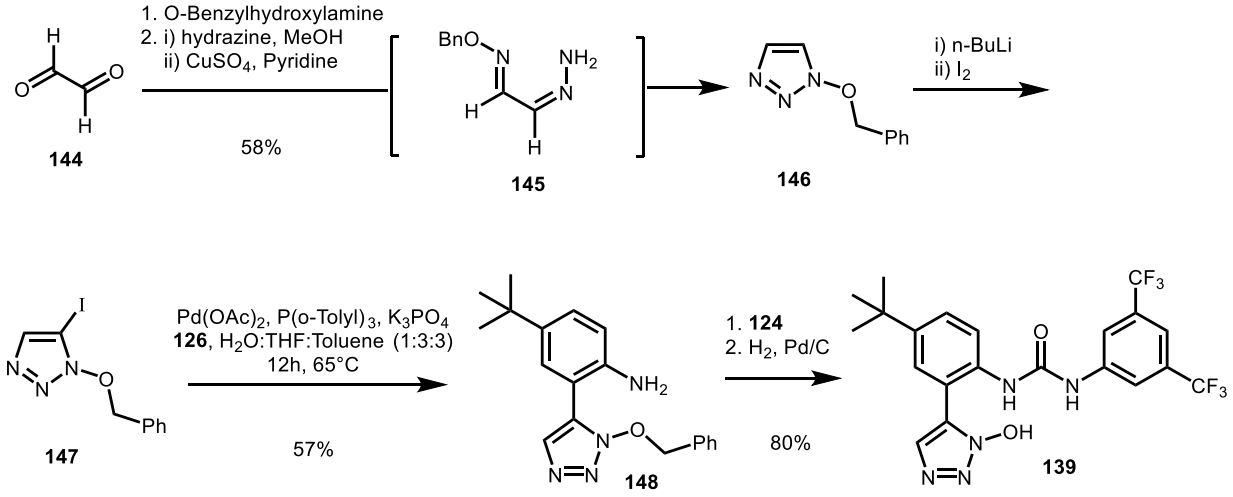

Scheme 2.13 Synthesis of 139

2.4.2 Testing triazoles as peptide coupling additive

Returning to our original intention of improving upon peptide coupling, screening triazole **138** and **139** as an additive for peptide coupling and comparing with the widely employed acyl transfer additive HOAt seemed to be the most appropriate experiment. Carpino has proposed that the pyridine nitrogen brings the amine into proximity to the activated acyl group to enhance reactivity (Figure 2.13 a).[19] We propose that our urea additive functions through a different mechanism, where the urea activates the carbonyl for first acyl transfer onto the triazole followed by acyl transfer to the amine (Figure 2.13 b). Other modes of participations can not be ruled out such as hydrogen bond between urea and amine and interactions between the carboxylate and urea before forming the *O*-acylisourea (Figure 2.13 c), potentially either beneficial or destructive for reactivity.

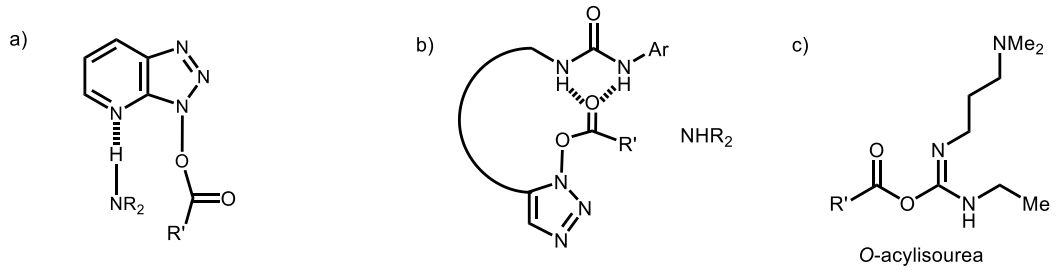

Figure 2.13 Proposed activation modes for a) HOAt, b) 138 and 139, c) *O*-acylisourea

The standard coupling reagent EDC•HCl was selected for the screening of the triazoles as additive. The peptide coupling of Boc protected glycine (**149**) and benzyl amine (**91**) was chosen as model system (Figure 2.14) and the reactions were performed in the presence of DIPEA as base in deuterated DMSO and the conversion was monitored by NMR. Triazole **139** gave a much slower conversion than the control reaction without the additive. This might be caused by a stable 3-N-acyl intermediate (**151**) being formed (Scheme 2.14). Linton and coworkers performed extensive studies showing that the *O*-acyl product is the kinetic product while the 3-*N*-acyl is the thermodynamically stable for HOBt.[122] However, after work up (24 h), only the peptide coupling product **150** and triazole **139** were isolated. If **139** was unreactive, caused by, for example, restricted rotation around the biaryl bond combined with steric bulk of the system preventing nucleophilic attack of the triazole on the *O*-acylisourea, then we should observe similar rates as the background reaction without additive.

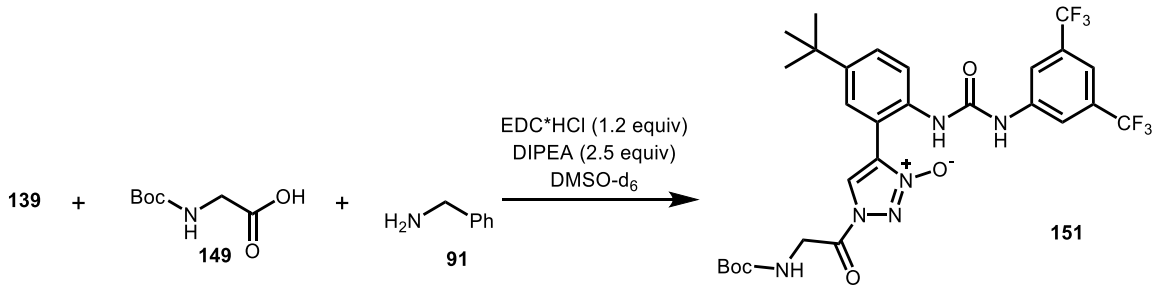

Scheme 2.14 Potential intermediate using additive 139

Pleasingly, benzotriazole **138** worked at par or moderately better than HOAt, showing that the urea indeed has a positive effect, but not as significant as we anticipated (Figure 2.14). It could be that the benzotriazole ester intermediate is already very activated and the final acyl transfer step

is not the rate determining step of the reaction.[123] Future investigations should focus on if **138** can supress racemization which has been the primary function of triazole additives.

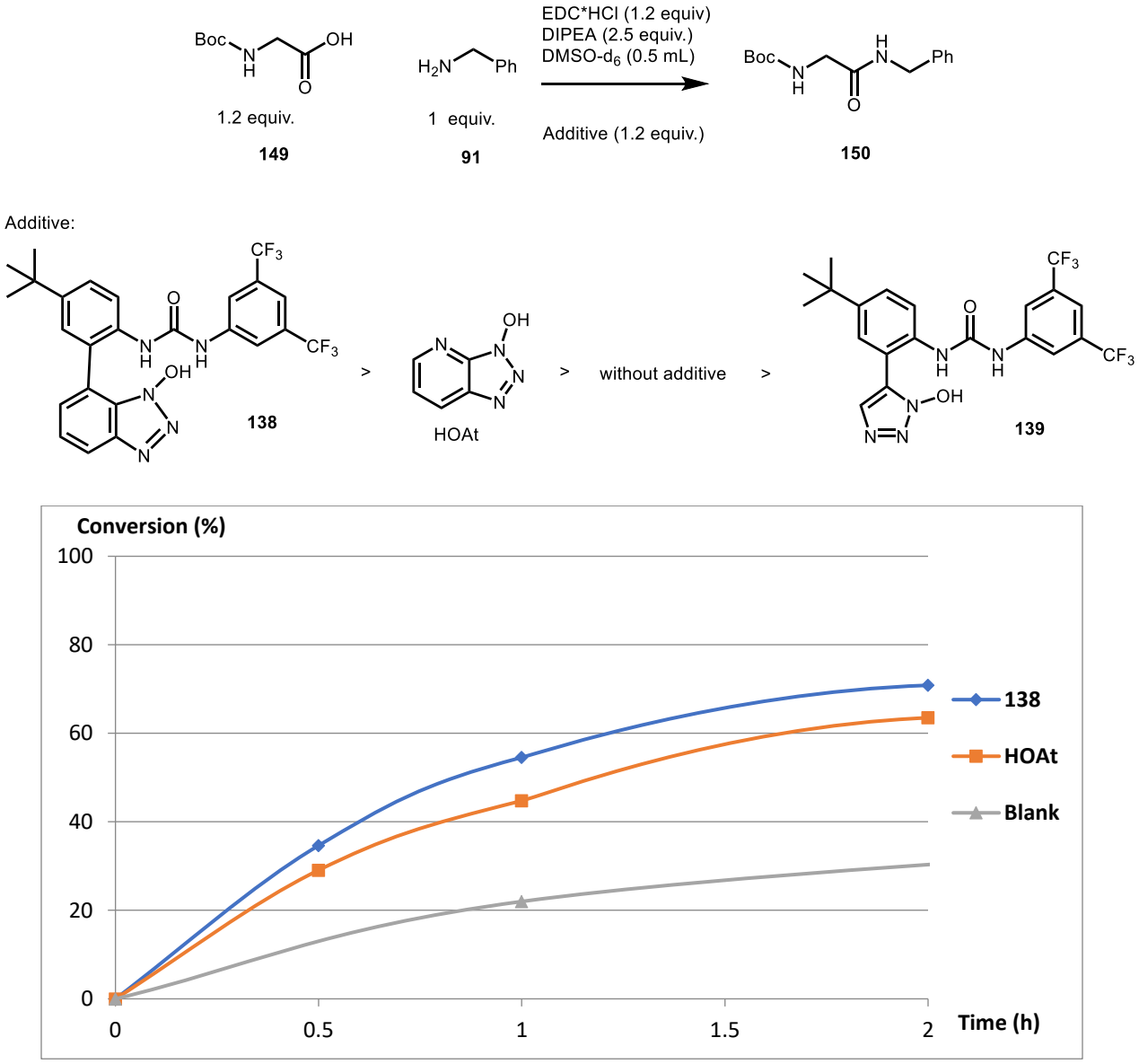

Figure 2.14 Testing of triazole 138 and HOAt for peptide coupling relative blank

2.5 Conclusion

The general trend observed from our studies was that increased proximity of the alcohol nucleophile to the urea provided a rate enhancement in the acylation of the hydroxyl group. No

difference between alkyl hydroxyl and aryl hydroxyl nucleophiles were observed for otherwise comparable scaffolds. Installing two electron withdrawing CF_3 groups rather than one had some effect on acylation but the effect was not as significant. We postulate that this trend should be true for other 2-point hydrogen bond donors, such as thiourea and guanidine, despite our thiourea showing no activity under identical conditions.

This study led to the development of a new type of peptide coupling co-reagent (**138**) which displayed a slight rate enhancement relative HOAt for peptide coupling which provided a proof of concept. However, due to higher synthetic complexity compared to HOAt, and the fact that it was not significantly more active, it is probably not a superior acyl transfer agent. However, the results presented herein have the potential to contribute to the future designs of urea based catalysts and reagents. Future work is needed to investigate the potential of racemization in the peptide formation which has been the main objective in the design of new coupling reagents and additives such as HOAt.[124] Furthermore, it would be interesting to investigate if the urea-triazole system could function as a general acyl transfer reagent such as DMAP.[125]

With the knowledge gained on proximity of the nucleophile, future studies might investigate an aldehyde with closer proximity to the urea. Unfortunately, due to time constraints, urea-aldehyde **152** has not been synthesized yet. More studies would be needed to conclude if hydrogen bond donors have the potential of activating a carboxylic acid enough for intramolecular attack by an imine.

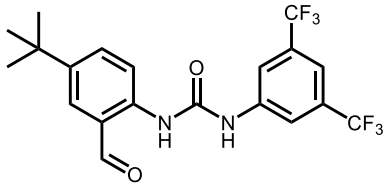

152

Scheme 2.15 New potential catalyst

2.6 Reference

[108] Fitzmaurice, R. J.; Kyne, G. M.; Douheret, D.; Kilburn, J. D.; *J. Chem. Soc., Perkin Trans.* 1, **2002**, 841.

[109] Berkessel, A.; Cleemann, F., Mukherjee, S. Muller, T. N., Lex, L.; *Angew.Chem. Int. Ed.* **2005**, 44, 807.

[110] Hughes, M. P.; Shang, M.; Smith, B. D.; *J. Org. Chem.* **1996**, 61, 4510.

[111] Li, X.; Deng, H.; Zhang, B.; Li, J. Y.; Zhang, L.; Luo, S. Z.; Cheng, J.-P. *Chem. Eur. J.* **2010**, 16, 450.

[112] Hof, K.; Lippert, K. M.; Schreiner, P. R. *In Science of Synthesis. Asymmetric Organocatalysis 2. Brønsted Base and Acid Catalysis and Additional Topics*; Maruoka, K., Ed.; Thieme: Stuttgart, NY, **2012**, pp 296 – 412.

[113] Gilli, P.; Pretto, L.; Bertolasi, V.; Gilli, G. *Acc. Chem. Res.* **2009**, 42, 33.

[114] Walvoord, R. R.; Huynh, P. N. H.; Kozlowski, M. C.; *J. Am. Chem. Soc.* **2014**, 136, 16055.

[115] Ishiyama, T.; Murata, M.; Miyaura, N.; *J. Org. Chem.*, **1995**, *60*, 7508.

[116] Jakab, G., Tancon, C.; Zhang, Z.; Lippert, K. M.; Schreiner, P. R. *Org. Lett*., **2012**, 14, 1724.

[117] Žabka, M.; Šebesta, R. *Molecules* **2015**, 20, 15500.

[118] Wittkopp, A.; Schreiner, P. R.; *Chem. Eur. J.,* **2003**, 9, 407.

[119] Rahaman, H.; Madarasz, A.; Papai, I.; Pihko, P. M.; *Angew. Chem. Int. Ed*. **2011**, 50, 6123.

[120] Steiner, T.*; Angew. Chem. Int. Ed.* **2002**, 41, 48.

[121] Uhlmann, P.; Felding, J.; Vedsø, P.; Begtrup, M.; *J. Org. Chem.* **1997,** *62,* 9177.

[122] Brink, B. D.; DeFrancisco, J. R.; Hillner, J. A.; Linton, B. R.; *J. Org. Chem*. **2011**, 76, 5258.

[123] Chan, L. C.; Cox, B. G.; *J. Org. Chem.* **2007**, 72, 8863.

[124] Carpino, L. A.; Imazumi, H.; Foxman, B. M.; Vela, M. J.; Henklein, P.; El-Faham, A.; Klose, J.; Bienert, M.; *Org. Lett.* **2000**, 2, 2253.

[125] Steglich, W.; Hofle, G. Angew. Chem. Int. Ed. **1969**, 8, 981.

Chapter 3

Development of the diazepane carboxylate catalyst for the Diels-Alder reaction

3.1 Ethyl diazepane carboxylate catalyst for the Diels-Alder reaction

In this chapter, we describe the development of an organocatalytic Diels-Alder cycloaddition using the achiral ethyl diazepane carboxylate catalyst developed in our lab by Dr. Dainis Kaldre for the Cope rearrangement (presented in chapter 1.5). Preliminary results were performed by Mr. Benjamin Zank and showed that catalyst **69** can catalyze the Diels-Alder between several α-substituted enals and CpH. The reminder of the investigations into optimization, reactivity and scope were performed by myself with the exception for DFT calculations performed by J. L. Gleason. The potential of the diazepane carboxylate as a general catalyst for the Diels-Alder reaction with α-substituted enals will be demonstrated. The catalyst gave good yields and *exo*-selectivity for a wide range of dienophiles and dienes.

3.1.1 Initial studies towards the Diels-Alder reaction

An important observation from our groups prior studies on the organocatalytic Cope rearrangement was that the substrates were α-substituted enals (**71**), yet the ethyl diazepane carboxylate could still efficiently catalyze the reaction (Figure 3.1). As presented in chapter 1, very few catalysts have been developed that can perform iminium ion catalysis with α-substituted enals due to the A-1,3 strain that is incurred in the iminium ion (**155**). We envisioned that the diazepane catalyst developed for the Cope rearrangement might be applicable in other areas. One obvious area of interest was the Diels-Alder reaction using an α-substituted enal. This is a classic reaction in organic chemistry, widely utilized in synthesis and, at the time when we began our study, no reports of enantioselective secondary iminium ion catalysis with α-substituted enals had been reported in literature. However, while this study was underway, Hayashi reported the use of prolinol **56** for the Diels-Alder reaction, between α-alkylacroleins and α-acyloxyacroleins with cyclopentadiene and the study also included acyclic dienes (isoprene and 2,3-dimethyl-1,3-butadiene) with α-acyloxyacrolein, presented in chapter 1.[95, 96]

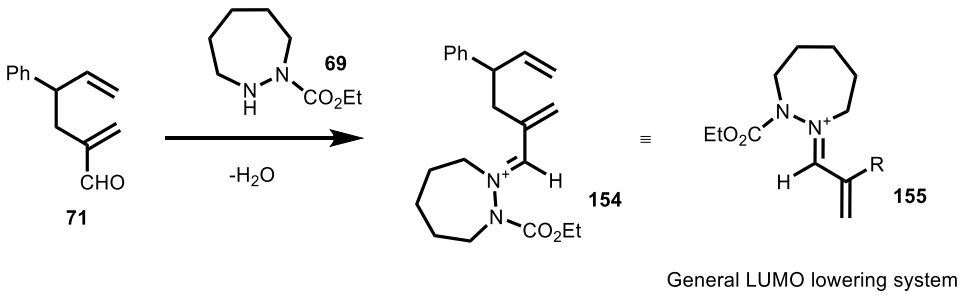

Figure 3.1 Iminium ion of 1,5-hexadiene-2-carboxaldehyde and generic α-substituted enal

A former undergraduate student in our laboratory, Benjamin Zank, was the first to test the Diels-Alder reaction between α-methylcinnamaldehyde (**156**) and CpH catalyzed by diazepane **69** (Table 3.1). The initial trial with 50 mol% catalyst and 50 mol% HCl co-catalyst only gave a low yield of Diels-Alder adduct **157** (7%, entry 1). Switching to the stronger acid TfOH, which had significantly improved rates in the Cope rearrangement, gave a promising yield of 89% (entry 2). Importantly, the catalyst loading could be reduced to only 5 mol%, providing the product in a comparably high yield (84%, entry 3). B. Zank went on to show that other α-substituted enals (α-benzylacrolein and α-bromoacrolein) are compatible with the diazepane catalyst. Furthermore, different dienes (1-acetoxy-1,3-butadiene, isoprene and 1,3-cyclohexadiene) were also reactive in the Diels-Alder reaction with methacrolein using the diazepane catalyst. This reactivity was a promising start for this project.

Table 3.1 Initial screening of the Diels-Alder reaction

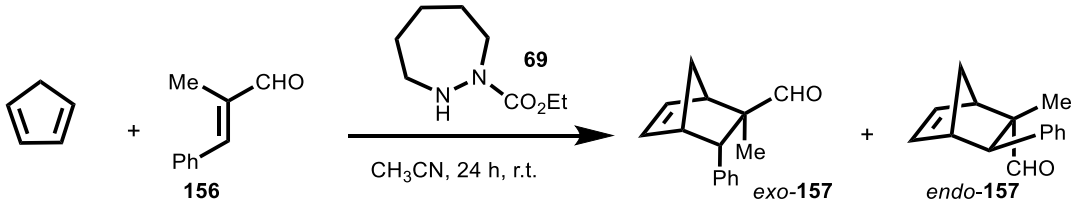

Entry	Catalyst loading	Acid	Yield
1	50 mol%	HCl (50 mol%)	7%
2	50 mol%	TfOH (50 mol%)	89%
3	5 mol%	TfOH (2 mol%)	84%

3.2 Optimization of reaction conditions

Optimization of reaction conditions for catalyst **69** had already been performed for the intramolecular Cope rearrangement with the 2-carboxaldehyde-1,5-dienes but a comprehensive screening of conditions was conducted to find the optimal conditions for the intermolecular Diels-Alder reaction.

3.2.1 Catalyst loading and acid co-catalyst

The first parameters that were investigated were the catalyst loading and acid co-catalyst for the Diels-Alder reaction between cyclopentadiene and α-methylcinnamaldehyde. The reactions were performed in NMR tubes in deuterated acetonitrile with internal standard and the conversions were monitored by NMR. The set up for these experiments is as follows: the catalyst was dissolved in appropriate solvent, acid and internal standard were added and mixed well. The aldehyde and finally diene were added and then the reaction mixture was stirred (or shaken if performed directly in a NMR tube). Conversion at 24 h was reported to consistently compare entries however, usually 2-6 time points were taken.

The optimization started with the initial conditions used by B. Zank, using 50 mol% catalyst with 50 mol% HCl (pKa -7) which gave 13% conversion in 24 h (Table 3.2). Switching to the more acidic triflic acid (pKa = -14) gave >95% conversion (entry 2) and when lowering catalyst loadings to 20, 10 and 5 mol%, only slight drops in conversion were observed (81%, 78% and 76%, respectively, entries 3-5). The weaker acid TFA (pKa = 0.2) only gave a trace of product (4%, entry 6). The 2:1 ratio of catalyst:acid was chosen for entry 3-6 because of a very exothermic polymerization reaction of CpH if even the slightest excess of TfOH was added. A solution to this was pre-forming the acid salt of diazepane **69** and then removing excess acid in high-vacuum. However, in some cases there was loss of acid over time under vacuum, regenerating the free base catalyst. It is noteworthy that all entries displayed high exo-selectivity.

Table 3.2. Catalyst loading and acid optimization

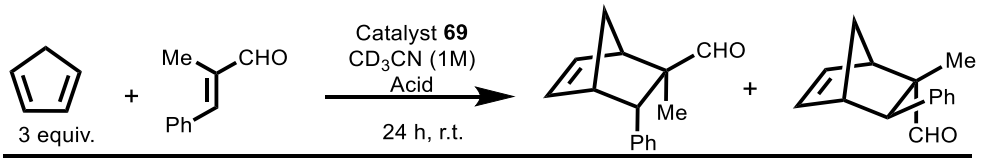

Entry	Cat. loading	Acid (mol%)	Conversion (%)	*Exo:Endo*
1	50	HCl (50%)	13	n.d.
2	50	TfOH (50%)	>95	16:1
3	20	TfOH (10%)	81	17:1
4	10	TfOH (5%)	78	21:1
5	5	TfOH (2.5%)	76	13:1
6	10	TFA (5%)	4	n.d.

3.2.2 Solvent screen

Solvents that are usually associated with iminium ion catalysis (see examples in chapter 1), were screened for the standard reaction between α-methylcinnamaldehyde and CpH using catalyst **69**. Switching from acetonitrile to another polar aprotic solvent such as nitromethane gave high conversion (>95%, entry 2, Table 3.3). Adding 5% water to the reaction-mixture killed the reactivity in both acetonitrile and nitromethane (entry 3 and 4). Methanol, dichloromethane and chloroform all had similar activity, around 20% conversion in 24 h (entries 5-7). Toluene, tetrahydrofuran and dimethyl sulfoxide gave no conversion (entries 8-10). Overall, the catalyst displays a significant solvent effect, where polar aprotic solvents like nitromethane or acetonitrile were superior but a solvent with similar dipole moment and higher dielectric constant such as DMSO gave no conversion. This reasons for this solvent effect are not yet understood.

Table 3.3 Solvent Screen

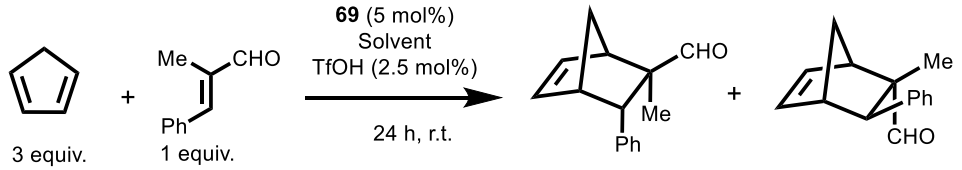

Entry	Solvent	Conversion (%)
1	CD_3CN	76
2	CD_3NO_2	>95
3	$CD_3CN:D_2O$ 19:1	-
4	$CD_3NO_2:D_2O$ 19:1	-
5	CD_3OD	18
6	CD_2Cl_2	22
7	$CDCl_3$	20
8	toluene-d_8	<5
9	THF	-
10	DMSO-d_6	-

3.2.3 Catalyst screening

To assess whether the ethyl diazepane carboxylate really was the superior catalyst, we screened a variety of hydrazides and primary and secondary amines (Figure 3.2). The acyclic hydrazide **49** gave 9% conversion while the 5-membered ring **50** only gave hint of product and 6-membered hydrazide **51** gave 6% (**49**, **50** and **51** were synthesized according to Tomkinson *et al.*[126]). These results followed the same trend as observed for the Cope rearrangement. The 7-membered hydrazide **69** provided 76% conversion. Inverse to what was observed with the Cope rearrangement, lower conversion was obtained with the 8-membered ring **70** (synthesized by Dainis Kaldre), potentially because of very rapid hydrolysis promoted by the highly strained iminium ion. MacMillan's imidazolidinone **40**, the benchmark catalyst for the Diels-Alder reaction,[78] had no activity for our model system. Jorgensen's diphenyl prolinol **56** which is known

to work with a select range of α-substituted enals (Chapter 1.4)[96] did not catalyze the cycloaddition of α-methylcinnamaldehyde with CpH. In fact, α-methylcinnamaldehyde is a very unreactive dienophile due to conjugation and steric bulk and is unprecedented as substrate in iminium ion catalysis, but have been used once in the thermal Diels-Alder reaction with 2,3-dimethyl-1,3-butadiene.[127] Work by Ishihara[97] and Maruoka[100] showed that primary amines had success with sterically encumbered enals. We explored some simple primary amines to investigate weather they could catalyze our model system to give insight to the reactivity of our hydrazide catalysts. Aniline (**67**) and benzyl amine (**91**) are more simple than the catalysts by Ishihara and Maruoka. However, the complexity of those catalysts is mainly to influence enantioselectivity and not reactivity. While aniline did show slight product formation (< 5%), benzyl amine was unreactive which demonstrates that our catalysts are more reactive with α-substituted enals. To support the hypothesis that the ethyl diazepane carboxylate catalyzed reaction proceeds via an iminium ion intermediate, we examined the *N*-methyl version of the catalyst (**158**) and found it was completely unreactive. Overall, this study confirmed that catalyst **69** was the most efficient catalyst.

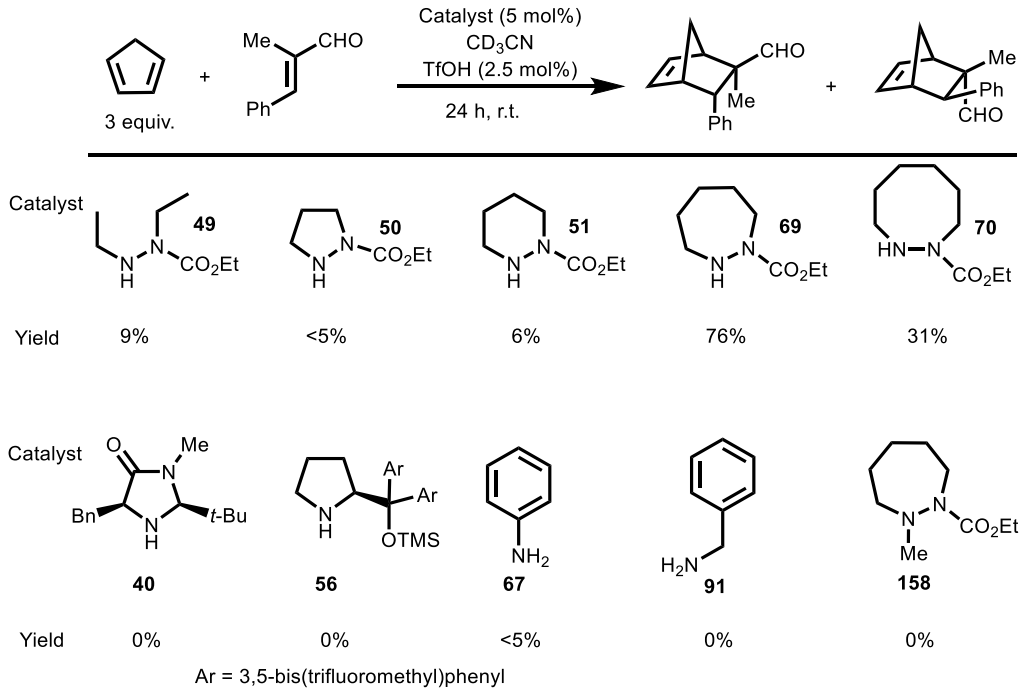

Figure 3.2 Catalyst Screening

3.3 Proton affinity, electron withdrawing group and kinetics

At this point we had a very active catalyst but we wanted to understand and explain why it had higher activity than the smaller hydrazide rings. Conventionally, most iminium ion catalysts in the literature are 5-membered imidazolidinone or pyrrolidine derivatives. There are a few exceptions such as Tomkinson's and Ogilvie's 6-membered hydrazides, piperidine for the Knoevenagel reaction and morpholine in asymmetric counterion-directed catalysis.[128] Bonini's group published a chiral aziridine carbinol for the Diels-Alder reaction and Friedel-Craft acylation.[129] Other 5-membered rings with different heteroatoms like a thiazolidine derived from cysteine have also been developed.[130] Apart from our work, the 7-membered ring is unprecedented in iminium ion catalysis, and its high reactivity was unusual and unexpected.

3.3.1 pKa and proton affinity

It is counterintuitive that a catalyst with a larger ring catalyst would be better at forming iminium ions considering that larger rings ought to incur higher A-1,3 strain due to a larger C-N-N bond angle (Figure 3.3). DFT calculations (performed by Dr. J. L. Gleason) show that by increasing the ring size from 5 to 7, the angle increased from 108.7° to 119.3°. The calculations also showed that the energy of the iminium ion increases by + 3.7 kcal/mol in going from the 5- to the 7-membered ring, which should disfavour iminium ion formation. However, we hypothesized that the stability of the iminium ion is not the key to reactivity. Rather, it is the formation of the iminium ion, a notion which has been previously supported by work from Tomkinson's group where correlation between higher catalytic activity and lower proton affinity was observed for their 5 and 6-membered hydrazides.[87] A crucial part of the formation of iminium ion is the initial proton transfer from the protonated ammonium of the catalyst to the carbonyl of the substrate as well as proton transfer in the tetrahedral intermediate. In separate work on simple iminium ion formation, Tomkinson and coworkers have suggested that these steps may be rate limiting.[131] A catalyst with lower proton affinity, meaning, a less basic catalyst, and therefor a more acidic ammonium, would promote these key steps. DFT calculated proton affinities showed a clear descending trend going to larger hydrazide rings (Figure 3.3 b). Calculations of the 5, 6 and 7-membered amine analogues **159-161** indicates that these are far more basic than their hydrazide

analogues (Figure 3.3 c). Proline derivative **198** has a higher proton affinity (by 6.9 kcal/mol) than the 5-membered hydrazide **50**. Experimental pKa values of 5, 6 and 7-membered hydrazides **50**, **51** and **69** were determined by standard titration and were found to decrease across the series; pKa 3.4 for **50**, 3.0 for **51** and 2.7 for **69**. The lower proton affinity is believed to produce the enhanced reactivity of the diazepane carboxylate.

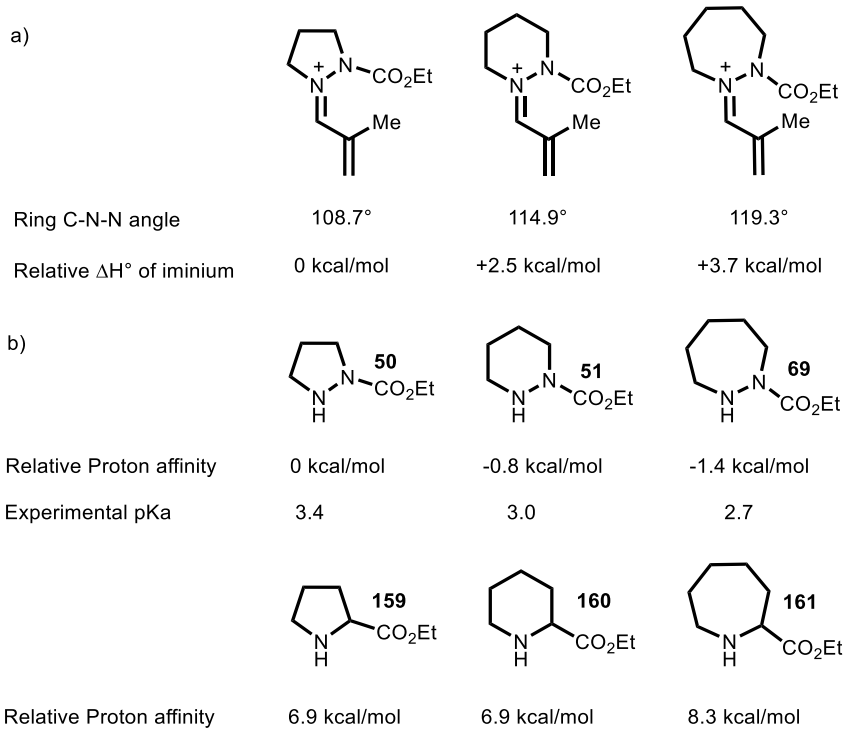

Figure 3.3 a) Calculated C-N-N bond angle and relative energy on iminium ion b) proton affinity for the 5 to 7-membered ring hydrazide series and their amine analogues

Several attempts were made to isolate or observe the iminium ion in the reaction, but these attempts were unsuccessful. Mixing diazepane **184** (chiral diazepane, see below) with methacrolein or α-methylcinnamaldehyde and perchloric acid (ratio 1:1:1) in deuterated solvents only showed the starting materials in the proton NMR spectrum. Similarly, for all prior screening reactions monitored by proton NMR, only peaks from starting materials and products were observed. Only when high catalyst loadings were used, and the reaction mixture was quenched with sodium borohydride, the reductive amination product could be isolated which supports its

existence and reactivity. These observations suggest that the iminium ion equilibrium lies far to the left.

3.3.2 Electron withdrawing groups

Given that proton affinity was found to be important, we chose to study the effects of the electron withdrawing group. We prepared acetate, trifluoroacetate, urea and thiourea protected hydrazides. The 6-membered ring was chosen because of slower kinetics with more reactive dienophiles such as tiglic aldehyde. The catalysts were synthesized in two steps from Boc piperazine **165**, itself prepared in 4 steps from *t*-butyl carbazate (**162**, Scheme 3.1). For methylacyl **166** and trifluoromethyl acyl **167**, acetic anhydride or trifluoracetic anhydride were used, respectively, and subsequent Boc deprotection with TFA yielded **166** and **167**. Benzyl isocyanate and benzyl thioisocyanate were used to install the urea and thiourea followed by milder phosphoric acid deprotection of the Boc group to give urea **168** and thiourea **169**, after attempts at TFA deprotection decomposed the intermediates.

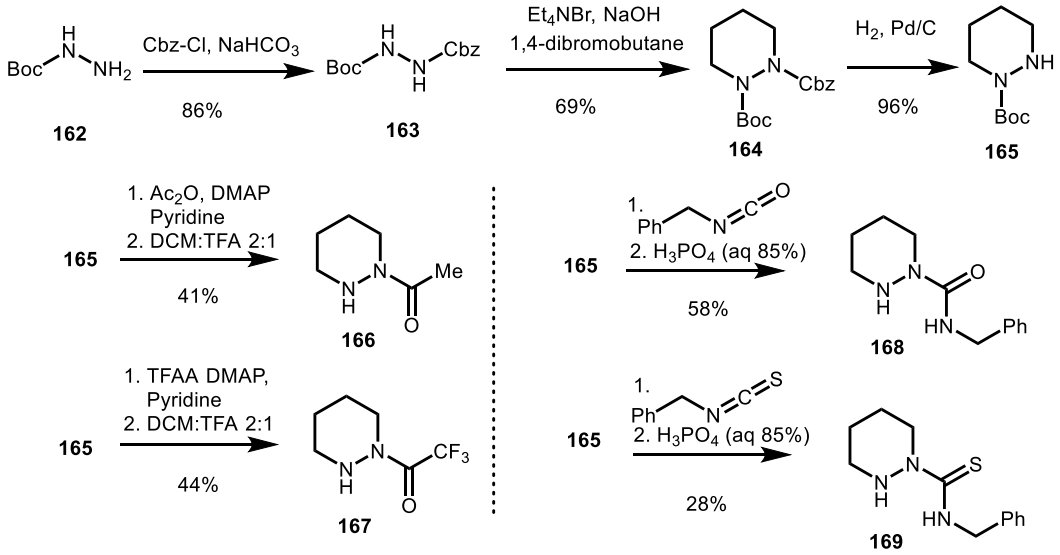

Scheme 3.1 Synthesis of 6-membered series

We were also interested in preparing sulfonamide derivatives but these turned out to be impossible to synthesize due to inherent instability of the sulfonyl hydrazine.[132] Scheme 3.2 displays attempts towards synthesizing tosylamide **270**. Although tosylation of piperazine **165**

proceeded cleanly, acidic deprotection conditions quickly gave decomposition and the only major product isolated was tolyl sulfinic acid (**170**). Other types of deprotection conditions like TMSOTf with 2,6-lutidine gave a complex crude and attempted thermal Boc removal returned mostly starting material. Alternatively, removal of the Boc protective groups followed by tosylation gave mainly decomposition, probably via **170** (Scheme 3.2, proposed mechanism), and some hydrazone **172**, arising via aerobic oxidation. The free hydrazines are unstable unless they are made into a salt and a pure sample converts into the corresponding hydrazone in less than 24 h in $CDCl_3$. Attempted reduction of hydrazone **171** with $NaCNBH_3$ or $NaBH_4$, again afforded only decomposition. Our proposed mechanism for decomposition is similar to work performed by Myers' group for deoxygenation reactions.[132]

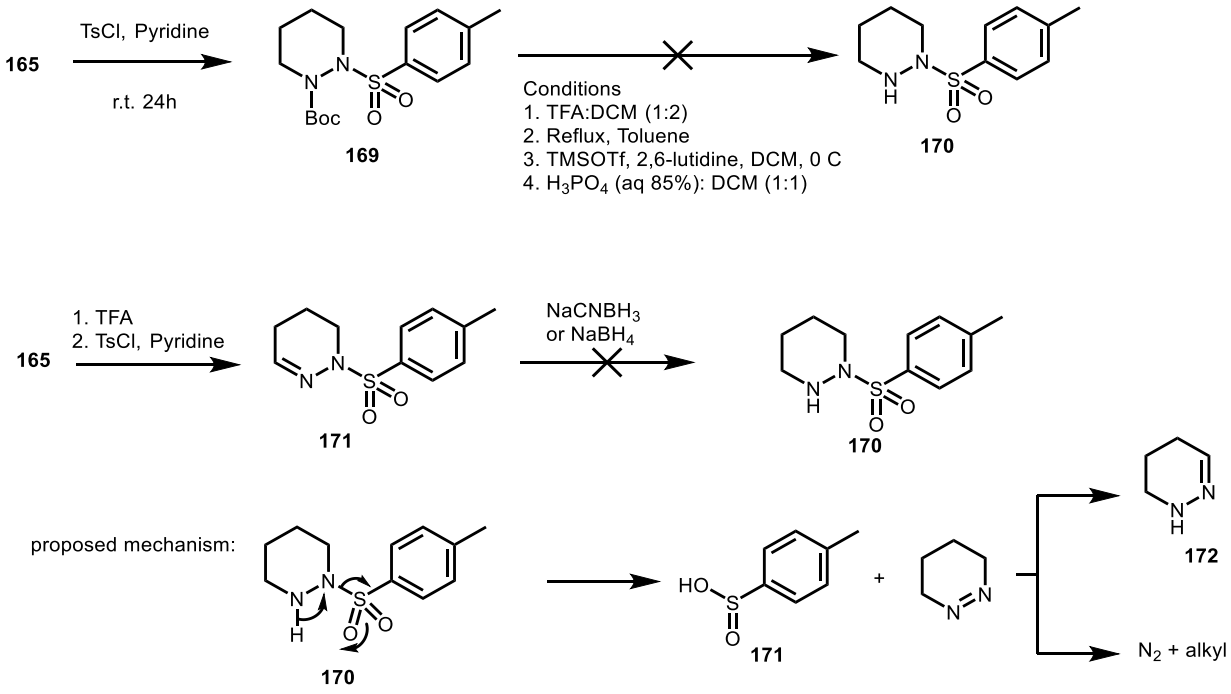

Scheme 3.2 Failed attempts towards structure 170

Assessing the various hydrazides prepared above showed a slight correlation between yield and proton affinity (Figure 3.4 and 3.5). Acetamide (**166**) and ethyl carbamate (**51**) have lower calculated proton affinity (PA) than urea (**168**). Both catalysts **166** and **51** gave better conversions supporting correlation between proton affinity and catalytic activity of the hydrazide. Trifluoroacetamide (**167**) was calculated to be far less basic than any other catalyst, PA = 206.5 kcal/mol vs 218.9 kcal/mol for diazepane **69**. However, trifluoroacetamide **167** provided a cloudy

solution once the triflic acid was added indicating solubility problem for the formed ammonium salt, and **167** had no activity. Thiourea **169** gave no conversion and NMR after 24 h showed no ^{1}H NMR signals of the catalyst indicating its decomposition under the reaction conditions.

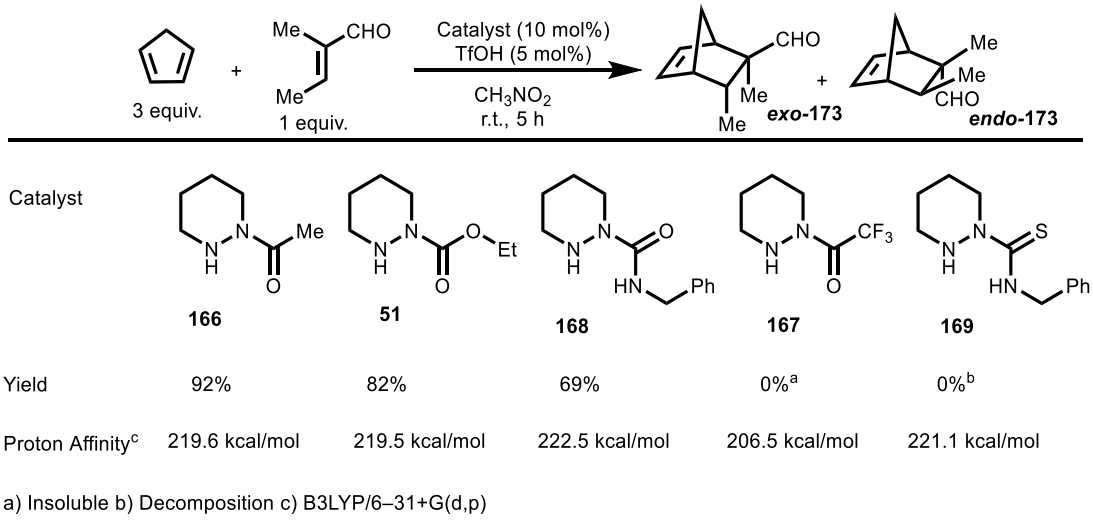

Figure 3.4 Conversion at 5 h and calculated proton affinity.

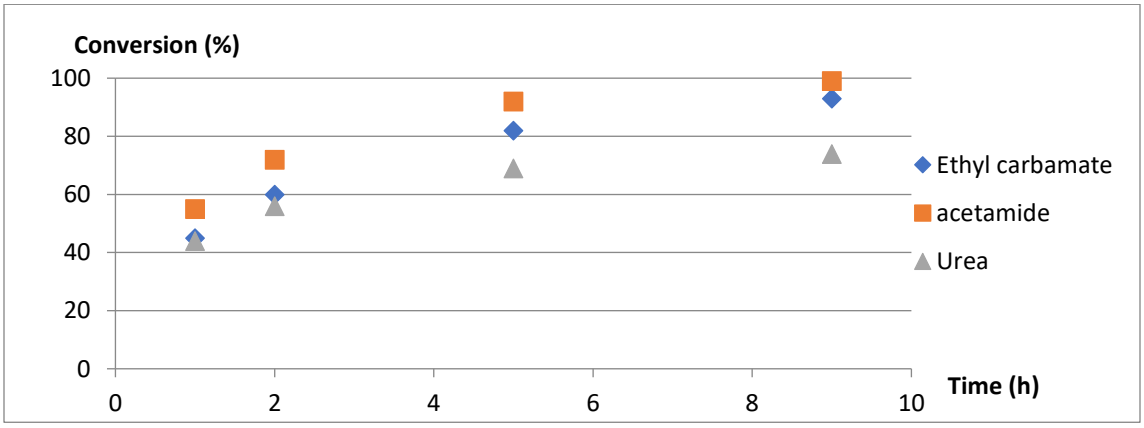

Figure 3.5 Graph showing conversion for 166, 51 and 168 against time

3.3.3 Diazepane carboxylate vs MacMillan's imidazolidinone catalyst

We compared the diazepane with MacMillan's imidazolidinone for the non-α-substituted enal cinnamaldehyde, where the rate-determining step is believed to be the cycloaddition (Figure 3.6).[78] Diazepane carboxylate **69** reached completion in 3h and had only slightly higher reactivity

than Macmillan's imidazolidinone catalyst **40** (82% conversion in 3 h). The diazepane is losing most of its edge for more reactive dienophiles where forming the iminium ion is not the rate determining step. The 6-membered hydrazide **51** only proceeds to 32% conversion in 3h. All three catalysts reached completion in 24 h and isolated yields over 90% with ~2:1 *exo:endo* selectivity. This shows that the diazepane catalyst **69** is still more reactive than the conventional imidazolidinone catalyst for a less sterically hindered enal but not as profound as has been observed for α-substituted enals.

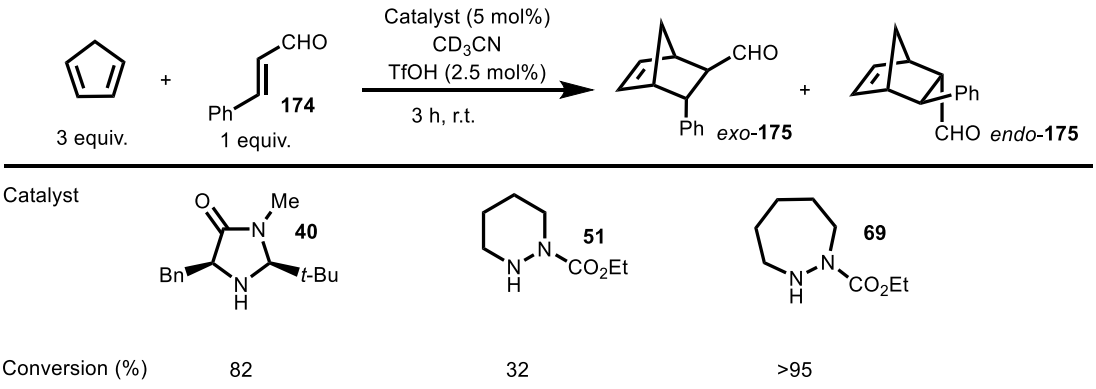

Figure 3.6 Comparing hydrazide 51 and 69 with 40 for non α-substituted enal

3.4 Scope of the Diels-Alder cycloaddition with catalyst 69

An examination of the scope of the Diels-Alder reaction with catalyst **69** showed that a wide variety of dienes and dienophiles can be used. The dienophile scope used CpH as the diene and standard reaction conditions with 10 mol% catalyst, 5 mol% TfOH, in nitromethane at 1 M with respect to the aldehyde (Figure 3.7). The smaller methacrolein and tiglic aldehyde were much more reactive than α-methylcinnamaldehyde and proceeded to completion in less than 5 h. Methacrolein achieved good *exo*-selectivity (*exo:endo* 7:1) and addition of the β-methyl group in tiglic aldehyde affords excellent *exo*-selectivity (*exo:endo* >19:1). The larger α-benzylacrolein also had high conversion and good *exo*-selectivity in 5 h (*exo:endo* 8:1) and **178** was isolated in 78% yield. α-Methylcinnamaldehyde and α-bromocinnamaldehyde were both slower as expected but gave high conversions and isolated yields (92% of **157** and 84% of **176**) in 20 h with great *exo*-selectivity (*exo:endo* 14:1 and *exo:endo* 15:1, respectively). Reactions of these enals are

unprecedented with iminium ion catalysis. The isolated yields for all adducts in Figure 3.7 are 78-92% with the exception of **177** (60%), presumably due to product volatility.

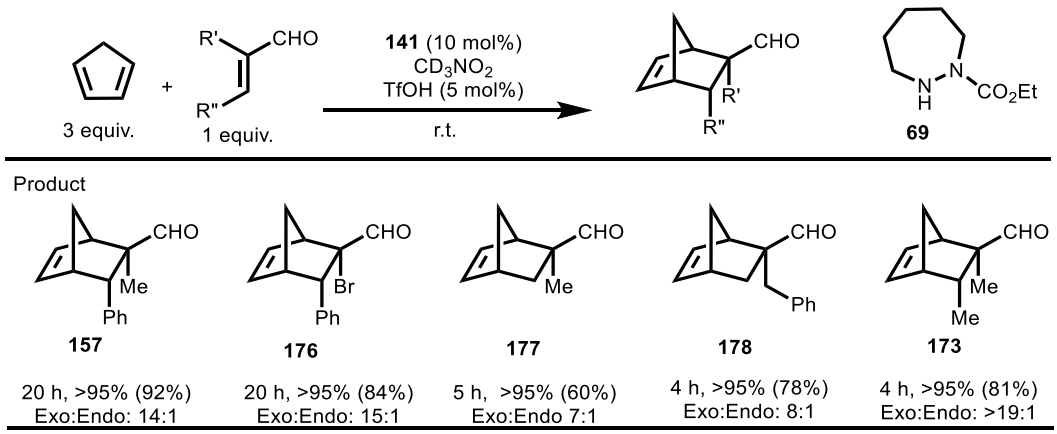

Exo:Endo ratio determined by 1H-NMR, isolated yield within parenthesis.

Figure 3.7 Dienophile scope of the Diels-Alder reaction

A variety of dienes were screened in reactions with methacrolein (Figure 3.8). They generally proceed with longer reaction times compared to the highly reactive CpH. Isoprene gave high yield (91%) and excellent regioselectivity and good yield (67%) was achieved for 2,3-dimethylbutadiene. Cyclohexa-1,3-diene and 1-acetoxy-1,3-butadiene were less reactive and needed higher catalyst loading and longer reaction times but both afforded high yields (78% and 62% isolated yield, respectively) with moderate *endo*-selectivity.

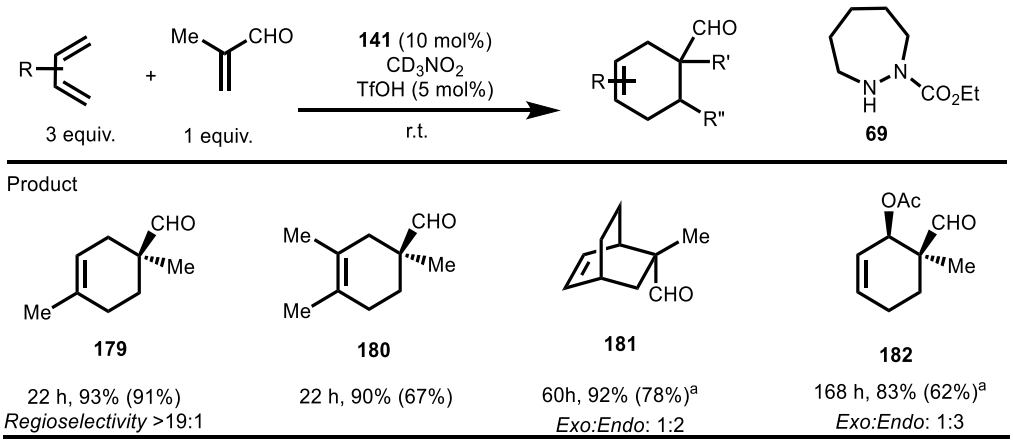

a) 20 mol% catalyst, 10 mol% TfOH. Exo:Endo ratio determined by 1H-NMR, isolated yield within parenthesis.

Figure 3.8 Diene scope of the Diels-Alder reaction

The study of achiral diazepane catalyst **69** was limited to these examples and was performed to confirm that the catalyst works for different dienes and dienophiles before progressing to the development of an enantioselective catalyst. The reactions presented in the next chapter will expand the scope even further.

3.5 Conclusion

Ethyl diazepane carboxylate has been established as excellent catalyst for iminium ion catalysis of α-substituted enals. Granted, both MacMillan's imidazolidinone and Jorgensen's prolinol are chiral catalyst with more bulk on the ring which might affect reactivity. Studies were performed on the catalyst to investigate and explain the advanced activity of catalyst **69**, and the key feature determined to be its lower proton affinity. A diverse scope was achieved with high conversions and yields and moderate to excellent regio- and diastereoselectivity were observed.

3.6 References

[126] Brazier, J. B.; Cavill, J. L.; Elliott, R. L.; Evans, G.; Gibbs, T. J. K.; Jones, I. L.; Platts, J. A.; Tomkinson, N. C. O.; *Tetrahedron* **2009**, *65*, 9961.

[127] Baldwin, J. E.; Lusch, M. J.; *J. Org. Chem.* **1979**, 44, 1923.

[128] Mayer, S.; List, B.; *Angew. Chem. Int. Ed.* **2006**, *45*, 4193.

[129] Bonini, B. F.; Capito, E.; Comes-Franchini, M.; Fochi, M.; Ricci,A.; Zwanenburg, B.; *Tetrahedron: Asymmetry* **2006**, *17*, 3135.

[130] Hayashi, Y.; Gotoh, H.; Tamura, T.; Yamaguchi, H.; Masui, R.; Shoji, M.; *J. Am. Chem. Soc.* **2005**, *127*, 16028.

[131] Evans, G. J. S.; White, K.; Platts, J. A.; Tomkinson, N. C. O.; *Org. Biomol. Chem.* **2006**, 4, 2616.

[132] Myers, A. G.; Movassaghi, M.; Zheng, B.; *J. Am. Chem. Soc.* **1997,** 119*,* 8572.

Chapter 4

Development of enantioselective diazepane carboxylate catalyst for the Diels-Alder reaction

4.1 Enantioselective diazepane carboxylate

This chapter describes the effort dedicated to developing an enantioselective version of the diazepane carboxylate catalyst presented in Chapter 3. While the reactivity and scope of catalyst **69** are excellent, reaching high enantioselectivity proved very difficult. The research mainly focused on three areas: to install bulky substituents on the ring, tuning the electron withdrawing group including chiral electron withdrawing groups and computational work to understand the selectivity. The conclusions of these studies led to a final catalyst containing a combination of a stereogenic centre on the ring and on the electron withdrawing group. This catalyst displayed good reactivity and high *exo*-, regio- and enantioselectivity for a wide range of alpha-substituted dienophiles for the Diels-Alder cycloaddition.

4.1.1 Design of enantioselective catalyst

There were three positions in diazepane carboxylate catalyst **69** that logically stood out as modifiable sites to develop a chiral catalyst (Figure 4.1). They were, on the C3 carbon adjacent to the proton-bearing nitrogen, on the C7 carbon adjacent to the nitrogen bearing the carbamate or incorporated into the electron withdrawing group. Among these possibilities, the first has the most precedent in the literature, including MacMillan's imidazolidinone and Jorgensen's prolinol.[78,133] The third have some precedent in proline derivatives.[134] The middle possibility, C7, is intriguing. While no other group has reported such a catalyst, in our prior preliminary work for the Cope rearrangement, C7 modification proved to give the highest enantioselectivity. We presume that this was due to a gearing effect where the C7 stereocenter would influence the conformation at the carbamate unit. One could also imagine introducing stereocenters at positions 4, 5 and/or 6; However, this was not part of the initial planning due to their remoteness from the site of reactivity.

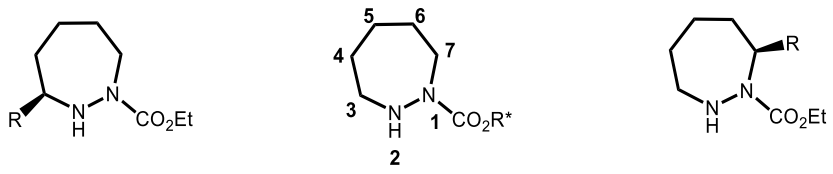

Figure 4.1 Potential substitutions of chiral catalysts

4.1.2 Synthesis of chiral catalyst

The first two chiral catalysts that were designed incorporated a phenyl or a benzyl at the C3 or C7 positions (Figure 4.2). Dainis Kaldre initially synthesized catalyst **78** with the phenyl group on C3 and with a Cbz group instead of ethyl carbamate and catalyst **80** with the phenyl group on C7 and ethyl carbamate. Both followed the same synthetic route (Scheme 4.1) which has been repeated for this project on multigram scale.

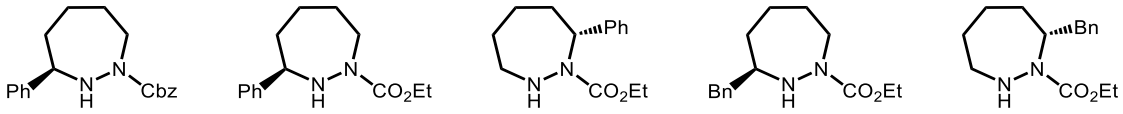

Figure 4.2 Structure of proposed catalysts

In order to have a better comparison between catalysts, we sought out to prepare the ethyl carbamate analogue (**183**) of catalyst **80**. The synthesis of ethyl carbamate catalyst **183** is similar to that of catalyst **80**.[135] Starting from 5-bromovaleric acid, the Weinreb amide was prepared and then phenyl Grignard reagent was added to form phenyl ketone **187** (Scheme 4.1). Corey-Bakshi-Shibata (CBS) reduction of the ketone afforded alcohol **188** in good yield (93%) and enantioselectivity (97% ee). After acetate protection of the alcohol, the bromide was displaced with *t*-butyl carbazate to form hydrazide **189**. Chemoselective acylation with ethyl chloroformate or benzyl chloroformate followed by mild deprotection of the acetate with potassium carbonate in methanol yielded hydrazide **190** or **191**, respectively. Compound **189** could be used for derivatization but the later intermediate **192,** with easily and orthogonally removable Cbz and Boc groups was chosen to reduce step count and provide maximum synthetic flexibility. Several attempts at closing the ring gave a loss in enantiopurity and low yield, affording a significant amount of styrene side-product by elimination. Higher concentrations gave partial racemization, probably due to competing S_N1 reaction. The Mitsunobu reaction gave perfect stereoretention but low yield. The most successful approach was mesylation of the alcohol at 0 °C with methanesulfonic anhydride followed by ring closure with sodium hydride in a highly dilute mixture (0.01 M) in THF/DMF (4/1) to give **192** (78% yield, 94% ee). The dilute conditions turned out to be essential to close the ring without a major loss in enantiopurity. Final Boc deprotection

gave hydrazide **78** in 97% yield and TFA deprotection followed by ethyl carbamate formation and hydrogenation provided catalyst **80** in 79% yield.

Alcohol **190** underwent the same sequence of mesylation, NaH ring closure and Boc deprotection to give ethyl carbamate catalyst **183** (52% yield, 92% ee). While screening could be achieved with this material (94% or 92% ee), this required scaling results for catalyst enantioselectivity, a process which may not be 100% reliable if any non-linear effects are present.

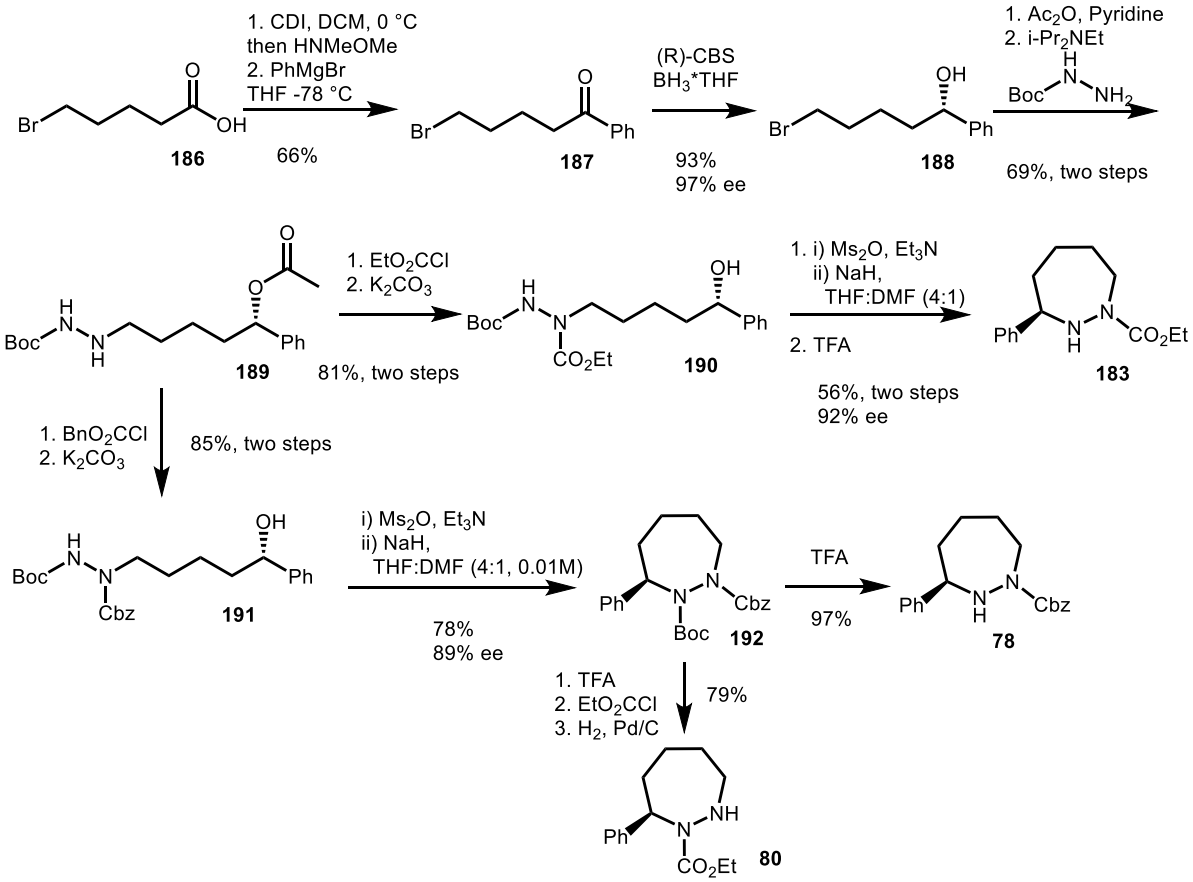

Scheme 4.1 Synthetic route to catalyst 183, 78 and 80

Inspired by the enantioselectivity induced by MacMillan's imidazolidinone catalyst we hypothesized that a benzyl group on the ring could be beneficial. Unfortunately, the synthetic scheme used for the phenyl catalyst could not be used for the benzyl catalyst. One of the key steps for the synthesis of the chiral diazepanes presented in this chapter is to introduce the stereocenter(s) in high enantioselectivity but no unified synthetic route has been found. The challenge of the benzyl group involves setting a stereogenic centre on an aliphatic chain without any major steric

bias. The CBS reduction employed for **183** would not be expected to give high ee. It was imagined that the stereogenic centre could come from the opening of chiral epoxide **196**. Unfortunately, direct enantioselective Shi or Jacobsen-Katsuki epoxidation on a terminal olefin with high enantiomeric excess did not have enough literature precedent. However, epoxidation of allyl benzene (90% yield) followed by Jacobsen hydrolytic kinetic resolution of the epoxide (38% yield) yielded enantiopure epoxide **196** (>99 % ee) in 2 steps from cheap, commercially-available starting material (Scheme 4.2). Epoxide **196** was opened at the terminal position by Cu catalyzed addition of allyl magnesium bromide to provide the desired chiral carbon skeleton **197** in 82% yield. A significant amount of effort was spent trying to displace sulfonate derivatives of alcohol **197** with different hydrazines without success. Usually no reaction was observed under mild conditions and with harsher conditions elimination to the styrene **199** was the major pathway. The Mitsunobu reaction was also tried on alcohol **197** using DIAD and PPh_3 with hydrazone **198** (the product of condensing Boc carbazate with acetone) but gave a complex crude mixture where the major product was again the elimination product **199**.

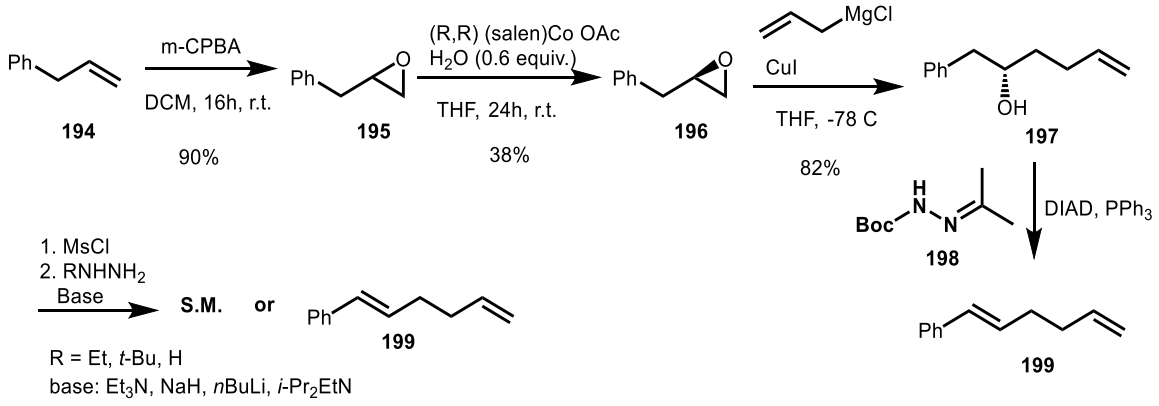

Scheme 4.2 Attempts towards synthesis of benzyl substituted catalyst

To solve the elimination problems noted above, we resorted to a stepwise introduction of the hydrazine. The more nucleophilic sodium azide was used to smoothly form the chiral azide which gave the amine **200** in 72% yield after Staudinger reduction (Scheme 4.3 a). The chiral amine was then converted to hydrazide **202** (86% yield BRSM) using oxaziridine **201** (Scheme 4.3 c)[136,137]. This reagent, developed by Armstrong and coworkers, acts as an electrophilic nitrogen source. The N-N coupling gave a tri-nitrogen species as a major by-product, however, using sub-stoichiometric amounts of oxaziridine and recovering and resubmitting any unreacted amine

starting material allowed for sufficient amount material to be processed. Cbz protection of hydrazide **202** followed by hydroboration oxidation gave alcohol **203** (2 steps, 64% yield). The alcohol **203** was mesylated and the ring was closed using TBAF as mild base. Amine bases or NaH were inferior in this reaction. A final series of carbamate modifications then gave C3 benzyl catalyst **184**. To introduce the benzyl on C7 (Scheme 4.3 b) the same pathway was used but with the introduction of the ethyl carbamate on hydrazide **202** and then hydroboration oxidation, mesylation, TBAF ring closure and finally TFA deprotection of the Boc group to yield catalyst **185** in 49% yield over 4 steps.

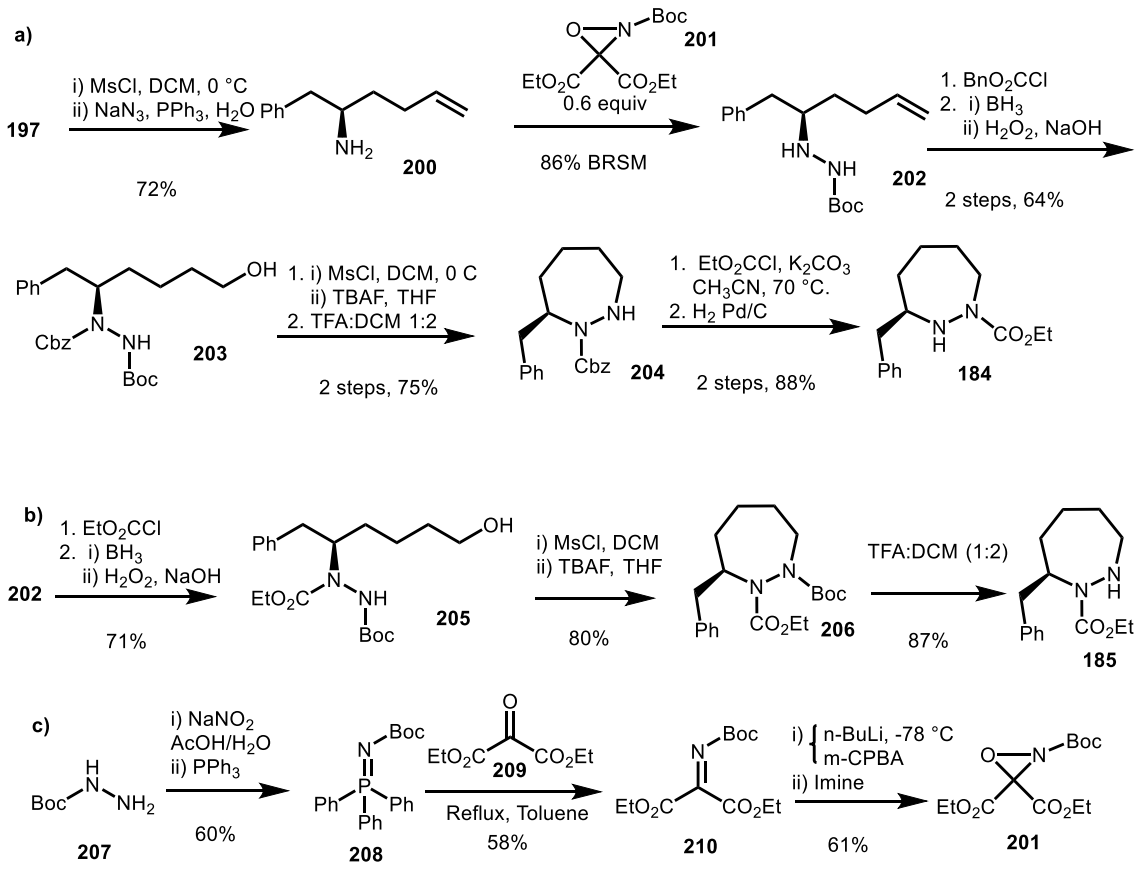

Scheme 4.3 Syntheses of benzyl substituted catalysts 184 and 185.

4.1.3 Screening of chiral catalysts

We began our initial screen of chiral catalyst using CpH and α-methylcinnamaldehyde under the optimized conditions from our prior work on achiral diazepane catalyst **69**. However,

lower reactivity was observed with the extra bulk around the nucleophilic nitrogen, preventing it from reaching completion within 24 h. Because of the limited reactivity of α-methylcinnamaldehyde, tiglic aldehyde was selected to be the model dienophile for the enantioselective reaction.

Upon screening with tiglic aldehyde and CpH, we found that both phenyl catalysts **78** and benzyl catalyst **184** with stereocenters on C3 adjacent to the NH, gave higher enantioselectivity than their counterpart substituted on C7 (Figure 4.3). However, in all cases, the enantioselectivity was very modest, with only 17-20% ee for the C3 substituted catalysts, versus 9% ee for both the C7 substituted catalyst (**80** and **185**). These results prompted us to explore the C3 substituted catalysts more in depth.

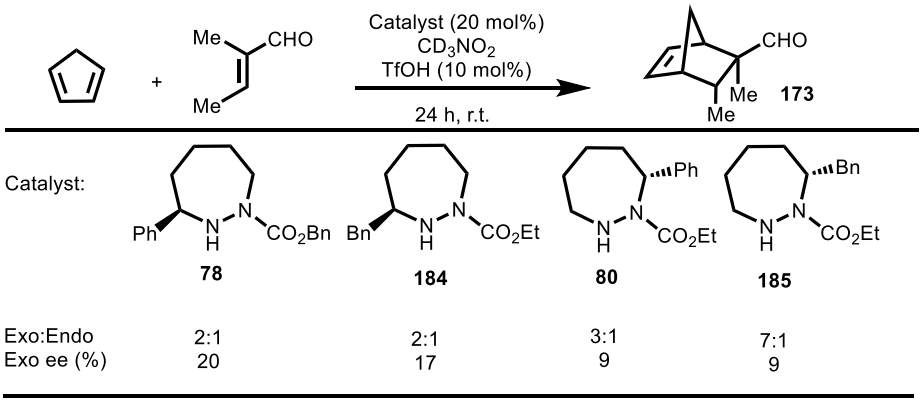

All conversions >90%. Exo:Endo ratio and conversion determined by 1H-NMR vs mesitylene as internal standard, ee determined by GLC using Chiraldex B-DM column.

Figure 4.3 Testing of chiral catalyst.[1]

4.1.4 Optimization of conditions for the Diels-Alder reaction

Our initial work discussed in Chapter 3 had optimized for reactivity and not enantioselectivity, so a new optimization was conducted for catalyst **78** (Table 4.1). Switching to another polar aprotic solvent like acetonitrile gave an increase in enantioselectivity (47% ee, entry 2) but with the same moderate exo selectivity. Perchloric acid gave similar results to TfOH (entry

[1] **Reaction run in NMR tube with 0.1 mmol of tiglic aldehyde (1 M), 0.5 mmol of CpH and 20 mol% of catalyst and 10 mol% of TfOH.**

3). Switching to the polar protic solvent EtOH gave moderate to good enantioselectivity for strong acids (TfOH, $HClO_4$, HCl, $PhSO_3H$ and Tf_2N) with high *exo* selectivity (entries 4-8) but with a slight drop in enantioselectivity for HCl. A strong acid is evidently required since the use of TFA led to no detectable conversion. Perchloric acid achieved higher enantioselectivity and *exo*-selectivity and was selected as the optimal acid co-catalyst for the Diels-Alder reaction. Generally, only the strength of the acid appears important for the catalytic system and not the type or size of the counter ion of the acid except for chloride which provided slightly lower enantioselectivity.

Investigation into other solvents such as brine, toluene and chloroform gave low to moderate enantiomeric excess (entries 9,10 and 12) while THF, *i*-PrOH/DCM 85/15 and *i*-PrOH (entries 11, 13 and 14) were nearly identical to EtOH. Brine only gave 80% conversion and was the only entry that is not over 90% conversion. Finally, cooling down the reaction gave better enantioselectivity and *exo*-selectivity as expected (entries 15 and 16). Other variables such as lower reaction concentrations (0.5 M and 0.2 M) did not change the enantioselectivity and using 2 equivalents of the diene relative to the dienophile did not affect the enantioselectivity. Later in this chapter, the electrostatic interactions that are believed to be dictating the stereochemical outcome of our catalyst system will be discussed. Briefly, the non-polar solvents, which promote and stabilize these interactions, unfortunately provided lower enantioselectivity in our system. In general, polar aprotic solvents promote reactivity better than protic solvents and non-polar solvents. However, no trend was observed for enantioselectivity. It was found that reasonably non-polar solvents such as toluene and chloroform provided moderate enantioselectivity (42 and 30% ee, respectively) while polar non-protic solvents such as acetonitrile provided comparable levels of enantioselectivity (40% ee). Thus, regarding stereoselectivity, no correlation between solvent polarity or dielectric constant has been found which sufficiently explains the observed solvent effects.[138]

Table 4.1. Screening of solvent and acid with catalyst 78

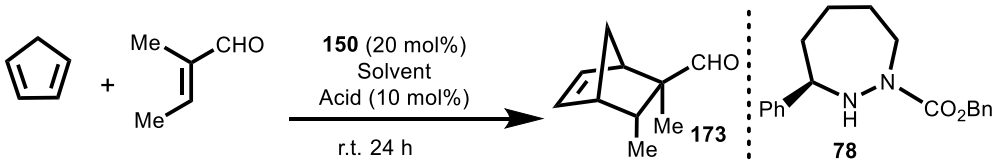

Entry	Solvent	Acid	Endo:Exo[a]	Exo ee (%)[b]
1	CH_3NO_2	TfOH	1:2	20
2	CH_3CN	TfOH	1:1.5	47
3	CH_3CN	$HClO_4$	1:2	40
4	EtOH	TfOH	1:9	62
5	EtOH	$HClO_4$	1:9	62
6	EtOH	HCl[c]	1:16	46
7	EtOH	$PhSO_3H$	1:9	58
8	EtOH	Tf_2NH	1:10	59
9	Brine[d]	$HClO_4$	1:8	44
10	$CHCl_3$	$HClO_4$	1:1.4	30
11	iPrOH:DCM (85:15)	$HClO_4$	1:6	62
12	Toluene	$HClO_4$	1:4	42
13	i-PrOH	$HClO_4$	1:6	59
14	THF	$HClO_4$	1:11	58
15	EtOH	$HClO_4$	1:11	64[e]
16	EtOH	$HClO_4$	<1:19	71[f]

All conversions > 90%.[a)] Determined by ^{1}H NMR. [b)] Determined by GLC. [c)] 20 mol% catalyst. [d)] 80% conversion [e)] 0 °C, [f)] -25 °C.

Benzyl substituted catalyst **184** gave very similar enantioselectivity to phenyl substituted catalyst **78** in our initial screen and was subjected to an additional smaller optimization for enantioselectivity parallel with that of catalyst **78** (Table 4.2). Analogous trends were observed for catalyst **184**, although they were not as pronounced (Entries 1-4). In this screening, brine gave the highest enantioselectivity. However, it was the only solvent that provided less than 90% conversion (71%, conversion, 37% ee, entry 5). Again, the highest enantioselectivity was observed for polar protic solvent EtOH (25% ee, entry 6) although the enantioselectivities were not as high as for catalyst **78** (62% ee).

Table 4.2. Optimization table for catalyst 184

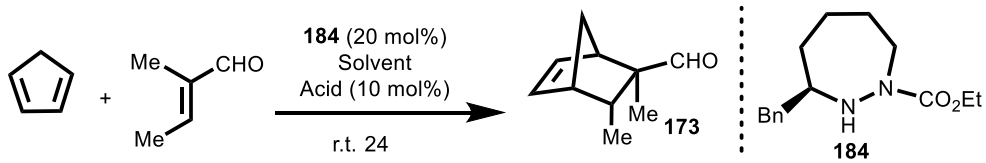

Entry	Solvent	Acid	*Endo:Exo*[a]	*Exo* ee (%)[b]
1	CD_3NO_2	TfOH	1:1.7	17
2	CD_3NO_2	HCl[c]	1:6	10
3	CH_3CN	TfOH	1:4	14
4	CH_3CN	$HClO_4$	1:5	16
5	Brine[d]	$HClO_4$	>1:19	37
6	EtOH	$HClO_4$	>1:19	25
7	MeOH:H_2O (9:1)	$HClO_4$	>1:19	14

All conversions > 90%. [a] Determined by ^{1}H NMR. [b] Determined by GLC. [c] 20 mol% cat. [d] 71 % yield

4.1.5 Divergent synthesis of chiral catalyst

Although improvements in enantioselectivity and *exo*-selectivity could be achieved, especially for catalyst **78** through optimization of solvent, acid co-catalyst and temperature, it was clear that it would be necessary to design and synthesize new catalysts to improve selectivity to more useful levels.

The alkyl and aryl catalyst above required unique, compound specific syntheses which was an inefficient method for derivatization. Several methods were envisioned to allow for late stage diversification of the catalyst to screen larger substituents and substituents with different polarity and potential for hydrogen bonding. Including an oxygen, which could serve as a point for modification via redox and addition chemistry, was considered to be the path with the highest synthetic utility.

In the retrosynthesis of the catalyst, we saw the potential in creating the diazepane dicarboxylate with a methyl alcohol group on position C3, quickly from 6-chlorohexanol. In the forward direction (Scheme 4.4), Swern oxidation of alcohol **212** to aldehyde **213** gave higher yield

(93%) and cleaner conversion than IBX. Aldehyde **213** underwent L-proline catalyzed alpha hydrazination with di-*t*-butyl azodicarboxylate **214** or dibenzyl azodicarboxylate **215** and was quenched with $NaBH_4$ to reduce the intermediate aldehydes to alcohols **216** and **217**. To evaluate enantioselectivity, a racemic sample used as a standard for chiral HPLC analysis was prepared with DL-proline and showed that that the hydrazination proceeded in 94% ee. Initial TBS protection of alcohol **214** followed by ring closing using NaH as the base gave a low yield of desired product. However, direct TBAF closure onto the primary chloride gave the diazepane dicarboxylate **216** in 69% yield without need for protection of the alcohol. Diazepanes **216** and **217** served common intermediates for seven other catalysts.

These diazepane alcohols **216** and **217** could, with only two synthetic modifications, be converted into two different types of diazepane catalysts, accessing a catalyst bearing either a simple methyl alcohol substituent (**219**) with the potential of hydrogen bonding and a bicyclic diazepane carbamate (**218**) by closing the alcohol on to the benzyl carbamate. Treating alcohol **216** with NaH failed to close onto the Boc group to the bicyclic lactone but closed well onto Cbz group (alcohol **217**). Bicyclic carbamate **218** was isolated in 57% yield after Cbz deprotection. Using intermediate **216**, Boc deprotection and a regioselective ethyl carbamate formation yielded catalyst **219** in 64% yield.

To further access different substituents on position C3, an one pot TEMPO/$NaClO_2$ oxidation[139] of alcohol **216** was performed to generate carboxylic acid **220** (75%). Carboxylic acid **220** served as a second branching point and could be used to directly access both the carboxylic acid and the methyl ester as substituents on C3 of the diazepane catalysts. Carboxylic acid **220** was first subjected to simultaneous Fisher esterification/Boc deprotection to provide methyl ester substituted catalyst **221** in 64% yield after selective ethyl carbamate formation. Simple Boc deprotection with TFA of diazepane **220** followed by ethyl carbamate formation gave carboxylic acid substituted **222**, albeit in low yield (21%).

The carboxylic acid **220** was methylated with MeI/K_2CO_3 and the resulting ester was treated with 2.5 equivalents of PhMgBr leading to an intermediate which closed onto the Boc group to form the diphenyl bicyclic carbamate **223** in 25% yield. It was assumed that this reaction would generate diphenyl methylalcohol **226** (Scheme 4.5) instead of **223** and then NaH would be required to close to the bicyclic carbamate **223**. However, bicyclic diazepane carbamate **223** could

smoothly be converted into two diazepane catalysts, either bearing a very bulky diphenylmethyl substituent on C3 (**224**) or a more substituted bicyclic diazepane carbamate (**225**). Hydrogenation of **223** gave the more substituted diphenylmethyl substituted **224** (72%), albeit with a *t*-butyl carbamate instead of ethyl carbamate. Finally, direct Boc deprotection of **223** gave the more substituted bicyclic lactone **225** in high yield.

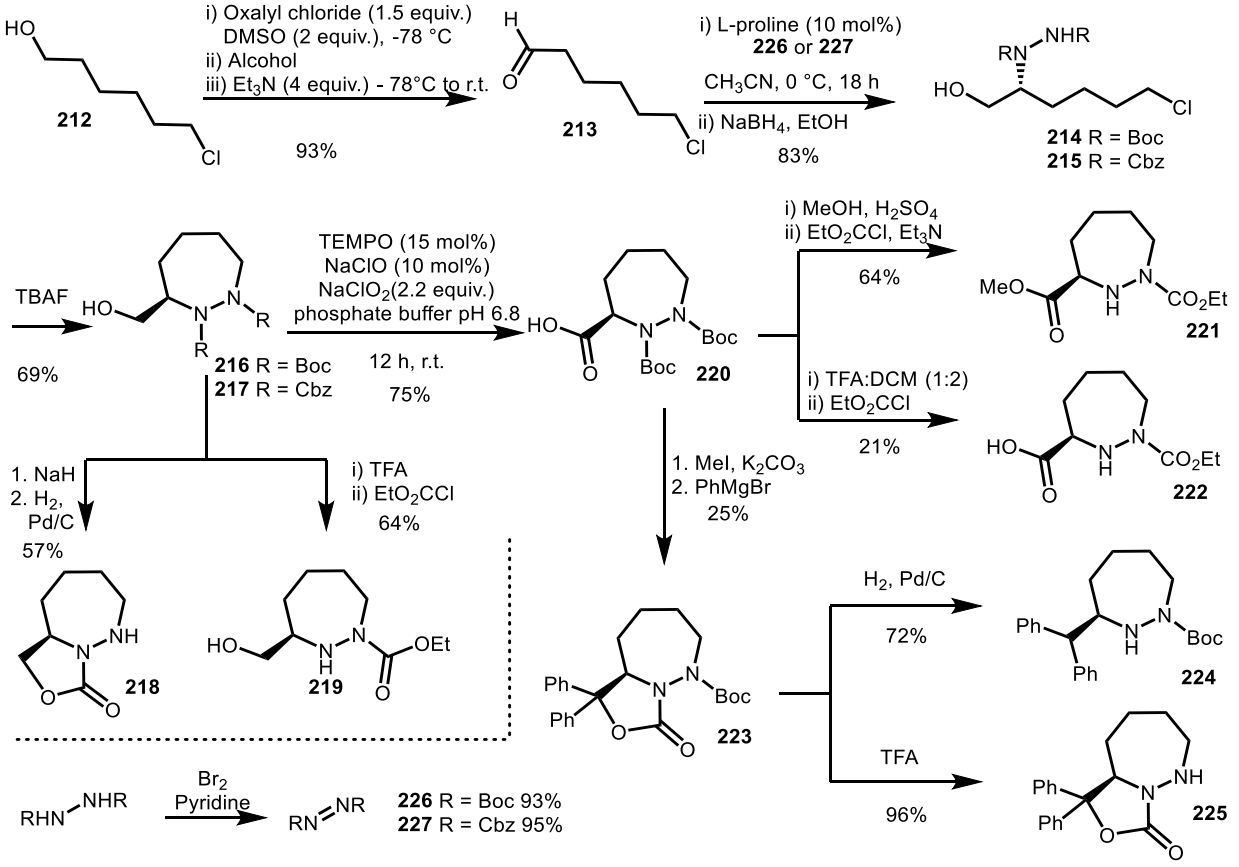

Scheme 4.4 Divergent route for C3 substituted catalysts

Our initial efforts towards **227**, a diphenylmethanol version of the catalyst, by methylating carboxylic acid **220** followed by Grignard reaction as described above gave, surprisingly, bicyclic carbamate **223**, which fortunately turned out to be a useful compound for further derivatization. In an alternative strategy, treatment of methyl ester **221** with 3 equiv. of PhMgBr gave diphenylmethanol **226** in low yield (23%). Attempts to add a TIPS group with TIPSOTf and 2,6-lutidine were unsuccessful and gave mostly decomposition with harsh conditions (Scheme 4.5). Effort towards **227** was ceased after the bulkier substituents produced poor enantioselectivity.

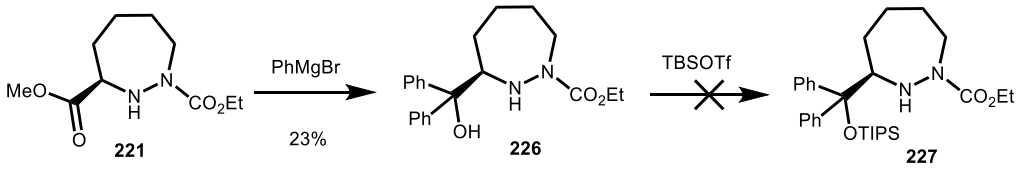

Scheme 4.5 Effort towards 227

We screened the new C3 substituted catalysts in our standard reaction and the results are summarized in Figure 4.4. Quite interestingly, the small methyl alcohol catalyst **219** gave the same moderate enantioselectivity, around 60% ee, as phenyl catalyst **183** and methyl ester catalyst **221**. However, the larger 1-naphthyl catalyst **226** (synthesized by Dainis Kaldre) gave a slight drop to 40% ee. More astonishingly, benzyl catalyst **184** gave 25% ee and the bulkier diphenylmethyl **224** only gave 10% ee. The bicyclic lactones catalysts **218** and the more substituted **225** also gave low enantioselectivity. Carboxylic acid catalyst **222** was tried under regular conditions without acid co-catalyst but the intramolecular carboxylic acid was not strong enough to carry out the reaction. Only 44% ee was achieved using perchloric acid as a co-catalyst. No consistent trend between size of the substituent and enantioselectivity was observed.

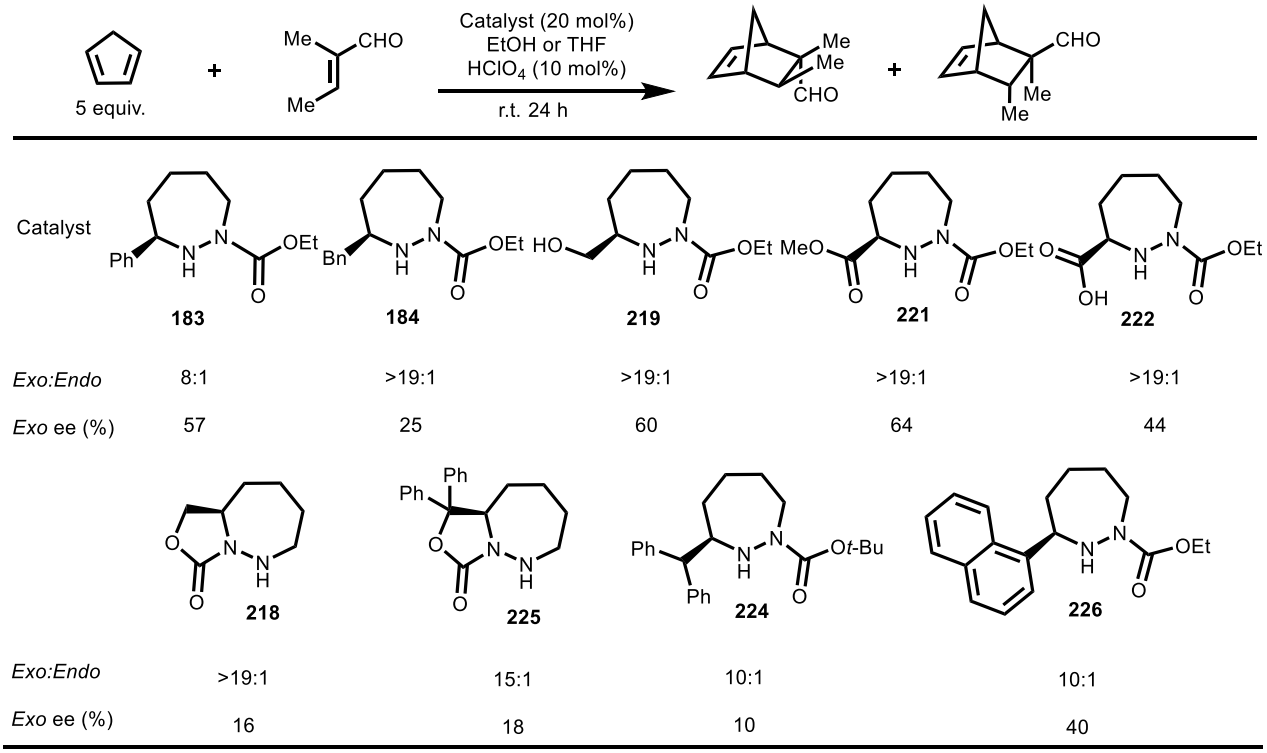

Exo:Endo ratio and conversion determined by 1H-NMR vs mesitylene as internal standard, ee determined by GLC using Chiraldex B-DM column.

Figure 4.4 Testing of synthesized catalyst[2]

4.2 Diazepane carboxylate with two chiral centers

With no clear trend observed by changing the groups at C3 it was clear that synthesizing additional C3 substituted diazepanes would not be the best approach to improve enantioselectivity. Instead, considering that (R)-**183** and (R)-**80** gave the same enantiomers of the Diels-Alder adducts, we envisioned that combining the two might have a cooperative effect to generate a superior catalyst (**228** Figure 4.5).

[2] **General conditions B: Reaction run in 0.5 dram screw cap vial with 0.1 mmol of tiglic aldehyde (1 M), 0.5 mmol of CpH and 20 mol% of catalyst and 10 mol% of TfOH in either THF or EtOH.**

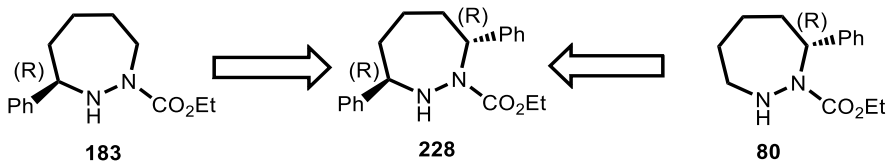

Figure 4.5 New design of catalyst

4.2.1 Synthesis of catalyst with two chiral centers

To synthesize the anti di-phenyl diazepane **228** we started with glutaric acid, which underwent double acyl chloride formation followed by Friedel-Craft acylation to form bis-phenyl ketone **229** (Scheme 4.6). Subsequent CBS reduction to give a statistical mixture of unreacted and mono- and di-reduced products using 1 equiv. borane afforded ketone **230** in 44% yield. Condensation of ketone **230** with ethyl carbazate yielded a 2:1 *E:Z* mixture of hydrazones **231**. The *E*-hydrazone **231** could be isolated in 49% yield after flash chromatography and the *Z* could be isomerized in $CDCl_3$ with a drop of acetic acid to a 1:1 *E:Z* mixture. Hydrazone alcohol **231** closed smoothly through a Mitsunobu reaction to the 7-membered hydrazone ring **232** in 92% yield. Unfortunately, both hydrogenation and tin hydride reduction of the closed hydrazone gave the syn product **233** exclusively. Other conditions such as (S)-TRIP with Hantzsch ester and K-selectride failed to reduce **277**. Initially, the proton NMR spectrum of **233** indicated two products thought to be the syn- and anti- di-phenyl, with clear, sharp and well-defined peaks and couplings, which is unusual for the diazepane ring (see experimental section). This is most likely caused by the large phenyl groups anchoring the structure raising the energy needed for conformational change. A COSY spectrum showed the expected correlations within the structures but also impossible correlations between the protons on the corresponding carbons (hence the proton on C3 of one isomer correlated to the proton on C3 of the other isomer). This indicated different conformations of **233** rather than diastereomers. This was confirmed by the fact that the ^{1}H-NMR peaks coalesce when heated to 70 °C in DMSO-d_6. Determination of the relative stereochemistry was achieved by first assignment using COSY and HSQC followed by NOESY correlations Scheme 4.6, which supports the syn di-phenyl relationship. This was later confirmed by a synthetic approach to the anti di-phenyl isomer, see Scheme 4.7.

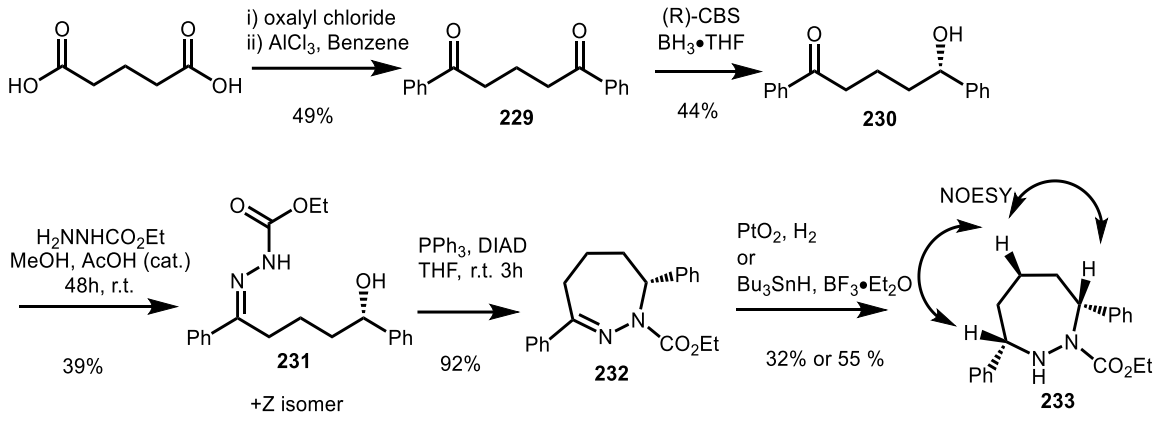

Scheme 4.6 Synthesis of catalyst 233 including relevant NOESY

The synthetic route for anti bis-phenyl **228** was revised, using the same CBS reduction of symmetric diketone **229**, in this case using excess of reducing agent to give the C2 symmetric diol **234** with dr 16:0:1 (SS, RR, SR/RS) in 87% yield (Scheme 4.7). Selective mono protection of diol **234** was carried out by forming the oxyanion with *n*-BuLi followed by addition of TBSCl. Excesses of both *n*-BuLi and TBSCl were essential to achieve a high yield (80%) and if 1 equiv. of each were used, only a moderate yield of monoprotected **235** was obtained. The remaining free hydroxyl group on **235** was transformed into the hydrazine by formation of the azide, Staudinger reduction to the amine and then N-N coupling with oxaziridine **236** providing hydrazide **237** in 82% yield (BRSM). Cbz protection of carbazate **237** followed by silyl deprotection gave alcohol **238** in good yield (70%, two steps). The latter was closed with NaH after mesylation to afford diazepane **239** in 74% yield. Hydrogenolysis of **239** gave the desired structure **240** and TFA deprotection gave the desired structure **241**.

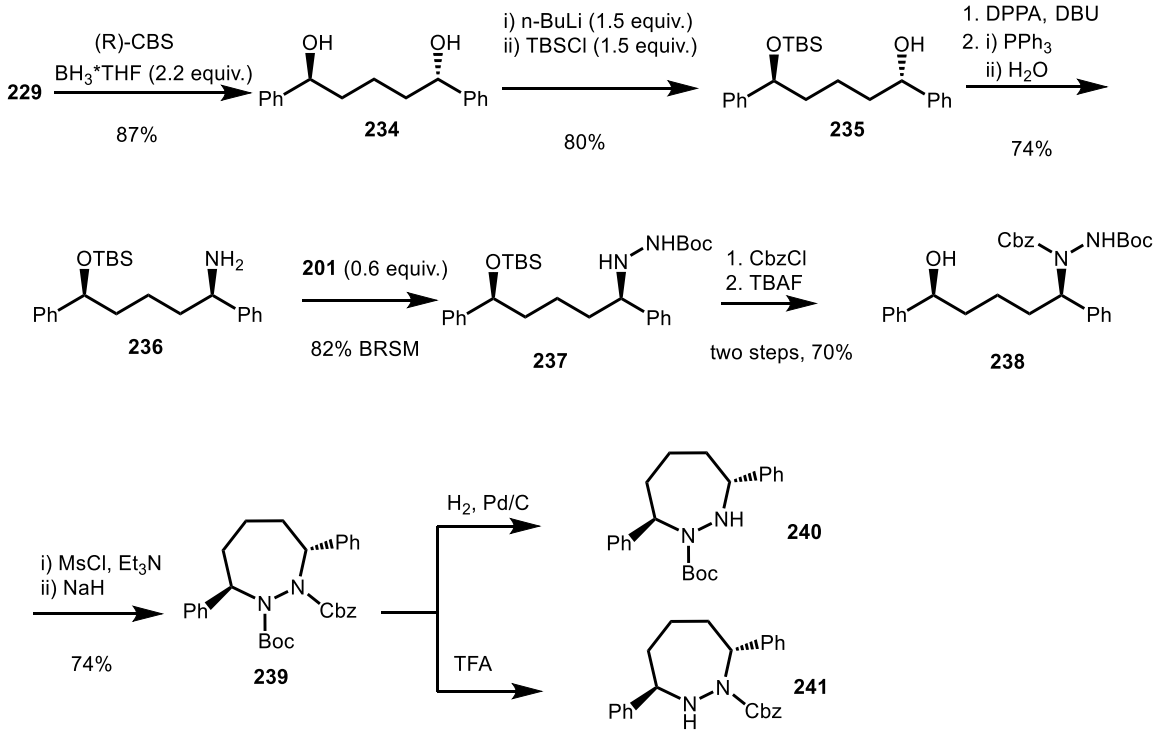

Scheme 4.7 Synthetic route for anti di-phenyl catalysts 240 and 241

We screened catalysts **233**, **240** and **241** under our standard conditions with CpH and tiglic aldehyde (Figure 4.6). Catalyst **233**, bearing cis-phenyl groups, afforded high yields, but the product was racemic. The pseudo C2-symmetric catalysts **240** and **241** unfortunately also afforded racemic product, this time in low yield. The yields of these reactions are similar to the proton-catalyzed reaction using *N*-methyl catalyst **158**, suggesting it is a proton catalyzed Diels-Alder reaction rather that iminium ion catalyzed reaction. Formation of the iminium ion may be prevented due to steric hindrance in the catalyst. The reasons for the high conversion but racemic product with diazepane **233** are not yet understood but it is expected to also be proton catalyzed. Calculations of the proton affinity of these catalysts could shine a light on why catalyst **233** gives higher conversion if it is shown that it has lower proton affinity.

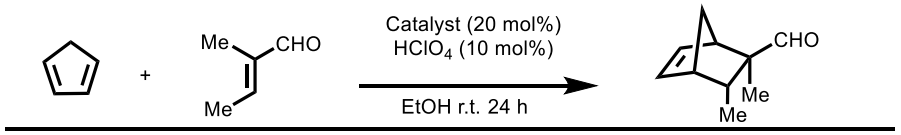

Catalyst	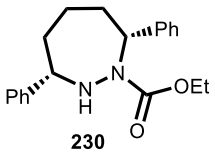 **230**	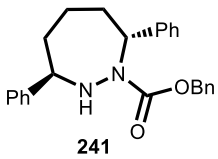 **241**	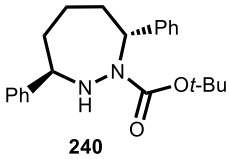 **240**
Conversion (%)	>95	20	15
Exo:Endo	10:1	7:1	3:1
Exo ee (%)	racemic	racemic	racemic

Exo:Endo ratio and conversion determined by 1H-NMR vs mesitylene as internal standard, ee determined by GLC using Chiraldex B-DM column.

Figure 4.6 Testing bis-phenyl catalyst for the Diels-Alder reaction

4.3 Exploring different electron withdrawing groups

After spending a significant amount of effort on synthesizing a catalogue of catalysts with various substituents on positions C3 and C7, our attention was refocused on the electron withdrawing group. The influence of this group on kinetics and reactivity was explored briefly in Chapter 3. The synthesis of catalysts bearing different electron withdrawing groups used common intermediate **192**, prepared previously. From diazepane **192**, either the Boc or Cbz groups could be removed as necessary, affording **242** and **78** in 98% and 97% yield, respectively (Scheme 4.8).

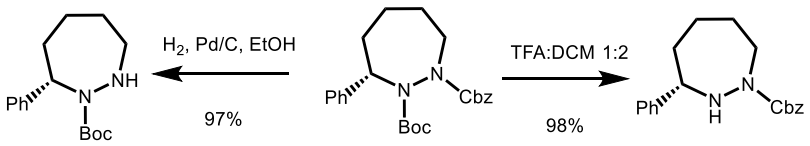

Scheme 4.8 Gram scale synthesis of 78 and 242.

4.3.1 Synthesis and screening of electron withdrawing groups on the distal nitrogen

To prepare a urea containing catalyst, **242** was allowed to react with benzyl isocyanate (Scheme 4.9). This reaction was surprisingly slow and required heating at reflux to proceed. Mild deprotection conditions were needed to avoid hydrolysing the urea, we therefore employed phosphoric acid instead of TFA which provided urea **243** in 67% yield. Phenyl amide **245** and *t*-butyl amide **244** were synthesized because of the favorable kinetics of amides in the achiral catalyst series, and also because pivaloyl, being a large group, might have a steric influence on the reaction. These were prepared in a straightforward fashion via acylation/deprotection affording pivaloyl **244** and benzylamide **245** in 93% and 71% yield, respectively. The trifluoromethyl amide **246** was synthesized in 83% yield to investigate what effect a strong electron withdrawing group would have on enantioselectivity and reactivity. 2-Chlorobenzoxazole turned out to be fairly unreactive so the Boc group on **242** was removed to give the more reactive hydrazine which reacted smoothly with 2-chlorobenzoxazole to afford benzoxazole **247** in 50% yield.

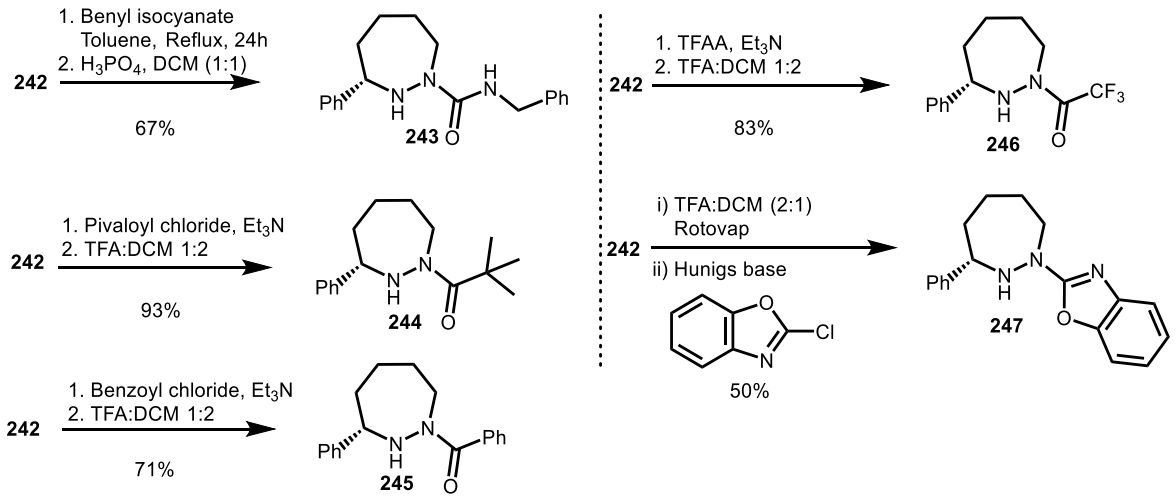

Scheme 4.9 Synthesis of different EWG with phenyl on C3 position.

Finally, because of a significant effect by the pivaloyl group (*vide infra*), it became important to synthesize pivaloyl **248** with a benzyl group on C3 to see if similar effect was observed (Scheme 4.10). This was prepared in the standard acylation of benzyl substituted **204** followed by hydrogenation of the Cbz group to afford **248** in 73% yield.

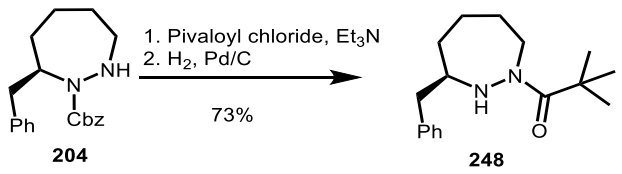

Scheme 4.10 Synthesis of pivaloyl carbamate with benzyl on C3 position

Screening of the 3-phenyldiazepanes bearing different electron withdrawing groups revealed significant changes in enantioselectivity (Figure 4.7). While there was very minor difference in enantioselectivity between different carbamates, a significant drop in enantioselectivity was observed with urea **243**. Further, phenylamide **245** gave almost racemic mixtures with slight preference for the R enantiomer, breaking the trend that had been observed for all other C3 substituted catalysts. This enantioinduction was insignificant at 5% ee but far over the margin of error. More significant yet was the result with pivaloyl **244** which continued this inversion in selectivity, with the R isomer now clearly predominating (43% ee). Catalyst **246** bearing trifluoroacetamide gave perfect conversion, in contrast to the achiral 6-membered hydrazide **167** presented in Chapter 4, but low enantioselectivity (10%). The higher reactivity with **246** relative to **167** may have been due to it is more soluble. Finally, using 2-benzoxazole **247** gave no conversion, even in solvents such as nitromethane and acetonitrile where the reaction is more rapid. This surprising reversal of enantiomer selectivity required more investigation. We also investigated the 3-benzyldiazepanes **184** and **248** and lower enantioselectivity for pivaloyl **248** were achieved (2% ee) than ethyl carbamate **184** (25% ee), but in this case affording the same enantiomer. Later in this chapter, DFT calculations will be used to explain the effect of EWG size on facial selectivity in the Diels-Alder reaction.

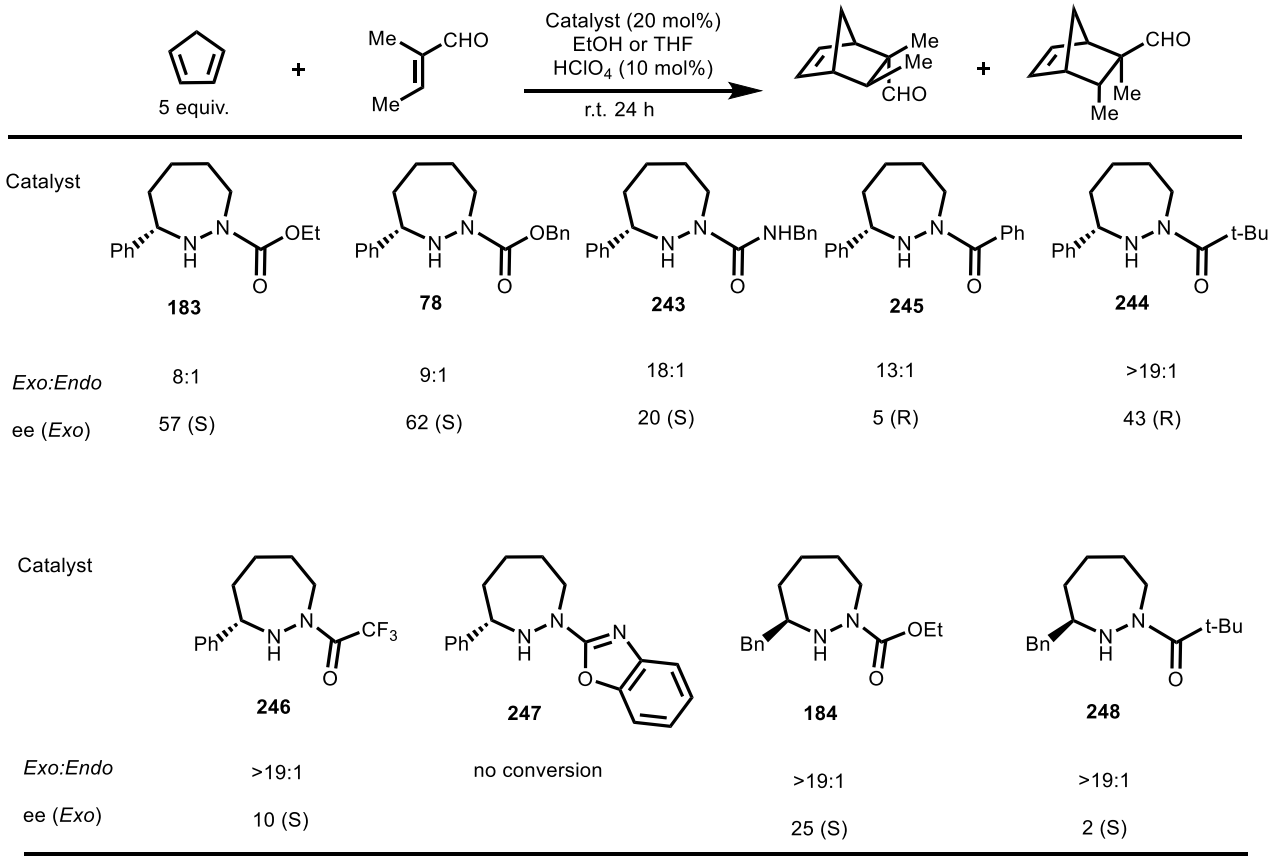

Exo:Endo ratio and conversion determined by 1H-NMR vs mesitylene as internal standard, ee determined by GLC using Chiraldex B-DM column. All but **247** gave conversion over 90%.

Figure 4.7 Screening of catalyst with different electron withdrawing groups

4.3.2 Testing of electron withdrawing group on the proximal nitrogen

Even though prior studies had showed that a stereocenter at the C7 position gave lower enantioselectivity than that at C3, considering the large effect that changing the carbamate had on facial selectivity, we wanted to quickly explore urea **250** and amide **251** with phenyl at C7. Urea **250** was prepared in 62% yield by first heating **78** in cyclohexyl isocyanate to install the cyclohexyl urea followed by Cbz deprotection (Scheme 4.11). Amide **251** was also prepared from Cbz protected **78** using standard acylation/deprotection in 70% yield.

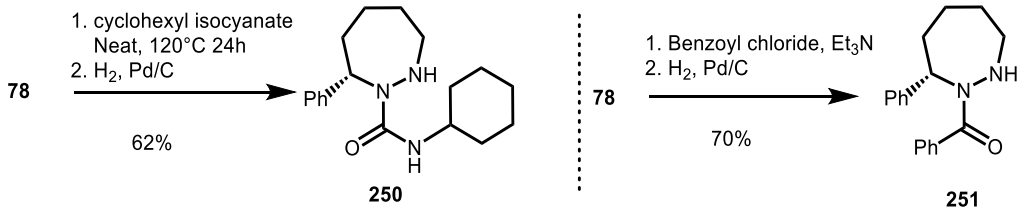

Scheme 4.11 Synthesis of urea and amide electron withdrawing groups with phenyl on C7.

The diazepanes with electron withdrawing group adjacent to the steric bulk were tested under our standard conditions (Figure 4.8). The same inversion of enantiomers was not observed for this series. Instead, disappointingly, both amide **251** and urea **250** simply generated slightly lower enantioselectivity (19% and 34% ee, respectively) and the *t*-butyl carbamate only gave a minor increase in ee (44% ee).

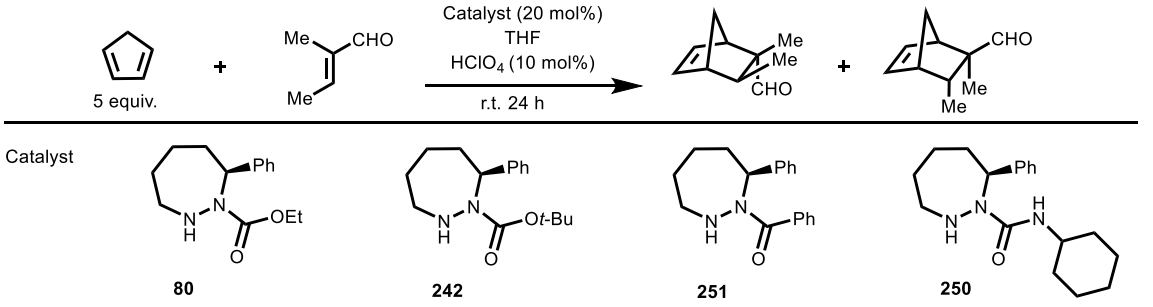

Catalyst				
	80	**242**	**251**	**250**
Exo:Endo	>19:1	>19:1	18:1	>19:1
Exo ee (%)	39	44	19	34

Exo:Endo ratio and conversion determined by 1H-NMR vs mesitylene as internal standard, ee determined by GLC using Chiraldex B-DM column. All conversions >90%.

Figure 4.8 Testing of carbamates with phenyl on C7

4.4 Other approaches for enantioselectivity

4.4.1. 6-membered ring catalyst

In addition to work with the diazepane, we also briefly investigated 6-membered ring hydrazides. Although they were less reactive, they should be conformationally more rigid and this

might improve the enantioselectivity of the catalyst. A former student in our group, Adamo Sulpizi, synthesized and tested benzyl piperazines **252** and **253** and showed that with tiglic aldehyde and CpH that good conversions and *exo*-selectivity can be achieved even with the 6-membered ring (Figure 4.9). However, the enantioselectivity was low in both cases (10% ee). Granted, these were tested in acetonitrile which is not normally the ideal solvent, but they gave lower enantioselectivity than the comparable diazepane **78** under identical conditions. Adamo Sulpizi also synthesized and tested **254,** which had previously been reported by Lee's group[140]. In our model system, hydrazine **254** gave no conversion. Finally, phenyl piperazines **255** and **256**, prepared by Samuel Plamondon, gave only partial completion for **255** in 24 h and only mid 20's ee's with good *exo*-selectivity's. Overall, none of these 6-membered rings proved to be superior to the diazepanes.

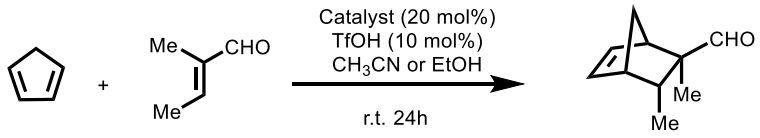

Catalyst	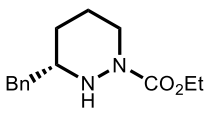	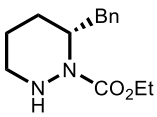	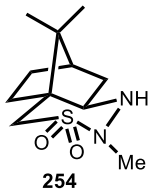	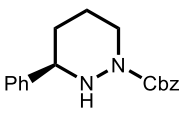	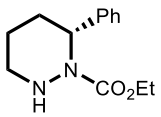
	252	**253**	**254**	**255**	**256**
Conversion (%)	>90	>90	No conversion	80	>90
Exo:Endo	16:1	12:1		12:1	>19:1
ee *Exo* (%)	10	10		24	27

Exo:Endo ratio and conversion determined by 1H-NMR vs mesitylene as internal standard, ee determined by GLC using Chiraldex B-DM column.

Figure 4.9 Testing of 6-membered ring catalyst

4.4.2 Chiral acid

Combining a chiral counterion with achiral iminium ion catalysts has had tremendous success in the last decade.[141] We wanted to see if there would be any impact in our Diels-Alder reaction in combining a chiral acid co-catalyst with an achiral diazepane catalyst. Using chiral phosphoric acid (R)-TRIP together with the simple ethyl diazepane carboxylate **69**, we observed no conversion with α-methylcinnamaldehyde but extremely quick conversion with methacrolein

(15 min). However, no enantioinduction was achieved in this process (Table 4.3). To figure out if the acidic background reaction was dominant, (R)-TRIP was combined with N-methyl diazepane **158.** This did show conversion, but was substantially slower. The acidic background reaction did display some enantioinduction from the phosphoric acid (13% ee) but not enough to warrant further exploration.

Table 4.3 Chiral acid counterion effect

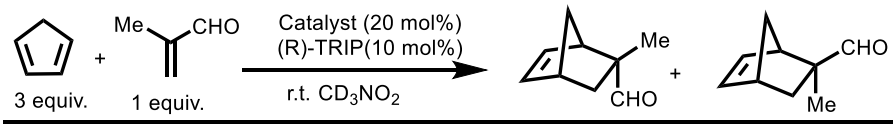

Catalyst	Time	Conversion (%)	Endo:Exo	Exo ee (%)
69	15 min	>90	1:10	1
158	48 h	91	1:8	13

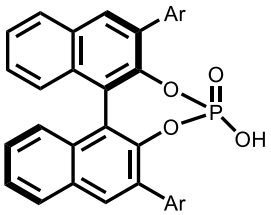

Ar = 2,4,6-^{i}Pr$_3$C$_6$H$_3$

(R)-TRIP

Exo:Endo ratio and conversion determined by 1H-NMR vs mesitylene as internal standard, ee determined by GLC using Chiraldex B-DM column.

4.4.3 Non α-substituted

We also screened non α-substituted iminium ion generated from cinnamaldehyde. Although the reaction went to completion with C3 or C7 substituted diazepane catalysts **78** and **80**, only slight *endo* selectivities (*endo:exo* 2:1) and modest enantioselectivities were observed (13% ee and 18% ee, respectively). As there are already a large number of catalysts developed for these substrates, no additional efforts towards optimization or catalyst screening were conducted.

4.5 DFT calculations of iminium ion

To gain insight into the unexpected result of inversion of enantioselectivity upon changing from carbamate to pivaloyl groups on the diazepane we employed DFT calculations at the

B3LYP/6-31G* level (performed by J. L. Gleason). The first DFT calculation was of the iminium ion of the simple achiral methyl diazepane carboxylate with methacrolein. The lowest energy conformation included two very interesting features (Figure 4.10). First the carbamate points straight up above the iminium ion with a 90-degree N-N twist and second, the iminium ion has *Z* geometry, putting the group towards the other nitrogen and under the carbamate. The *Z* geometry is favoured over *E* by 1.3 kcal/mol and reflects the smaller size of the hydrazide nitrogen versus the C3 methylene group.

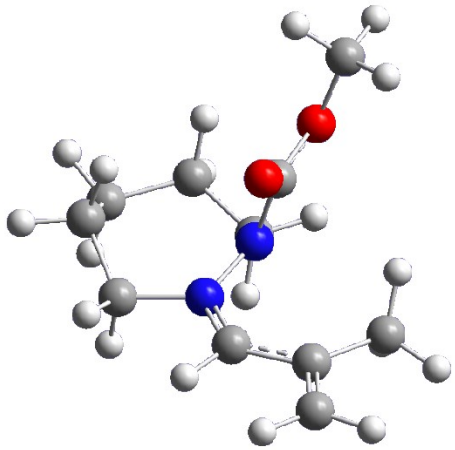

Figure 4.10 Iminium ion of methyl diazepane carboxylate and methacrolein. B3LYP/6-31G* level

DFT calculations of the iminium ion of the chiral ring **183** (methyl carbamate) with methacrolein displayed the same N-N twist of 90°, having the carbamate pointing on the same face (down) as the phenyl (Figure 4.11 a). The iminium ion geometry this time was less surprisingly the *Z* iminium. The second lowest energy conformation is the N-N twist (Figure 4.11 b), where the carbamate is pointing into the other face (up) relative to before. This species was 0.67 kcal/mol less stable. What is significant in both Figure 4.11 a) and b) is that the chiral bulk, the phenyl group, is not pointing into either the top or the bottom face of the iminium, but away from the ring in a pseudo equatorial fashion. This, together with the direction of the iminium, could explain why the size of the chiral group does not have a large effect on the enantioselectivity.

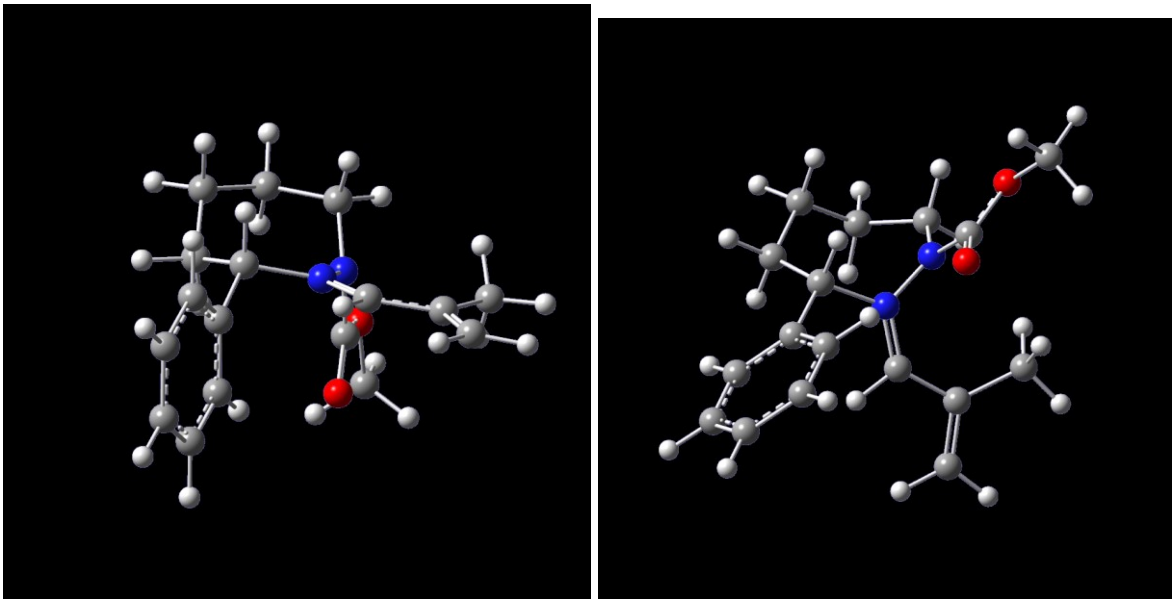

Figure 4.11 DFT calculations of iminium ion from 183 (methyl carbamate) and methacrolein. a) The lowest energy conformation, b) the second lowest energy conformation energy. B3LYP/6-31G* level

Importantly, DFT calculations for the pivaloyl **244** with methacrolein showed that the lowest energy iminium ion is the opposite N-N twist, with the pivalyl group pointing up relative to the chiral phenyl group which is pointing down/away (Figure 4.12). This compared to the methyl carbamate in Figure 4.11 where the carbamate was pointing in the same direction as the chiral phenyl group. We postulate that this conformational change leads to the change in enantiomer selectivity in the Diels-Alder reaction with catalyst **244**.

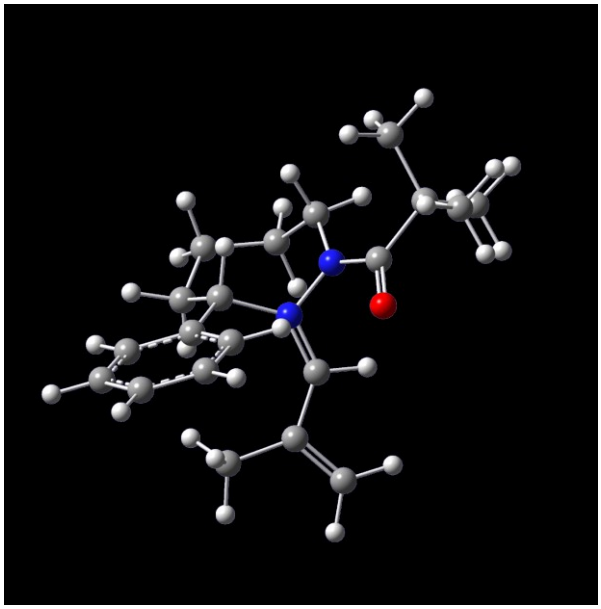

Figure 4.12 DFT calculations for iminium ion of 244 and methacrolein. B3LYP/6-31G* level

All of the carbamate catalysts gave the same major enantiomer. Reducing the aldehydes **177** and **173** to the corresponding alcohols with $NaBH_4$, followed by the formation of the (R)-Mosher ester to afford **258** and **259**, allowed for comparison with literature (Scheme 4.12).[142,143,144] From this it was determined that (S)-**78** predominantly gives Diels-Alder adducts (*S*)-**177** and (*S*)-**173** with the S-configuration (Scheme 4.12).

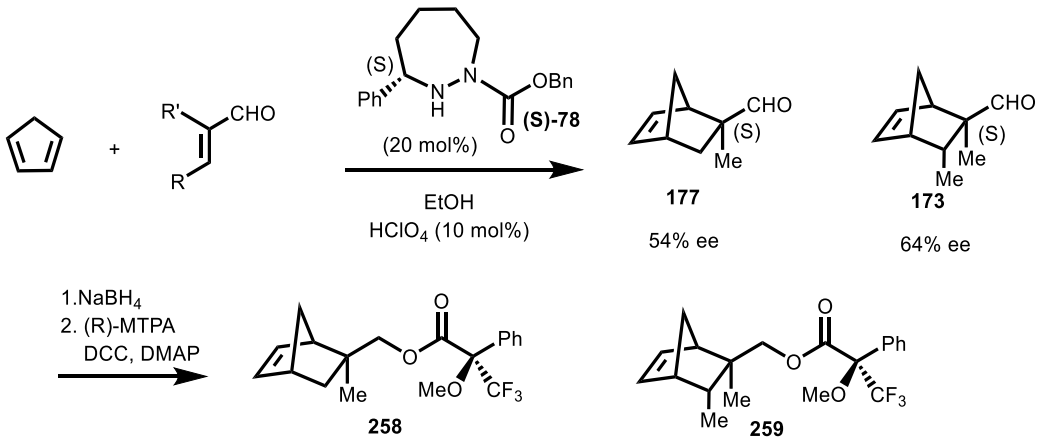

Scheme 4.12 Mosher ester of the Diels-Alder adduct of methacrolein and tiglic aldehyde with CpH

After determining the absolute stereochemistry, it was clear that the diene must approach the iminium ion from the face bearing the greatest amount of steric bulk based on the DFT model. Although initially surprising, DFT calculations eventually confirmed this. The lowest energy transition state involves the steric bulk (phenyl) being pseudo equatorial pointing away from the ring system and the carbamate pointing straight down with a 90° twist of the N-N bond (Figure 4.13). Importantly, this does not block that face but instead directs the diene by stabilizing the build up of positive charge on the C-4 position on the diene via an electrostatic interaction with the carbamate oxygen.

a) 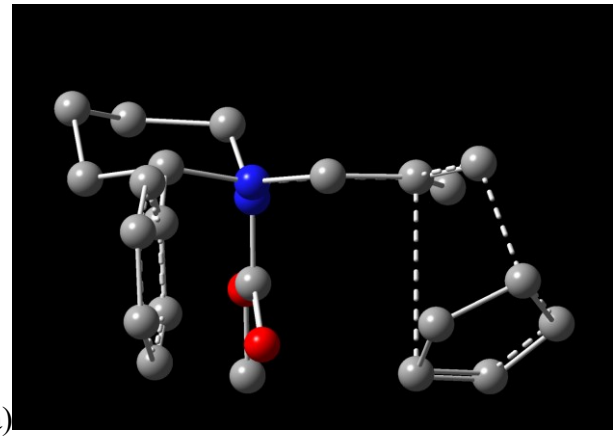 b) 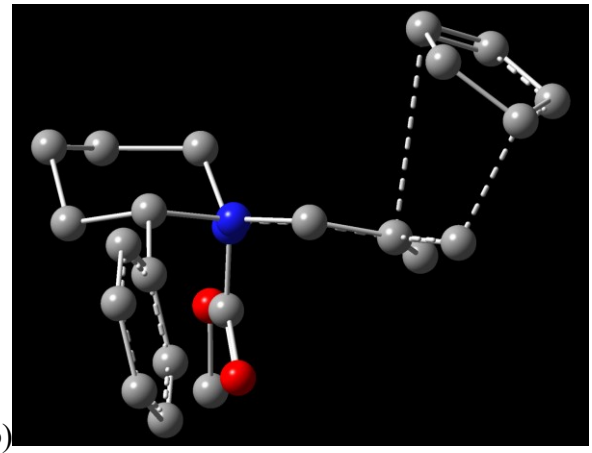

Figure 4.13 The Diels-Alder transition state for the lowest iminium ion conformations with a) bottom face approach (favoured) and b) top face approach (disfavoured) of diene. Hydrogens omitted for clarity. B3LYP/6-31G* level

If the transition state depicted in Figure 4.13 b) were the second lowest in energy, we would be able to achieve high enantioselectivity as the difference in energy is 2.55 kcal/mol. Unfortunately, the second lowest energy transition state arises from the other N-N twist of the catalyst (Figure 4.14). This directs the cycloaddition from the opposite face with an energy difference of 0.7 kcal/mol, which aligns closely with the observed enantioselectivity.

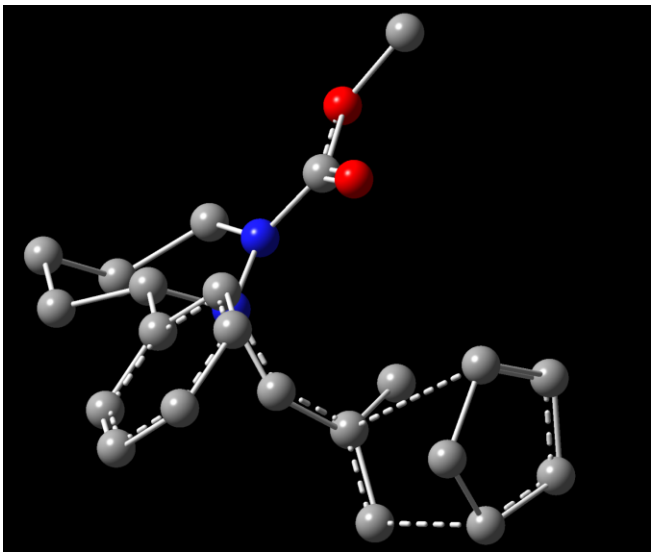

Figure 4.14 Second lowest energy transition state. Protons omitted for clarity. B3LYP/6-31G* level

This is not the first example of an iminium ion catalyzed reaction not being determined by steric hindrance. An interesting study from Pihko and co-workers showed that *trans*-2,5-diphenylpyrrolidine catalyzed Mukaiyama-Michael additions. They also showed by DFT calculation that enantioselectivity arose from attractive non-covalent dispersion interaction, not steric hindrance.[145] This article questions the paradigm in iminium ion catalysis, and organocatalysis in general, that steric encumbrance from chiral bulk on the catalyst is the main source of enantioinduction.

Based on these observations, we designed a catalyst which would disfavour the conformation with undesired N-N twist. By replacing the hydrogen at position C7 anti to the phenyl on position C3 with a methyl group (**266**, Scheme 4.16), the desired N-N twist should be favoured with 2.3 kcal/mol and the catalyst should not be as sterically encumbered as the bis-phenyl variant.

4.6 Synthesis of 266

The synthesis of catalyst **266** started with epoxidation and oxidative cleavage of 1-phenyl-cyclohexene (**260**) to afford aldehyde **261** in 91% yield (Scheme 4.13). α-Hydrazination of

aldehyde **261** followed by chemoselective reduction of the aldehyde hydrazide adduct with 0.5 equivalents of sodium borohydride smoothly generated hydrazide **262** with good yield (75%) and enantioselectivity (94% ee). Alcohol **262** was then deoxygenated by forming the thioimidazole followed by radical cleavage to form ketone **263** (86% BRSM). The phosphorous hydrogen source sodiumhypophosphite[146] gave 7% yield, which unfortunately was not as clean and high yielding as the more conventional tributyltin hydride. Alternative attempts at direct deoxygenation from **262** with conditions developed by Myers group using *o*-nitrobenzenesulfonylhydrazide under Mitsunobu conditions (PPh_3, DIAD) gave more than 9 spots on the TLC and no hint of product in the crude.[132, 147] Ketone **263** was reduced by CBS reduction and the resulting alcohol **264** was mesylated and the ring was closed with NaH to give **265** in 62% yield. Deprotection of both Boc groups and addition of the ethyl carbamate at -78 °C ultimately gave catalyst **266** with high regioselectivity (>19:1). Running the final acylation reaction at room temperature or 0 °C gave no better than 10:1 regioselectivity.

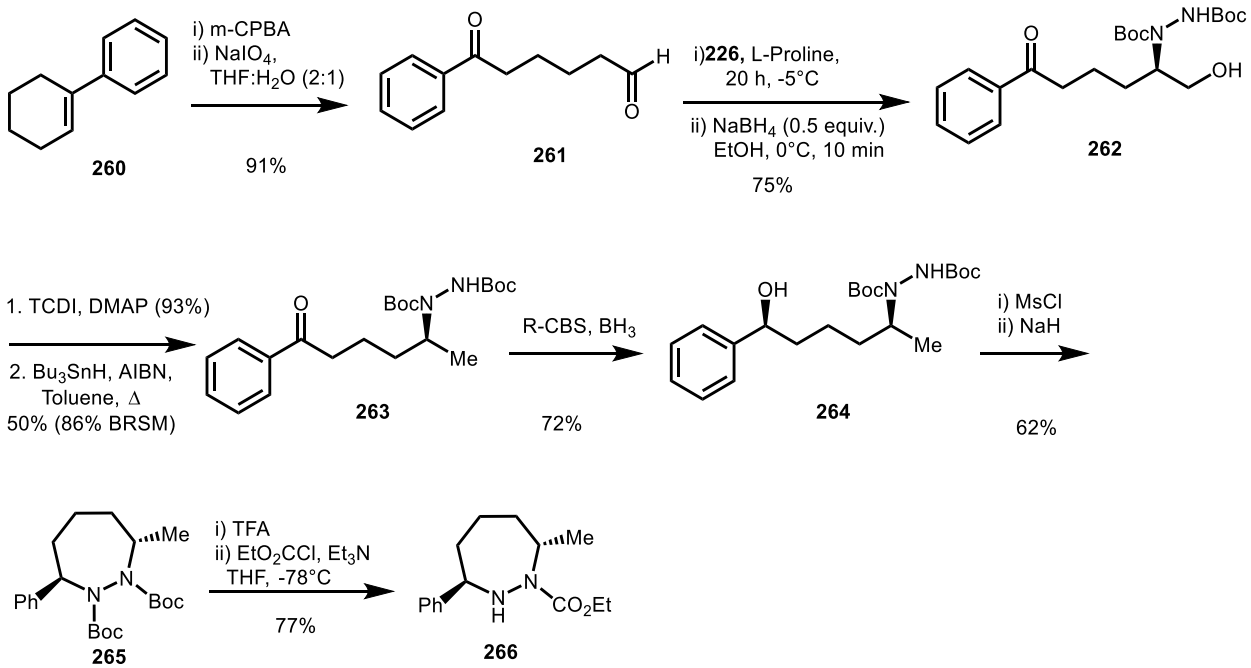

Scheme 4.13 Synthesis of catalyst 266.

To our surprise, use of catalyst **266** with tiglic aldehyde and CpH gave high conversion and good *exo*-selectivity but with only 6% ee for *exo*. This result was not predicted by DFT calculations for reasons that remain unclear. The ee for the endo adduct was around 50%, which

would be inconsistent with simple acid catalysis which would give a racemic product. More studies are needed to fully understand these results.

4.7 Screening chiral electron withdrawing groups

After extensive exploration of chiral catalysts based on ring substitution and different electron withdrawing groups for both reactivity and enantioselectivity, we chose to evaluate chiral carbamates. A series of chiral carbamates (**268**, **269** and **270**) were synthesized from the corresponding alcohols as shown in Scheme 4.14 a) (i.e., borneol, (S)-1-phenylethanol, (S)-2-octanol) by first preparing the chloroformates. Diazepane dicarboxylate **267** was deprotected to the free hydrazine and then reacted with the chloroformates in the presence of base. The free hydrazine oxidizes quickly to the corresponding hydrazone unless it is stored as a salt or prepared right before use. (-)-Menthylchloroformate is commercially available and was allowed to react directly with free diazepane (Scheme 4.14 b) to afford **271** in 59% yield.

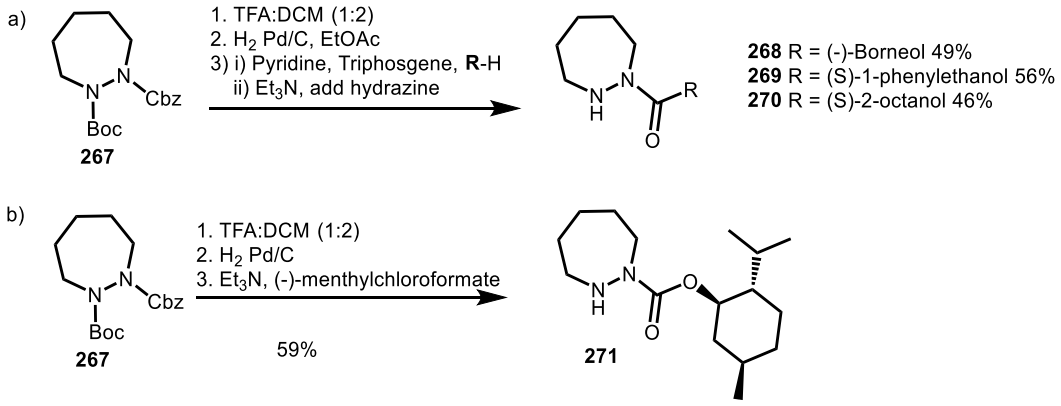

Scheme 4.14 Synthesis of diazepane with chiral carbamates

Upon screening under standard conditions, (-)-Menthyl carbamate **271** achieved the highest, but still modest enantioselectivity (15% ee, Figure 4.15). The large (-)-borneol carbamate **268** gave a negligible ee of 4%, 1-phenylethanol carbamate **269** gave 11% ee and the carbamate of 2-octanol (**270**) gave a similar ee (8%).

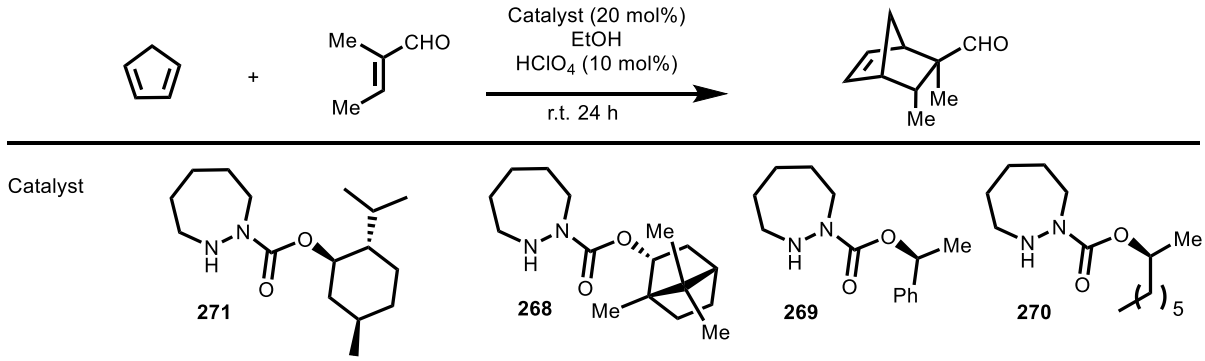

Catalyst	**271**	**268**	**269**	**270**
Exo:Endo	11:1	8:1	12:1	>19:1
Exo ee (%)	15	4	11	8

Exo:Endo ratio and conversion determined by 1H-NMR vs mesitylene as internal standard, ee determined by GLC using Chiraldex B-DM column. All conversions > 90%.

Figure 4.15 Testing of chiral carbamates

As will be seen below, while the enantioselectivities with chiral carbamates were low, they could be used to augment the enantioselectivity of the ring substituted catalysts. We were therefore interested in testing the 8-phenylmenthyl version, which has classically been used as a chiral auxiliary. (-)-8-Phenylmenthol was synthesized from (-)-β-citronellol (**272**), starting with Swern oxidation to (-)-citronellal followed by diastereoselective carbonyl-ene cyclization with $ZnBr_2$ to form (-)-isopulegol (**273**) in 46% yield (Scheme 4.15).[148] The phenyl migration was performed using conditions recently developed by Shenvi's group where the the sulfonyl **274** is first formed and then $Mn(dpm)_3$ (**278**) and $PhSiH_3$ are used to give (+)-8-phenylmethol (**275**).[149] The reaction mechanism starts with a hydrogen atom transfer to the olefin followed by a radical attack from the tertiary radical to the ipso position of the phenylsulfonyl which yields the product after a Truce-Smiles rearrangement plus a sulfite radical which was reported to react with the manganese complex preventing catalytic turnover. The $Mn(dpm)_3$ reagent (**278**) was prepared by simply mixing $MnSO_4$ (**276**) and 2,2,6,6-tetramethyl-3,5-heptanedione (**277**) and then isolated by filtration.[150]

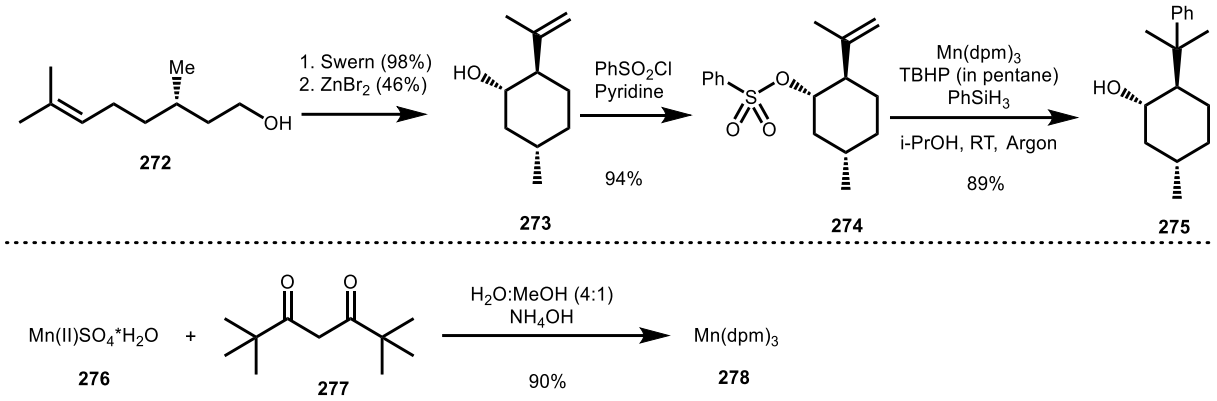

Scheme 4.15 Synthesis of (-)-8-phenylmenthol 275

Catalyst **279** the with 8-phenylmenthyl group was synthesized in an identical fashion as that shown in scheme 4.14 a). Catalyst **269** bearing the 1-phenylethylcarbamate gave nearly the same ee (11%) as the menthyl carbamate (15% ee). We hypothesized that the size difference between the phenyl and the methyl in catalyst **269** was the key aspect for its enantioinduction and designed catalyst **280** bearing the 1-*t*-butylethyl carbamate. Catalyst **280** was synthesized using (S)-3,3-dimethylbutan-2-ol as shown above. Screening catalyst **279** and **280** under our standard conditions with tiglic aldehyde and CpH achieved slightly lower ee's (13% and 6% ee, respectively, Figure 4.16). No clear trend between enantioinduction and the size and type of carbamate was observed. The same ambiguity is observed with the stereocenter on the ring, which was partially explained by DFT calculations.

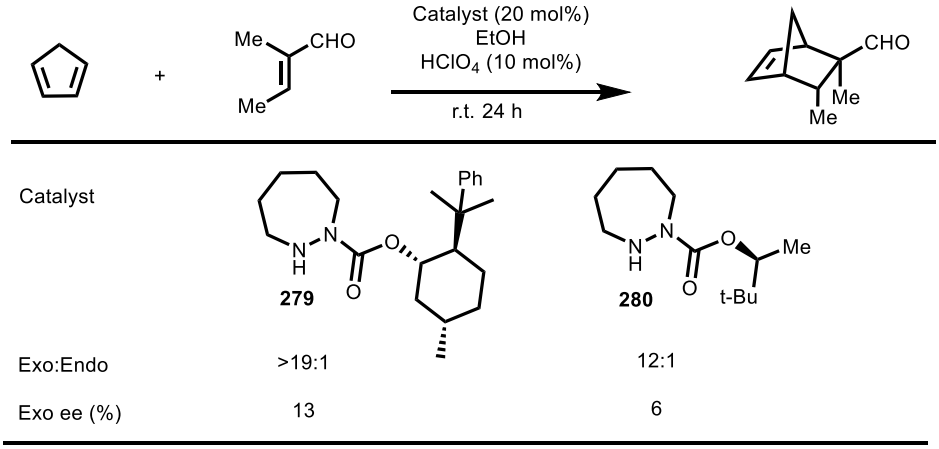

Exo:Endo ratio and conversion determined by 1H-NMR vs mesitylene as internal standard, ee determined by GLC using Chiraldex B-DM column. All conversions >90%.

Figure 4.16 Testing of chiral carbamates 279 and 280

4.8 Dual effect of chiral group on ring and carbamate

Although the chiral carbamates alone gave poor enantioinduction, we hypothesized that there might be the potential of combining their effect with the more effective ring-substituted catalysts. In particular, the stereocenters would be well removed from one another and might lend themselves to a classic matched/mismatched phenomenon.[151]

4.8.1 Synthesizing and screening matched/mismatched effect

Catalysts **281** and **282** with the C3 phenyl group and either (+)-menthyl and (-)-menthyl carbamate, respectively, were synthesized as for the simple carbamates (Scheme 4.14 b) but starting from C3 phenyl substituted diazepane **78**. We were delighted to find that the non-natural (+)-menthol gives a matched case with catalyst **281** provided the Diels-Alder product in 71% ee at room temperature, an improvement of 9% ee (Figure 4.17). Correspondingly, catalyst **282** bearing the (-)-menthyl group afforded the Diels-Alder adduct in 46% ee, a drop of 16% ee. These results are an excellent example of matched/mismatched behaviour.

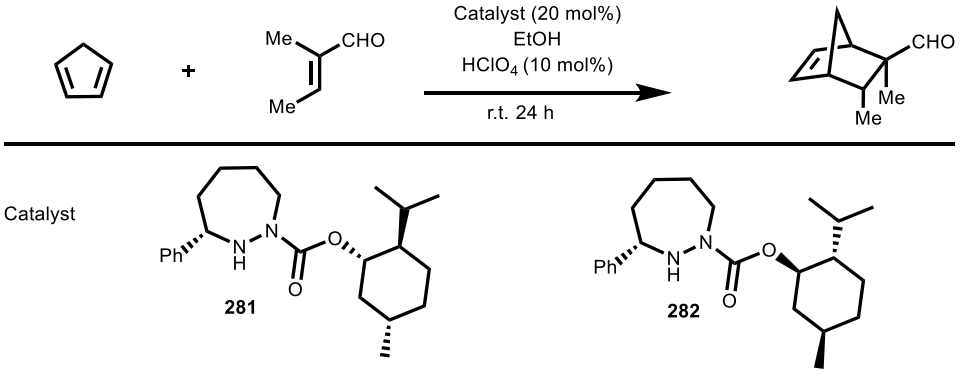

Exo:Endo	8:1	8:1
Exo ee (%)	71	46

All conversions >90%. Exo:Endo ratio and conversion determined by 1H-NMR vs mesitylene as internal standard, ee determined by GLC using Chiraldex B-DM column.

Figure 4.17 Match and mismatch case combining chirality on the ring with chiral carbamate

A follow-up solvent optimization for matched catalyst **281** showed that THF gave similar enantioselectivity but slightly better *exo*-selectivity (*exo*:*endo* 11:1 versus 8:1) and, as usual, a slightly cleaner reaction where very minor (<5%) by-products, including acetal formation and oxa Michael addition, are observed when using alcohol as the solvent (Table 4.4). Non-polar solvents like hexanes and toluene worked with this greasier version of the catalyst but achieved moderate enantioselectivity (56% and 63% ee, respectively).

Table 4.4 Solvent and temperature optimization

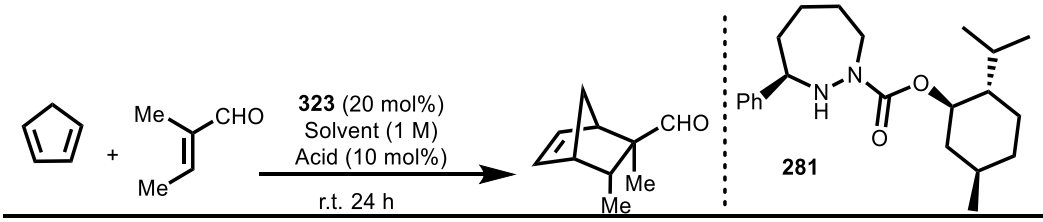

Entry	Solvent	Acid	ExoEndo[a]	Exo ee (%)[b]	Conditions
1	EtOH	$HClO_4$	8:1	71	-
2	THF	$HClO_4$	11:1	67	-
3	EtOH	$HClO_4$	12:1	75	-10°C
4	THF	$HClO_4$	11:1	78	-20°C
5	Hexanes	$HClO_4$	5:1	56	-
6	Toluene	$HClO_4$	4:1	63	-

a. Exo:Endo ratio and conversion determined by 1H-NMR vs mesitylene as internal standard.
b. ee determined by GLC using Chiraldex B-DM column or HPLC using Chiralcel OD column.
All conversions >90%.

Notably, we wondered whether matched/mismatched behaviour might extend to other catalysts. Methyl ester **221** gave 64% ee (vs 62% ee for **78**) in the reaction of CpH with tiglic aldehyde and we were interested to see if it would also improve with a menthyl carbamate. Catalyst **283** was synthesized in the same fashion as **221** (Scheme 4.4) through a one pot acid catalyzed Boc deprotection/Fischer esterification followed by regioselective carbamate formation with (-)-menthyl chloroformate (Scheme 4.16). Catalyst **283** was tested under the standard conditions and was close to identical to the results observed with **281** (70% versus 71% ee).

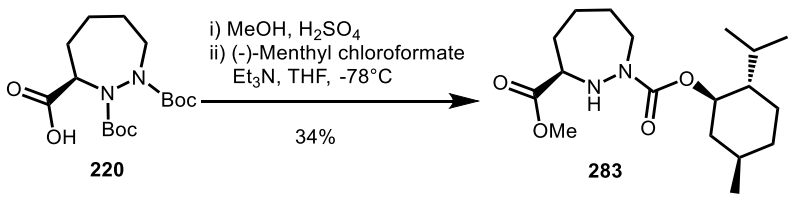

Scheme 4.16 Synthesis of 283

4.8.2 Synthesis of dienophiles and catalyst 281

With an improved catalyst in hand, we sought to examine its scope with a range of dienophiles. Some of the dienophiles had to be synthesized and they are shown in Scheme 4.17. For α-*t*-butylacrolein (**284**), the synthesis started from 3,3-dimethyl-1-butene which was transformed into the primary alcohol **285** by hydroboration. The alcohol was oxidized with Bobbitt's salt[152] which gave cleaner reaction than either Swern or IBX. The methylene was introduced by pyrrole catalyzed methylenation of formaldehyde.[153] α-*i*-Propylacrolein (**293**) and α-ethylacrolein (**292)** were synthesized through the same steps from commercially available alcohols **289** and **288**. α-Benzylacrolein (**294**) was easily derived from hydrocinnamaldehyde **290** through α-methylenation. Cyclopentene-1-carboxaldehyde **297** was synthesized through oxidative cleavage of diol **296** followed by intramolecular aldol condensation. Finally, α-benzyl-β-methylacrolein (**300**) was synthesized according to a procedure by Sarpong *et al*. through an unusual double Heck reaction.[154]

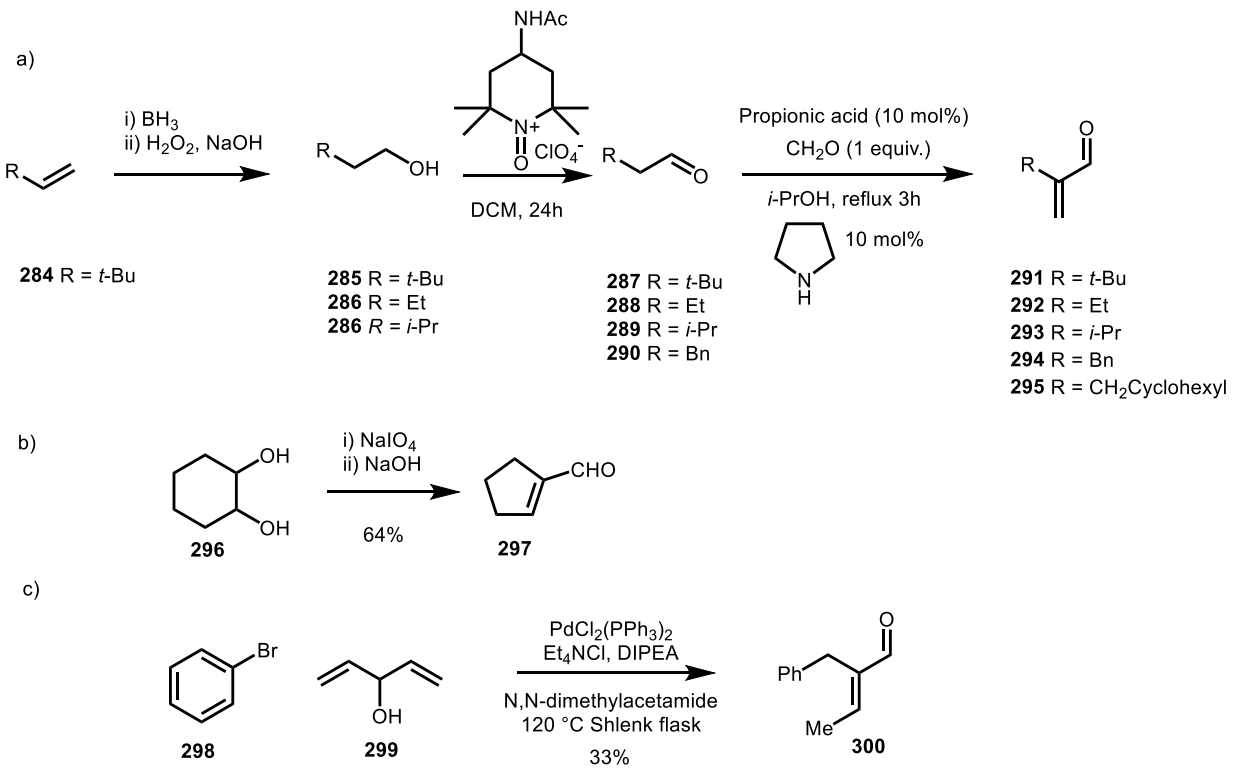

Scheme 4.17 Synthesis of dienophiles

To prepare enantiopure catalyst **281**, the Boc group was removed from **192** with TFA and then the Cbz group was removed by hydrogenation under acidic conditions to form the hydrazine HCl salt which was recrystallized in EtOAc/MeOH (20/1) to yield material with over 99% ee enantiopurity in preparation for the final catalyst **281** (Scheme 4.18).

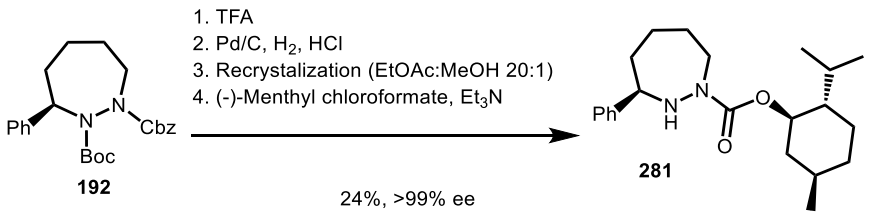

Scheme 4.18 Synthesis of enantiopure catalyst

4.8.3 Scope of catalyst 281 with acyclic diene isoprene and α-substituted enals

The acyclic diene isoprene gave good conversions and high regioselectivity but unfortunately only moderate enantioselectivity was achieved with the dienophiles α-benzylacrolein and methacrolein (49% ee for **301** and 55% ee for **179**, Figure 4.18). The conversion was high (>90%, mesitylene as internal standard) and isolated yields were not determined.

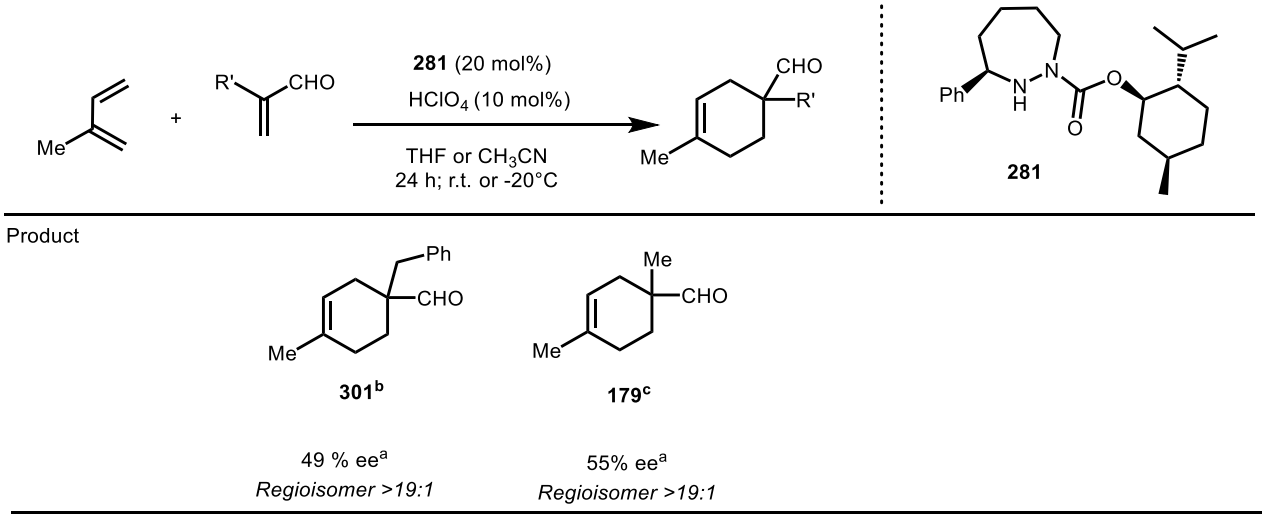

a) ee determined by reducing the aldehyde to the corresponding alcohol and subsequently synthesizing the (R)-MTPA Mosher ester. b) THF, r.t. c) CH_3CN, -20 °C

Figure 4.18 Scope of acyclic diene

4.8.4 Scope of catalyst 281 with dienophiles and CpH

Screening catalyst **281** with the series of dienophiles above and commercially available dienophiles were performed at -20 °C under otherwise standard conditions. Enals with very bulky α-substituents showed poor reactivity with catalyst **281** with both α-*t*-butylacrolein (**291**) and α-*i*-propylacrolein (**293**) showing no conversion. α-*t*-Butylacrolein (**291**) also showed no reaction with the simple unsubstituted ethyl diazepane carboxylate **69** while α-*i*-propylacrolein (**293**) gave only moderate conversion (45%) with catalyst **69** in 48 h. α-Benzyl-β-methyl-acrolein **300** also gave no conversion with catalyst **281** but gave moderate conversion (51%) with **69** in 48 h.

Less hindered aldehydes proved to be more effective (Figure 4.19). Our model system of tiglic aldehyde and CpH still reached completion in 24 h even at -20 °C providing the product in 77% yield with 75% ee and 12:1 *exo:endo* selectivity.

α-Substituted enals without β-substituents such as α-ethylacrolein fortunately gave similar enantioselectivity (**303**: 75% yield, 71% ee, 7:1 *exo:endo*). The reaction of dienophiles bearing larger α-substituents provided very high enantioselectivity, showing that the diazepane catalyst is capable of achieving excellent enantioselectivity. α-benzylacrolein gave adduct **178** in good yield (85%) with high enantioselectivity (92% ee) and with good *exo*-selectivity (10:1 *exo*:*endo*). The Diels-Alder adduct **302** from the reaction of CpH with α-(cyclohexylmethyl)acrolein was isolated in 85% yield and in excellent enantioselectivity (95% ee).

The less reactive α-methylcinnamaldehyde and α-bromocinnamaldehyde did not show any activity in both ethanol and THF but the reaction proceeded smoothly in acetonitrile giving products **157** and **176**, respectively. However, extended reaction times (144 h) were necessary for these new chemical entities. Diels-Alder product **157** was isolated in 65% yield with 78% ee with and the α-Br substituted **176** gave higher yield (77%) and similar enantioselectivity in 72% ee, both with good *exo*-selectivity.

We continued the exploration of the scope with cyclic dienes and explored the reaction of CpH with 1-cyclohexene-1-carboxaldehyde which gave moderate conversion and enantioselectivity (**304**: 69% yield, 72% ee, 13:1 *exo:endo*). The smaller 5-membered ring 1-cyclopentene-1-carboxaldehyde gave both lower enantioselectivity (52% ee) and *exo*-selectivity (3:1 *exo*:*endo*), the reasons for which are not yet understood.

Overall, a varied scope of α-substituted enals provided good enantioselectivity and regioselectivity and the results have recently been published.[155] Additionally, β-substituents were also tolerated while still providing high yields and selectivity. 5-membered and 6-membered ring enals were also compatible with our catalyst **281** and provided moderate to good yields and enantioselectivities. Generally, larger α-substituents provided very high enantioselectivity while smaller substituents provided moderate enantioselectivity. The isolated yields for the reactions were good to high e*xo*-selectivity remained great throughout the scope.

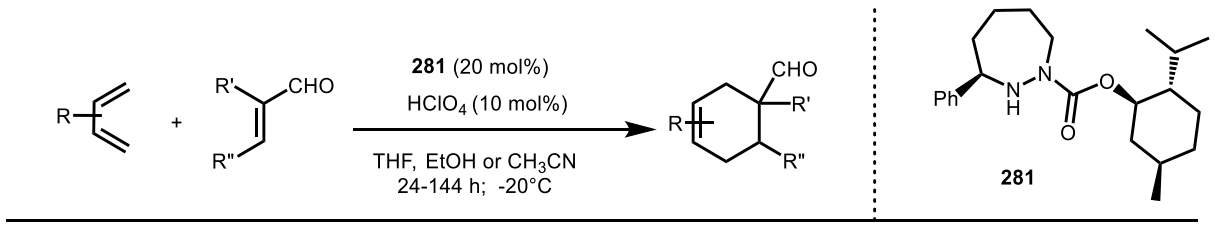

Product				
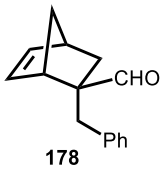 **178**	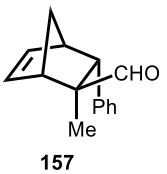 **157**	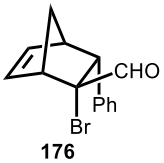 **176**	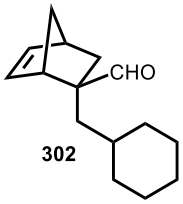 **302**
85%, 24 h[a] 92% ee (96:4 er) *Exo:Endo* 10:1	65%, 144 h[b] 70% ee (85:15 er) *Exo:Endo* 10:1	77%, 144 h[b] 72% ee (86:14 er) *Exo:Endo* 11:1	81%, 24 h[a] 95% ee (97:3 er) *Exo:Endo* 11:1
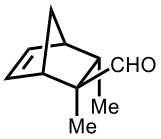 **(R)-173**	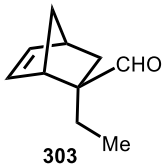 **303**	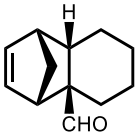 **304**	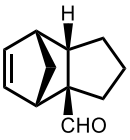 **305**
77%, 24 h[a] 75% ee (87:13 er) *Exo:Endo* 12:1	75%, 24 h[a] 71% ee (86:14 er) *Exo:Endo* 9:1	69%, 72 h[a] 72% ee (86:14 er) *Exo:Endo* 13:1	81%, 24 h[c] 52 % ee (76:24 er) *Exo:Endo* 3:1

Exo:Endo ratio determined by ^{1}H-NMR intergration. ee determined by GLC using Chiraldex B-DM column, HPLC using Chiralcel OD column or by reducing the aldehyde to the corresponding alcohol and subsequently synthesizing the (R)-MTPA Mosher ester. Mosher ester was also used to determine absolute configuration.
a) THF b) CH_3CN c) EtOH

Figure 4.19 Scope of the Diels-Alder reaction with catalyst 281

4.9 Conclusion

We have developed an enantioselective catalyst for the Diels-Alder reaction of α-substituted enals. A wide variety of chiral diazepanes have been synthesized and screened in this reaction in attempts to find a catalyst that is highly enantioselective. We have performed extensive studies, both experimental and *in silico* DFT calculations (Dr. J. L. Gleason) to provide insight into the reactivity and selectivity of the catalysts and how these properties may be improved. The conclusions of our studies led us to synthesize diazepane **281** possessing a stereogenic centre at

C3 of the diazepane ring bearing a phenyl group matched with a chiral menthyl carbamate on the distal position for improved enantioinduction.

Catalyst **281** gives good to high yields, moderate to excellent *exo*- and enantioselectivity for unreactive (α-bromocinnamaldehyde, α-methylcinnamaldehyde) and sterically encumbered α-substituted enals in the enantioselective Diels-Alder reaction. A few of the Diels-Alder reactions disclosed achieved enantioselectivities over 90% with most others providing enantioselectivity between 70 to 80% ee.

One of the most fundamental results gained from this project was establishing the origins of enantioinduction in this catalyst system. DFT calculations of the transition state revealed that the enantioinduction is a result of electrostatic interactions between the carbamate and the diene, directing the diene approach from one face towards the iminium ion rather than through sterically hindering the approach of the diene. This is a unique mode of enantioinduction for iminium ion catalysis as the conventional model for inducing selectivity relies on steric hindrance to differentiate different approaches of the diene. By illustrating the use of electrostatic interactions to influence the stereochemical outcome of this reaction these studies provide the potential to influence and positively impact future catalyst design.

The catalysts synthesized in this chapter have also been used for the other projects in our group; Cope rearrangement (Dr. Dainis Kaldre), polyene cyclization (Samuel Plamondon and Josefine Warnica) and oxy-Cope rearrangement (Ryan Barrett and Donald Campbell). Quite interestingly, the Diels-Alder reaction achieves higher enantioselectivity from the C3 substituted diazepanes. This is opposite to that observed in the intramolecular Cope rearrangement and the polyene cyclization investigated by other students in our lab, which show higher enantioinduction using catalysts with the stereogenic centre on the C7 position, adjacent to the nitrogen bearing the carbamate. For the polyene cyclization, the 6-membered hydrazide has been the most successful catalyst for enantioselectivity and based on work performed in this chapter, the matched/mismatched cases of that catalyst have been synthesized and have shown improved results.

Recently, we published a Michael addition using our achiral ethyl diazepane carboxylate (**69**) including my part of catalyst synthesis and screening (Scheme 4.19).[156] Dr. Florent Larnaud,

a former post doctoral fellow in our lab, spearheaded this project. My contribution to this project was minor and thus has been omitted from this thesis.

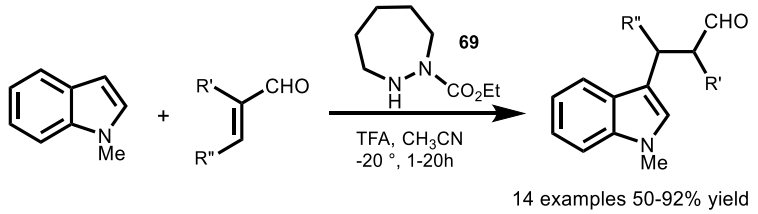

Scheme 4.19 Ethyl diazepane carboxylate catalyzed Michael addition

The diazepane is a new and exciting scaffold in iminium ion catalysis that has already performed a variety of reactions with moderate to excellent reactivity and selectivity. These catalysts have the potential of becoming even more selective through continuing work being performed in our group. Future work for the Diels-Alder reaction would be to investigate enantioselectivity for acyclic dienes and intramolecular Diels-Alder reactions.

4.10 References

[133] Marigo, M.; Wabnitz, T. C.; Fielenbach, D.; Jørgensen, K. A.; *Angew. Chem. Int. Ed*. **2005**, 44, 794.

[134] Jiang, J.; He, L.; Luo, S-W.; Cun, L-F.; Gong L-Z.; *Chem*. *Commun*., **2007**, 736.

[135] Kaldre, D.; 2016, Development of Hybrid Drugs for Cancer Treatment and Studies in Asymmetric Organocatalysis, PhD, McGill University, Montreal Canada.

[136] Armstrong, A.; Jones, L. H.; Knight, J. D.; Kelsey, R. D.; *Org. lett.* **2005**, *7*, 713.

[137] Armstrong, A.; Cooke, R. S.; *Chem. Commun.,* **2002**, 904.

[138] Reichardt, C.; *Chem. Rev.* **1994**, 94, 2319.

[139] Zhao, M.; Eiichi Mano J. L.; Song Z.; Tschaen D. M.; Grabowski E. J. J.; Reider P. J.; *J Org Chem*. **1999***,* 2564

[140] He, H. Pei, B-J.; Chou, H. H.; Tian, T.; Chan, W-H., Lee, A. W. M.; *Org. Lett.*, **2008**, 10, 2421.

[141] Mayer, S.; List, B.; *Angew. Chem. Int. Ed.* **2006**, *45*, 4193.

[142] Corey, E. J.; Loh, T.-P.; *J. Am. Chem. Soc.* **1991**, *113*, 8966.

[143] Kubota, K.; Hamblett, C. L.; Wang, X.; Leighton, J. L.; *Tetrahedron* **2006**, *62*, 11397.

[144] Ishihara, K.; Kurihara, H.; Matsumoto, M.; Yamamoto, H.; *J. Am. Chem. Soc.* **1998**, 120, 6920.

[145] Kemppainen, E. K.; Sahoo, G.; Piisola, A.; Hamza, A.; Kotai, B.; Papai, I.; Pihko, P. M.; *Chem. Eur. J.* **2014**, 20, 5983.

[146] Tavera-Mendoza L. E.; Quach T. D.; Dabbas, B.; Hudon, J.; Liao, X.; Palijan, A,; Gleason, J. L.; White, J. H.; *Proc. Natl. Acad. Sci.* **2008**, 105, 8250.

[147] Myers, A. G. Movassaghi, M. Zheng, B.; *J Org. Chem*, **1997**, 7507.

[148] Nakatani, Y.; Kawashima, K.; *Synthesis* **1978**, 1978, 147.

[149] Crossley, S. W. M.; Martinez, R. M.; Guevara-Zuluaga, S.; Shenvi, R. A.; *Org. Lett.* **2016**, 18, 2620.

[150] Iwasaki, K. Wan, K. K.; Oppedisano, A.; Steven W. M. Crossley, S. W. M.; Shenvi, R. A.; *J. Am. Chem. Soc.* **2014**, 136, 1300.

[151] Masamune, S.; Choy, W.; Petersen, J. S.; Sita, L. R,; *Angew. Chem. Int. Ed. Engl.* **1985**, 24,1.

[152] Bobbitts, J. M.; *J. Org. Chem.* **1998**, *63*, 9367.

[153] Erkkilä, A.; Pihko, P. M.; *J. Org. Chem.*, **2006**, 71, 2538.

[154] Ndungu, J. M.; Larson, K. K.; Sarpong, R.; *Org Lett.* **2005**, 5845.

[155] N. O. Haggman, B. Zank, H. Jun, D. Kaldre, J. L. Gleason; *Eur. J. Org. Chem.* **2018**, 5412.

[156] Larnaud, F.; Sulpizi, A.; Häggman, N. O.; Hughes, J. M. E.; Dewez, D. F.; Gleason, J. L.; *Eur. J. Org. Chem*, **2017**, 2637.

CONTRIBUTIONS TO KNOWLEDGE

We have showed that a series of urea-alcohols can quickly be synthesized via a modular synthetic approach using common intermediates and similar reactions. This approach could be utilized to study more parameters that influence urea hydrogen bonding chemistry. These urea-alcohols showed that the proximity of a nucleophile to the urea was key with higher reactivity afforded to more closely associated systems. We developed a new type of acyl transfer agent for peptide coupling reactions, that showed similar or slightly better activity than HOAt.

We have expanded the development of a novel catalyst for the Diels-Alder reaction and optimized it for reactivity with α-substituted α,β-unsaturated aldehydes to provide good yields and moderate to excellent diastereo- and enantioselectivity. Contributions to the synthesis of C3 and/or C7 substituted 1,2-diazepanes have been made through a variety of different routes to access these chiral 7-membered rings routinely in fewer than 10 steps and with high enantiopurity. Most importantly, we have development of a new class of organocatalysts that are compatible with notoriously unreactive α-substituted enals. This highlights the possibility of establishing systems that extend the scope of the reactions that are currently performed with proline derivatives, imidazolidinones, and other 5-membered ring pyrrolidine catalysts. The most remarkable feature of this catalyst is its unconventional direction of the diene through electrostatic interactions from the carbamate rather than steric hindrance which is the usual mode of enantioinduction by iminium ion catalysts.

Conclusion

In part A we briefly described our attempts towards developing a novel organocatalyst for amide bond formation. The bifunctional catalyst design contained a hydrogen bond donor to activate and coordinate to the carboxylate and an aldehyde to activate the amine by bringing it into proximity of the carboxylate to promote nucleophilic attack. After the initial catalyst design proved unsuccessful, the project pivoted to investigate one of the key potential issues of the catalyst design; the position of the nucleophile relative the hydrogen bond donor.

A catalogue of ureas with different length linkers to a nucleophilic hydroxyl group was synthesized and tested for reactivity with valine based oxazolone. Replacing the imine nucleophile with a hydroxyl group ignores the differences in geometry between the two nucleophiles (*i.e.* the limited number of orientations the imine may adopt relative to the hydroxyl group). However, this modification was considered an adequate compromise for studying the effect of the nucleophile's position. The general trend observed from was that increased proximity of the alcohol nucleophile to the urea provided a rate enhancement in the acylation of the hydroxyl group. Installing a second electron withdrawing trifluoromethyl groups had some effect on acylation but the effect was not as significant as nucleophile position. This study led to the development of a new type of peptide coupling co-reagent which contained a urea and a 1-hydroxylbenzotriazole through an aryl linker.

The developed peptide coupling co-reagent displayed a slight rate enhancement relative HOAt for peptide coupling using EDC as the coupling reagent which provided a proof of concept. However, the results are complicated by the fact that EDC mediated peptide couplings rely on an initial activation of the carboxylate which is usually considered to be the rate limiting step. Future work is required to investigate the potential of racemization in the peptide formation which has been the main objective in the design of new coupling reagents and additives such as HOAt. Furthermore, it would be of interest to investigate a system other than peptide coupling where acyl transfer is the key step to find out if the urea-triazole system could function as a general acyl transfer reagent.

With the knowledge gained on nucleophile proximity, future studies may again investigate the initial catalyst design incorporating an aldehyde closer to the urea. More studies would also be

needed to conclude if hydrogen bond donors have the potential to sufficiently activate carboxylates towards nucleophilic imine attack.

In part B, we described the development a new type of enantioselective iminium ion catalyst, a 7-membered ring diazepane carboxylate, and applied it towards the Diels-Alder reaction. The 7-membered ring was originally developed in our research group by Dainis Kaldre for the organocatalytic Cope rearrangement of substituted 2-formyl-1,5-hexadienes. The substrates for the Cope rearrangement can also be described as α-substituted α,β-unsaturated aldehydes which are typically not compatible with secondary amine catalyst due to a significant A-1,3 strain in the formed iminium ion. To investigate if the diazepane carboxylate could be a general catalyst for α-substituted enals, we explored its activity in the Diels-Alder reaction. It proved to be an active catalyst and a diverse scope was achieved with high yields and moderate to excellent regio- and diastereoselectivity. Studies were performed on the catalyst to investigate and explain the superior activity, with the key feature identified to be its lower proton affinity. The ethyl diazepane carboxylate has been established as excellent catalyst for iminium ion catalysis of α-substituted enals.

Following the success of the achiral diazepane carboxylate catalyst, we wished to develop an enantioselective version for the Diels-Alder reaction of α-substituted enals. A wide variety of chiral diazepanes were synthesized and screened in attempts to find a highly enantioselective catalyst. We performed extensive studies, including experimental and *in silico* DFT calculations to provide insight into the reactivity and selectivity of these catalysts and how their properties may be improved. The conclusions of our studies led us to synthesize a diazepane possessing a stereogenic centre at C3 of the diazepane ring bearing a phenyl group matched with the chiral menthyl carbamate on the distal position for improved enantioinduction.

The catalyst provided good to high yields, moderate to excellent *exo*- and enantioselectivity for unreactive and sterically encumbered α-substituted enals in the enantioselective Diels-Alder reaction with a few of the Diels-Alder reactions disclosed achieved enantioselectivities over 90%. Insight into the transition state revealed that the enantioinduction is a result of electrostatic interactions between the carbamate and the diene, directing the diene approach towards the iminium ion. This is a unique mode of enantioinduction for iminium ion catalysis as steric

hindrance providing a preferred approach of the diene from one face is the conventional model to rationalize enantioselectivity.

The chiral catalysts described in this thesis have also been evaluated for reactivity in several other projects in our group; Cope rearrangement (Dr. Dainis Kaldre) and polyene cyclization (Samuel Plamondon and Josefine Warnica). These different and diverse projects illustrate that these hydrazide-based molecules are a new and exciting scaffold in iminium ion catalysis and have already been shown to perform a variety of reactions with moderate to excellent reactivity and selectivity. These catalysts have the potential of becoming even more selective through continuing efforts in our group. Future work around the Diels-Alder reaction would need to investigate enantioselectivity for acyclic dienes and intramolecular Diels-Alder reactions. The new electrostatic based model of enantioinduction observed in the Diels-Alder transition state will influence the development of other iminium ion catalyst and may also impact the design of other types of catalysts.

5 Experimental

Thin-layer chromatography (TLC) was carried out on glass plates, coated with 250 μm of 230-400 mesh silica gel that was saturated with the F-254 indicator. TLC plates were visualized using ultraviolet light and/or by exposure to an acidic solution of cerium (IV) ammonium molybdate followed by heating, a basic solution of potassium permanganate followed by heating or an acidic solution of *p*-anisaldehyde followed by heating. Flash column chromatography was carried out on 230-400 mesh silica gel (Silicycle) using reagent grade solvents.

Materials. All commercial reagents were used without further purification with the following exceptions tetrahydrofuran and diethyl ether were distilled from sodium benzophenone ketyl. Triethylamine, dichloromethane and toluene were distilled from calcium hydride. DMF was dried using 4 Å MS. *N*-Butyllithium was titrated with sec-butanol in toluene using 2,2'-dipyridyl as an indicator. Alkyl halides were passed through basic alumina prior to use.

Instrumentation. Infrared (IR) spectra were obtained using a Perkin-Elmer Spectrum One FT-IR spectrophotometer. NMR spectra were recorded at 300, 400, 500 MHz Varian or 400, 500 MHz Bruker spectrometers. Chemical shifts (δ) were internally referenced to the residual proton resonance $CDCl_3$ (δ 7.26 ppm), CD_3OD (δ 3.31 ppm), $(CD_3)_2SO$ (δ 2.50 ppm), CD_3NO_2 (δ 4.33 ppm). Coupling constants (J) are reported in Hertz (Hz). HRMS was obtained by Dr. Nadim Saadeh or Dr. Alexander S. Wahba at McGill University Department of Chemistry. Chiral HPLC was performed using AGILENT Infinity 1260 with Chiraldex OD or OB-H column (0.46 x 25 cm). Chiral GC was performed using HP 6890 series with Astec Chiraldex B-DM (30 m × 0.25 mm) column. Details of chromatographic conditions were indicated under each compound in experimental part. Structures generated with Chemdraw Professional 15.1. NMR data was processed with Mestrenova v11.

5.1 Synthesis of urea-alcohols

General procedure A for borane reduction of carboxylic acid: In a dry RBF, carboxylic acid (1 equiv.) was dissolved in THF (0.2 M) and cooled to 0 °C. BH_3*THF (1 M in THF, 1.2 equiv.) was added dropwise to the carboxylic acid solution after which the ice bath was removed and the reaction was stirred for 8-24 h. After consumption of starting material is complete according to TLC, the reaction was quenched by careful addition of H_2O at 0 °C and diluted with ethyl acetate. The layers were separated, and the aqueous layer was extracted with ethyl acetate and the combined organic layers were washed with saturated aq. sodium bicarbonate solution, water and brine, dried with anhydrous sodium sulfate and the solvent was removed under reduced pressure. The crude material was purified by flash column chromatography on silica gel (ethyl acetate in hexanes as eluent) to yield the product.

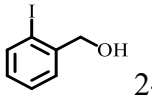

2-Iodobenzyl alcohol (**SI-1**) Synthesized according to general procedure A in and characterization agrees with literature.[3]

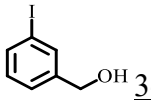

3-Iodobenzyl alcohol (**SI-2**). Synthesized according to general procedure A and characterization agrees with literature.[4]

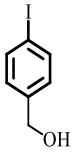

4-Iodobenzyl alcohol (**SI-3**). Synthesized according to general procedure A and characterization agrees with literature.[5]

[3] Sigma-Aldrich (Spectral data were obtained from Advanced Chemistry Development, Inc.)
[4] Sigma-Aldrich (Spectral data were obtained from Advanced Chemistry Development, Inc.)
[5] Gibson SE, Mainolfi N, Kalindjian SB, Wright PT, White AL. *Chem. Eur. J.* **2005**, 11, 69–80.

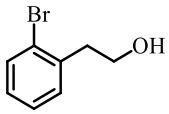

2-(2-bromophenyl)ethan-1-ol (**SI-4**). Synthesized according to general procedure A and characterization agrees with literature.[6]

General procedure B for TBS protection: The alcohol (1 equiv.) was dissolved in DMF (0.25 M). Imidazole (1.3 equiv.), DMAP (0.05 equiv.) and TBSCl (1.2 equiv.) were added and the reaction mixture was stirred until TLC indicates the alcohol was consumed. The reaction mixture was diluted with EtOAc and washed with H_2O, HCl (1 M) and brine. The organic phase was dried with anhydrous sodium sulfate and the solvent was removed under reduced pressure. The crude material was purified by flash column chromatography on silica gel (ethyl acetate in hexanes as eluent) to yield the product.

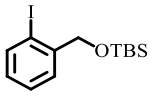

tert-butyl((2-iodobenzyl)oxy)dimethylsilane (**98**). Synthesized according to general procedure B and characterization agrees with literature.[7]

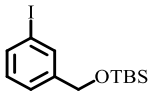

tert-butyl((3-iodobenzyl)oxy)dimethylsilane (**86**). Synthesized according to general procedure B and characterization agrees with literature.[8]

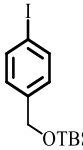

tert-butyl((4-iodobenzyl)oxy)dimethylsilane (**99**) Synthesized according to general procedure B and characterization agrees with literature.[9]

[6] Reich, H. J.; Goldenberg, W. S.; Sanders, A. W.; Jantzi, K. L.; Tzschucke, C. C. J. Am. Chem. Soc. 2003, 125, 3509-3521.
[7] Lautens, M.; Paquin, J-F.; Piguel, S.; Dahlmann, M. *J. Org. Chem*. **2001**, 66, 8127.
[8] Jian, H.; Tour, J. M.; *J. Org. Chem.* **2003**, 68, 5091.
[9] Smith, A.B. III, Rucker, P.V., Brouard, I., Freeze, B.S., Xia, S., and Horwitz, S.B. *Org. Lett*., **2005**, 7, 5199.

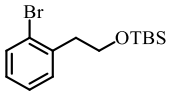

(2-bromophenethoxy)(tert-butyl)dimethylsilane (**100**). Synthesized according to general procedure B and characterization agrees with literature.[10]

General procedure C for boronic acid formation: The halide (1 equiv.) was dissolved in Et_2O (0.1 M) and cooled to - 78 °C. *n*-Buli (2 equiv.) was added dropwise and the solution was stirred for 30 min. B(O*i*-Pr)$_3$ was added and the reaction mixture was allowed to slowly reach rt. (the addition order of *n*-BuLi and triisopropylborate have been changed at times) After 2 h, HCl (1 M) was added carefully to quench the reaction and hydrolyse the borate. After 1 h, the phases were separated and the organic phase was washed with brine. The organic phase was dried with anhydrous sodium sulfate and the solvent was removed under reduced pressure. The crude material was purified by flash column chromatography on silica gel (ethyl acetate in hexanes as eluent) to yield the product.

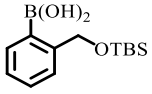

(2-(((tert-butyldimethylsilyl)oxy)methyl)phenyl)boronic acid (**101**) Synthesized according to general procedure C and was isolated as waxy solid in 78% yield. R_f = 0.28 (1/2 Hex/EtOAc) ^{1}H NMR (500 MHz, Methanol-d_4) δ 7.45 – 7.07 (m, 4H), 4.81 (s, 2H), 0.99 (s, 9H), 0.17 (s, 6H). ^{13}C NMR (126 MHz, MeOD) δ 143.77, 130.81, 127.85, 126.02, 125.03, 65.51, 25.15, 18.17, -6.71 (Missing ipso carbon: C-B(OH)$_2$). IR (film cm^{-1}) 3303, 2929, 2857, 1612, 1474, 1457, 1418, 1370, 1292, 1553, 1221, 1084, 972, 846, 776, 721. HRMS (ESI): calcd for $C_{15}H_{27}BNaO_3Si$ [M + Na + (MeOH)$_2$] 317.1718, found 317.1726.

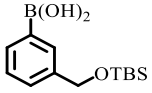

(3-(((tert-butyldimethylsilyl)oxy)methyl)phenyl)boronic acid (**87**) Synthesized according to general procedure C and was isolated as white crystals in 86% yield. R_f = 0.22 (3/1 Hex/EtOAc). ^{1}H NMR (400 MHz, CD_3OD) δ 7.83 – 7.57 (m, 2H), 7.56 – 7.18 (m, 2H), 4.69 (s, 2H), 0.94 (s, 9H), 0.10 (s, 6H). ^{13}C NMR (100 MHz, CD_3OD) δ 139.94, 132.41, 131.76, 128.22,

[10] Bell*, R. A.;* Dickson*, K. C.;* Valliant*, J. F. Can. J. Chem*. **1999**, 77*,* 146.

127.22, 65.16, 25.28, 17.97, -6.14 (Missing ipso carbon: C-B(OH)$_2$). IR (film cm^{-1}) 2955, 2929, 2857, 1606, 1430, 1338, 1253, 1193, 1078. HRMS (ESI): calcd for $C_{13}H_{23}BNaO_3$ [M + Na] 289.1405, found 289.1403.

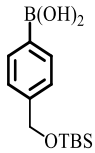

(4-(hydroxymethyl)phenyl)boronic acid (**102**) Synthesized according to general procedure B and characterization agrees with literature.[11]

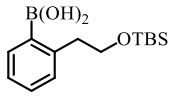

(2-(2-((tert-butyldimethylsilyl)oxy)ethyl)phenyl)boronic acid (**103**). Synthesized according to general procedure C and was isolated as waxy solid in 80% yield. R_f = 0.29 (3/1 Hex/EtOAc). ^{1}H NMR (500 MHz, Methanol-d_4) δ 7.63 (d, J = 7.2 Hz, 1H), 7.35 (t, J = 7.4 Hz, 1H), 7.20 (t, J = 7.4 Hz, 1H), 7.16 (d, J = 6.8 Hz, 1H), 4.20 (t, J = 5.4 Hz, 2H), 2.90 (t, J = 5.4 Hz, 2H), 0.93 (s, 9H), 0.07 (s, 6H). ^{13}C NMR (126 MHz, MeOD) δ 145.47, 132.34, 132.32, 130.70, 126.24, 125.63, 64.07, 32.04, 24.87, 17.54, -4.88 (Missing ipso carbon: C-B(OH)$_2$). IR (film cm^{-1}) 3385, 3019, 2953, 2930, 2888, 2857, 1603, 1404, 1351, 1298, 1021. HRMS (ESI): calcd for $C_{14}H_{24}O_3BSi$ [M - H] 279.1593, found 279.1589.

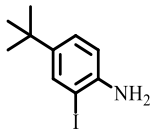

4-*t*-butyl-2-iodoaniline (**105**)

Prepared by ortho iodination of 4-*t*-butylaniline according to Iskra *et al* and characterization agrees with literature.[12]

[11] Magnus, N. A.; Anzeveno, P. B.; Coffey, D. S.; Hay, D. A.; Laurila, M. E.; Schkeryantz, J. M.; Shaw, B. W.; Staszak,. M. A. *Org. Process Res. Dev.* **2007**, 11, 560.
[12] J. Iskra, S. Stavber, M. Zupan, *Synthesis*, **2004**, 1869.

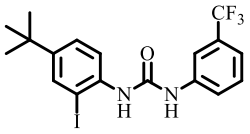

1-(4-(tert-butyl)-2-iodophenyl)-3-(3-(trifluoromethyl)phenyl)urea (**110**)

Prepared according to the procedure for **111** using aniline **105** and trifluoromethyl)aniline and was isolated as fluffy white crystals in 44% yield. R_f = 0.33 (2/1 Hex/EtOAc) ^{1}H NMR (400 MHz, Acetone-d_6) δ 9.12 (s, 1H), 8.11 (s, 1H), 7.95 (d, J = 8.6 Hz, 1H), 7.86 (d, J = 2.2 Hz, 1H), 7.71 (d, J = 8.1 Hz, 1H), 7.57 – 7.43 (m, 3H), 7.34 (d, J = 7.7 Hz, 1H), 1.33 (s, 9H). ^{13}C NMR (100MHz, $CO(CD_3)_2$): δ 152.3, 148.5, 140.8, 137.3, 135.7, 130.6 (q, ^2J = 33 Hz), 129.7, 126.0, 123.9 (q, ^1J = 270 Hz), 122.8, 121.8, 118.4 (q, ^3J = 4 Hz), 114.7 (q, ^3J = 4 Hz), 90.6, 33.9, 30.6. IR (film cm^{-1}) 3332, 2956, 1659, 1556, 1339, 1127. HRMS (ESI): calcd for $C_{26}H_{27}F_3IN_2NaO_2$ [M + Na] 485.0308, found 485.0314.

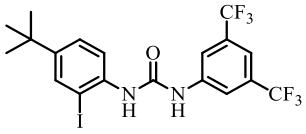

1-(3,5-bis(trifluoromethyl)phenyl)-3-(4-(tert-butyl)-2-iodophenyl)urea (**111**)

3,5-Bis(trifluoromethyl)aniline (0.64 g, 4.09 mmol) and CDI (0.71 g, 4.38 mmol) were dissolved in (12 mL) and stirred over night. Aniline **105** (0.42 g, 0.15 mmol) was added and the reaction mixture was again stirred over night. Ethyl acetate was added and the solution was washed with water and brine. The organic phase was dried with anhydrous magnesium sulfate and the solvent was removed under reduced pressure. The crude material was purified by flash column chromatography on silica gel (5 to 10% gradient ethyl acetate in hexanes as eluent) to yield the product (0.44 g, 55%) as fluffy white crystals. R_f = 0.35 (4/1 Hex/EtOAc) ^{1}H NMR (500 MHz, Acetone-d_6) δ 9.38 (s, 1H), 8.21 (s, 2H), 7.91 (d, J = 8.6 Hz, 1H), 7.86 (d, J = 2.2 Hz, 1H), 7.63 (m, 2H), 7.46 (dd, J = 8.6, 2.2 Hz, 1H), 1.31 (s, 9H). ^{13}C NMR (126 MHz, Acetone-d_6) δ 152.39, 149.05, 141.90, 136.83, 135.79, 131.64 (q, ^2J = 34 Hz), 126.04, 123.54 (q, ^1J = 273 Hz), 123.30, 118.22 (q, ^3J = 3 Hz), 114.87 (q, ^3J = 4 Hz), 91.37, 33.92, 30.58. IR (film cm^{-1}) 3293, 3114, 2971,

1657, 1572, 1520, 1472, 1383, 1275, 1174, 1129, 883. HRMS (ESI): calcd for $C_{19}H_{17}F_6IN_2NaO$ [M + Na] 553.0182, found 553.0187.

General procedure D for Suzuki cross coupling: $Pd(OAc)_2$ (0.07 equiv.) and PPh_3 (0.35 equiv.) were mixed in toluene and stirred for 1 h. A solution of the halide (1 equiv.) and boronic acid (1.3 equiv.) in THF was added followed by Na_2CO_3 (0.5 M). The reaction mixture was heated to 65 °C until TLC indicated consumption of halide. The reaction mixture was cooled down and filtered through celite, rinsed with ethyl acetate. The organic solution was washed with HCl (1 M) and brine, dried with anhydrous magnesium sulfate and the solvent was removed under reduced pressure. The crude material was purified by flash column chromatography on silica gel (gradient of ethyl acetate in hexanes as eluent) to yield the TBS protected product.
The TBS protected product was dissolved in MeOH followed by PTSA (20 mol%). The solution was stirred until TLC showed that the SM was consumed. The reaction mixture was diluted with EtOAc and washed with K_2CO_3 (aq. sat.) and brine, dried with anhydrous magnesium sulfate and the solvent was removed under reduced pressure. The crude material was purified by flash column chromatography on silica gel (gradient of ethyl acetate in hexanes as eluent) to yield the product.

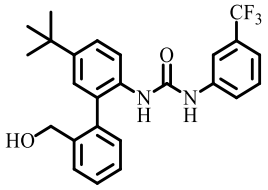

1-(5-(tert-butyl)-2'-(hydroxymethyl)-[1,1'-biphenyl]-2-yl)-3-(3-(trifluoromethyl)phenyl)urea (**112**). Synthesized according to general procedure D and was isolated as white crystals in 27% yield. R_f = 0.51 (3/1 Hex/EtOAc). ^{1}H NMR (300 MHz, Chloroform-*d*) δ 7.72 (d, *J* = 8.5 Hz, 1H), 7.48 – 7.07 (m, 11H), 7.02 (s, 1H), 4.35 (d, J_{AB} = 13 Hz, 2H), 1.30 (s, 9H). ^{13}C NMR (75 MHz, $CDCl_3$) δ 153.4, 147.6, 138.9, 138.4, 138.1, 132.8, 131.1 (q, ^{2}J=32Hz), 130.5, 129.3, 129.2, 128.4, 128.3, 127.3, 125.7, 122.9, 122.8, 119.6 (q, ^3J = 4 Hz), 116.3 (q, ^3J = 4 Hz), 63.1, 34.5, 31.4. Missing **C**F_3 and **C**-CF_3 (weak signals due to *J*-coupling). IR (film cm^{-1}) 3325, 2962, 1738, 1665, 1562, 1522, 1336, 1124, 698. HRMS (ESI): calcd for $C_{25}H_{26}F_3N_2O_2$ [M + H] 443.1941, found 443.1938.

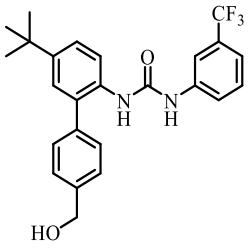

1-(5-(tert-butyl)-4'-(hydroxymethyl)-[1,1'-biphenyl]-2-yl)-3-(3-(trifluoromethyl)phenyl)urea (**116**)

Synthesized according to general procedure D and was isolated as off-white crystals in 85% yield. ^{1}H NMR (400 MHz, Acetonitrile-d_3) δ 7.89 – 7.82 (m, 2H), 7.76 (s, 1H), 7.50 – 7.34 (m, 7H), 7.29 – 7.25 (m, 2H), 6.92 (s, 1H), 4.64 (d, J = 5.6 Hz, 2H), 1.34 (s, 9H). ^{13}C NMR (101 MHz, CD_3CN) δ 153.55, 147.52, 141.85, 141.00, 138.29, 133.90, 133.30, 130.90 (q, ^{2}J = 33 Hz), 130.17, 129.82, 127.77, 127.75, 125.49, 124.91 (q, ^{1}J = 273 Hz), 123.44, 122.48, 119.11 (q, ^{3}J = 4 Hz), 115.39 (q, ^{3}J = 4 Hz), 63.99, 34.57, 31.18. IR (film cm^{-1}) 3331, 1962, 1663, 1561, 1523, 1494, 1447, 1396, 1337, 1296, 1222, 1166, 1110, 1071, 792, 737, 699. HRMS (ESI): [M + Na] for $C_{25}H_{25}F_3N_2NaO_2$ found 465.1748 calcd 465.1760

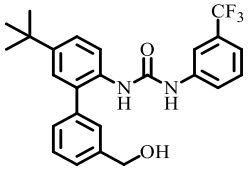

1-(5-(tert-butyl)-3'-(hydroxymethyl)-[1,1'-biphenyl]-2-yl)-3-(3-(trifluoromethyl)phenyl)urea (**114**) **.**

Synthesized according to general procedure D and was isolated as white fluffy crystals in 90% yield. R_f = 0.41 (2/1 Hex/EtOAc) ^{1}H NMR (500 MHz, Chloroform-*d*) δ 7.81 – 7.66 (m, 2H), 7.60 – 7.04 (m, 10H), 6.74 (s, 1H), 4.56 (s, 2H), 3.90 – 3.56 (m, 1H), 1.35 (s, 9H). ^{13}C NMR (126 MHz, $CDCl_3$) δ 153.51, 147.69, 140.12, 139.31, 139.17, 133.19, 131.73, 131.11 (q, ^{2}J = 33 Hz), 129.30, 129.12, 128.43, 127.40, 127.05, 125.60, 123.91 (q, ^{1}J = 271 Hz), 122.77, 122.42, 119.45 (q, ^{3}J = 3 Hz), 116.01 (q, ^{3}J = 4 Hz), 64.93, 34.45, 31.36. IR (film cm^{-1}) 3328, 2942, 1663, 1563, 1521, 1494, 1447, 1397, 1337, 1297, 1228, 1166, 1123, 1071, 909, 793, 733, 699. HRMS (ESI): calcd for $C_{25}H_{25}F_3N_2NaO_2$ [M + Na] 465.1760, found 465.1755.

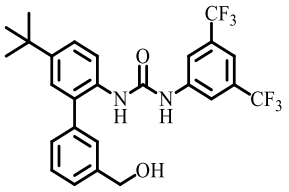

1-(3,5-bis(trifluoromethyl)phenyl)-3-(5-(tert-butyl)-3'-(hydroxymethyl)-[1,1'-biphenyl]-2-yl)urea (**115**)

Synthesized according to general procedure D and was isolated as white crystals in 75% yield. R_f = 0.36 (3/1 Hex/EtOAc). ^{1}H NMR (400 MHz, Chloroform-*d*) δ 8.38 (s, 1H), 7.80 (s, 2H), 7.71 (d, *J* = 8.6 Hz, 1H), 7.44 (s, 1H), 7.39 – 7.24 (m, 2H), 7.24 – 7.09 (m, 4H), 6.91 (s, 1H), 4.54 (s, 2H), 4.31 – 3.86 (bs, 1H), 1.33 (s, 9H). ^{13}C NMR (101 MHz, $CDCl_3$) δ 153.29, 147.65, 140.30, 139.54, 139.23, 132.60, 131.95 (q, ^2J = 33 Hz), 131.27, 129.36, 129.12, 128.76, 127.41, 127.33, 125.46, 123.15 (q, ^1J = 273 Hz), 122.11, 118.45 (q, ^3J = 4 Hz), 115.70 (q, ^3J = 4 Hz), 64.98, 34.39, 31.28. IR (film cm^{-1}) 3315, 2969, 1738, 1661, 1604, 1561, 1519, 1483, 1336, 1296, 1227, 1216, 1163, 1122, 790, 698, 657. HRMS (ESI): calcd for $C_{26}H_{24}F_6N_2NaO_2$ [M + Na], 533.1634 found 533.1650.

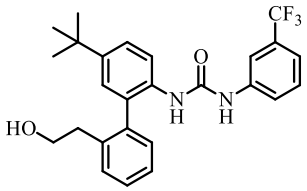

1-(5-(tert-butyl)-2'-(2-hydroxyethyl)-[1,1'-biphenyl]-2-yl)-3-(3-(trifluoromethyl)phenyl)urea (**117**)**.**

Synthesized according to general procedure D and was isolated as white crystals in 16% yield. ^{1}H NMR (400 MHz, Chloroform-*d*) δ 7.78 (d, *J* = 8.6 Hz, 1H), 7.61 (s, 1H), 7.52 – 6.99 (m, 11H), 3.65 (m, 2H), 2.98 (s, 1H), 2.64 (m, 2H), 1.32 (s, 9H). ^{13}C NMR (101 MHz, $CDCl_3$) δ 153.52, 147.02, 139.07, 139.06, 137.12, 132.60, 132.50, 131.10 (q, ^2J = 33 Hz), 130.69, 129.29, 129.24, 128.19, 127.49, 126.68, 125.32, 122.53, 121.90, 119.44 (q, ^3J = 4 Hz), 116.13 (q, ^3J = 4 Hz), 62.30, 35.27, 34.39, 31.37. **C**F_3 signal could not be found but one weak peak at 125.22 ppm is unassigned. IR (film cm^{-1}) 3336, 2962, 1668, 1560, 1522, 1337, 1166. HRMS (ESI): calcd for $C_{26}H_{28}N_2O_2F_3$ [M + H] 457.2086, found 457.2095.

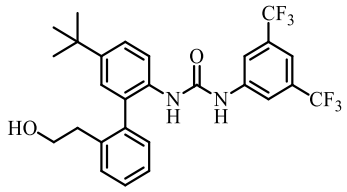

1-(3,5-bis(trifluoromethyl)phenyl)-3-(5-(tert-butyl)-2'-(2-hydroxyethyl)-[1,1'-biphenyl]-2-yl)urea (**118**)

Synthesized according to general procedure D using 2 equiv. boronic acid and was isolated as white crystals in 70% yield. ^{1}H NMR (400 MHz, Chloroform-*d*) δ 7.94 – 7.60 (m, 4H), 7.47 – 7.11 (m, 8H), 3.99 – 3.52 (m, 2H), 2.94 – 2.39 (m, 3H), 1.33 (s, 9H). ^{13}C NMR (101 MHz, $CDCl_3$) 152.9, 147.3, 140.4, 139.2, 137.0, 132.33, 132.30, 132.2 (q, ^{2}J = 33 Hz), 130.9, 129.0, 128.3, 127.6, 126.8, 123.1 (q, ^{1}J = 271Hz), 121.6, 118.5 (q, ^{3}J = 4 Hz), 115.7 (q, ^{3}J = 4 Hz), 62.4, 35.0, 34.4, 31.4 IR (film cm^{-1}) 3344, 2964, 1671, 1572, 1523, 1474, 1386, 1294. HRMS: calcd for $C_{27}H_{27}N_2O_2F_6$ [M + H] 525.19712, found 525.19759.

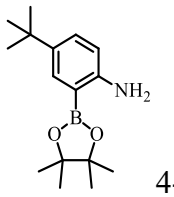

4-(tert-butyl)-2-(4,4,5,5-tetramethyl-1,3,2-dioxaborolan-2-yl)aniline (**126**)

Halide **105** (0.50 g, 1.82 mmol) was dissolved in 1,4-dioxane and then triethylamine (1.01 mL, 7.27 mmol), $Pd(dppf)_2Cl_2$*DCM (119 mg, 0.15 mmol, 0.08 equiv.) and borane (792 µL, 5.46 mmol) was added. The atmosphere was exchanged for argon and the orange reaction mixture was heated to 100 °C for 3 h. The reaction mixture which had turned black was cooled down and filtered through celite, rinsed with ethyl acetate. The organic solution was washed with brine, dried with anhydrous magnesium sulfate and the solvent was removed under reduced pressure. The crude material was purified by flash column chromatography on silica gel (gradient of 5 to 15% ethyl acetate in hexanes as eluent) to yield the product (0.265 mg, 53%) as white crystals. R_f = 0.73 (80/20 Hex/EtOAc). ^{1}H NMR (500 MHz, $CDCl_3$) 7.66 (d, 1H, 2.4Hz), 7.30 (dd, 1H, 2.5Hz and 8.4Hz), 6.60 (d, 1H, 8.4Hz), 4.68 (s, 2H), 1.37 (s, 12H), 1.33 (s, 9H). ^{13}C NMR (126 MHz, $CDCl_3$) δ 151.41, 139.32, 132.82, 130.07, 114.80, 83.39, 33.86, 31.57, 24.95. (No signal from **C**-B) IR (film cm^{-1}): 3486, 3388, 2963, 1617, 1571, 1500, 1415, 1366, 1353, 1319, 1302, 1254, 1142, 1122, 964, 856. HRMS (ESI): calcd for $C_{16}H_{27}BNO_4$ [M + H] 276.2132, found 276.2142.

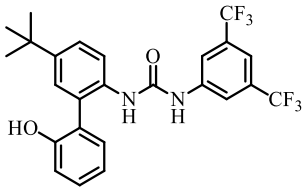

1-(3,5-bis(trifluoromethyl)phenyl)-3-(5-(tert-butyl)-2'-hydroxy-[1,1'-biphenyl]-2-yl)urea (**128**) Aniline **127** (33 mg, 0.14 mmol) was dissolved in $CHCl_3$ and **124** (88 mg, 0.28 mmol) was added. The reaction mixture was stirred over night and HCl (1 M) was added. The layers were separated and the organic phase was washed with brine, dried with anhydrous magnesium sulfate and the solvent was removed under reduced pressure. The crude material was purified by flash column chromatography on silica gel (gradient of 20 to 35% ethyl acetate in hexanes as eluent) to yield the product (17 mg, 25%) as beige waxy crystals. R_f = 0.15 (3/1 Hex/EtOAc). ^{1}H NMR (400 MHz, Chloroform-*d*) δ 8.08 – 7.78 (m, 3H), 7.59 (d, *J* = 8.4 Hz, 1H), 7.55 – 7.50 (m, 2H), 7.46 – 7.36 (m, 2H), 7.25 (m, 2H), 7.05 – 6.91 (m, 3H), 1.39 (s, 9H). ^{13}C NMR (101 MHz, $CDCl_3$) δ 153.90, 152.93, 150.17, 139.59, 132.33, 132.00, 131.95, 131.30, 129.90, 129.09, 126.37, 125.40, 124.55, 120.97, 119.25, 116.06, 34.73, 31.35. Weak signals for **C**F_3 and **C**-CF_3, most likely at 122 ppm and 132 ppm, respectively, are not included. IR (film cm^{-1}) 3339, 2968, 1738, 1665, 1574, 1519, 1386, 1277, 1180, 1135. HRMS (ESI): calcd for $C_{25}H_{23}N_2O_2F_6$ [M+H] 497.1658, found 497.1657.

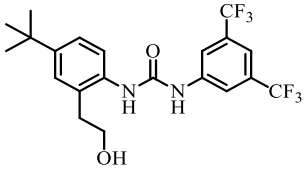

1-(3,5-bis(trifluoromethyl)phenyl)-3-(4-(tert-butyl)-2-(2-hydroxyethyl)phenyl)urea (**122**) A RBF was charged olefin **120** (75 mg, 0.18 mmol) and a stir bar under argon atmosphere and THF (4 mL) was added. The solution was cooled to 0 °C followed by addition of borane (1 M in THF, 175 µL, 0.18 mmol). The reaction was allowed to reach room temperature and stirred over night. Hydrogen peroxide (30 wt%, 59 µL, 0.53 mmol) and NaOH (2 M in water, 263 µL, 0.53 mmol) was added and the reaction mixture was stirred for additional 6 h. The reaction mixture was quenched with water and ether was added. The layers were separated and the organic phase was washed with brine, dried with anhydrous magnesium sulfate and the

solvent was removed under reduced pressure. The crude material was purified by flash column chromatography on silica gel (gradient of 15 to 30% ethyl acetate in hexanes as eluent) to yield the product (22 mg, 29%) as beige waxy crystals. R_f = 0.25 (3/1 Hex/EtOAc). ^{1}H NMR (500 MHz, Acetonitrile-d_3) δ 8.14 – 8.03 (m, 3H), 7.93 (s, 1H), 7.60 (s, 1H), 7.54 (d, J = 8.2 Hz, 1H), 7.35 – 7.28 (m, 2H), 3.80 (td, J = 6.0, 4.0 Hz, 2H), 3.25 (t, J = 4.3 Hz, 1H), 2.85 (t, J = 6.1 Hz, 2H), 1.34 (s, 9H). ^{13}C NMR (126 MHz, CD_3CN) δ 153.07, 147.83, 142.00, 134.19, 132.81, 131.42 (q, ^2J = 33 Hz) 127.34, 124.45, 123.69, 123.61 (q, ^1J = 270Hz) 118.24 (q, ^3J = 4 Hz), 114.83 (q, ^3J = 4 Hz), 63.18, 34.64, 33.98, 30.63. IR (film cm^{-1}) 3328, 3116, 2960, 1662, 1572, 1471, 1383, 1273, 1170, 1229, 881, 681. HRMS (ESI): calcd for $C_{21}H_{23}N_2O_2F_6$ [M + H] 449.1658, found 449.1657.

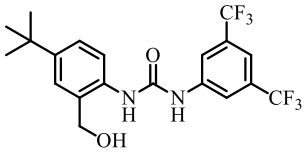

1-(3,5-bis(trifluoromethyl)phenyl)-3-(4-(tert-butyl)-2-(hydroxymethyl)phenyl)urea (**122**) Olefin **120** (45 mg, 0.11 mmol) was dissolved in DCM (5 mL) and cooled to -78 °C. Ozone was bubbled through the reaction mixture for 30 min to give a heavenly blue colour. The reaction mixture was allowed to reach room temperature after which borane (2 M in THF, 211 μL, 0.42 mmol) was added and stirred for 12 h. The reaction mixture was quenched with water and then transferred to a separatory funnel. The layers were separated and the organic phase was washed with $NaHCO_3$ and brine, dried with anhydrous magnesium sulfate and the solvent was removed under reduced pressure. The crude material was purified by flash column chromatography on silica gel (gradient of 10 to 30% ethyl acetate in hexanes as eluent) to yield the title product (22 mg, 33%) as white crystals. R_f = 0.44 (2/1 Hex/EtOAc). ^{1}H NMR (400 MHz, Chloroform-d) δ 7.86 (d, J = 8.3 Hz, 4H), 7.62 (d, J = 8.4 Hz, 1H), 7.50 (s, 1H), 7.36 (dd, J = 8.4, 2.3 Hz, 1H), 7.28 (d, J = 2.3 Hz, 1H), 4.69 (s, 2H), 3.11 – 2.62 (bs, 1H), 1.28 (s, 9H). ^{13}C NMR (101 MHz, $CDCl_3$) δ 153.57, 148.62, 140.14, 133.76, 132.18 (q, ^2J = 33 Hz), 131.25, 126.69, 126.44, 123.80, 123.11 (q, ^1J = 274 Hz), 118.93 (q, ^1J = 4 Hz), 116.27 (q, ^1J = 3 Hz), 63.98, 34.39, 31.19. IR (film cm^{-1}) 3321, 2966, 1670, 1575, 1387, 1305, 1277, 1180, 1133. HRMS (ESI): calcd for $C_{20}H_{20}F_6N_2NaO_2$ [M + Na] 457.1321, found 457.1325.

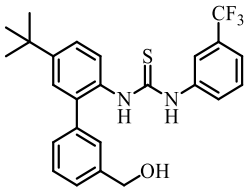

1-(5-(tert-butyl)-3'-(hydroxymethyl)-[1,1'-biphenyl]-2-yl)-3-(3-(trifluoromethyl)phenyl)thiourea (**132**)

Aniline **105** (68 mg, 0.18 mmol) and isothiocyanate **108** (56 mg, 0.27 mmol) were dissolved in DCM. DMAP (1 mg, 0.009 mmol) was added and the reaction mixture was stirred over night. The reaction mixture was filtered through a plug of silica and the solvent was removed under reduced pressure. The crude was dissolved in MeOH:Et_2O (1:1, 5mL) and PTSA (1 crystal) was added and stirred for 1 h. Ethyl acetate was added and the organic phase was washed with brine, dried with anhydrous magnesium sulfate and the solvent was removed under reduced pressure. The crude material was purified by flash column chromatography on silica gel (gradient of 10 to 15% ethyl acetate in hexanes as eluent) to yield the title product (18 mg, 21%) as white crystals. Significant decomposition of the thiourea to urea during the chromatography was observed. ^{1}H NMR (500 MHz, Chloroform-*d*) δ 7.99 (s, 1H), 7.59 – 7.32 (m, 11H), 7.25 (d, J = 1.9 Hz, 1H), 4.73 (s, 2H), 2.49 (s, 1H), 1.39 (s, 9H). ^{13}C NMR (126 MHz, $CDCl_3$) δ 180.05, 152.02, 141.82, 138.39, 138.17, 137.66, 131.21 (q, ^2J = 30 Hz), 130.72, 129.33, 129.13, 128.89, 128.27, 127.85, 127.25, 127.08, 126.69, 126.22, 123.57 (q, ^1J = 273 Hz), 123.18 (q, ^3J = 3 Hz), 122.12 (q, ^3J = 4 Hz), 64.96, 34.88, 31.28. IR (film cm^{-1}) 3211, 2964, 2839, 1738, 1601, 1524, 1302, 1165, 1124. HRMS (ESI): calcd for $C_{25}H_{26}F_3N_2OS$ [M + H] 459.1712, found 459.1726.

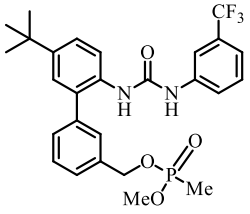

(5'-(tert-butyl)-2'-(3-(3-(trifluoromethyl)phenyl)ureido)-[1,1'-biphenyl]-3-yl)methyl methyl methylphosphonate (**136**)

Dimethyl methylphosphonate (49 µL, 0.45 mmol) was dissolved in DCM (4 mL). Oxalyl chloride (38 µL, 0.45 mmol) was added and the reaction mixture was refluxed for 4 h. The solvent was removed under reduced pressure and then dissolved in THF (2 mL). Et_3N (126 µL, 0.90 mmol)

and **114** (20 mg, 0.045 mmol) were added and the reaction was stirred overnight. The reaction mixture was quenched with water and DCM was added. The layers were separated and the organic phase was washed with water and brine, dried with anhydrous magnesium sulfate and the solvent was removed under reduced pressure. The crude material was purified by flash column chromatography on silica gel (gradient of 10 to 25% ethyl acetate in hexanes as eluent) to yield the title product (14 mg, 57%) as white crystals. ^{1}H NMR (500 MHz, Chloroform-*d*) δ 9.29 (s, 1H), 8.23 (d, *J* = 8.7 Hz, 1H), 7.81 (d, *J* = 9.2 Hz, 1H), 7.63 – 7.49 (m, 4H), 7.46 – 7.37 (m, 3H), 7.33 (t, *J* = 8.0 Hz, 1H), 7.27 – 7.24 (m, 1H), 7.16 (d, *J* = 7.7 Hz, 1H), 5.20 – 5.03 (m, 2H), 3.61 (d, *J* = 11.3 Hz, 3H), 1.46 (d, *J* = 17.5 Hz, 3H), 1.33 (s, 9H). Et_2O impurity. ^{13}C NMR (126 MHz, $CDCl_3$) δ 153.02, 145.48, 140.77, 139.43, 135.56, 133.25, 130.80 (q, ^{2}J = 23 Hz), 130.66, 130.50, 130.11, 130.03, 129.31, 127.80, 126.64, 125.58, 124.08 (q, ^{1}J = 272 Hz), 121.10, 120.69, 118.08 (q, ^{3}J = 4 Hz), 114.72 (q, ^{3}J = 4 Hz), 69.59, 52.49, 34.26, 31.39, 11.34 (d, ^{1}J = 144 Hz) ^{1}H-^{31}P HMBC correlation between proton at 9.29 ppm and phosphorous at 32 ppm. IR (film cm^{-1}) 3353, 2958, 1711, 1568, 1520, 1495, 1447, 1397, 1338, 1295, 1209, 1164, 1119, 1198, 1055, 1010, 916, 792, 701, 658. HRMS (ESI): calcd for $C_{27}H_{30}F_3N_2NaO_4P$ [M + Na] 557.1787, found 557.1788.

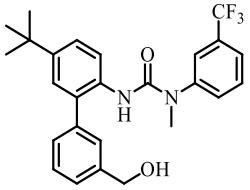

3-(5-(tert-butyl)-3'-(hydroxymethyl)-[1,1'-biphenyl]-2-yl)-1-methyl-1-(3-(trifluoromethyl)phenyl)urea (**134**). ^{1}H NMR (400 MHz, Chloroform-*d*) δ 8.16 (d, *J* = 8.7 Hz, 1H), 7.47 (d, *J* = 7.9 Hz, 1H), 7.44 – 7.32 (m, 3H), 7.25 (d, *J* = 7.1 Hz, 2H), 7.21 – 7.05 (m, 3H), 6.97 (d, *J* = 7.4 Hz, 1H), 6.28 (s, 1H), 4.63 (s, 2H), 3.28 (s, 3H), 1.31 (s, 9H).^{13}C NMR (101 MHz, $CDCl_3$) δ 153.98, 145.72, 143.27, 141.52, 138.91, 133.19, 132.34 (q, ^{2}J = 23 Hz), 130.98, 130.73, 130.55, 128.87, 127.78, 127.42, 126.48, 125.87, 125.47, 124.16 (t, *J* = 4 Hz, might contain one more carbon peak), 119.47, 64.87, 37.14, 34.28, 31.39. Missing **C**F_3. IR (film cm^{-1}) 3403, 2960, 2951, 1665, 1510, 1330, 1130. HRMS (ESI): calcd for $C_{26}H_{27}F_3N_2NaO_2$ [M + Na] 479.1917, found 449.1924.

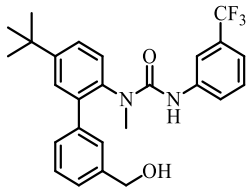

1-(5-(tert-butyl)-3'-(hydroxymethyl)-[1,1'-biphenyl]-2-yl)-1-methyl-3-(3-(trifluoromethyl)phenyl)urea (**135**). ^{1}H NMR (500 MHz, Chloroform-*d*) δ 7.50 (s, 2H), 7.41 – 7.17 (m, 9H), 6.36 (s, 1H), 4.64 (s, 2H), 3.07 (s, 3H), 1.40 (s, 9H). ^{13}C NMR (126 MHz, cdcl$_3$) δ 154.28, 152.15, 141.62, 139.71, 139.27, 138.98, 136.87, 130.99 (q, ^{2}J = 16 Hz), 129.12, 128.89, 128.82, 128.15, 127.41, 126.70, 126.63, 126.31, 123.92 (q, ^{1}J = 273 Hz), 122.61, 119.39 (q, ^{3}J = 4 Hz), 116.14 (q, ^{2}J = 4 Hz), 64.94, 37.09, 34.87, 31.31. IR (film cm^{-1}) 3422, 2950, 2926, 1662, 1533, 1444, 1324, 1125. HRMS (ESI): calcd for $C_{26}H_{27}F_3N_2NaO_2$ [M + Na], calcd 479.1917, found 479.1916.

General procedure for acylation of urea-alcohols with oxazolones

The urea-alcohol (1 equiv.) was dissolved in $CDCl_3$ (0.2 M on urea-alcohol) in a NMR tube. Oxazolone **94** (2.0 equiv.) and internal standard were added and an initial ^{1}H-NMR was taken (time 0 h). Et_3N (1.5 equiv.) was added and ^{1}H-NMR spectra were taken to monitor the reaction. Conversion was determined by integration of the urea-alcohol (C**H**$_2$OH except for phenol where the proton on oxazolone) relative internal standard and monitor the disappearance of the peak. Only one product forms in all reactions (where reaction occur) and determining conversion based on integration of acyl product or disappearance of oxazolone gives the same result.

5.2 Acyl transfer agent

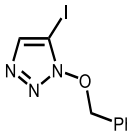

1-(benzyloxy)-5-Iodo-1,2,3-triazole. (**147**)

Synthesized according to Begtrup and coworkers.[13] ^{1}H NMR (400 MHz, $CDCl_3$) 7.62 (s, 1H), 7.43-7.38 (m, 5H), 5.45 (s, 2H). ^{13}C NMR (100 MHz, $CDCl_3$) 139.2, 132.1, 130.5, 130.1, 129.0, 119.4, 83.2, 72.3. IR (film, cm^{-1}) 3132, 3065, 3033, 2961, 2895, 1499, 1471, 1455, 1397, 1220,

[13] P. Uhlmann, J. Felding, P. Vedsø, and M. Begtrup *J. Org. Chem.* **1997,** *62,* 9177.

1108, 957, 826, 727, 691. HRMS (ESI): calcd for $C_9H_8IN_3NaO$ [M + Na] 323.9604, found 323.9601.

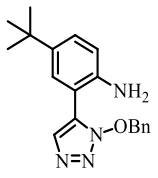

1-(Benzyloxy)-5-(2-amino-4-*tert*butyl-phenyl)-1,2,3-triazole (**148**)

Synthesized according to general procedure D using P(*o*-tolyl)$_3$ instead of PPh_3 as ligand and K_3PO_4 instead of $NaHCO_3$ as base. Isolated in 57% yield (54 mg) as a yellow wax. ^{1}H NMR (400 MHz, $CDCl_3$) 7.71 (s, 1H, 4-H), 7.29-7.24 (m, 3H), 7.20 (d, 1H), 7,18 (d, 1H), 7.07 (m, 2H), 6.68 (d, 7.1 Hz), 5.31 (s, 2H). ^{13}C NMR (100 MHz, $CDCl_3$) 142.3, 141.33, 132.2, 131.8, 130.0, 129.9, 129.6, 128.5, 128.2, 127.3, 116.1, 109.3, 82.6, 34.0, 31.4. IR (film cm^{-1}): 3011, 2964, 2870, 1738, 1602, 1525, 1450, 1311, 1254, 1165, 1124, 1070,796, 737, 697. HRMS (ESI): calcd for $C_{19}H_{23}N_4O$ [M + H] 323.1866, found 323.1870.

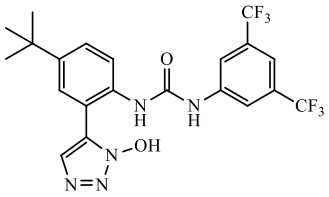

1-(3,5-bis(trifluoromethyl)phenyl)-3-(4-(tert-butyl)-2-(1-hydroxy-1H-1,2,3-triazol-5-yl)phenyl)urea (**139**)

Prepared according to the same procedure for **138** and isolated as off-white crystals in 80% yield. ^{1}H NMR (400 MHz, DMSO-d_6) δ 11.95 (s, 1H), 10.76 (bs, 1H), 9.80 (s, 1H), 8.20 (s, 2H), 7.84 (s, 1H), 7.69 (d, J = 8.6 Hz, 1H), 7.57 (s, 1H), 7.43 (d, J = 10.5 Hz, 1H), 7.35 (s, 1H), 1.32 (s, 9H). ^{13}C NMR (126 MHz, CD_3OD) δ 155.04, 148.53, 143.37, 135.81, 133.03 (q, ^2J = 30 Hz), 128.35, 128.01, 122.71, 125.40, 124.83 (q, ^1J = 270 Hz), 119.14 (q, ^3J = 4 Hz), 115.60 (q, ^3J = 5 Hz), 35.24, 31.66 (1 missing). IR (film cm^{-1}) 3033, 2986, 1703, 1574, 1472, 1373, 1274, 1127. HRMS (ESI): [M + H] for $C_{21}H_{19}F_6N_5NaO_2$ found 510.1324, calcd 510.1335.

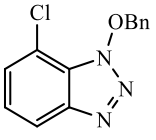

1-(benzyloxy)-7-chloro-1H-benzo[*d*][1,2,3]triazole (**142**)

Prepared according to literature in 41% yield.[14] ^{1}H NMR (400 MHz, Chloroform-*d*) δ 7.93 (dd, *J* = 7.7, 3.2 Hz, 1H), 7.57 – 7.24 (m, 7H), 5.58 (d, *J* = 4.0 Hz, 2H). ^{13}C NMR (101 MHz, $CDCl_3$) δ 144.95, 132.33, 130.10, 129.77, 128.77, 128.52, 125.27, 125.20, 118.91, 115.42, 84.07. IR (film cm^{-1}) 3035, 2889, 1876, 1577, 1495, 1453, 1416, 1343, 1242, 1096, 948, 900, 840, 789, 730, 691. HRMS (ESI): [M + Na] for $C_{13}H_{10}ClN_3NaO$ found 282.0405, calcd 282.0405. mp 85-86 °C.

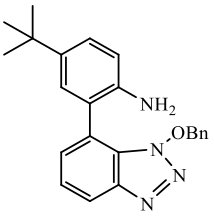

2-(1-(benzyloxy)-1H-benzo[d][1,2,3]triazol-7-yl)-4-(tert-butyl)aniline (**143**)

Synthesized according to general procedure D using SPhos instead of PPh_3 as ligand and K_2CO_3 instead of $NaHCO_3$ as base in a Schlenk bomb at 100 ˚C in Toluene:water. Isolated in 61% yield as white crystals. ^{1}H NMR (500 MHz, Chloroform-*d*) δ 8.06 (dd, *J* = 8.0, 1.4 Hz, 1H), 7.59 – 7.43 (m, 2H), 7.43 – 7.18 (m, 5H), 6.93 – 6.76 (m, 3H), 5.13 – 4.89 (AB, q, 2H), 3.53 (s, 2H), 1.28 (s, 9H). ^{13}C NMR (126 MHz, $CDCl_3$) δ 144.35, 142.17, 141.32, 132.17, 130.06, 129.70, 129.35, 128.38, 128.16, 126.67, 125.85, 125.06, 122.73, 121.07, 119.51, 115.58, 83.30, 34.02, 31.53. IR (film cm^{-1}) 3471, 3359, 2960, 1621, 1508. 1496. HRMS (ESI): [M + Na] for $C_{23}H_{24}N_4NaO$ found 395.1846, calcd 395.1842.

[14] R. R. Holmes, R. P. Bayer *J. Am. Chem. Soc*., **1960**, 3454.

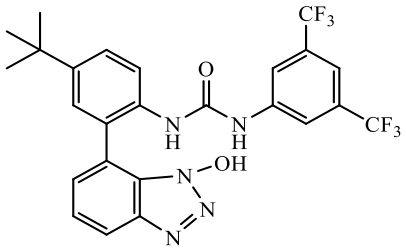

1-(3,5-bis(trifluoromethyl)phenyl)-3-(4-(tert-butyl)-2-(1-hydroxy-1H-benzo[d][1,2,3]triazol-7-yl)phenyl)urea (**138**)

Prepared according to the same procedure for **128** with subsequent benzyl deprotection: in EtOH using 10 mol% Pd/C and bubbled hydrogen gas for 1h. Filtered through celite and then purified by flash column chromatography on silica gel (gradient of 10 to 40% ethyl acetate in hexanes as eluent) to yield the title product in 89% yield as white crystals. ^{1}H NMR (500 MHz, DMSO-d_6) δ 13.17 (s, 1H), 9.48 (s, 1H), 8.03 (d, J = 8.4 Hz, 1H), 7.95 (d, J = 1.6 Hz, 2H), 7.89 (d, J = 8.6 Hz, 1H), 7.78 (s, 1H), 7.58 (s, 1H), 7.52 – 7.41 (m, 2H), 7.38 (d, J = 7.0 Hz, 1H), 7.28 (d, J = 2.4 Hz, 1H), 1.32 (s, 9H).^{13}C NMR (126 MHz, CD_3OD) δ 147.79, 141.58, 133.48, 131.66 (q, ^{2}J = 33 Hz), 128.54, 128.15, 125.66, 125.04, 124.23, 123.35 (q, ^{1}J = 271 Hz), 117.70 (q, ^{3}J = 4 Hz), 114.33 (q, ^{3}J = 3 Hz), 33.95, 30.37 (broad weak peaks from benzotriazole not assigned). IR (film cm^{-1}) 3353, 3371, 1657, 1575, 1388, 1276. HRMS (ESI): [M - H] for $C_{25}H_{20}F_6N_5O_2$ found 536.1526, calcd 536.1527.

Procedure for peptide coupling:

In a NMR tube, N-(tert-Butoxycarbonyl)glycine (1.2 equiv.), benzyl amine (1.0 equiv., 0.010 mmol) and diisopropylethylamine (2.5 equiv.) were dissolved in DMSO-*d*6 (0.5 mL). Acyl transfer agent (1.2 equiv.) was added and a ^{1}H-NMR was taken (time = 0 h). EDC-HCl (1.2 equiv.) was added and the reaction was monitored by 1H-NMR (time = 5 min, 15 min, 30 min, 1 h, 1.5 h, 2 h and 15 h). Conversion was determined by integration of PhC**H**$_2$NH$_2$ (δ = 3.98 ppm) versus PhC**H**$_2$NHC(O)C (δ = 4.29 ppm).

5.3 Synthesis of diazepane catalysts

Note: Spectra for hydrazine dicarboxylate and diazepane carboxylate have several semi-stable conformations giving very broad peaks in the NMR and either to many or too few ^{13}C peaks. ^{1}H-COSY, ^{1}H-^{13}C-HMQC and ^{1}H-^{13}C HMBC were taken for almost all diazepane rings and hydrazine dicarboxylates for characterization.

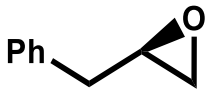

(R)-2-benzyloxirane (**196**)

Prepared according to Schaus *et al.* [15]

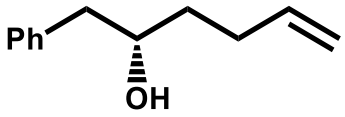

(S)-1-phenylhex-5-en-2-ol (**197**)

Prepared according to Sharma *et al.* [16]

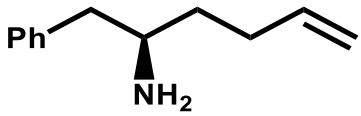

(R)-1-phenylhex-5-en-2-amine (**200**)

A flask with alcohol **197** (3.85 g, 21.85 mmol, 1 equiv.) was equipped with a septum and evacuated and backfilled with argon three times and then added dry DCM (25 mL) and cooled to 0 °C. Freshly distilled Et_3N (6.09 mL, 43.70 mmol, 2.0 equiv.) was added followed by MsCl (2.03 mL, 26.22 mmol, 1.2 equiv.). The solution is stirred for 30 minutes and then quenched with saturated aqueous $NaHCO_3$ (15 mL). DCM (20 mL) was added and the phases were separated and the water layer was extracted with DCM (10 mL) and the combined organic layers were dried with anhydrous Na_2SO_4, filtered and the concentrated under reduced pressure (without heating). The crude was dissolved in DMF (60 mL) and NaN_3 (2.56 g, 39.33 mmol, 1.8 equiv.), PPh_3 (7.45 g, 28.40 mmol) and water (0.78 mL, 43.3 mmol, 2 equiv.) were added and the reaction mixture was stirred over night. The reaction was quenched with NaOH (1 M) and then EtOAc was added. The layers were separated, and the aqueous layer was extracted with ethyl acetate and the combined organic layers

[15] Schaus, S. E., Brandes, B. D., Larrow, J. F., Tokunaga, M., Hansen, K. B., Gould, A. E., Furrow, M. E. & Jacobsen, E. N. *J. Am. Chem. Soc.*, **2002,** 124, 1307.
[16] Sharma H, Santra S, Debnath J, Antonio T, Reith M, Dutta A. *Bioorg. Med. Chem*. **2014** 311.

were washed with saturated aq. sodium bicarbonate solution, water and brine, dried with anhydrous sodium sulfate and the solvent was removed under reduced pressure. The crude material was purified by flash column chromatography on silica gel (ethyl acetate with 1% Et_3N in hexanes) to yield the title product (2.75 g, 72%). R_f = 0.36 (9/1 DCM/MeOH). ^1H NMR (400 MHz, Chloroform-*d*) δ 7.40 – 7.17 (m, 5H), 5.89 – 5.66 (m, 3H), 5.08 (dq, *J* = 17.2, 1.7 Hz, 1H), 5.03 – 4.96 (m, 1H), 3.32 (p, *J* = 6.7 Hz, 1H), 2.93 (q, *J* = 6.2 Hz, 2H), 2.36 – 2.02 (m, 2H), 1.73 (q, *J* = 7.3 Hz, 2H). ^{13}C NMR (101 MHz, $CDCl_3$) 139.6, 138.5, 129.3, 128.4, 126.2, 114.7, 52.21, 44.7, 36.8, 30.6. IR (film cm^{-1}) ν_{max} 3368, 3283, 3027, 2974, 2917, 2847, 1639, 1495, 1453, 909, 741, 700. HRMS: (ESI) [M+H] for $C_{12}H_{18}N$ found 176.1427, calcd 176.1434. HPLC of benzoyl amide: 87% ee. CHIRALCEL OD (4.6 × 250 mm), Hex:iPrOH 90:10. 1 mL/min, 254 nm (ref 360 nm). 9.477 min (minor) and 10.758 min (major). Racemic mixture made through the same synthesis from achiral epoxide.

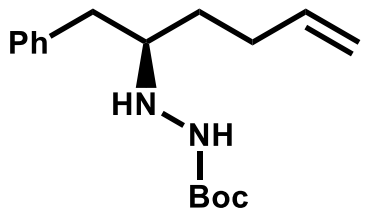

tert-butyl-(R)-2-(1-phenylhex-5-en-2-yl)hydrazine-1-carboxylate (**202**).

A solution of oxaziridine **201** (0.56 g, 1.92 mmol, 0.4 equiv.) in toluene (5 mL) was added to amine **200** (0.84 g, 4.80 mmol, 1.0 equiv.) in toluene (5 mL). After 5 min, the solvent was removed under reduced pressure and the crude material was purified by flash column chromatography on silica gel (ethyl acetate with 1% Et_3N in hexanes) to yield the product (0.51 g, 92%) as a pale yellow viscous oil. R_f = 0.61 (3/1 Hex/EtOAc, CAM stained). ^1H NMR (400 MHz, $CDCl_3$) δ 7.34-7.21 (5H, m), 6.21 (1H, broad s, CHN**H**), 5.80, (1 H, m, CH_2C**H**=CH_2), 5.03 (1H, dd, ^3J =17.4 and ^2J = 1.6Hz), 4.96 (1H, dd, ^3J =10.4 and ^2J = 1.5 Hz), 4.08 (1H, bs, N**H**Boc), 3.23 (1H, bs, BnC**H**NH), 2.72 (2H, m, PhC**H**$_2$CH), 2.17 (2H, m, $CHCH_2C$**H**$_2CH$=CH_2), 1.51 (11H, m, CHC**H**$_2CH_2CH$=CH_2 and C(C**H**$_3$)3) ppm. ^{13}C NMR (100 MHz, $CDCl_3$) δ 156.7, 138.9, 138.4, 129.3, 128.5, 126.2, 114.7, 80.3, 60.4, 39.4, 31.1, 29.8, 28.4 ppm. IR (film cm^{-1}) ν_{max} 3313, 3028,

2978, 2932, 1706, 1454, 1367, 1275, 1157, 910, 735, 699. HRMS (ESI): [M+H] for $C_{17}H_{22}N_2O_2$ found 291.2063, calcd 291.2067.

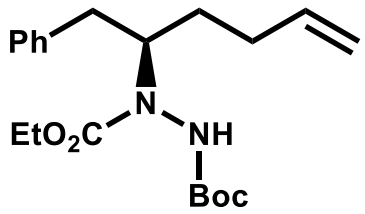

2-(tert-butyl) 1-ethyl (R)-1-(6-hydroxy-1-phenylhexan-2-yl)hydrazine-1,2-dicarboxylate (**SI-5**)

202 (269 mg, 0.926 mmol) was dissolved in chloroform (10 mL) was cooled in a ice bath to 0 °C. Added $NaHCO_3$ (aq. 1M, 10 mL) followed by dropwise addition of ethyl chloroformate (124 µL, 1.4 equiv., 1.30 mmol). The solution was stirred for 2.5 h and then brought up to room temperature and the phases were separated. The organic phase was washed with aqueous $NaHCO_3$ (satur'd., 3x10 mL), brine (20 mL). The solvent was removed *in vacuo* and the crude product was purified with silica gel chromatography (5/1 Hexanes/EtOAc) to yield the title product as a colourless oil (269 mg, 80%). R_f = 0.29 (4/1 Hex/EtOAc. CAM stained) ^{1}H NMR (400 MHz, $CDCl_3$) δ 7.31-7.12 (m, 5H, Ar-**H**), 6.29-5.68 (m, 2H, N**H** and CH_2C**H**=CH_2), 5.10-4.86 (m, 2H, CHC**H₂**), 4.59-3.94 (m, 3H, N-C**H** and C**H₂**CH_3), 3.22-2.57 (m, 2H, PhC**H**$_2$CH), 2.39-2.08 (m, 2H, $CHCH_2C$**H**$_2CH=CH_2$), 2.90-1.39 (m, 11H, C(C**H₃**)$_3$) and CHC**H**$_2CH_2CH=CH_2$), 1.35-1.10 (m, 3H, CH_2C**H₃**) ppm. ^{13}C NMR (125 MHz, $CDCl_3$) δ (rotomers) 156.02, 138.19, 128.93, 128.48, 126.32, 114.72, 81.07, 62.01, 59.54, 57.97, 39.30, 30.59, 28.13, 14.43. IR (film cm^{-1}) ν_{max} 3286, 3064, 2979, 1750, 1704, 1368, 1289, 1240, 1148, 1051, 1031, 911, 747, 700. HRMS: (ESI) [M+Na] for $C_{20}H_{30}N_2NaO_4$ found 385.2107, calcd 385.2098.

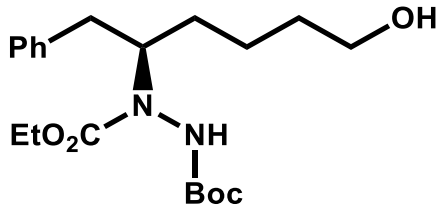

2-(tert-butyl) 1-ethyl (R)-1-(6-hydroxy-1-phenylhexan-2-yl)hydrazine-1,2-dicarboxylate (**205**)

9-BBN (1 M in THF, 4.46 mL, 2.23 mmol) was added to a solution of olefin **SI-5** (269 mg, 0.743 mmol) in THF (25 mL) at 0 °C. After 3 h, the ice bath was removed and the H_2O_2 (0.4mL, 3.71 mmol) and NaOH (1M, 0.37 mL, 3.71 mmol) was added to the solution and the mixture was stirred over night. EtOAc (25 mL) and H_2O (10 mL) was added to the solution and the phases were separated. The organic phase was washed with H_2O (2x10 mL) and brine (10 mL), dried with Na_2SO_4 and the solvent was removed *in vacuo*. **205** was isolated as a viscous oil (0.197 mg, 71%) after silica gel chromatography (40% EtOAc/Hexanes). R_f = 0.14 (2/1 Hex/EtOAc) ^{1}H NMR (400 MHz, $CDCl_3$) δ 7.40-6.95 (m, 5H, Ar**H**), 6.69-5.71 (m, 1H, N**H**), 4.58-3.92 (m, 3H, $CH_3C\mathbf{H_2}$ and C**H**N), 3.65-3.42 (bs, 2H, C$\mathbf{H_2}$OH), 3.18-2.37 (m, 3H, O**H** and PhC$\mathbf{H_2}$), 1.88-1.07 (m, 18H, $CH_2C\mathbf{H_3}$ CHC$\mathbf{H_2}$C$\mathbf{H_2}$C$\mathbf{H_2}$$CH_2$OH and C(C$\mathbf{H_3}$)$_3$) ppm. ^{13}C NMR (100 MHz, $CDCl_3$) δ 156.59, 138.64, 128.82, 128.51, 126.37, 81.58, 62.10, 39.28, 32.06, 28.14, 22.08, 20.58, 14.41 ppm. IR (film cm^{-1}) ν_{max} 3288, 3026, 2979, 2933, 1695, 1413, 1368, 1288, 1241, 1158, 1030, 750, 701. HRMS: (ESI) [M+Na] for $C_{20}H_{32}N_2NaO_5$ found 403.2205, calcd 403.2203

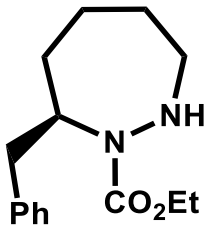

Ethyl (R)-7-benzyl-1,2-diazepane-1-carboxylate (**185**)

Alcohol **205** (190 mg, 0.50 mmol, 1 equiv.) was dissolved in dry DCM (10 mL) under argon and cooled to 0 °C. Freshly distilled Et_3N (0.14 mL, 1.00 mmol, 2 equiv.) was added followed by MsCl (47 μL, 0.60 mmol, 1.2 equiv.). The solution is stirred for 15 minutes and then quenched with saturated aqueous NH_4Cl (10 mL). The phases were separated and the organic layer was washed with more NH_4Cl, brine and dried with anhydrous Na_2SO_4, filtered and the concentrated under reduced pressure (without heating). The mesyl crude was used immediately without further purification by dissolving the oil in dry THF (15 mL) and adding TBAF (1 M in THF, 3 equiv.). The reaction was monitored by TLC and quenched with saturated aqueous NH_4Cl after 6 h when the starting material was consumed. The solution was extracted with EtOAc and the organic phase was washed with more NH_4Cl, brine, dried with anhydrous $MgSO_4$, filtered and concentrated *in*

vacuo. The crude was purified with flash chromatography over silica gel to give diazepane **206** (145 mg, 80% yield) as a wax film.

The Boc protected diazepane **206** (70 mg, 0.193 mmol) was dissolved in a mixture of DCM:TFA (2:1, 3 mL). The solution was stirred for 1 h and then solvent and excess TFA were removed under reduced pressure. EtOAc (25 mL) and $NaHCO_3$ (25 mL) were added to the flask and then transferred to a separatory funnel. The phases were separated and the organic phase was washed with $NaHCO_3$ and brine, dried with anhydrous Na_2SO_4, filtered and evaporated *in vacuo*. The crude material was purified by flash column chromatography on silica gel (gradient of 30% to 45% ethyl acetate in hexanes as eluent) to yield the product as a amorphous white solid (44 mg, 87% yield). R_f = 0.15 (3/1 Hex/EtOAc). ^{1}H NMR (500 MHz, CD_3OD) 7.28 – 7.05 (m, 5H), 4.25 - 3.52 (m, 3H), 2.99 – 2.58 (m, 4H), 2.07-0.93 (m, 9H). ^{13}C NMR (101 MHz, CD_3OD) δ 161.04, 160.54, 143.26, 142.87, 132.89, 132.89, 131.74, 131.74, 129.62, 129.62, 65.18, 62.69, 62.08, 54.59, 54.19, 44.19, 44.19, 37.40, 37.40, 28.20, 28.20, 17.17, 17.17. IR (film cm^{-1}) ν_{max} 3312, 3062, 3026, 2979, 2926, 2852, 1689, 1448, 1403, 1330, 1216, 1124,1099, 1031, 758, 745, 700. HRMS (ESI): [M+Na] for $C_{15}H_{22}N_2NaO_2$ found 285.1574, calcd 285.1573.

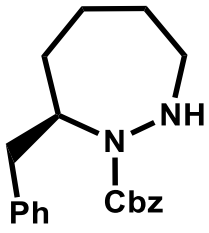

benzyl (R)-7-benzyl-1,2-diazepane-1-carboxylate (**204**)

Synthesized according to the procedure for **185** from hydrazine **203** and isolated as white crystals in 75% yield, two steps. R_f = 0.86 (1/1 Hex/EtOAc). ^{1}H NMR (400 MHz, Methanol-d_4) broad signals due to conformers δ 7.40 – 6.97 (m, 10H), 5.13 – 4.52 (m, 3H), 4.33 – 3.96 (m, 1H), 3.04 – 2.50 (m, 4H), 1.96 – 1.04 (m, 6H). ^{13}C NMR (101 MHz, MeOD) To many signals due to conformers, major peaks listed δ 156.77, 156.41, 139.12, 138.88, 136.63, 136.28, 128.97, 128.19, 128.09, 127.93, 127.89, 127.77, 127.71, 127.66, 127.55, 125.82, 125.76, 67.11, 66.94, 60.15, 58.95, 58.36, 50.76, 50.25, 48.39, 48.17, 47.96, 47.75, 47.54, 47.32, 47.11, 40.40, 40.09, 33.26, 32.65, 30.70, 24.30, 24.24, 19.63, 13.22. IR (film cm^{-1}) 3316, 3063, 3029, 2926, 2852, 1686, 1495,

1449, 1400, 1328, 1283, 1214, 1121, 1093, 735, 697. HRMS: (ESI) [M+H] for $C_{20}H_{25}N_2O_2$ found 325.1908, calcd 325.1911.

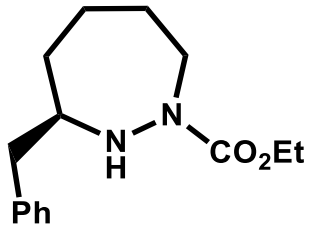

Ethyl (R)-3-benzyl-1,2-diazepane-1-carboxylate (**184**)

Ethyl carbamate formation according to the procedure for **202** followed by Cbz deprotection: The Cbz protected diazepane (65 mg, 0.16 mmol) was dissolved in EtOH (5 mL) under argon atmosphere. Pd/C (10 mol%) was added and hydrogen gas was bubbled through the reaction mixture. After 1 h, the reaction mixture was filtered through celite and the solvent was removed under reduced pressure. The crude material was purified by flash column chromatography on silica gel (5-10% gradient of ethyl acetate in hexanes as eluent) to yield the product (42 mg, 97%). Was isolated as wax film (88% yield, 2 steps). ^{1}H NMR (500 MHz, Methanol-d_4) Conformers giving broad signals δ 7.33-7.21 (m, 5H), 4.23 – 3.72 (m, 3H), 3.30 – 2.88 (m, 2H), 2.86 – 2.41 (m, 2H), 1.97 – 1.58 (m, 4H), 1.45 – 0.89 (m, 5H). ^{13}C NMR (126 MHz, MeOD) (broad signals due to conformers, major peaks listed) δ 156.52, 138.58, 128.93, 128.11, 126.05, 61.90, 61.41, 60.63, 40.38, 35.94, 26.56, 23.36, 13.57. IR (film cm^{-1}) 3327, 3062, 3027, 2980, 2930, 2859, 1694, 1496, 1453, 1408, 1381, 1262, 1175, 1111, 759, 744, 700. HRMS (ESI): [M+Na] for $C_{15}H_{22}N_2NaO_2$ found 285.1576, calcd 285.1573.

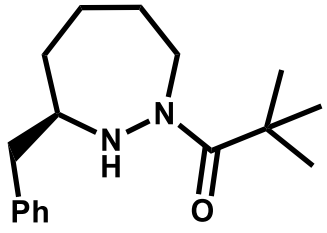

(R)-1-(3-benzyl-1,2-diazepan-1-yl)-2,2-dimethylpropan-1-one (**248**)

Synthesized according to the procedure for **245**. R_f = 0.33 (3/1 Hex/EtOAc). ^{1}H NMR (400 MHz, Chloroform-*d*) broad signals due to conformers δ 7.48 – 7.00 (m, 5H), 3.87-3.51 (m, 2H),

3.35 – 3.05 (m, 1H), 2.89-2.81 (m, 1H), 2.74 – 2.55 (m, 1H), 1.94-1.21 (m, 15H). ^{13}C NMR (101 MHz, $CDCl_3$) (broad signals due to conformers, major peaks listed) δ 138.70, 129.33, 128.41, 126.34, 50.79, 41.73, 38.78, 33.31, 28.02, 27.18. IR (film cm^{-1}) 3265, 3027, 2927, 2859, 1612, 1495, 1473, 1453, 1399, 1355, 1210, 991, 699. HRMS (ESI): [M+H] for $C_{17}H_{26}N_2NaO$ found 297.1933, calcd 297.1937.

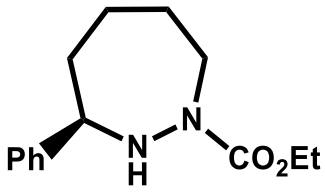

ethyl (R)-3-phenyl-1,2-diazepane-1-carboxylate (**183**)

The flask with alcohol **191** (synthesized according to Kaldre *et al.*)[17] (100 mg, 0.27 mmol, 1 equiv., 91% ee) was equipped with a septum and evacuated and backfilled with argon three times and then added dry DCM (12 mL) and cooled to 0 °C. Freshly distilled Et_3N (53 µL, 0.38 mmol, 1.4 equiv.) was added followed by Ms_2O (25 µL, 0.32 mmol, 1.2 equiv.). The solution is stirred for 30 minutes and then quenched with saturated aqueous $NaHCO_3$ (15 mL). DCM (10 mL) was added and the phases were separated and the water layer was extracted with DCM (10 mL) and the combined organic layers were dried with anhydrous Na_2SO_4, filtered and the concentrated under reduced pressure (without heating). The mesyl crude was used immediately without further purification by dissolving the wax in dry THF (10 mL) and DMF (2.5 mL) and adding NaH (60% in oil, 16 mg, 0.41 mmol). The reaction mixture was stirred over night and then quenched with $NaHCO_3$ (aq. satur'd) solution was extracted with EtOAc and the organic phase was washed with NH_4Cl, brine, dried with anhydrous Na_2SO_4, filtered and concentrated *in vacuo*. The crude was dissolved in DCM (2 mL) and TFA (1 mL) was added. The solution was stirred for 1 h and then reduced under vacuum. EtOAc (25 mL) and $NaHCO_3$ (25 mL) was added to the flask and then transferred to a separatory funnel. The phases were separated and the organic phase was washed with $NaHCO_3$ and brine, dried with anhydrous Na_2SO_4, filtered and evaporated *in vacuo*. The product was purified with flash chromatography (silica gel, Hex/EtOAc 80/20 to 70/30) to afford diazepane **183** (37.9 mg, 56% yield over 3 steps, 91% ee) as a thin film. ^{1}H NMR (400 MHz, Chloroform-*d*)

[17] Kalde, D.; Gleason J. L. *Angew. Chem. Int. Ed.* **2016**, 55, 11557.

broad signals due to conformers δ 7.58 – 7.21 (m, 5H), 4.92 – 3.72 (m, 5H), 3.34 (s, 1H), 2.18 – 1.41 (m, 6H), 1.32 (t, *J* = 7.1 Hz, 3H). ^{13}C NMR (101 MHz, $CDCl_3$) broad signals due to conformers, major peaks listed δ 157.02, 142.22, 128.49, 127.54, 127.31, 66.13, 65.25, 61.69, 47.95, 47.69, 37.90, 37.60, 27.33, 24.29, 14.80. IR (film cm^{-1}) 3303, 3030, 2908, 2930, 2871, 1691, 1447, 1406, 1380, 1261, 1177, 1109, 1076, 1026, 758, 670. HRMS (ESI): [M+H] for $C_{14}H_{21}N_2O_2$ found 249.1600, calcd 249.1598.

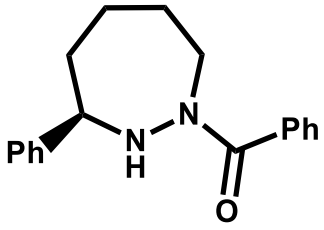

(R)-phenyl(3-phenyl-1,2-diazepan-1-yl)methanone (**245**)

To a solution of Boc Hydrazide **242** (100 mg, 0.36 mmol, 92% ee, 1 equiv.) in DCM (1 mL) was added Et_3N (150 µL, 1.1 mmol, 3.0 equiv.), DMAP (1 crystal, catalytic amount), Benzoyl chloride (84 µL, 0.72 mmol, 2.0 equiv.). The reaction was stirred for 12 h and monitored by TLC which indicated the starting material was consumed. DCM (10 mL) and saturated aqueous $NaHCO_3$ (10 mL) was added to the reaction mixture and the organic phase was dried with $MgSO_4$, filtered. After evaporation of the solvent, the residue ran through a silica plug (hexanes:EtOAc 80:20) and was deprotected according to the same Boc deprotection procedure as **183**. The residue was purified by flash chromatography (silica gel, Hexanes/EtOAc 95:5 to 80:20) to afford **245** (72 mg, 71% yield, 92% ee) as a clear oil. ^{1}H NMR (400 MHz, $CDCl_3$) δ 7.58 – 6.74 (m, 10H, Ar-**H**), 5.73 (s, 1H C(O)N**H**Bn), 4.14 (dd, *J* = 6.3 Hz and 0.9 Hz, 1H, PhC**H**NHN), 3.79 – 3.42 (m, 2H, C**H₂**NNH), 2.16 – 1.70 (m, 5H, PhCHC**H₂**C**H₂**C**H₂**), 1.69-1.53 (m, 1H PhCHCH$_2$C**H**$_2$CH$_2$). ^{13}C NMR (101 MHz, $CDCl_3$) δ 170.36, 142.27, 136.04, 129.85, 128.60, 128.54, 127.71, 127.44, 127.00, 65.15, 51.26, 37.83, 27.93, 24.15. IR (film cm^{-1}) 3320, 3060, 2931, 1627, 1493, 1446, 1397, 699. HRMS (ESI): [M+H] for $C_{18}H_{21}N_2O$ found 281.1647, calcd 281.1648.

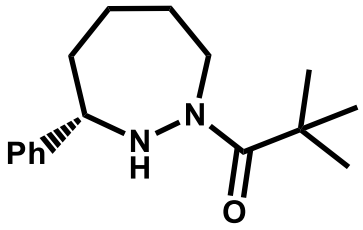

(S)-2,2-dimethyl-1-(3-phenyl-1,2-diazepan-1-yl)propan-1-one (**244**)

Prepared according to the procedure for **245** in 93% yield using pivaloyl chloride. R_f = 0.34 (3/1 Hex/EtOAc) ^{1}H NMR (400 MHz, Chloroform-*d*) broad signals due to conformers δ 7.66 – 7.06 (m, 5H), 5.55-5.47 (m, 1H), 4.26 – 3.24 (m, 3H), 2.26 – 0.98 (m, 15H). ^{13}C NMR (101 MHz, $CDCl_3$) broad signals due to conformers, major peaks listed δ 142.59, 128.45, 127.33, 125.94, 65.90, 50.65, 37.46, 28.55, 28.05. IR (film cm^{-1}) 3285, 2927, 2864, 1612, 1483, 1396, 1212, 753, 699. HRMS: [M+H] for $C_{16}H_{25}N_2O$ found 261.1963, calcd 261.1961.

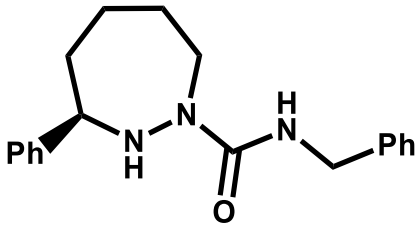

(R)-N-benzyl-3-phenyl-1,2-diazepane-1-carboxamide (**243**)

Boc protected compound **242** (35 mg, 0.13 mmol, 1 equiv.) was dissolved in toluene (1mL). Benzyl isocyanate was added and the flask was equipped with a condenser and the reaction mixture was refluxed for 24h. TLC indicated 1 major new product, starting material and several smaller spots, probably from decomposition so the reaction was stopped. The mixture was concentrated *in vacuo*. The crude was dissolved in DCM (1 mL) and 85% aqueous phosphoric acid (0.5 mL) was added and stirred for 16 h. The reaction was quenched by NaOH (0.5 M) and extracted with DCM. The organic phase was dried with Na_2SO_4, filtered and concentrated *in vacuo*. The residue was purified with flash chromatography (silica gel, Hexanes/EtOAc 1/1) to give **243** as a viscous clear oil. R_f = 0.08 (3/1 Hex/EtOAc). ^{1}H NMR (500 MHz, $CDCl_3$) broad signals due to conformers δ 7.46 – 7.14 (m, 10H, Ar-**H**), 6.66 (s, 1H), 4.53 – 4.33 (m, 2H, PhC**H$_2$**NH), 4.15 – 3.88 (m, 2H), 3.78 (d, *J* = 7.7 Hz, 1H), 3.61-3.54 (m, 1H), 2.11 – 1.76 (m, 5H), 1.70 – 1.47 (m, 1H). ^{13}C NMR (126 MHz, $CDCl_3$) broad signals due to conformers, major peaks listed δ 159.35, 143.54, 140.02, 128.64, 128.47, 127.41, 127.38, 126.96, 126.67, 66.24, 49.45, 44.13, 35.22, 27.34, 27.02. IR (film

cm^{-1}) 3401, 3265, 3029, 2927, 1643, 1527. HRMS (ESI): [M-H] for $C_{20}H_{23}N_2O_3$ found 310.1906, calcd 310.1914.

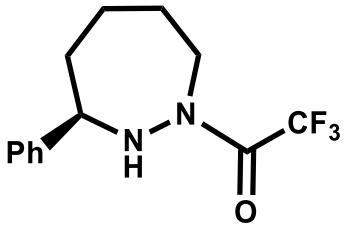

(R)-2,2,2-trifluoro-1-(3-phenyl-1,2-diazepan-1-yl)ethan-1-one (**246**)

Prepared according to the procedure for **245** in 83% yield using trifluoroacetic anhydride. ^{1}H NMR (400 MHz, Chloroform-*d*) δ 7.52 – 7.20 (m, 5H), 4.21 – 3.83 (m, 2H), 3.75 – 3.54 (m, 1H), 2.08 – 1.51 (m, 6H). ^{13}C NMR (101 MHz, $CDCl_3$) broad signals due to conformers, major peaks listed δ 142.03, 141.19, 128.65, 128.57, 128.38, 128.36, 127.96, 127.62, 127.23, 126.69, 118.17, 115.33, 66.11, 64.88, 49.91, 49.80, 49.77, 37.24, 35.91, 31.59, 27.56, 26.99, 25.31, 23.66, 22.66, 14.12. HRMS (ESI): calcd for $C_{13}H_{15}N_2OF_3Na$ [M+Na] 295.1029, found 295.1021.

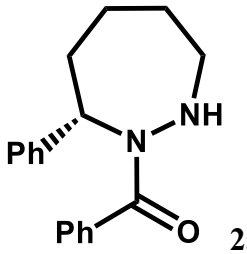

251. Repeated according to Kaldre, D. **2015**, *Development of Hybrid Drugs for Cancer Treatment and Studies in Asymmetric Organocatalysis*, Doctorial dissertation, McGill University, Department of Chemistry, Montreal, Canada.

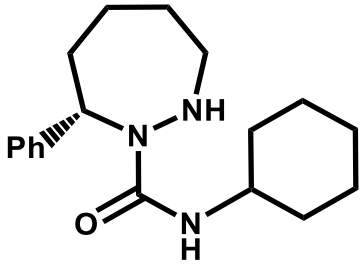

(S)-N-cyclohexyl-7-phenyl-1,2-diazepane-1-carboxamide (**250**)

Cyclohexyl isocyanate was added to a dry flask containing Cbz protected hydrazide **78** (80 mg, 0.26 mmol, 92% ee) equipped with a stir bar and a septum. The system was evacuated and backfilled with argon three times and then heated to 125 °C for 20 h. The solvent was evaporated and the residue was purified with flash chromatography (silica gel, Hexanes/EtOAc 3/1) to afford urea/Cbz intermediate (R_f = 0.77 Hexanes/EtOAc 3/2). Deprotection of Cbz group as above afforded the product (45 mg, 58%) as white crystals. R_f = 0.66 (Hex/EtOAc 3:2). ^{1}H NMR (400 MHz, Chloroform-*d*) δ 7.23 (m, 5H), 5.35 (m, 2H), 3.58 (m, 1H), 3.13 (m, 1H), 2.78 (m, 1H), 2.43 – 0.72 (m, 17H). ^{13}C NMR (101 MHz, $CDCl_3$) δ 158.17, 158.13, 143.58, 129.89, 128.56, 126.62, 125.57, 60.85, 53.44, 51.69, 48.60, 48.49, 35.07, 33.98, 33.95, 33.91, 32.95, 31.56, 29.69, 25.73, 25.31, 25.01, 24.97, 24.61. IR (film cm^{-1}) 3392, 3291, 2926, 2851, 1636, 1509, 1449, 1265, 893. HRMS (ESI): [M-H] for $C_{18}H_{27}NaNO$ found 324.2052, calcd 324.2046.

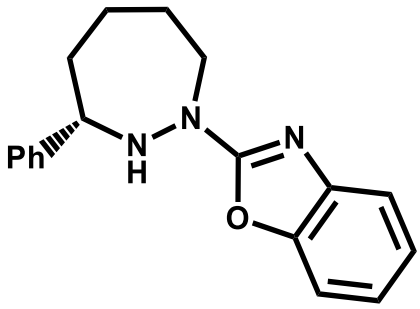

(S)-2-(3-phenyl-1,2-diazepan-1-yl)benzo[d]oxazole (**247**)

In a round bottom flask equipped with a stir bar, **242** (50 mg, 0.18 mmol) was dissolved in DCM (2 mL) and then TFA (1 mL) was added. The reaction mixture was evaporated under vacuum and flushed with Argon. THF (5 mL) was added to dissolve the diazepane*TFA salt followed by Hunigs base (158 µL, 0.90 mmol) and 2-chlorobenzoxazole (41 µL, 0.36 mmol). The reaction was stirred for 18 h and then EtOAc and $NaHCO_3$ (aq., satur'd) were added. The phases were separated and the organic phase was washed with water and brine, dried with anhydrous sodium sulfate and the solvent was removed under reduced pressure. The crude material was purified by flash column chromatography on silica gel (10-20% ethyl acetate in hexanes as eluent) afforded the product as a white crystal (26.5 mg, 50%). R_f = 0.56 (3/1 Hex/EtOAc). ^{1}H NMR (400 MHz, Chloroform-*d*) δ 7.71 – 7.56 (m, 3H), 7.55 – 7.27 (m, 6H), 5.77 (s, 1H), 5.21 (ddt, *J* = 11.9, 6.0, 1.6 Hz, 1H), 4.81 (dt, *J* = 10.8, 1.5 Hz, 1H), 3.82 (tt, *J* = 12.0, 1.6 Hz, 1H), 2.08 – 1.67 (m, 5H), 1.41 (dtdd, *J* = 14.6, 12.5, 4.0, 1.8 Hz, 1H). ^{13}C NMR (101 MHz, $CDCl_3$) δ 162.76, 149.27, 143.50, 142.05, 128.60,

127.71, 127.33, 124.03, 120.41, 116.29, 108.83, 64.71, 49.83, 38.12, 27.29, 24.20. IR (film cm^{-1}) 3287, 3060, 329, 2929, 2855, 1817, 1628, 1570, 1458, 1244, 738, 700. HRMS (ESI): [M+H] for $C_{18}H_{20}N_3O$ found 294.1597, calcd 294.1601.

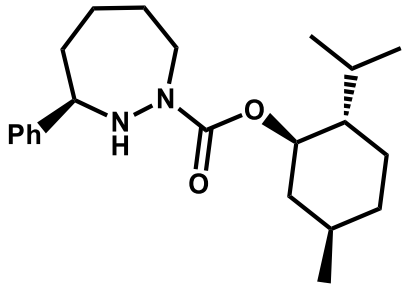

(1R,2S,5R)-2-isopropyl-5-methylcyclohexyl (R)-3-phenyl-1,2-diazepane-1-carboxylate (**281**)

Diazepane carboxylate **78** (900 mg, 2.90 mmol) was dissolved in MeOH (50 mL). Acetyl chloride (0.83 mL, 11.6 mmol) was added and after stirring for 10 min, Pd/C (10 mol%) was added. Hydrogen gas was bubbled through the solution for 30 min and then the reaction mixture was filtered though celite and the solvent was removed under reduced pressure. EtOAc (45 mL) was added and heated to reflux and MeOH (~1 mL) was added until the crystals were dissolved. The solution was allowed to slowly cool down over night. The crystals (220 mg, 32%) were collected by filtration.

The crystals (110 mg, 0.52 mmol) was dissolved in DCM (8 mL) under argon atmosphere and cooled to 0 °C after which Et_3N (288 µL, 2.07 mmol) and (-) menthyl chloroformate (122 µL, 0.57 mmol) were added. The reaction was stirred for 1 h and then allowed to reach rt. The reaction was quenched with $NaHCO_3$ (aq, sat.) and extracted with EtOAc. The phases were separated and the organic phase was washed with brine, dried with anhydrous sodium sulfate and the solvent was removed under reduced pressure. The crude material was purified by flash column chromatography on silica gel (5-15% gradient of ethyl acetate in hexanes as eluent) to yield the product. R_f = 0.70 (3/1 Hex/EtOAc). ^{1}H NMR (500 MHz, 87 °C, DMSO-d_6) ^{1}H NMR (500 MHz, DMSO-d_6) δ 7.38 (d, J = 7.1 Hz, 2H), 7.32 (t, J = 7.6 Hz, 2H), 7.25 (t, J = 7.2 Hz, 1H), 4.82 (s, 1H), 4.53 (td, J = 10.8, 4.4 Hz, 1H), 4.03 – 3.95 (m, 1H), 3.82 (dt, J = 13.8, 7.1 Hz, 1H), 3.27 (dt, J = 13.1, 5.7 Hz, 1H), 3.01 (s, 1H), 2.09 – 1.96 (m, 1H), 1.98 – 1.59 (m, 8H), 1.55 – 1.33 (m, 3H), 1.15 – 0.97 (m, 2H), 0.89 (dd, J = 18.3, 6.8 Hz, 7H), 0.80 (d, J = 7.0 Hz, 3H). ^{13}C NMR (126 MHz,

87 °C, dmso-*d6*) δ 155.18, 142.22, 127.74, 126.66, 126.47, 74.55, 63.66, 47.75, 46.66, 40.82, 36.41, 33.48, 30.47, 26.59, 25.89, 23.48, 23.24, 21.28, 19.91, 16.21. IR (film cm^{-1}) 3318, 2927, 2869, 1689, 1397, 1259, 1176, 1107, 757, 700. HRMS (ESI): [M+Na] for $C_{22}H_{34}N_2NaO_2$ found 381.2522, calcd 381.2512.

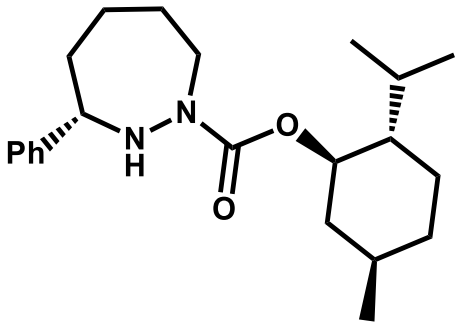

(1R,2S,5R)-2-isopropyl-5-methylcyclohexyl (S)-3-phenyl-1,2-diazepane-1-carboxylate (**282**)

Prepared according to the ethyl carbamate formation procedure for **183** using (+)-methyl chloroformate to give the product in 59% yield. R_f = 0.69 (3/1 Hex/EtOAc). ^{1}H NMR (400 MHz, Chloroform-*d*) δ 7.56 – 6.94 (m, 5H), 4.80 – 4.27 (m, 2H), 4.19 – 3.60 (m, 2H), 3.25 (m, 1H), 2.20 – 1.13 (m, 12H), 1.11 – 0.60 (m, 12H). ^{13}C NMR (101 MHz, $CDCl_3$) δ 156.80, 155.93, 142.46, 142.26, 128.43, 127.47, 127.38, 127.11, 75.74, 75.53, 66.63, 65.05, 47.97, 47.69, 47.49, 47.30, 41.69, 38.53, 37.50, 34.36, 31.43, 29.71, 27.41, 27.12, 26.45, 26.02, 24.32, 23.71, 22.89, 22.05, 21.10, 20.77, 16.59, 15.84. IR (film cm^{-1}) 3304, 2926, 2868, 1692, 1450, 1397, 1260, 1177, 1108, 700. HRMS (ESI): [M+Na] for $C_{22}H_{34}N_2NaO_2$ found 381.2506, calcd 381.2512.

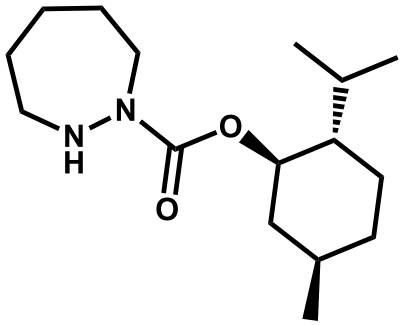

271 Repeated according to Kaldre, D. **2015**, *Development of Hybrid Drugs for Cancer Treatment and Studies in Asymmetric Organocatalysis*, Doctorial dissertation, McGill University, Department of Chemistry, Montreal, Canada.

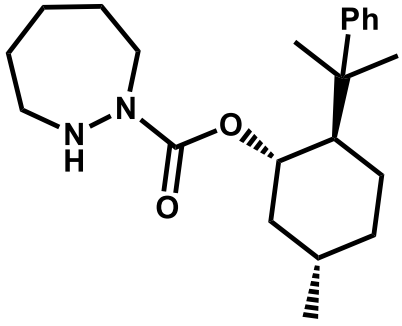

(1S,2R,5S)-5-methyl-2-(2-phenylpropan-2-yl)cyclohexyl 1,2-diazepane-1-carboxylate (**279**)

Chloroformate prepared from corresponding alcohol according to literature.[18] Carbamate prepared according to the ethyl carbamate formation procedure for **183** to give the title product in 87% yield. ^{1}H NMR (400 MHz, Chloroform-*d*) δ 7.41 – 7.01 (m, 5H), 4.88 – 4.65 (m, 1H), 3.81 (m, 1H), 3.23 – 2.28 (m, 4H), 2.27 – 0.69 (m, 23H). ^{13}C NMR (101 MHz, $CDCl_3$) δ 155.74, 154.98, 153.10, 151.76, 127.80, 125.33, 124.96, 75.75, 75.25, 68.22, 50.96, 50.84, 50.11, 47.66, 47.47, 42.51, 42.04, 39.80, 39.24, 34.74, 31.32, 30.47, 29.73, 29.40, 27.45, 27.18, 26.81, 26.29, 26.21, 26.08, 25.27, 24.86, 21.84. IR (film cm^{-1}) 3346, 2924, 2868, 1684, 1399, 1193, 1127,1092, 762, 699. HRMS (ESI): calcd for $C_{22}H_{35}N_2O_2$ [M+H] 359.2693, found 359.2695.

[18] Sajra, S.; Bhowmick, M.; Maji, B.; Sinha, D.; *J. Org. Chem*., **2007**, 72, 4872.

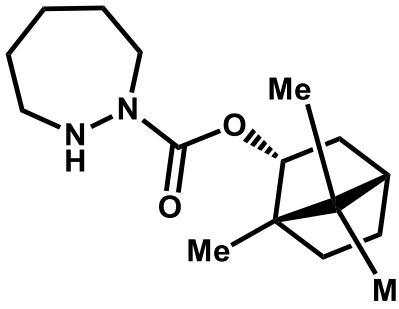

N-94G (1S,2R,4S)-1,7,7-trimethylbicyclo[2.2.1]heptan-2-yl 1,2-diazepane-1-carboxylate (**268**)

Chloroformate prepared from corresponding alcohol according to literature.[16] Carbamate prepared according to the ethyl carbamate formation procedure for **183** to give the title product in 49% yield. ^{1}H NMR (400 MHz, Chloroform-*d*) δ 4.81 (ddd, *J* = 9.9, 3.5, 2.1 Hz, 1H), 4.59 (s, 1H), 3.50 (td, *J* = 6.5, 1.6 Hz, 2H), 2.92 (dq, *J* = 5.0, 2.4 Hz, 2H), 2.34 (tt, *J* = 13.9, 4.0 Hz, 1H), 1.99 – 1.46 (m, 9H), 1.41 – 1.09 (m, 2H), 1.07 – 0.66 (m, 10H). ^{13}C NMR (101 MHz, $CDCl_3$) δ 156.90, 80.99, 50.50, 48.81, 48.39, 47.68, 44.85, 37.05, 29.51, 28.06, 27.62, 27.37, 25.36, 19.70, 18.84, 13.51. IR (film cm^{-1}) 3319, 2930, 1692, 1402, 1389, 1344, 1192, 1128, 1022. HRMS (ESI): [M+Na] for $C_{16}H_{28}NaN_2O_2$ found 303.2054, calcd 303.2043.

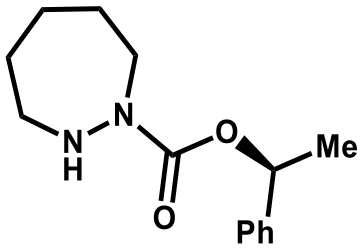

(S)-1-phenylethyl 1,2-diazepane-1-carboxylate (**269**)

Chloroformate prepared from corresponding alcohol according to literature.[16] Carbamate prepared according to the ethyl carbamate formation procedure for **183** to give the title product in 56% yield. ^{1}H NMR (500 MHz, Chloroform-*d*) δ 7.48 – 7.16 (m, 5H), 5.86 (m, 1H), 4.62 (m, 1H), 3.59 (m, 2H), 3.06 – 2.82 (m, 2H), 1.90 – 1.71 (m, 2H), 1.71 – 1.49 (m, 7H). ^{13}C NMR (126 MHz, $CDCl_3$) δ 156.05, 142.36, 128.48, 128.07, 127.69, 125.78, 73.63, 67.34, 50.77, 48.35, 29.64, 27.56, 25.35, 22.92. IR (film cm^{-1}) 3317, 2929, 2853, 1693, 1396, 1193, 1127, 699. HRMS (ESI): [M+Na] for $C_{14}H_{20}NaN_2O_2$ found 271.1413, calcd 271.1417.

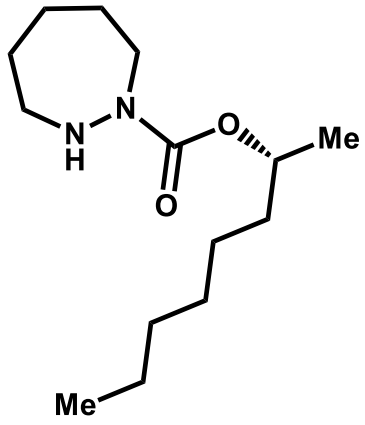

(R)-octan-2-yl 1,2-diazepane-1-carboxylate (**270**)

Chloroformate prepared from corresponding alcohol according to literature.[16] Carbamate prepared according to the ethyl carbamate formation procedure for **183** to give the title product in 46% yield.

^{1}H NMR (400 MHz, Chloroform-*d*) δ 4.81 (m, 2H), 3.48 (m, 2H), 2.92 (m, 2H), 1.86 – 1.14 (m, 19H), 0.94 – 0.79 (m, 3H). ^{13}C NMR (101 MHz, $CDCl_3$) δ 156.24, 72.31, 52.12, 48.13, 36.24, 31.72, 29.61, 29.10, 27.56, 25.34, 25.28, 22.52, 20.38, 14.00. IR (film cm^{-1}) 3318, 2928, 2857, 1693, 1398, 1193,1124. HRMS (ESI): [M+Na] for $C_{14}H_{28}N_2O_2Na$ found 279.2036, calcd 279.2043.

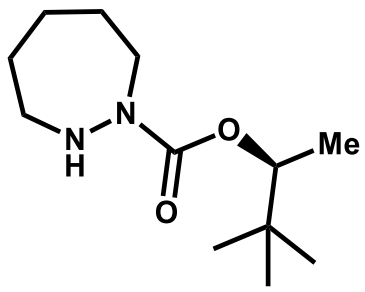

(S)-3,3-dimethylbutan-2-yl 1,2-diazepane-1-carboxylate (**280**)

Chloroformate prepared from corresponding alcohol according to literature.[16] Carbamate prepared according to the ethyl carbamate formation procedure for **183** to give the title product in 36% yield. ^{1}H NMR (400 MHz, Chloroform-*d*) δ 4.94 – 4.50 (m, 2H), 3.55 (m, 2H), 2.97 (m, 2H), 1.89 – 1.56 (m, 6H), 1.29 (m, 1H), 1.19 (d, J = 6.4 Hz, 3H), 0.94 (s, 9H). ^{13}C NMR (101 MHz, $CDCl_3$) δ 156.58, 79.08, 69.13, 48.24, 34.42, 34.13, 31.74, 29.70, 29.60, 28.50, 27.64, 25.81, 25.38, 15.32. HRMS (ESI): [M+Na] for $C_{12}H_{24}N_2O_2Na$ found 251.1722, calcd 251.1730.

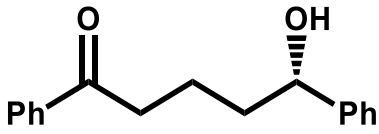

(S)-5-hydroxy-1,5-diphenylpentan-1-one (M-52) (**230**)

Synthesized according to the procedure for **264** using 1 equiv. of borane and spectra agree with literature.[19] HPLC Chiralcel OB-H, 1mL/min, 85:15 Hex:iPrOH, 31.97 min (minor), 39.32 (major), 95% ee. Racemic sample for HPLC prepared by $NaBH_4$ (0.4 equiv.) reduction.

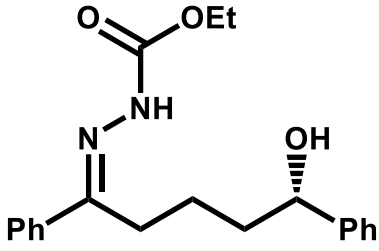

ethyl (S,E)-2-(5-hydroxy-1,5-diphenylpentylidene)hydrazine-1-carboxylate M-53H (**231**)

Ethyl carbazate (76 mg, 0.73 mmol) was added to **230** (156 mg, 0.61 mmol) in MeOH (5 mL). A drop of acetic acid was added and the reaction was monitored by TLC. After 48 h, the reaction mixture was concentrated under reduced pressure. The crude material was purified by flash column chromatography on silica gel (gradient of 30% to 45% ethyl acetate in hexanes as eluent) to yield the product (81 mg, 0.24 mmol, 39%) as an oil. R_f = 0.41 (1/1 Hex/EtOAc). ^{1}H NMR (400 MHz, $CDCl_3$) δ 9.19 (s, 1H), 7.85 – 7.70 (m, 2H), 7.49 – 6.94 (m, 8H), 4.81 (t, *J* = 5.5 Hz, 1H), 4.30 (ddq, *J* = 14.5, 7.4, 3.6 Hz, 2H), 2.92 – 2.70 (m, 2H), 1.87 – 1.66 (m, 4H), 1.35 (t, *J* = 7.1 Hz, 3H). ^{13}C NMR (101 MHz, $CDCl_3$) δ 152.11, 144.61, 137.25, 129.12, 128.59, 128.44, 127.72, 126.45, 125.71, 74.91, 61.98, 37.13, 26.56, 22.74, 14.70. IR (film cm^{-1}) 3490, 3255, 3029, 2932, 1718, 1530, 1494, 1235, 1056, 765, 699. HRMS (ESI): [M-H] for $C_{20}H_{23}N_2O_3$ found 339.1715, calcd 339.1714.

[19] Lagasse, F., Tsukamoto, M., Welch, C., and Kagan, H.B. *J.Am. Chem.Soc*., **2003***,* 7490.

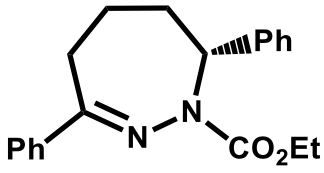

ethyl (R)-3,7-diphenyl-4,5,6,7-tetrahydro-1H-1,2-diazepine-1-carboxylate (**232**)

DIAD (78 µL, 0.39 mmol) was added to a solution of PPh_3 (116 mg, 0.44 mmol) in THF (2 mL) under argon at 0 °C. **231** (75 mg, 0.22 mmol) in THF (2 mL) was added and the reaction mixture was allowed to reach rt. After being stirred for 4 h, the reaction mixture was concentrated under reduced pressure. The crude material was purified by flash column chromatography on silica gel (gradient of 10% to 20% ethyl acetate in hexanes as eluent) to yield the product (65 mg, 0.20 mmol, 92%) as a clear oil. R_f = 0.53 (2/1 Hex/EtOAc). ^{1}H NMR (400 MHz, $CDCl_3$) Broad signals due to conformers δ 7.93-7.86 (m, 2H), 7.56 – 7.19 (m, 8H), 5.34-5.27 (m, 1H), 4.24-4.06 (m, 2H), 3.17 – 3.02 (m, 1H), 2.96 (m, 1H), 2.13 – 1.58 (m, 4H), 1.21-1.14 (m, 3H). ^{13}C NMR (101 MHz, $CDCl_3$) Broad signals due to conformers, major peaks listed δ 172.20, 155.19, 136.55, 130.65, 128.54, 128.43, 127.32, 126.77, 126.25, 61.78, 31.89, 28.29, 18.18, 14.51. IR (film cm^{-1}) 3028, 2980, 2937, 2866,1694, 1449, 1400, 1374, 1313, 1106, 766, 696. HRMS (ESI): [M+H] for $C_{20}H_{23}N_2O_2$ found 323.1749, calcd 323.1754.

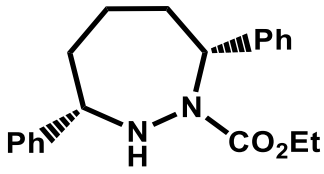

ethyl (3S,7R)-3,7-diphenyl-1,2-diazepane-1-carboxylate (**233**)

Hydrazone **232** (60 mg, 0.19 mmol) was dissolved in EtOH (2 mL) under argon atmosphere. PtO_2 (4.4 mg, 0.019 mmol) was added and H_2 was bubbled through the mixture for 1 h. The reaction mixture was filtered through celite, rinsed with EtOAc. The solution was evaporated under reduced pressure and the crude material was purified by flash column chromatography on silica gel (gradient of 5% to 10% ethyl acetate in hexanes as eluent) to yield the product (20 mg, 32%) as a waxy solid. R_f = 0.82 (2/1 Hex/EtOAc). ^{1}H NMR (500 MHz, Chloroform-*d*) 2 conformations (peaks coalescence at 70 ˚C in CD_3CN) (40:60) δ 7.59 – 7.12 (m, 10H), 5.10 (dd, *J* = 10.6, 7.4 Hz, 0.4H) 4.92 (dd, *J* = 10.6, 7.4 Hz, 0.6H), 4.76 – 4.67 (m, 0.6H), 4.40-4.45 (m, 0.4H), 4.35-4.27 (m,

0.4H) 4.15 (m, 1.6H), 3.95 (m, 1H), 2.32 – 2.14 (m, 2H), 2.14 – 1.79 (m, 3H), 1.78 – 1.55 (m, 1H), 1.27 (m, 3H). ^{13}C NMR (126 MHz, $CDCl_3$) 2 conformers, major peaks listed δ 157.07, 156.12, 143.71, 143.45, 141.98, 141.87, 128.63, 128.53, 128.30, 128.23, 127.81, 127.65, 127.43, 127.29, 127.02, 126.95, 126.63, 126.38, 67.57, 66.94, 61.85, 61.72, 61.66, 60.94, 38.50, 38.05, 35.52, 35.07, 26.33, 25.46, 25.27, 14.76, 14.62. IR (film cm^{-1}) 3302, 3061, 3030, 2929, 2852, 1690, 1491, 1402, 1380, 1328, 1275, 1171, 1107, 1072, 1022, 933, 750, 698. HRMS (ESI): [M+H] for $C_{20}H_{25}N_2O_2$ found 325.1908, calcd 325.1911.

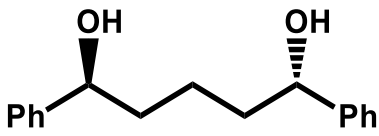

(1S,5S)-1,5-diphenylpentane-1,5-diol (**234**)

Synthesized according to the procedure for **264** using 2.2 equiv. of borane to give the product in 87% yield and the physical and spectral data for this compound matched previously reported data.[20] dr:16:0:1 of SS, RR and SR/RS. HPLC: CHIRALCEL OB-H, Hex:iPrOH 85:15. 1 mL/min, 220 nm (ref 360 nm). 12.63 min (major, SS), 22.39 min (minor, RR) and 26.68 min (minor, RS and SR). Racemic made through the reduction with $NaBH_4$ (2 equiv.) in a 1(SS):1(RR):1.5 (meso, RS and SR) ratio.

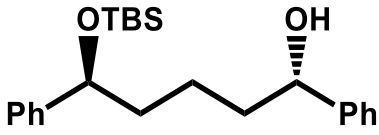

(1S,5S)-5-((tert-butyldimethylsilyl)oxy)-1,5-diphenylpentan-1-ol (**235**)

Diol **234** (0.80 g, 3.13 mmol) was dissolved in THF under argon atmosphere and cooled to -78 °C. *n*-BuLi (2.29 M; 2.0 mL, 4.49 mmol) was added dropwise and the reaction was allowed to reach rt. TBSCl (0.68 g, 4.49 mmol) was added and the reaction was stirred over night. The reaction was quenched by careful addition of H_2O at 0 °C and diluted with ethyl acetate. The layers were

[20] Lagasse, F., Tsukamoto, M., Welch, C., and Kagan, H.B. *J.Am. Chem.Soc*., **2003***,* 7490

separated, and the aqueous layer was extracted with ethyl acetate and the combined organic layers were washed with saturated aq. sodium bicarbonate solution, water and brine, dried with anhydrous sodium sulfate and the solvent was removed under reduced pressure. The crude material was purified by flash column chromatography on silica gel (10% ethyl acetate in hexanes as eluent) to yield the product (0.70 g, 80%) as white crystals. R_f = 0.84 (2/1 Hex/EtOAc). ^{1}H NMR (400 MHz, Chloroform-*d*) δ 7.45 – 7.14 (m, 10H), 4.72 – 4.56 (m, 2H), 1.92 – 1.54 (m, 4H), 1.54 – 1.33 (m, 2H), 0.92 (d, *J* = 2.1 Hz, 9H), 0.05 (s, 3H) -0.11 (s, 3H). ^{13}C NMR (101 MHz, $CDCl_3$) δ 145.75, 144.84, 128.43, 128.03, 127.50, 126.86, 125.90, 125.85, 75.07, 74.60, 40.89, 39.06, 25.90, 22.20, 18.25, -4.56, -4.92. IR (film cm^{-1}) 3363, 3063, 3029, 2929, 2857, 1453, 1256, 1094, 1066, 835. HRMS (ESI): [M+Na] for $C_{23}H_{34}NaO_2Si$ found 393.2220, calcd 393.2220.

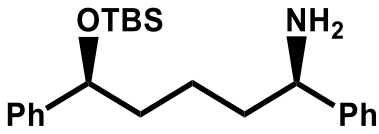

tert-butyl 2-((1R,5S)-5-((tert-butyldimethylsilyl)oxy)-1,5-diphenylpentyl)hydrazine-1-carboxylate (**236**)

Synthesized according to the procedure for **200** with the modification using DPPA (1.2 equiv.) and DBU (1.2 equiv.) to form azide and subsequent Staudinger reduction gave the title product in 74% yield. R_f = 0.26 (9/1 DCM/MeOH (1% Et_3N)). ^{1}H NMR (400 MHz, Chloroform-*d*) δ 7.45 – 7.15 (m, 10H), 4.66 (dd, *J* = 7.6, 4.7 Hz, 1H), 3.90 (q, *J* = 6.3, 5.7 Hz, 1H), 1.97 – 1.58 (m, 4H), 1.50 – 1.23 (m, 2H), 0.92 (d, *J* = 3.2 Hz, 9H), 0.04 (s, 3H), -0.10 (s, 3H). ^{13}C NMR (101 MHz, $CDCl_3$) δ 146.71, 145.78, 128.43, 128.03, 126.87, 126.85, 126.33, 125.84, 74.92, 56.22, 40.91, 39.71, 25.92, 22.71, 18.26, -4.55, -4.91. IR (film cm^{-1}) 3370, 3312, 2929, 2856, 1603, 1453, 1256, 1092, 1068, 835, 775, 699. HRMS (ESI): [M+H] for $C_{23}H_{36}NOSi$ found 370.2560, calcd 370.2561.

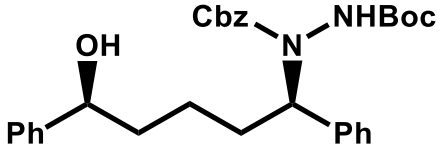

1-benzyl 2-(tert-butyl) 1-((1R,5S)-5-hydroxy-1,5-diphenylpentyl)hydrazine-1,2-dicarboxylate (**238**)

The sequence N-N coupling, Cbz protection and TBAF deprotection is performed according to the procedures for **202**, **203** and **183**, respectively to give **238** (46%, 3 steps) as white crystals. R_f = 0.23 (3/1 Hex/EtOAc). ^{1}H NMR (400 MHz, Chloroform-*d*) δ 7.50-7.08 (m, 15H), 6.50 – 4.50 (m, 5H), 2.69 – 0.71 (m, 16H). ^{13}C NMR (101 MHz, $CDCl_3$) (rotomers) δ 156.03, 145.02, 139.20, 135.96, 128.95, 128.90, 128.48, 128.39, 128.18, 128.04, 127.84, 127.33, 126.97, 126.28, 125.84, 125.69, 81.28, 74.30, 68.17, 65.21, 41.63, 39.05, 38.56, 37.19, 30.60, 28.40, 28.11, 27.31, 26.22, 22.86, 22.70. IR (film cm^{-1}) 3285, 3031, 2978, 2935, 1700, 1455, 1409, 1367, 1296, 1245, 1157, 1053, 1026. HRMS (ESI): [M+Na] for $C_{30}H_{36}N_2NaO_5$ found 527.2506, calcd 527.2516.

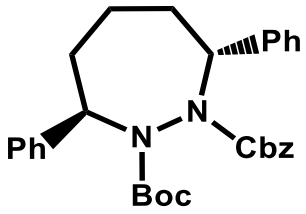

1-benzyl 2-(tert-butyl) (3R,7R)-3,7-diphenyl-1,2-diazepane-1,2-dicarboxylate (**239**)

Prepared according to the ring closing procedure for **183** to give the product in 74% yield (68 mg). R_f = 0.76 (3/1 Hex/EtOAc). ^{1}H NMR (500 MHz, Chloroform-*d*) Broad signals due to conformers δ 7.72 – 6.95 (m, 15H), 5.49 – 4.62 (m, 4H), 2.50 – 1.76 (m, 6H), 1.41 – 1.01 (m, 9H). ^{13}C NMR (126 MHz, $CDCl_3$) (conformers) δ 155.97, 155.95, 155.36, 155.20, 154.47, 154.26, 153.64, 153.47, 143.87, 142.79, 142.74, 141.78, 141.71, 141.36, 141.18, 138.97, 136.12, 136.03, 135.61, 135.43, 129.03, 128.97, 128.90, 128.61, 128.56, 128.39, 128.37, 128.28, 128.24, 128.20, 128.13, 128.10, 128.07, 128.06, 127.99, 127.94, 127.89, 127.87, 127.83, 127.80, 127.76, 127.72, 127.62, 127.58, 127.54, 127.42, 127.38, 127.20, 127.13, 127.11, 126.96, 126.92, 126.74, 126.32, 126.14, 81.28, 81.25, 81.22, 81.16, 81.09, 69.75, 68.12, 67.97, 67.89, 67.64, 65.97, 65.13, 64.96, 64.27, 63.93, 63.81, 63.20, 62.69, 31.68, 31.33, 30.87, 30.57, 30.15, 29.89, 29.74, 29.61, 29.56, 29.42, 28.15, 28.02, 27.74, 27.68, 24.81, 24.19, 24.13, 23.71, 22.74. IR (film cm^{-1}) 3064, 3032, 2935, 1701, 1455, 1393, 1367, 1344, 1142, 1028. HRMS: [M+Na] for $C_{30}H_{34}NaN_2O_4$ found 509.2413, calcd 509.2411.

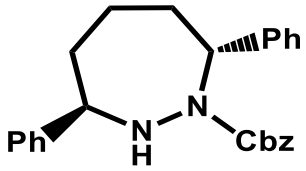

benzyl (3R,7R)-3,7-diphenyl-1,2-diazepane-1-carboxylate (**241**)

Prepared according to Boc deprotection procedure for **183** to afford the title product (24 mg, 96%) R_f = 0.79 (3/1 Hex/EtOAc). ^{1}H NMR (400 MHz, Chloroform-*d*) Broad signals due to conformers δ 7.69 – 6.68 (m, 15H), 5.29 – 4.05 (m, 5H), 2.51 – 1.74 (m, 6H). ^{13}C NMR (101 MHz, $CDCl_3$) Broad signals due to conformers, major peaks listed δ 136.13, 128.35, 128.26, 127.85, 127.82, 127.61, 127.38, 126.79, 126.40, 126.34, 67.38, 64.56, 23.89. IR (film cm^{-1}) 3030, 2928, 1694, 1494, 1397, 1326, 1262, 1127. HRMS (ESI): [M+Na] for $C_{25}H_{26}NaN_2O_2$ found 409.1882, calcd 409.1886

Bicyclic **118** synthesized according to Dainis Kaldre thesis which includes characterization for the intermediates.

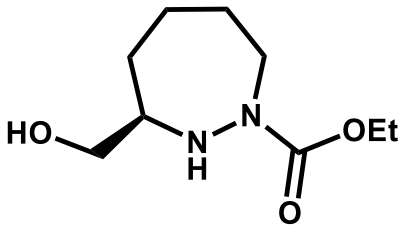

ethyl (R)-3-(hydroxymethyl)-1,2-diazepane-1-carboxylate (**219**)

The Boc protected diazepane **216** (0.21 g, 0.47 mmol) was dissolved in a mixture of DCM:TFA (2:1, 3 mL). The solution was stirred for 1 h and then reduced under reduced pressure. The crude was dissolved in $CHCl_3$ (5 mL) and EtO_2CCl (68 µL, 0.71 mmol) and $NaHCO_3$ (1M, 5 mL) were added and the reaction mixture was stirred for 1 h. EtOAc (25 mL) and $NaHCO_3$ (25 mL) were added to the flask and then transferred to a separatory funnel. The phases were separated and the organic phase was washed with $NaHCO_3$ and brine, dried with anhydrous Na_2SO_4, filtered and evaporated *in vacuo*. The crude material was purified by flash column chromatography on silica gel (30-35% gradient of ethyl acetate in hexanes as eluent) to yield the product (61 mg, 64%). R_f = 0.13 (2/1 Hex/EtOAc). ^{1}H NMR (500 MHz, Chloroform-*d*) δ 4.32-3.96 (m, 3H), 3.72 – 3.15 (m, 4H), 3.08-2.89 (m, 1H), 2.00 – 1.38 (m, 5H), 1.31 – 1.13 (m, 4H). ^{13}C NMR (126 MHz, $CDCl_3$) δ 158.04, 64.13, 62.03, 61.52, 49.51, 30.82, 28.44, 23.87, 14.63. IR (film cm^{-1}) 3420, 2981, 2929,

2864, 1673, 1411,1381, 1336, 1263, 1182, 1120, 1035. HRMS (ESI): [M+Na] for $C_9H_{18}N_2NaO_3$ found 225.1212, calcd 225.1210.

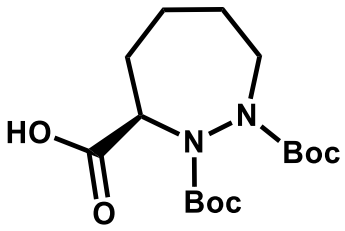

(R)-1,2-bis(tert-butoxycarbonyl)-1,2-diazepane-3-carboxylic acid (**220**)

Procedure according to lit.[21] and title compound was isolated as white crystals in 75% yield. R_f = 0.32 (2/1 Hex/EtOAc). ^{1}H NMR (400 MHz, Chloroform-*d*) rotomers δ 4.56 – 4.06 (m, 2H), 3.02 – 2.79 (m, 1H), 2.44 – 2.22 (m, 1H), 2.19 – 1.99 (m, 1H), 1.85 – 1.42 (m, 22H). ^{13}C NMR (101 MHz, $CDCl_3$) rotomers δ 177.24, 173.01, 172.51, 158.49, 158.21, 153.42, 152.54, 84.30, 84.19, 83.70, 82.57, 66.38, 64.22, 61.95, 51.77, 51.47, 49.75, 44.66, 33.65, 32.16, 29.28, 29.07, 28.08, 28.05, 28.00, 27.94, 27.73, 27.63, 26.68, 26.25, 26.15, 24.96, 23.95. IR (film cm^{-1}) 2978, 2934, 1718, 1654, 1458, 1416, 1367, 1151. HRMS (ESI): [M+Na] for $C_{16}H_{28}N_2NaO_6$ found 367.1839, calcd 367.1840.

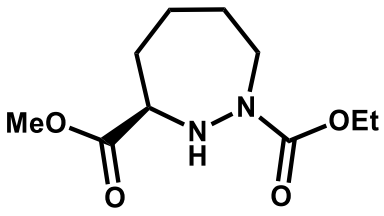

1-ethyl 3-methyl (R)-1,2-diazepane-1,3-dicarboxylate (**221**)

Carboxylic acid (80 mg, 0.23 mmol) was dissolved in MeOH and 5 drops sulfuric acid (conc.) was added. After 2 h, the reaction mixture was concentrated under reduced pressure. The crude was dissolved in $CHCl_3$ (4 mL) and EtO_2CCl (29 μL, 0.30 mmol) and $NaHCO_3$ (1M, 4 mL) were added and the reaction mixture was stirred for 1 h. $NaHCO_3$ (aq. sat.) and EtOAc were added and the phases were separated and the organic phase was washed with water and brine, dried with anhydrous sodium sulfate and the solvent was removed under reduced pressure. The crude material

[21] Zhao, M.; Eiichi Mano J. L.; Song Z.; Tschaen D. M.; Grabowski E. J. J.; Reider P. J.; *J Org Chem*. ***1999***, *2564*

was purified by flash column chromatography on silica gel (20-25% gradient of ethyl acetate in hexanes as eluent) to yield the product in 64% yield. R_f = 0.36 (2/1 Hex/EtOAc) ^{1}H NMR (400 MHz, Chloroform-*d*) δ 5.42-4.84 (m, 1H), 4.22-4.09 (m, 2H), 3.85-3.71 (m, 5H), 3.38 – 3.23 (m, 1H), 2.10 – 1.93 (m, 1H), 1.93 – 1.39 (m, 5H), 1.29 (t, *J* = 7.1 Hz, 3H). ^{13}C NMR (101 MHz, $CDCl_3$) conformers δ 172.31, 77.33, 61.81, 52.07, 48.73, 31.82, 23.92, 14.69. IR (film cm^{-1}) 3326, 2935, 1739, 1697, 1446, 1407, 138, 1211, 1184. HRMS (ESI): [M+Na] for $C_{10}H_{18}N_2NaO_4$ found 253.1163, calcd 253.1159.

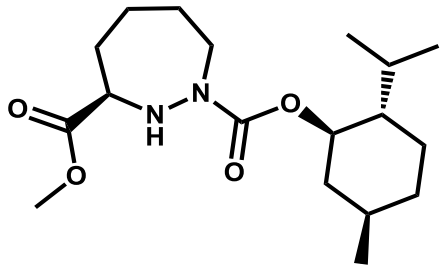

1-((1R,2S,5R)-2-isopropyl-5-methylcyclohexyl) 3-methyl (R)-1,2-diazepane-1,3-dicarboxylate (**283**)

Prepared according to the procedure for **221** with (-)-menthol chloroformate instead of ethyl chloroformate and was isolated as a think film in 34% yield. ^{1}H NMR (500 MHz, Chloroform-*d*) δ 5.44 – 4.88 (m, 1H), 4.65-4.55 (m, 1H), 3.95-3.59 (m, 5H), 3.38-3.18 (m, 1H), 2.15 – 1.57 (m, 9H), 1.57 – 0.76 (m, 15H). ^{13}C NMR (126 MHz, $CDCl_3$) δ 172.24, 156.52, 69.12, 62.32, 52.09, 48.58, 47.37, 41.46, 34.27, 34.04, 31.92, 31.83, 31.39, 29.69, 29.67, 29.65, 29.36, 29.25, 29.09, 27.61, 26.62, 26.13, 24.85, 23.94, 23.64, 22.69, 22.03, 20.78, 20.69, 16.57, 14.12. IR (film cm^{-1}) 3305, 2928, 2869, 1740, 1691, 1397, 1210, 1179, 1114. HRMS (ESI) calc. for $C_{18}H_{32}N_2NaO_4$ [M+Na] 363.2254, found 363.2255.

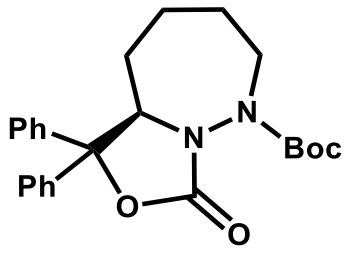

tert-butyl (R)-8-oxo-6,6-diphenylhexahydro-1H,8H-oxazolo[3,4-b][1,2]diazepine-1-carboxylate (**223**)

K_2CO_3 (241 mg, 1.74 mmol) and MeI (65 µL, 1.05 mmol) were added to carboxylic acid **220** (300 mg, 0.87 mmol) in DMF (3 mL). The reaction mixture was stirred for 16 h after which EtOAc and water were added. The phases were separated and the organic phase was washed with water and brine, dried with anhydrous sodium sulfate and the solvent was removed under reduced pressure. The crude material was purified by flash column chromatography on silica gel (10-15% gradient ethyl acetate in hexanes as eluent) to yield the product (215 mg, 69%). The methyl ester (200 mg, 0.56 mmol) was dissolved in THF and the solution was cooled to 0 °C. PhMgBr (464 µL, 1.39 mmol, 3M in THF) was added dropwise after which the reaction mixture was allowed to reach rt. After 1 h, the reaction mixture was cooled down to 0 °C again and the reaction was quenched with NH_4Cl (aq, sat.) and extracted with EtOAc. The phases were separated and the organic phase was washed with brine, dried with anhydrous sodium sulfate and the solvent was removed under reduced pressure. The crude material was purified by flash column chromatography on silica gel (5-15% gradient of ethyl acetate in hexanes as eluent) to yield the product (83 mg, 36%) as a white powder. ^{1}H NMR (400 MHz, Chloroform-*d*) δ 7.76 – 6.67 (m, 10H), 4.99 – 4.36 (m, 1H), 3.89-3.60 (m, 1H), 3.45 – 3.00 (m, 1H), 1.83 – 1.08 (m, 15H). ^{13}C NMR (101 MHz, $CDCl_3$) δ 154.92, 153.80, 142.87, 139.52, 128.51, 128.39, 128.21, 127.94, 126.38, 125.80, 86.38, 81.92, 65.25, 49.15, 46.75, 32.82, 30.74, 29.48, 28.24, 27.84, 27.05, 22.86. IR (film cm^{-1}) 2932, 1776, 1709, 1367, 1155. HRMS (ESI) calc. for $C_{28}H_{28}N_2NaO_4$ [M+Na] 431.19413, found 431.1933.

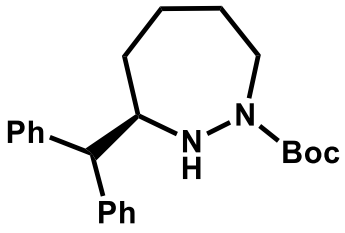

tert-butyl (R)-3-benzhydryl-1,2-diazepane-1-carboxylate (**224**)

Prepared according to the benzyl deprotection procedure for **184** to yield the title product in 72% yield as a thick oil. ^{1}H NMR (400 MHz, Chloroform-*d*) δ 7.77 – 7.04 (m, 10H), 4.86 – 3.71 (m, 4H), 3.09 (s, 1H), 1.96 – 1.24 (m, 15H). ^{13}C NMR (101 MHz, $CDCl_3$) δ 141.89, 128.84, 128.60, 128.27, 128.25, 126.68, 126.34, 80.21, 67.10, 59.16, 56.11, 49.71, 32.13, 28.60, 28.42, 22.44. IR (film cm^{-1}). HRMS (ESI) calc. for $C_{23}H_{30}N_2NaO_4$ [M+Na] 389.2199, found 389.2201.

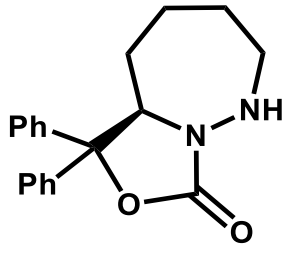

(R)-6,6-diphenylhexahydro-1H,8H-oxazolo[3,4-b][1,2]diazepin-8-one (**225**)

Prepared according to the Boc deprotection procedure for **185** to give the product in 96% yield as white crystals. ^{1}H NMR (400 MHz, Chloroform-*d*) δ 7.57 – 7.17 (m, 10H), 4.73 – 4.50 (m, 2H), 3.24 – 2.87 (m, 2H), 1.89 – 1.39 (m, 5H), 1.09 – 1.00 (m, 1H). ^{13}C NMR (101 MHz, $CDCl_3$) δ 156.32, 142.61, 139.42, 128.53, 128.37, 128.13, 127.85, 126.63, 126.07, 86.03, 65.46, 49.50, 30.92, 30.19, 22.48. IR (film cm^{-1}) 3304, 2926, 2854, 1755, 1449. HRMS (ESI) calc. for $C_{19}H_{21}N_2O_2$ [M+H] 309.15975, found 309.1598.

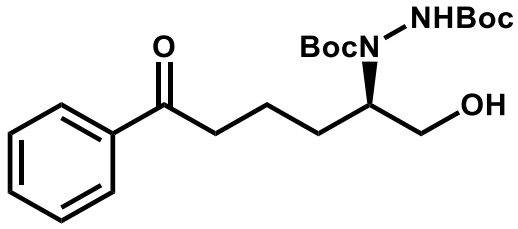

di-tert-butyl (R)-1-(1-hydroxy-6-oxo-6-phenylhexan-2-yl)hydrazine-1,2-dicarboxylate (**262**)

Aldehyde **261** prepared according to literature.[22] Aldehyde **261** (2.29 g, 9.95 mmol) and hydrazone **226** (2.65 g, 13.93 mmol) were dissolved in CH_3CN (50 mL) and cooled to -5 °C. L-proline (115 mg, 1.0 mmol) was added and the reaction mixture was stirred at -5 °C for 24 h. The reaction was quenched by adding EtOH (10 mL) and $NaBH_4$ (263 mg, 6.69 mmol) and stirred for 15 min. HCl (1M) was added and the mixture was extracted twice with EtOAc. The organic phases were combined and washed with brine, dried with anhydrous sodium sulfate and the solvent was removed under reduced pressure. The crude material was purified by flash column

[22] Wang, Y.; Du, H.; *J. Org. Chem.*, **2010**, 3503.

chromatography on silica gel (25% ethyl acetate in hexanes as eluent) to yield the product (3.13 g, 75%). R_f = 0.55 (1/1 Hex/EtOAc). ^{1}H NMR (400 MHz, Chloroform-*d*) δ 7.94 (t, *J* = 5.9 Hz, 2H), 7.64 – 7.50 (m, 1H), 7.45 (t, *J* = 7.6 Hz, 2H), 6.78-6.58 (m, 1H), 4.86 – 3.96 (m, 2H), 3.66 – 3.20 (m, 2H), 3.09 – 2.89 (m, 2H), 1.98 – 1.18 (m, 21H). ^{13}C NMR (101 MHz, $CDCl_3$) (conformers) δ 200.32, 199.62, 158.48, 157.88, 155.96, 155.53, 136.86, 133.12, 128.60, 128.00, 127.91, 125.82, 82.25, 82.00, 81.91, 81.23, 77.30, 62.32, 62.20, 60.37, 57.94, 37.64, 37.51, 28.20, 28.14, 28.10, 27.43, 27.12, 20.08, 19.89. IR (film cm^{-1}) 3402, 3192, 2972, 1712, 1393, 1344, 1291, 1162, 1130, 1068, 737. HRMS (ESI): [M+Na] for $C_{22}H_{34}N_2NaO_6$ found 445.2305, calcd 445.2309.

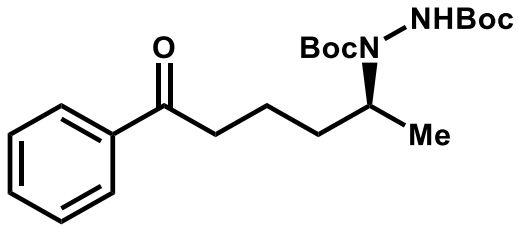

di-tert-butyl (S)-1-(6-oxo-6-phenylhexan-2-yl)hydrazine-1,2-dicarboxylate (**263**)

DMAP (89 mg, 0.73 mmol) and TCDI (1.96 g, 11.0 mmol) were added to a solution of alcohol **262** (3.10 g, 7.3 mmol) in DCM (35 mL). After 24 h, the solvent was removed under reduced pressure and the crude was purified by flash column chromatography on silica gel (20% ethyl acetate in hexanes as eluent) to yield the thionylimidazole activated alcohol (95% yield). In a dry, three-necked flask under inert atmosphere quipped with condenser and septa, the activated alcohol (3.2 g, 6.0 mmol) was dissolved in toluene (150 mL) and AIBN was added. The reaction mixture was refluxed Bu_3SnH (3.23 mL, 12.0 mmol) was added in portions of 0.5 mL in 10 min intervals. After stirring for 1 h. The reaction was cooled down to rt and EtOAc and KF (0.70 g, 12 mmol) was added and the suspension was stirred for 30 min and then filtered through a SiO_2 plug (tin waste, toxic). The solvent was removed under reduced pressure and the crude was purified by flash column chromatography on silica gel (15% ethyl acetate in hexanes as eluent) to yield the product (2.4 g, 50%). R_f = 0.83 (2/1 Hex/EtOAc). ^{1}H NMR (400 MHz, Chloroform-*d*) Broad signals due to conformers δ 7.96 – 7.81 (m, 2H), 7.55 – 7.44 (m, 1H), 7.43 – 7.36 (m, 2H), 6.42 – 5.54 (m, 1H), 4.38 – 3.97 (m, 1H), 3.07 – 2.76 (m, 2H), 1.80 – 0.78 (m, 25H). ^{13}C NMR (101 MHz, $CDCl_3$)

Broad signals due to conformers, major peaks listed δ 155.07, 136.99, 132.95, 128.55, 128.05, 126.95, 80.85, 52.04, 33.47, 28.64, 28.54, 28.27, 28.19, 27.84, 27.07, 26.83, 23.44, 17.52, 15.26, 13.68, 13.59. IR (film cm^{-1}) 3323, 2929, 2856, 1742, 1703, 1393, 1367, 1241, 1158. HRMS (ESI): [M+Na] for $C_{22}H_{34}N_2NaO_5$ found 429.2354, calcd 429.2360. Enantioselectivity determined by HPLC: 98% ee. CHIRALCEL OD (4.6 × 250 mm), Hex:iPrOH 90:10. 1 mL/min, 220 nm (ref 360 nm). 6.46 min (minor) and 7.45 min (major). Racemic mixture made through the same synthesis using DL-proline.

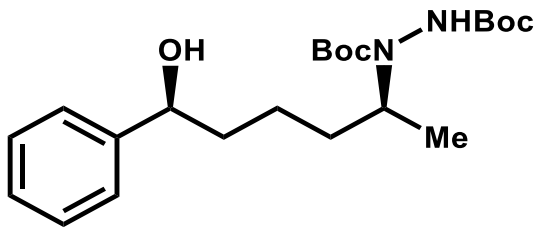

di-tert-butyl 1-((2S,6S)-6-hydroxy-6-phenylhexan-2-yl)hydrazine-1,2-dicarboxylate (**264**)

In a dry RBF under argon atmosphere, (R)-2-methyl-CBS-oxazaborolidine (80 mg, 0.30 mmol) was dissolved in THF (5 mL). The solution was cooled to 0 °C and borane (3 mL, 2.95 mmol, 1M in THF) was added. A solution of ketone **263** (600 mg, 1.47 mmol) in THF (5 mL) at 0 °C was cannulated slowly over to the borane solution. The reaction mixture was stirred for 1 h after complete addition after which it was quenched carefully with water. The suspension was transferred to a separatory funnel and extracted twice with EtOAc. The organic phase were combined and washed with HCl (0.1 M) and brine, dried with anhydrous sodium sulfate and the solvent was removed under reduced pressure. The crude material was purified by flash column chromatography on silica gel (30-35% gradient of ethyl acetate in hexanes as eluent) to yield the product (437 mg, 75%). R_f = 0.21 (2/1 Hex/EtOAc) ^{1}H NMR (400 MHz, Chloroform-*d*) Broad signals due to conformers δ 7.36-7.17 (m, 5H), 6.44 – 6.02 (m, 1H), 4.72 – 3.95 (m, 2H), 2.97 – 2-71 (m, 1H), 1.94 – 0.78 (m, 27H). ^{13}C NMR (101 MHz, $CDCl_3$ Broad signals due to conformers, major peaks listed) δ 155.74, 155.06, 145.04, 128.27, 127.22, 125.84, 80.72, 74.17, 60.38, 52.32, 38.97, 38.95, 28.24, 28.18, 27.82, 26.80, 20.97, 17.99, 17.52, 14.16, 13.59. IR (film cm^{-1}) 3313, 2978, 2934, 1702, 1394, 1367, 1248, 1159. HRMS (ESI): [M+Na] for $C_{22}H_{36}N_2NaO_5$ found 431.2505, calcd 431.2516.

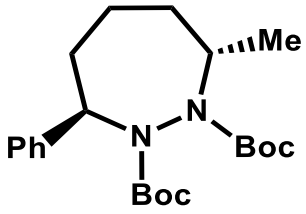

di-tert-butyl (3S,7R)-3-methyl-7-phenyl-1,2-diazepane-1,2-dicarboxylate (**265**)

Prepared according to the procedure for **183** to give the product in 62% yield (removed a close similar impurity which was believed to be diastereomers). R_f = 0.69 (2/1 Hex/EtOAc) ^{1}H NMR (400 MHz, Chloroform-*d*) δ 7.80 – 7.06 (m, 5H), 5.17 – 4.09 (m, 2H), 2.47 – 0.62 (m, 27H). ^{13}C NMR (101 MHz, $CDCl_3$) Too many signals due to conformers, major peaks listed δ 155.26, 154.95, 154.93, 154.65, 154.48, 154.40, 154.25, 154.04, 145.02, 144.05, 143.36, 142.42, 128.00, 127.87, 127.84, 127.73, 127.49, 127.36, 126.85, 126.80, 126.75, 126.67, 126.45, 126.27, 126.17, 80.85, 80.77, 80.66, 80.59, 80.53, 80.47, 80.35, 67.98, 66.01, 64.77, 62.92, 60.30, 56.11, 55.58, 54.56, 54.15, 53.40, 34.34, 33.62, 32.93, 32.26, 32.01, 31.91, 31.85, 31.44, 28.47, 28.37, 28.26, 28.15, 28.08, 28.00, 27.92, 23.96, 23.89, 23.47, 23.42, 18.68, 18.39, 16.86, 16.83. IR (film cm^{-1}) 2976, 2932, 1697, 1455, 1390, 1365, 1333, 1172, 1150. HRMS (ESI): [M+Na] for $C_{22}H_{34}N_2NaO_4$ found 413.2401, calcd 413.2411.

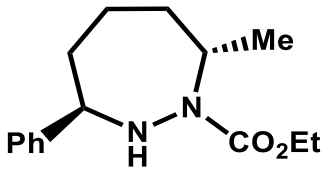

ethyl (3R,7S)-7-methyl-3-phenyl-1,2-diazepane-1-carboxylate (**266**)

Diazepane dicarboxylate **265** (100 mg, 0.26 mmol) was dissolved in DCM (2 mL) and TFA (1 mL). After 2 h, the solvent and excess TFA were removed under reduced pressure. The crude was dissolved in THF under argon atmosphere and cooled to -78 °C after which Et_3N (107 µL, 0.77 mmol) and ethyl chloroformate (37 µL, 0.38 mmol) were added. The reaction was stirred for 1 h and then allowed to reach rt. The reaction was quenched with $NaHCO_3$ (aq, sat.) and extracted with EtOAc. The phases were separated and the organic phase was washed with brine, dried with anhydrous sodium sulfate and the solvent was removed under reduced pressure. The crude material was purified by flash column chromatography on silica gel (5-15% gradient of ethyl acetate in hexanes as eluent) to yield the product (52 mg, 77% yield). R_f = 0.65 (2/1 Hex/EtOAc). ^{1}H NMR

(500 MHz, Chloroform-*d*) δ 7.53 – 7.17 (m, 5H), 5.19 – 3.62 (m, 5H), 2.08 – 1.57 (m, 6H), 1.46 – 1.02 (m, 6H). ^{13}C NMR (126 MHz, $CDCl_3$) Due to conformers, major peaks described: δ 143.32, 128.30, 127.48, 127.30, 64.47, 61.30, 57.17, 53.44, 34.20, 33.52, 29.72, 23.77, 14.58, 1.04. IR (film cm^{-1}) 3313, 2929, 2860, 1690, 1377, 1285, 1100, 699. HRMS (ESI): [M+Na] for $C_{15}H_{22}N_2NaO_2$ found 285.1565, calcd 285.1587. Regioselectivity (97:3) and enantioselectivity (>98:2 er). Determined by HPLC: CHIRALCEL OD (4.6 × 250 mm), Hex:iPrOH 99:1. 1 mL/min, 214 nm (ref 360 nm). 6.38 min (minor regioisomer) and 7.18 min (major regioisomer). Undesired cis-diastereomers removed during flash chromatography purification in either this step or after the previous ring closing step Enantiomer at 9.65 min is less than 2%, too small/broad to integrate. Reference mixture made from racemic-**263** through the same synthesis but using $NaBH_4$ instead of CBS/BH_3 in the reduction.

5.4 Synthesis of 6-membered catalysts

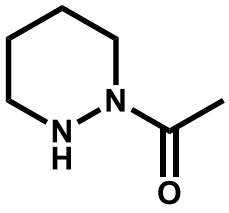

1-(tetrahydropyridazin-1(2H)-yl)ethan-1-one (**166**)

Prepared according to the procedure for **245** to give the product in 41% yield. ^{1}H NMR (500 MHz, Methanol-d_4) δ 3.67-3.56 (m, 2H), 2.93-2.88 (m, 2H), 2.14 (s, 3H), 1.76-1.42 (m, 4H). ^{13}C NMR (126 MHz, $CDCl_3$) δ 172.23, 48.27, 42.70, 25.65, 23.96, 20.77. IR (film cm^{-1}) 3475, 3251, 2937, 2857, 1627, 1524, 1439, 1404, 1354, 1263, 1196, 967, 896. HRMS (ESI): [M+Na] for $C_6H_{12}N_2NaO$ found 151.0841, calcd 151.0842.

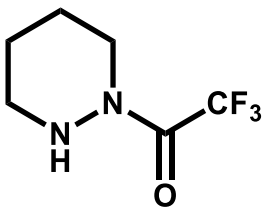

2,2,2-trifluoro-1-(tetrahydropyridazin-1(2H)-yl)ethan-1-one (**167**)

Prepared according to the procedure for **245** to give the product in 44% yield. ^{1}H NMR (500 MHz, Chloroform-*d*) δ 3.71 – 3.55 (m, 2H), 3.04 – 2.91 (m, 2H), 1.87 – 1.64 (m, 4H). ^{13}C NMR (126 MHz, $CDCl_3$) δ 157.40 (q, ^{2}J = 34 Hz), 116.73 (q, ^{1}J = 287 Hz), 48.17, 44.22, 24.94, 23.67. IR (film cm^{-1}) 3278, 2947, 2862, 1686, 1445, 1219, 1151, 998, 898, 664. HRMS (ESI): [M+Na] for $C_6H_9F_3N_2NaO$ found 205.0561, calcd 205.0559.

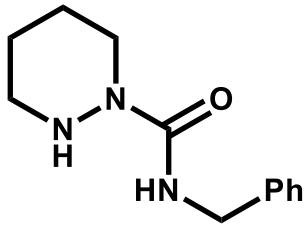

N-benzyltetrahydropyridazine-1(2H)-carboxamide (**168**)

Prepared according to the procedure for **243** using benzylisocyanate to give the product in 58% yield. ^{1}H NMR (500 MHz, Chloroform-*d*) δ 7.35 – 7.12 (m, 5H), 6.69 (t, *J* = 6.1 Hz, 1H), 4.37 (d, *J* = 6.1 Hz, 2H), 3.37 – 3.22 (m, 1H), 2.78 (m, *J* = 5.7 Hz, 2H), 1.70 – 1.45 (m, 4H). ^{13}C NMR (126 MHz, $CDCl_3$) δ 157.87, 140.12, 128.44, 127.41, 126.93, 47.24, 43.96, 43.30, 25.53, 23.95. IR (film cm^{-1}) 3401, 3236, 3030, 2936, 2854, 1647, 1521, 1496, 1454, 1254, 1154. HRMS (ESI): [M+Na] for $C_{12}H_{17}N_3NaO$ found 242.1264, calcd 242.1264.

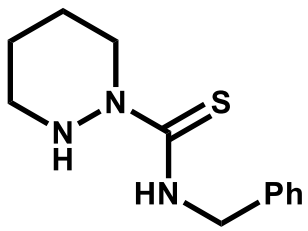

N-benzyltetrahydropyridazine-1(2H)-carbothioamide (**169**)

Prepared according to the procedure for **243** using benzylisothiocyanate to give the product in 28% yield. ^{1}H NMR (400 MHz, $CDCl_3$) 8.10 (s, 1H, NC(S)N**H**CH_2), 7.27-7.36 (m, 5H, Ar-**H**), 4.83 (d, 2H, J= 5.2 Hz, PhC**H$_2$**NH), 4.25 (bs, 2H, CH_2C**H$_2$**NC(S)CH_2Ph), 3.20 (t, 1H, 7.6 Hz CH_2CH_2N**H**N), 2.88 (m, 2H, CH_2C**H$_2$**NH), 1.79 (m, 2H, C**H$_2$**CH_2NC(S)CH_2Ph), 1.66 (m, 2H, C**H$_2$**CH_2NH). ^{13}C NMR (100 MHz, $CDCl_3$) 180.6, 138.5, 128.6, 127.8, 127.4, 48.9, 47.4, 25.5, 23.8. IR (film cm^{-1}) 3318, 3220, 2937, 2853, 1692, 1525, 1474, 1454, 1369, 1347, 1250, 1128, 856. HRMS (ESI): [M+Na] for $C_{12}H_{17}N_3NaS$ found 258.1030, calcd 258.1035.

5.5 Diels-Alder scope

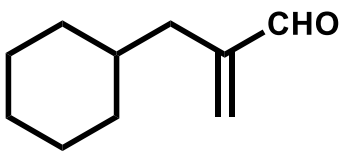

2-(cyclohexylmethyl)acrylaldehyde (**294**)

Prepared from 3-cyclohexylpropanal by α-methylenation according to literature.[23] ^{1}H NMR (500 MHz, Chloroform-*d*) δ 9.55 (s, 1H), 6.23 (d, *J* = 1.1 Hz, 1H), 6.04 (d, *J* = 0.9 Hz, 1H), 2.16 (d, *J* = 7.0 Hz, 2H), 1.74 – 1.62 (m, 5H), 1.29 – 1.08 (m, 4H), 0.94 – 0.82 (m, 2H). ^{13}C NMR (126 MHz, $CDCl_3$) δ 194.90, 148.77, 135.17, 36.25, 35.70, 33.10, 26.44, 26.17. IR (film cm^{-1}) 2923, 2851, 1697, 1448. HRMS (ESI): calcd for $C_{10}H_{17}O$ [M+H] 153.12739, found 153.12751.

Aldehydes **291-295** were prepared according to literature and distilled prior to use.[23] **297** and **300** were prepared according to literature.[24, 25] CpH was cracked right before using.

General procedure for Diels-Alder reaction: In a small vial equipped with a stir bar, catalyst **281** (20 mol%) was dissolved in appropriate solvent (1 M on aldehyde). Perchloric acid (10 mol%) was added and the reaction was cooled to – 20 °C in a cryostat. The vial was quickly taken out of the cryostat and prechilled (-20 °C in freezer) aldehyde (1 equiv.) and diene (5 equiv.) were added quickly and the vial was capped and returned to the cryostat. After indicated time, the reaction mixture was purified directly by flash column chromatography on silica gel (gradient of 5% to 15% ethyl acetate in hexanes as eluent) to yield the Diels-Alder product.

Achiral catalyst **69** used to synthesize racemix mixtures for HPLC or GLC references. First spectrum is the racemic followed by the spectrum of the Diels-Alder adduct by catalyst **281**.

[23] Erkkilä, A.; Pihko, P. M.; *J. Org. Chem.*, **2006**, 71, 2538.
[24] Huang, F.; Yao, Z-K.; Wang, Y.; Wang, Y.; Zhang, J.; Yu, Z.-X.; *Chem.–Asian J.*, **2010**, 5, 1555.
[25] Ndungu, J. M.; Larson, K. K.; Sarpong, R.; *Org Lett.* **2005**, 5845.

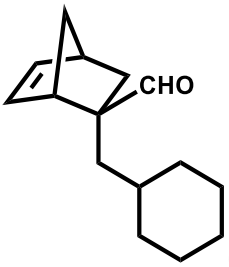

(1S,2R,4S)-2-(cyclohexylmethyl)bicyclo[2.2.1]hept-5-ene-2-carbaldehyde (**302**)

Prepared according to general procedure for Diels-Alder in THF for 24 h and was isolated as an oil in 81% yield as an *Exo*:*Endo* mixture. R_f = 0.59 (9/1 Hex/EtOAc). ^{1}H NMR (400 MHz, Chloroform-*d*) *exo* δ 9.74 (s, 1H), 6.29 (dd, *J* = 5.6, 3.0 Hz, 1H), 6.09 (dd, *J* = 5.7, 3.1 Hz, 1H), 2.93 (bs, 1H), 2.86 (bs, 1H), 2.24 (dd, *J* = 11.9, 3.9 Hz, 1H), 1.68-1.55 (m, 6H), 1.39 – 1.05 (m, 6H), 0.96 – 0.76 (m, 3H). ^{13}C NMR (101 MHz, $CDCl_3$) δ 206.19, 139.64, 133.23, 58.48, 47.92, 46.97, 43.66, 42.68, 35.58, 34.49, 34.13, 33.54, 26.29, 26.26, 26.16. IR (film cm^{-1}) 3062, 2921, 2850, 2807, 2697, 1718, 1448. HRMS (ESI): calcd for $C_{15}H_{23}O$ [M+H] 219.1743, found 219.1744. The diastereoselectivity (*exo:endo* ratio 89:11) determined by ^{1}H NMR integration: δ 9.74 (s, 1H, C*H*O, *exo*), 9.49 (s, 1H, C*H*O, *endo*). Enantioselectivity (ee = 95%) was determine by reducing the aldehyde to the alcohol using $NaBH_4$; GC (Astec CHIRALDEX B-DM 30 m × 0.25 mm column, 145 °C) t_R = *Exo* (minor) 47.3 min. (4.531 Au), *Exo* (major) 48.5 min. (164.74 Au).

Racemix mixture:

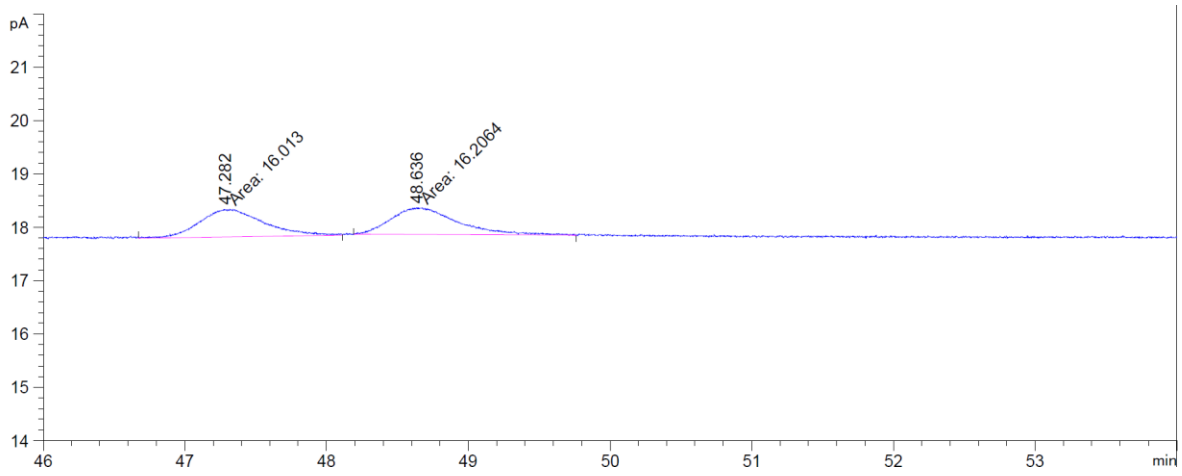

Chiral adduct:

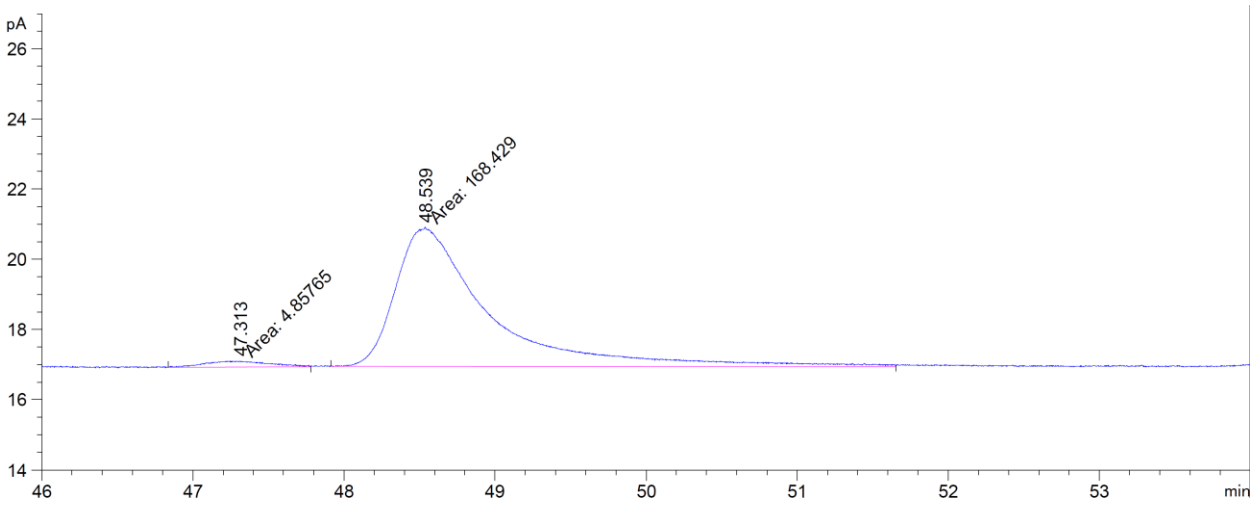

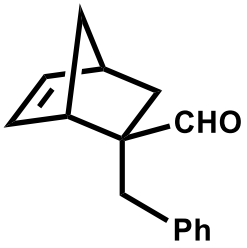

(1S,2S,4S)-2-benzylbicyclo[2.2.1]hept-5-ene-2-carbaldehyde (**178**)

R_f = 0.64 (9/1 Hex/EtOAc) Prepared according to general procedure for Diels-Alder in THF for 24 h and was isolated as an oil in 85% yield as an *Exo*:*Endo* mixture. The physical and spectral data for this compound matched previously reported data.[26] ^{1}H NMR (500 MHz, Chloroform-*d*) δ 9.78 (s, 1H), 7.32 – 7.15 (m, 3H), 7.13 – 7.03 (m, 2H), 6.42 (dd, *J* = 5.7, 3.0 Hz, 1H), 6.28 (dd, *J* = 5.7, 3.0 Hz, 1H), 3.03 – 2.97 (m, 2H), 2.94-2.90 (bs, 1H), 2.74 (d, *J* = 14.2 Hz, 1H), 2.23 (dd, *J* = 12.2, 3.9 Hz, 1H), 1.45 (d, *J* = 8.9, 1H), 1.31 (d, *J* = 9.0, 1H), 1.04 (dd, *J* = 12.1, 2.8 Hz, 1H). ^{13}C NMR (126 MHz, $CDCl_3$) exo: δ 206.10, 140.13, 137.90, 133.28, 129.43, 128.38, 126.42, 59.86, 47.51, 47.31, 42.62, 41.65, 33.09. The diastereoselectivity (*exo:endo* ratio 91:9) determined by ^{1}H NMR integration: δ 9.78 (s, 1H, C*H*O, *exo*), 9.50 (s, 1H, C*H*O, *endo*). Enantioselectivity (ee = 92%) was determine by reducing the aldehyde to the corresponding alcohol using $NaBH_4$: GLC (Astec CHIRALDEX B-DM 30 m × 0.25 mm column, isotherm 147 °C) t_R = *Exo* (minor) 56.1 min. (21.55 Au), *Exo* (major) 57.5 min. (525.46 Au).

[26] T. Kano, Y. Tanaka, K. Osawa, T. Yurino, K. Maruoka, *Chem. Comm*., **2009**, 1956.

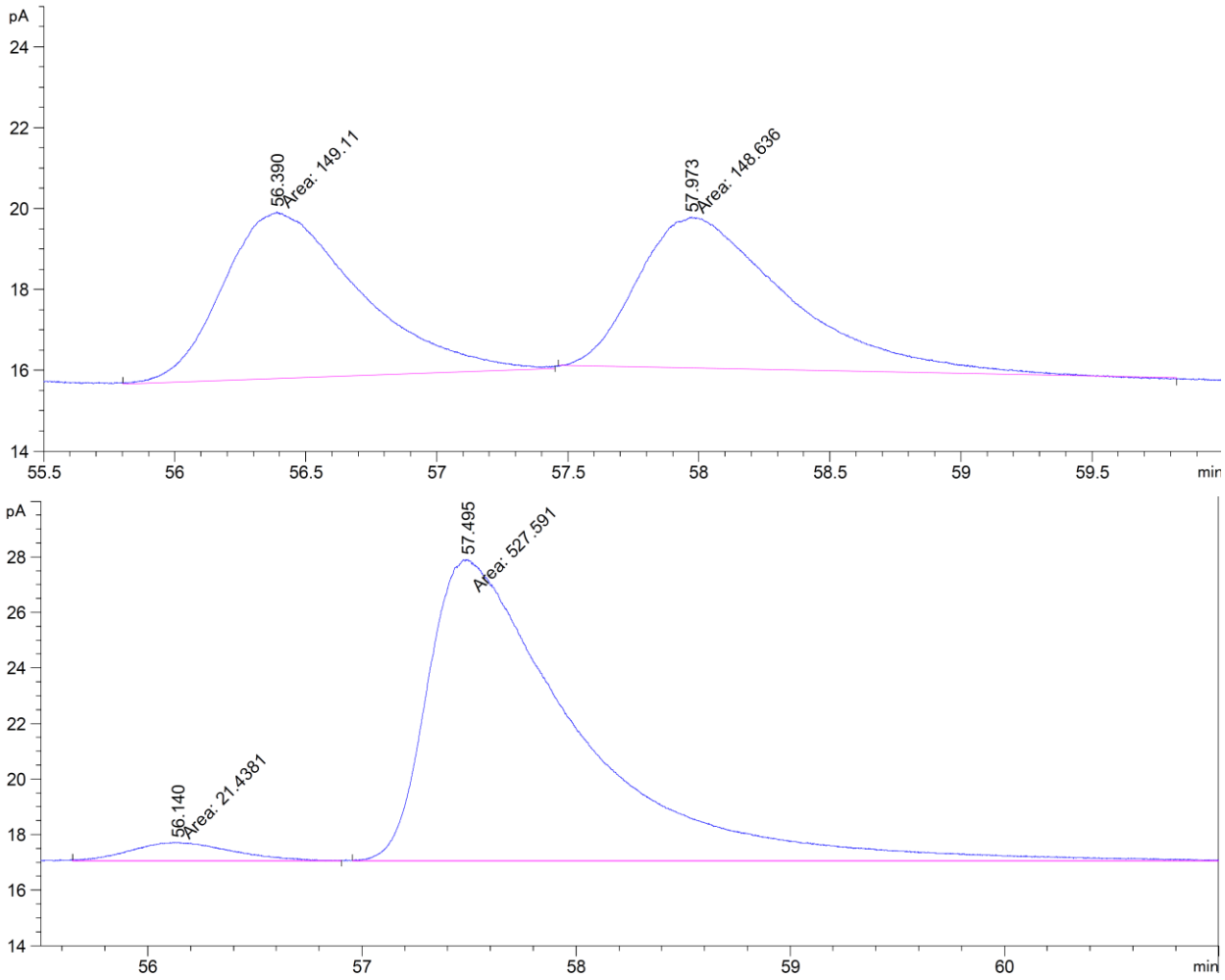

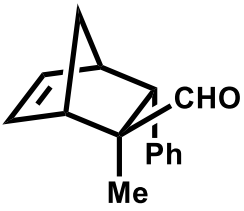

(1S,2S,3R,4R)-2-methyl-3-phenylbicyclo[2.2.1]hept-5-ene-2-carbaldehyde

(**157**)

Prepared according to general procedure for Diels-Alder in CH_3CN for 144 h and was isolated as an oil in 65% yield as an *Exo*:*Endo* mixture. R_f = 0.56 (4/1 Hex/EtOAc). ^{1}H NMR (500 MHz, Chloroform-*d*) *exo:* δ 9.76 (s, 1H), 7.23 (t, *J* = 7.4 Hz, 2H), 7.17 (t, *J* = 7.3 Hz, 1H), 7.11 (d, *J* = 7.3 Hz, 2H), 6.66 (dd, *J* = 5.7, 2.9 Hz, 1H), 6.29 (dd, *J* = 5.7, 3.3 Hz, 1H), 3.94 (d, *J* = 3.0 Hz, 1H), 3.22 (bs, 1H), 2.97 (bs, 1H), 1.62 (d, *J* = 8.8 Hz, 1H), 1.55 (d, *J* = 7.6 Hz, 1H), 0.69 (s, 3H). ^{13}C

NMR (126 MHz, $CDCl_3$) δ 205.02, 140.83, 138.50, 135.22, 129.22, 128.08, 126.26, 58.76, 50.14, 49.59, 48.50 (**C**H2 and **C**HC(H)Ph, assigned based on COSY and HSQC correlations), 17.59. The diastereoselectivity (*exo:endo* ratio 91:9) determined by ^{1}H NMR integration: δ 9.76 (s, 1H, C*H*O, *exo*), 9.55 (s, 1H, C*H*O, *endo*). Enantioselectivity (71% ee) was determined by reducing aldehyde to alcohol with $NaBH_4$ and subsequently forming the benzoate ester of the alcohol and analyzed by HPLC (Chiralcel OD, Hex:*i*-PrOH 99:1, 0.6 mL/min) t_R = 10.0 min (*exo* minor), 13.3 min (*exo* major). HRMS (APCI) of alcohol: calcd for $C_{15}H_{19}O$ [M+H] 215.1430, found 215.1431.

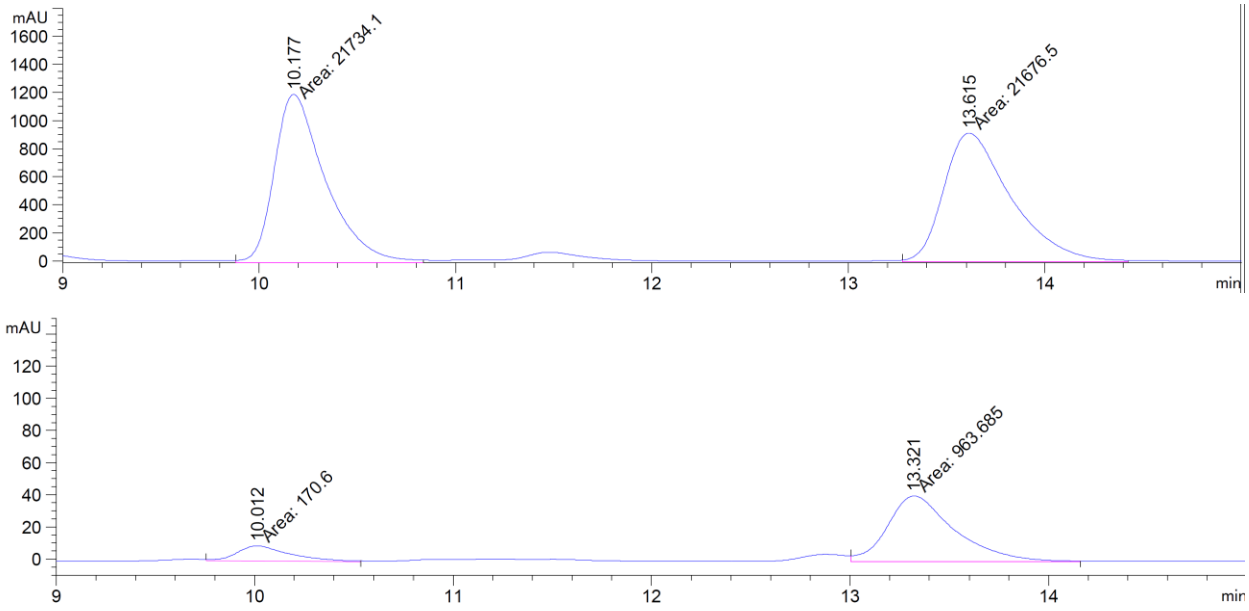

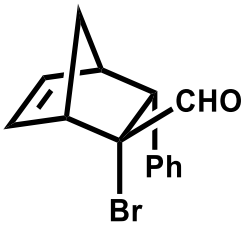

(1S,2R,3R,4R)-2-bromo-3-phenylbicyclo[2.2.1]hept-5-ene-2-carbaldehyde (**176**)

Prepared according to general procedure for Diels-Alder in CH_3CN for 144 h and was isolated as an oil in 77% yield as an *Exo*:*Endo* mixture. R_f = 0.73 (3/1 Hex/EtOAc). NMR (400 MHz, Chloroform-*d*) δ 9.64 (s, 1H), 7.41 – 7.10 (m, 6H), 6.74 (dd, *J* = 5.7, 3.0 Hz, 1H), 6.30 (dd, *J* = 5.7, 3.2 Hz, 1H), 4.06 (d, *J* = 2.8 Hz, 1H), 3.47 (bs, 1H), 3.32 (bs, 1H), 1.81 (dt, *J* = 9.3, 2.0 Hz, 1H), 1.69 – 1.59 (m, 1H). ^{13}C NMR (101 MHz, $CDCl_3$) δ 191.80, 140.26, 138.19, 135.61, 129.68, 127.76, 126.83, 81.24, 51.11, 48.85, 48.28, 47.25. The diastereoselectivity (*exo:endo* ratio 92:8)

determined by ^{1}H NMR integration: δ 9.64 (s, 1H, C*H*O, *exo*), 9.49 (s, 1H, C*H*O, *endo*). Enantioselectivity (72% ee) was determined by reducing aldehyde to alcohol with $NaBH_4$ and subsequently forming the benzoate ester of the alcohol and analyzed by HPLC (Chiralcel OD, Hex:*i*-PrOH 98:2, 1.0 mL/min) t_R = 9.7 min (minor) and 22.3 min (major).

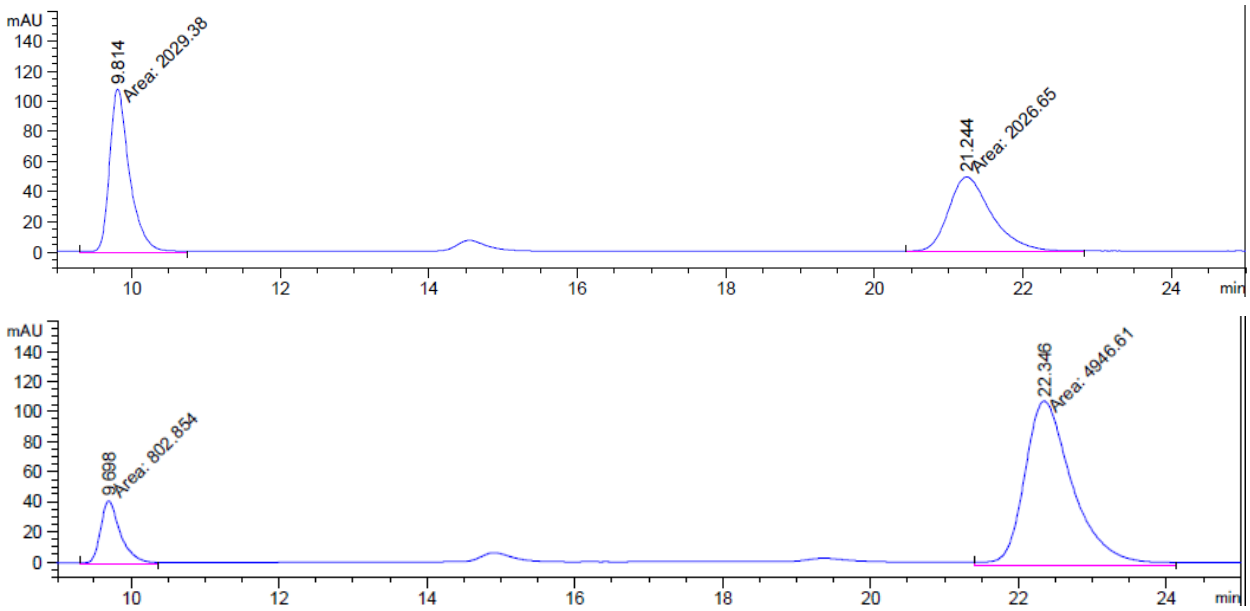

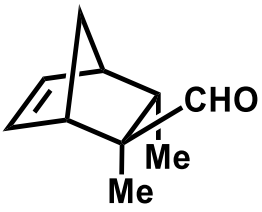

(1S,2R,3S,4R)-2,3-dimethylbicyclo[2.2.1]hept-5-ene-2-carbaldehyde (**173**)

Prepared according to general procedure for Diels-Alder in THF for 24 h and was isolated as an oil in 77% yield as an *Exo*:*Endo* mixture. The physical and spectral data for this compound matched previously reported data.[27] R_f = 0.51 (4/1 Hex/EtOAc). The diastereoselectivity (*exo:endo* ratio 92:8) determined by ^{1}H NMR integration: δ 9.63 (s, 1H, C*H*O, *exo*), 9.38 (s, 1H, C*H*O, *endo*). Enantioselectivity (ee = 75%) was determine by reducing the aldehyde to the corresponding alcohol using $NaBH_4$: GLC (Astec CHIRALDEX B-DM 30 m × 0.25 mm column, isotherm 110 °C) t_R = Exo (major) 16.6 min, Exo (minor) 17.7 min. Absolute configuration (R) was determined

[27] Ishihara, K.; Kurihara, H.; Matsumoto, M.; Yamamoto, H. *J. Am. Chem. Soc.* **1998**, 120, 6920.

by conversion of the alcohol to the (*R*)-Mosher ester and comparing with literature (^{1}H NMR integration (500 MHz, $CDCl_3$): δ 4.34 (d, 1H, major), 4.28 (d, 1H, minor), 4.23 (d, 1H, minor), 4.17 (d, 1H, major).[28]

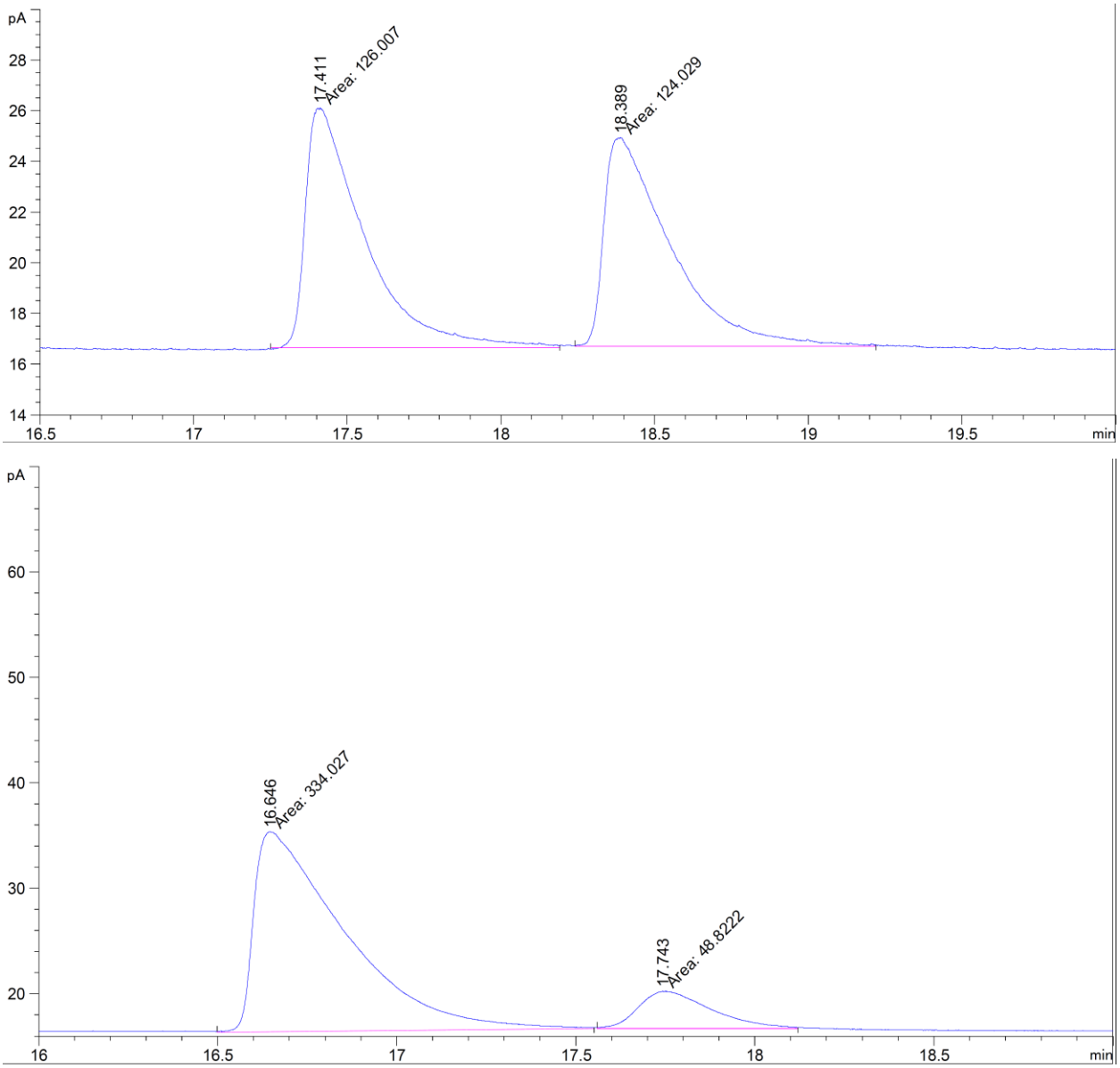

[28] Kubota, K.; Hamblett, C. L.; Wang, X.; Leighton, J. L. *Tetrahedron* **2006**, 62, 11397.

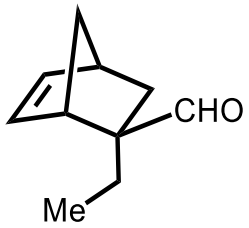

(1S,2R,4S)-2-ethylbicyclo[2.2.1]hept-5-ene-2-carbaldehyde (**303**)

Prepared according to general procedure for Diels-Alder in THF for 24 h and was isolated as an oil in 75% yield as an *Exo*:*Endo* mixture. The physical and spectral data for this compound matched previously reported data.[29] ^{1}H NMR (400 MHz, Chloroform-*d*) δ 9.72 (s, 1H), 6.29 (dd, *J* = 5.7, 3.0 Hz, 1H), 6.10 (dd, *J* = 5.7, 3.1 Hz, 1H), 2.97 (bs, 1H), 2.87 (bs, 1H), 2.16 (dd, *J* = 12.0, 3.9 Hz, 1H), 1.64 – 1.27 (m, 5H), 0.80 (t, *J* = 7.5 Hz, 3H). The diastereoselectivity (*exo:endo* ratio 90:10) determined by ^{1}H NMR integration: δ 9.72 (s, 1H, C*H*O, *exo*), 9.45 (s, 1H, C*H*O, *endo*). Enantioselectivity (ee = 71%) was determine by reducing the aldehyde to the corresponding alcohol using $NaBH_4$: GLC (Astec CHIRALDEX B-DM 30 m × 0.25 mm column, isotherm 97 °C) t_R = Exo (major) 33.3 min, Exo (minor) 34.0 min. (*endo* at 29.8 and 31.2 min)

[29] Sprott, K. T.; Corey, E. J.; *Org. Lett.* **2003**, 2465.

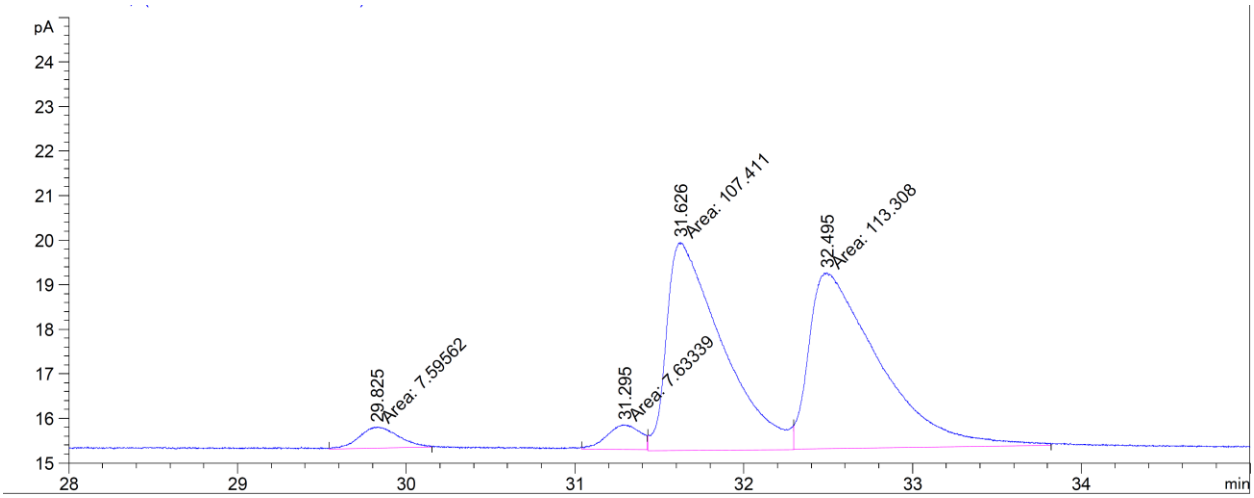

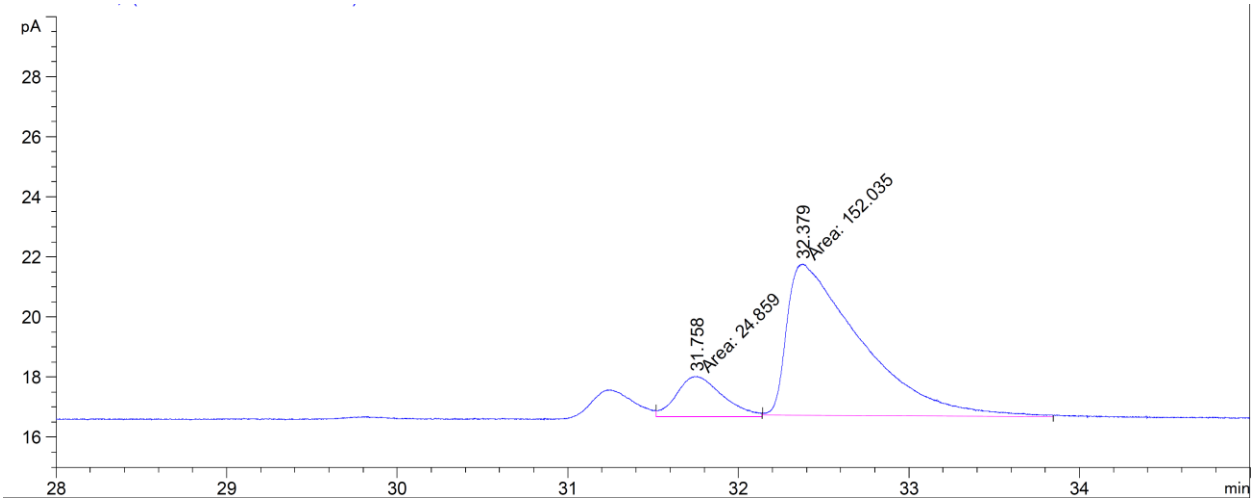

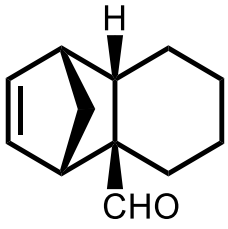

(1R,4S,4aS,8aS)-1,5,6,7,8,8a-hexahydro-1,4-methanonaphthalene-4a(4H)-carbaldehyde (**304**)

Prepared according to general procedure for Diels-Alder in EtOH for 72 h (73% conversion vs mesitylene) and was isolated as an oil in 69% yield as an *Exo*:*Endo* mixture. The physical and spectral data for this compound matched previously reported data.[30] ^{1}H NMR (500 MHz, Chloroform-*d*) δ 9.66 (s, 1H), 6.29 (dd, *J* = 5.7, 3.0 Hz, 1H), 6.19 (dd, *J* = 5.7, 3.2 Hz, 1H), 2.87 – 2.79 (m, 2H), 2.45 (ddd, *J* = 12.9, 5.5, 3.5 Hz, 1H), 1.79 (ddd, *J* = 13.8, 5.8, 1.5 Hz, 1H), 1.60 – 1.48 (m, 3H), 1.37 (dt, *J* = 8.5,

[30] Hayashi, Y.; Rohde, J. J.; Corey, E. J.; *J. Am. Chem. Soc.,* **1996** 5503

1.8 Hz, 1H), 1.31 – 1.16 (m, 3H), 1.11 (td, J = 13.5, 6.3 Hz, 1H), 0.72 (qd, J = 13.1, 4.1 Hz, 1H). ^{13}C NMR (126 MHz, $CDCl_3$) δ 206.42, 138.16, 134.52, 57.57, 48.54, 46.86, 46.05, 39.54, 24.86, 24.35, 19.85, 18.07. The diastereoselectivity (*exo:endo* ratio 72:28) determined by ^{1}H NMR integration: δ 9.66 (s, 1H, C*H*O, *exo*), 9.50 (s, 1H, C*H*O, *endo*). Enantioselectivity (ee = 72%) was determine by reducing the aldehyde to the corresponding alcohol using $NaBH_4$: GLC (Astec CHIRALDEX B-DM 30 m × 0.25 mm column, isotherm 120 °C) t_R = Exo (minor) 50.2 min, Exo (major) 52.0 min.

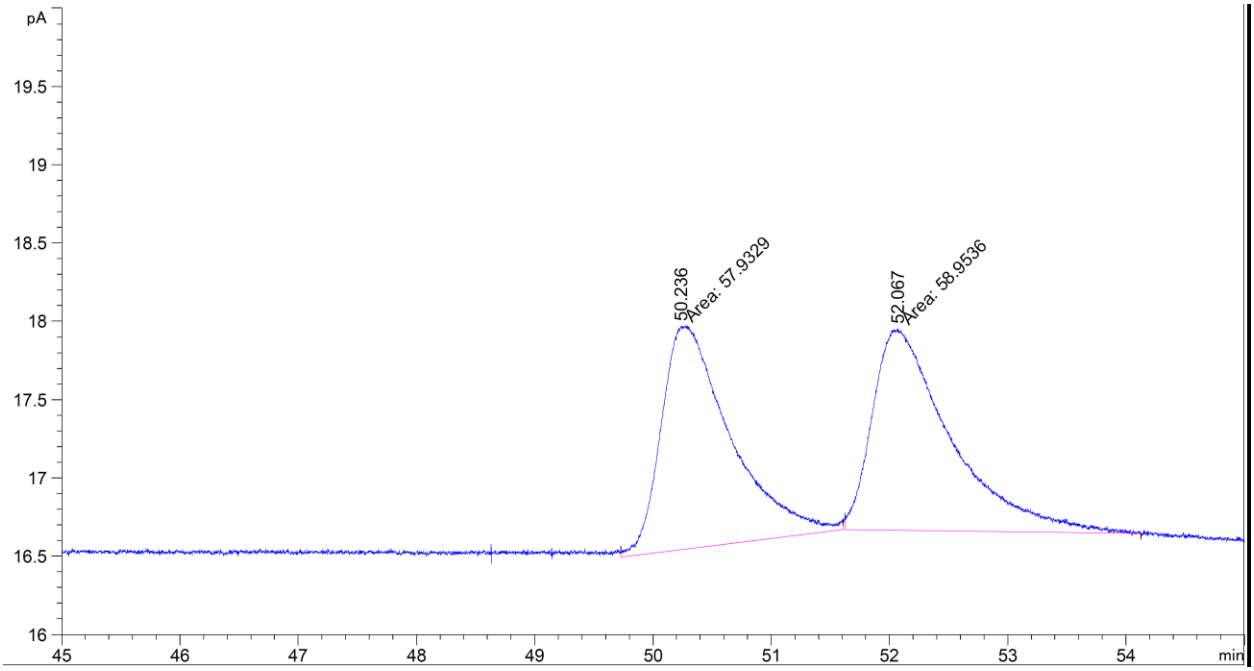

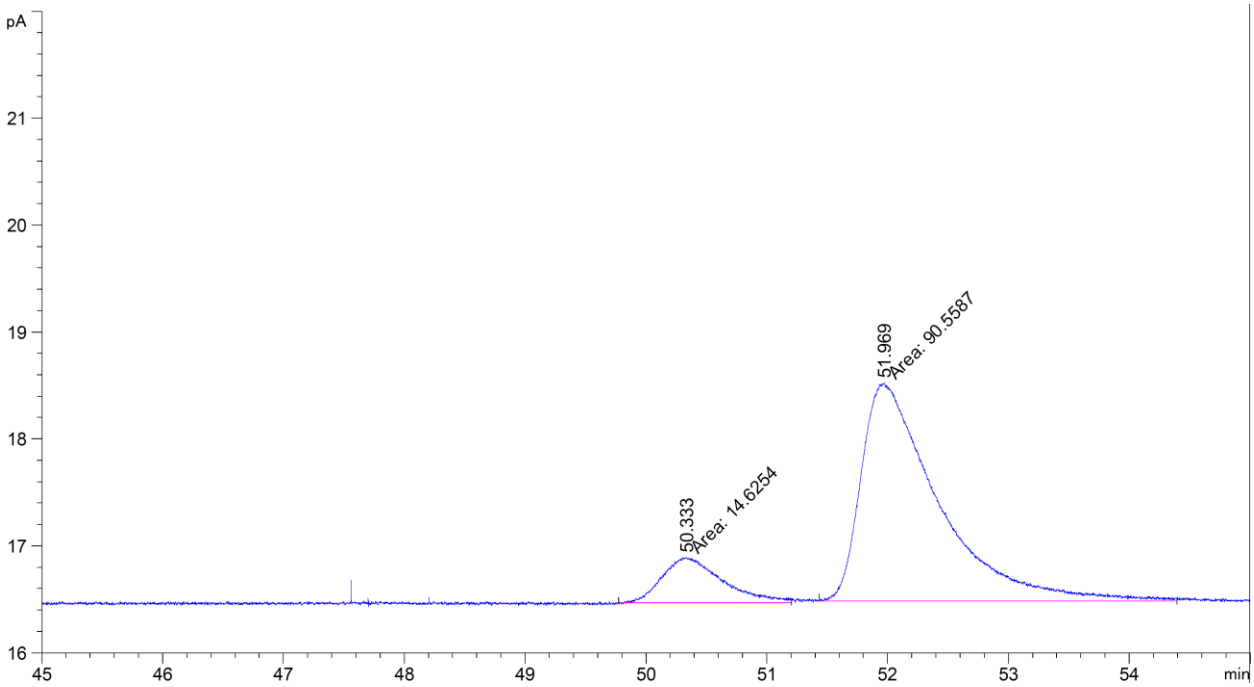

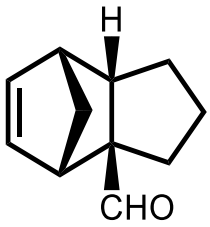

(3aS,4S,7R,7aS)-1,2,3,4,7,7a-hexahydro-3aH-4,7-methanoindene-3a-carbaldehyde (**305**)

Prepared according to general procedure for Diels-Alder in THF for 24 h and was isolated as an oil in 81% yield as an *Exo*:*Endo* mixture. The physical and spectral data for this compound matched previously reported data.[31] ^{1}H NMR (500 MHz, Chloroform-*d*) δ 9.75 (s, 0.76H), 6.32 (dd, *J* = 5.8, 2.9 Hz, 0.76H), 6.28 – 6.15 (m, 1.4H), 2.97 (s, 0.76H), 2.94 – 2.81 (m, 1.5H), 1.98 – 1.52 (m, 7H), 1.36 – 1.09 (m, 3H). The diastereoselectivity (*exo:endo* ratio 72:28) determined by ^{1}H NMR integration: δ 9.75 (s, 1H, C*H*O, *exo*), 9.46 (s, 1H, C*H*O, *endo*). Enantioselectivity was determined by reduction with $NaBH_4$ to the corresponding alcohol, conversion to the (R)-MTPA ester derivative and 1H NMR integration (500 MHz, $CDCl_3$): δ 2.69 (bs, 1H, minor), 2.64 (bs, 1H, major).

[31] Ryu, D. H.; Lee, T. W.; Corey, E. J.; *J. Am. Chem. Soc.* **2002**, 9992.

5.6 Spectra (^{1}H and ^{13}C NMR)

5.6.1 Urea Project

112

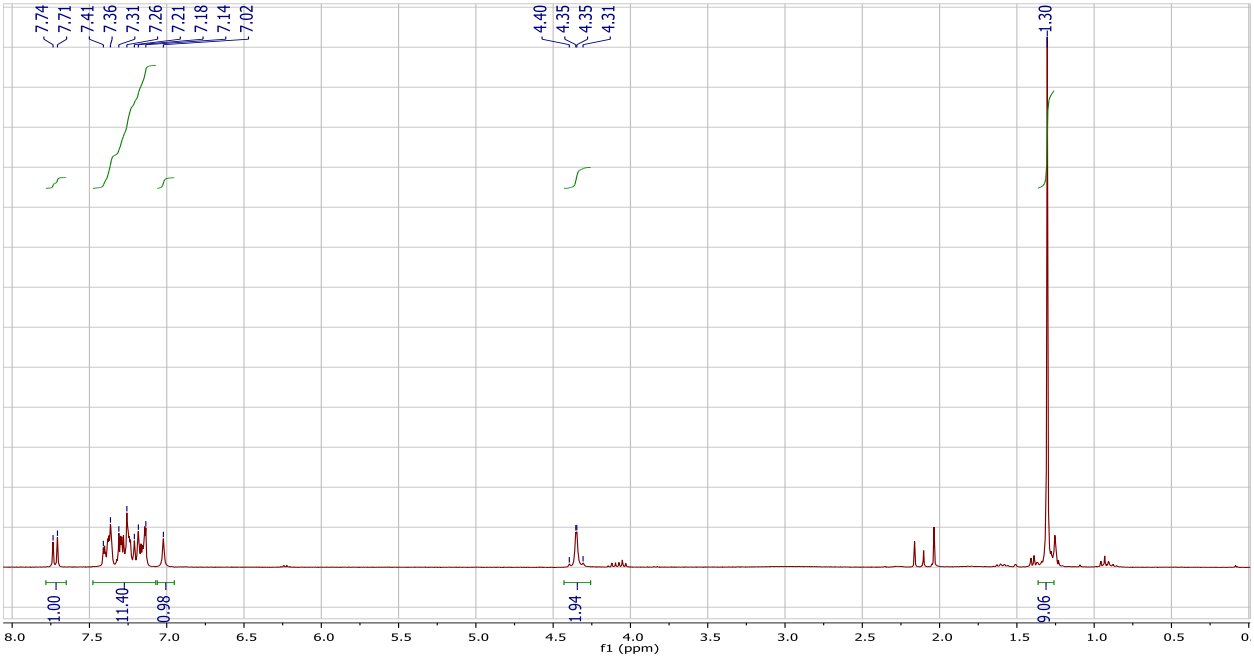

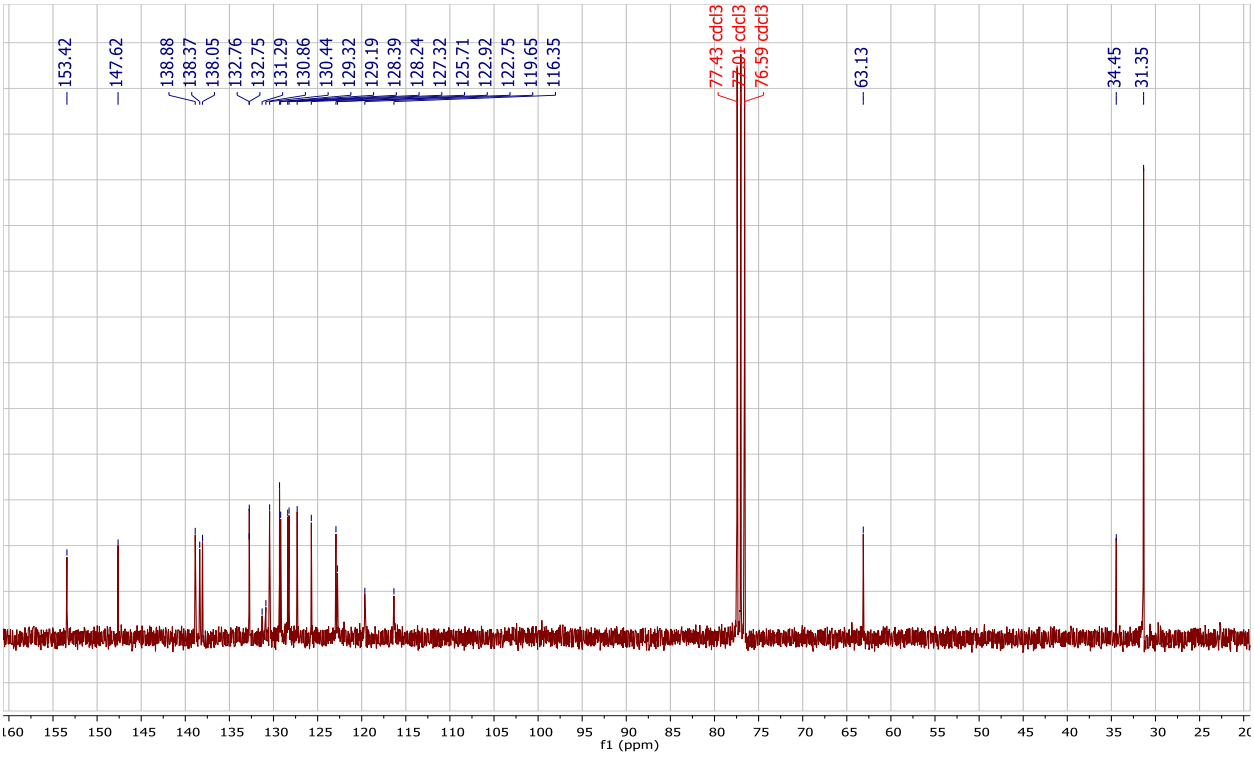

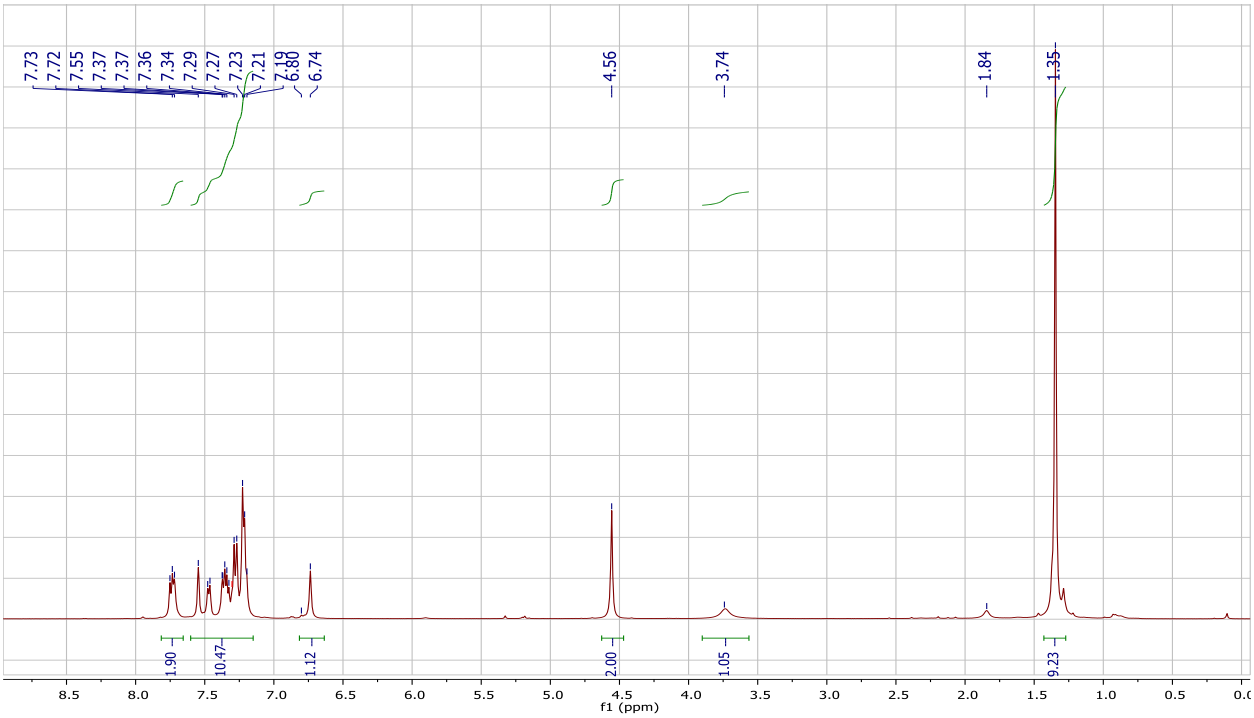
7.73
7.72
7.55
7.37
7.37
7.36
7.34
7.29
7.27
7.23
7.21
7.19
6.80
6.74
4.56
3.74
1.84
1.35
1.90
10.47
1.12
2.00
1.05
9.23
f1 (ppm)

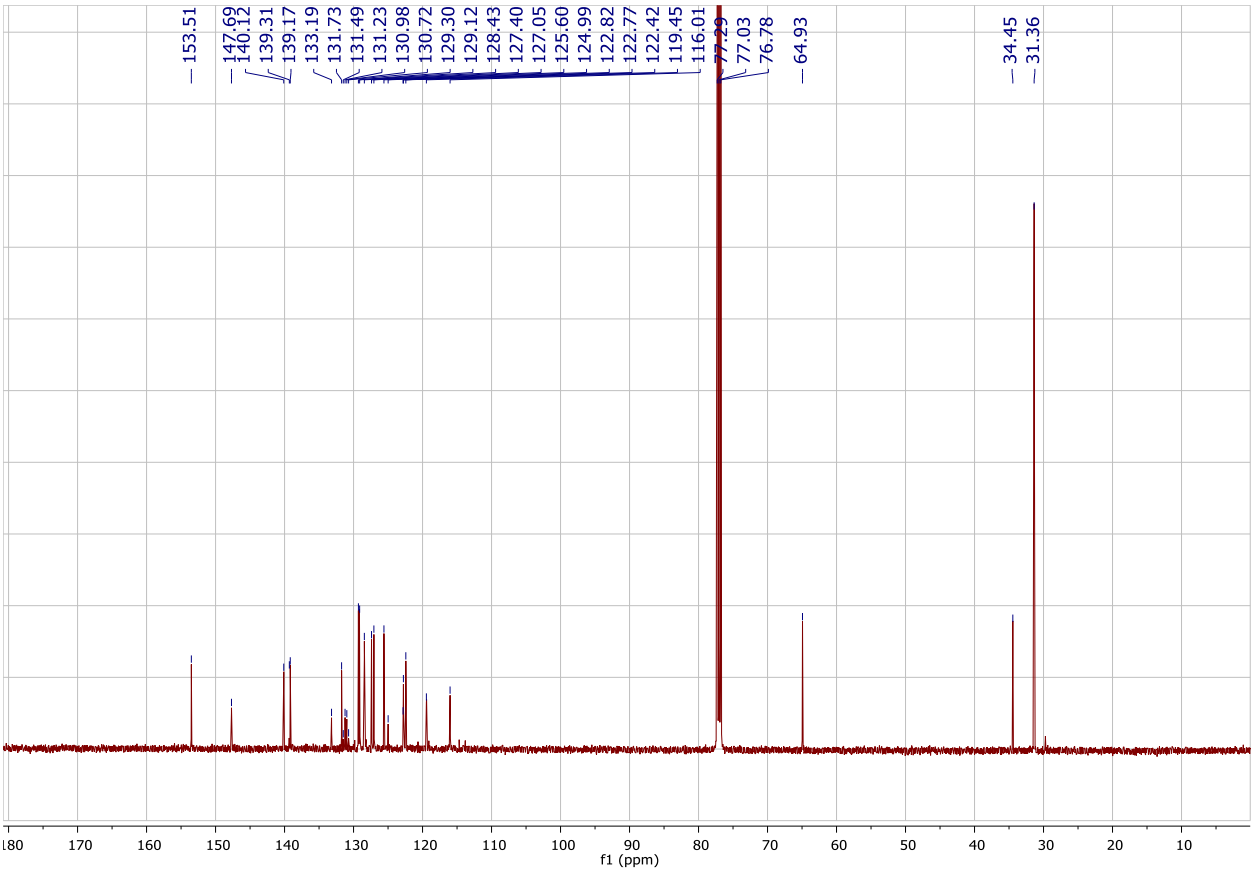
153.51
147.69
140.12
139.31
139.17
133.19
131.73
131.49
131.23
130.98
130.72
129.30
129.12
128.43
127.40
127.05
125.60
124.99
122.82
122.77
122.42
119.45
116.01
77.29
77.03
76.78
64.93
34.45
31.36
f1 (ppm)

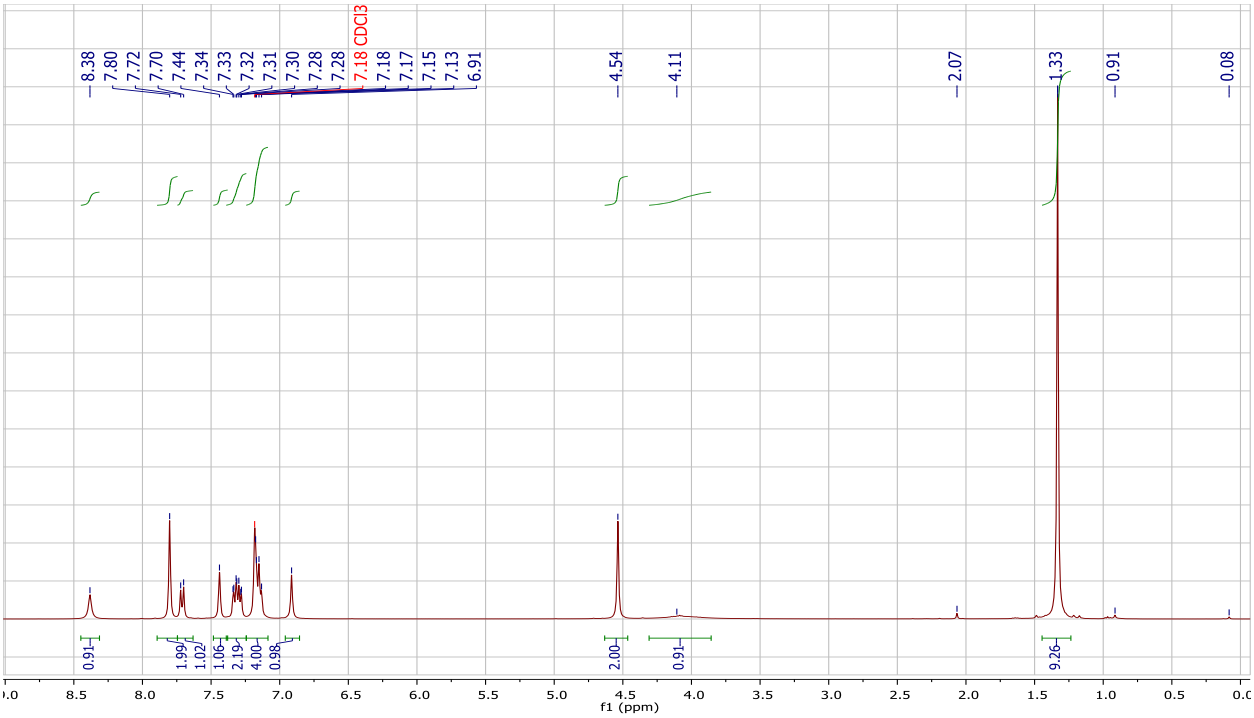
8.38
7.80
7.72
7.70
7.44
7.34
7.33
7.32
7.31
7.30
7.28
7.28
7.18 CDCl3
7.18
7.17
7.15
7.13
6.91
4.54
4.11
2.07
1.33
0.91
0.08
0.91
1.99
1.02
1.06
2.19
4.00
0.98
2.00
0.91
9.26
f1 (ppm)

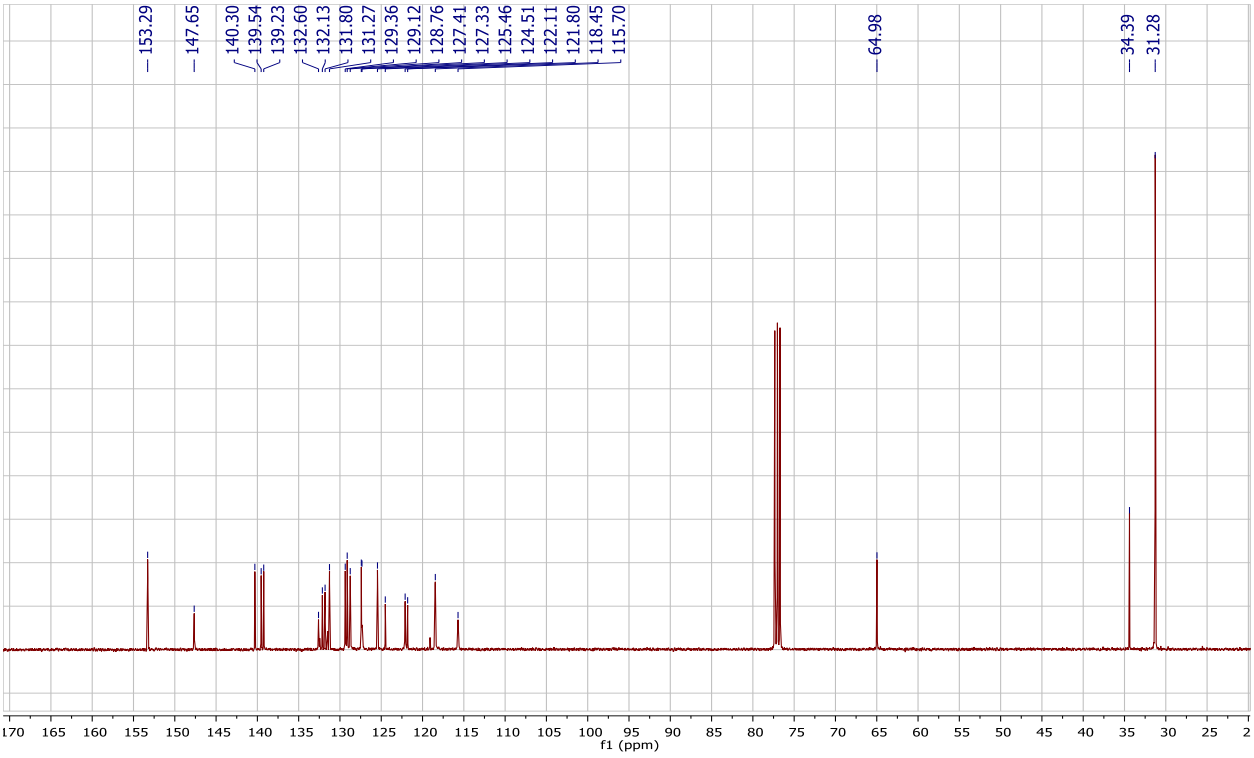
153.29
147.65
140.30
139.54
139.23
132.60
132.13
131.80
131.27
129.36
129.12
128.76
127.41
127.33
125.46
124.51
122.11
121.80
118.45
115.70
64.98
34.39
31.28
f1 (ppm)

117

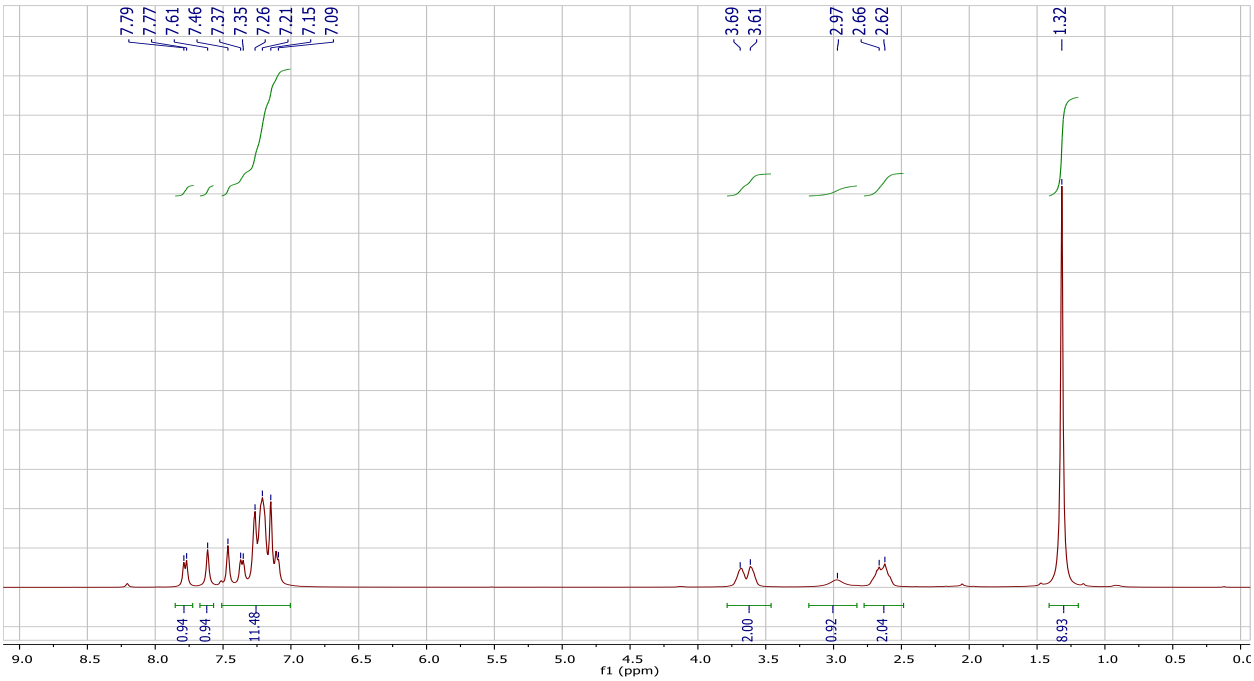
7.79
7.77
7.61
7.46
7.37
7.35
7.26
7.21
7.15
7.09
3.69
3.61
2.97
2.66
2.62
1.32
0.94
0.94
11.48
2.00
0.92
2.04
8.93
f1 (ppm)

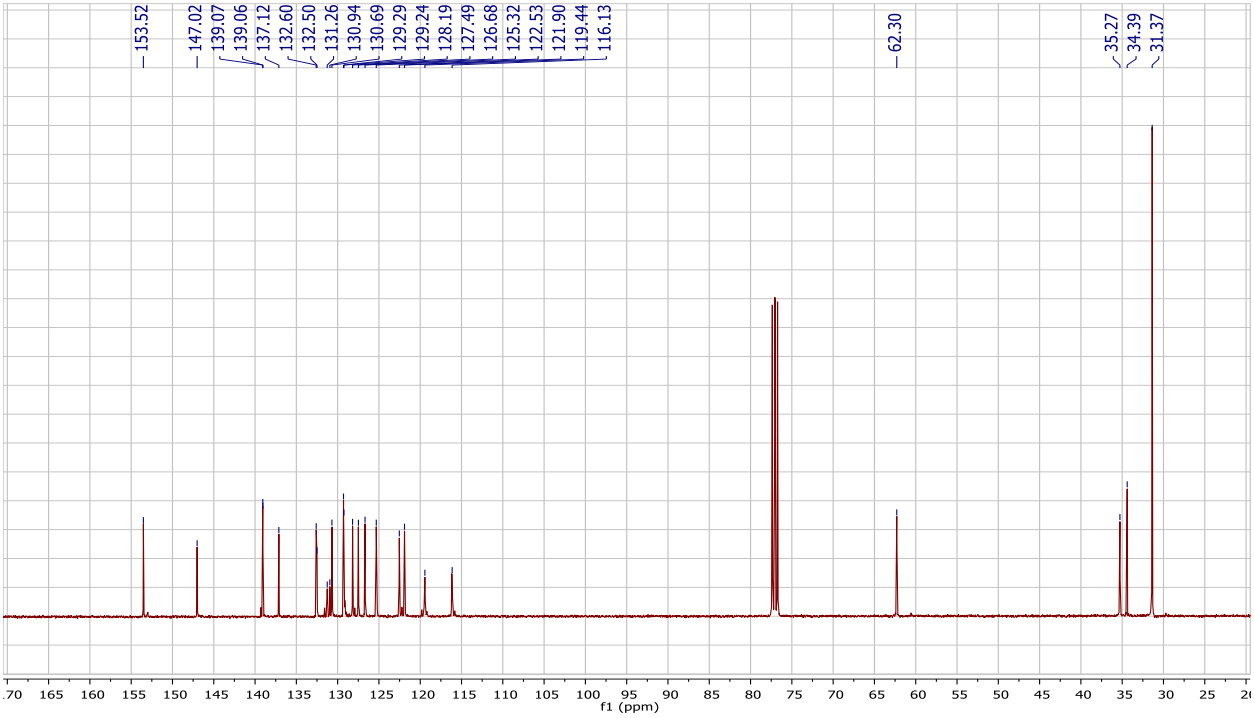
153.52
147.02
139.07
139.06
137.12
132.60
132.50
131.26
130.94
130.69
129.29
129.24
128.19
127.49
126.68
125.32
122.53
121.90
119.44
116.13
62.30
35.27
34.39
31.37
f1 (ppm)

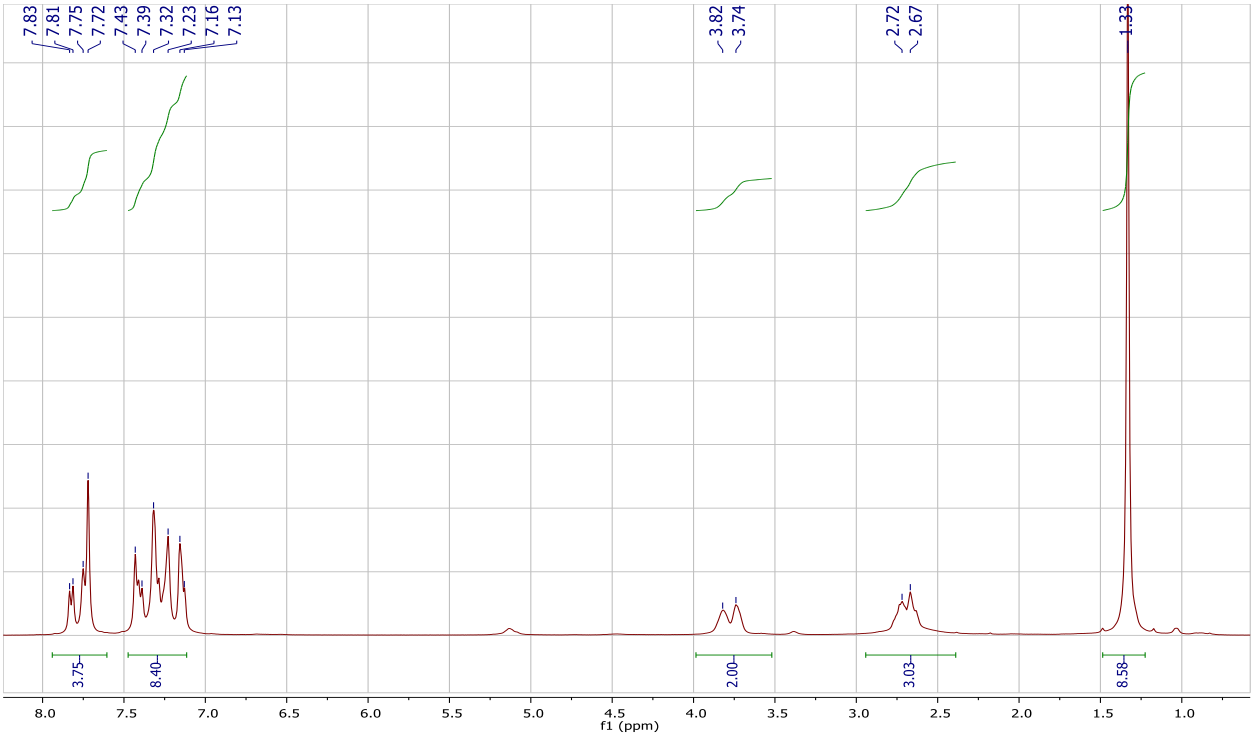
7.83
7.81
7.75
7.72
7.43
7.39
7.32
7.23
7.16
7.13
3.82
3.74
2.72
2.67
1.33
3.75
8.40
2.00
3.03
8.58
f1 (ppm)

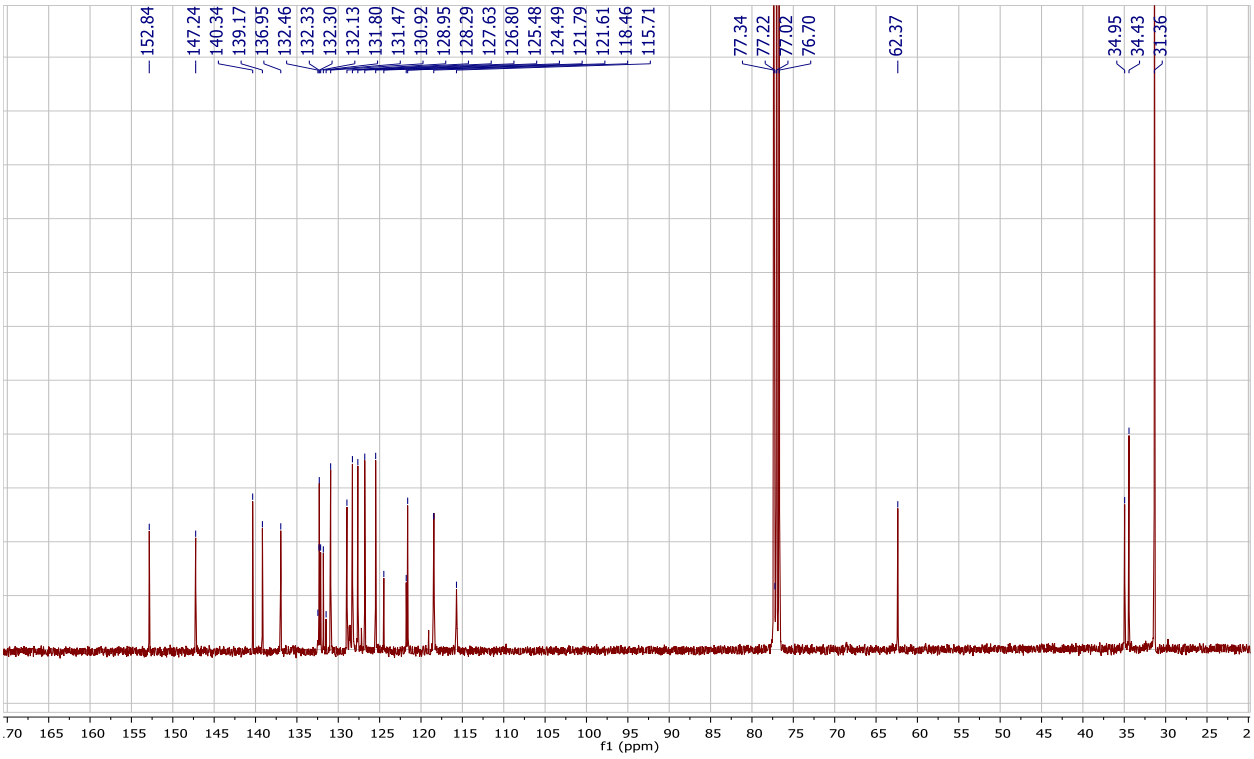
152.84
147.24
140.34
139.17
136.95
132.46
132.33
132.30
132.13
131.80
131.47
130.92
128.95
128.29
127.63
126.80
125.48
124.49
121.79
121.61
118.46
115.71
77.34
77.22
77.02
76.70
62.37
34.95
34.43
31.36
f1 (ppm)

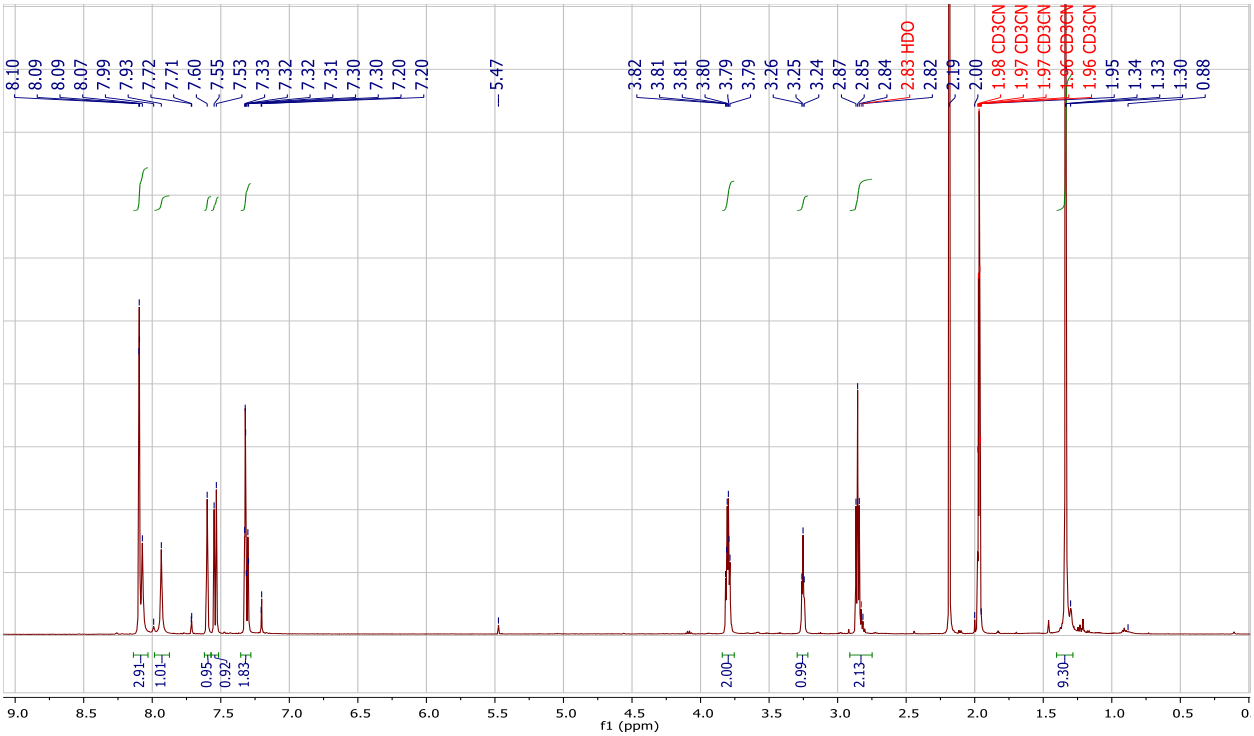
8.10
8.09
8.09
8.07
7.99
7.93
7.72
7.71
7.60
7.55
7.53
7.33
7.32
7.32
7.31
7.30
7.30
7.20
7.20
5.47
3.82
3.81
3.81
3.80
3.79
3.79
3.26
3.25
3.24
2.87
2.85
2.84
2.83 HDO
2.82
2.19
2.00
1.98 CD3CN
1.97 CD3CN
1.97 CD3CN
1.96 CD3CN
1.96 CD3CN
1.95
1.34
1.33
1.30
0.88
2.91
1.01
0.95
0.92
1.83
2.00
0.99
2.13
9.30
f1 (ppm)

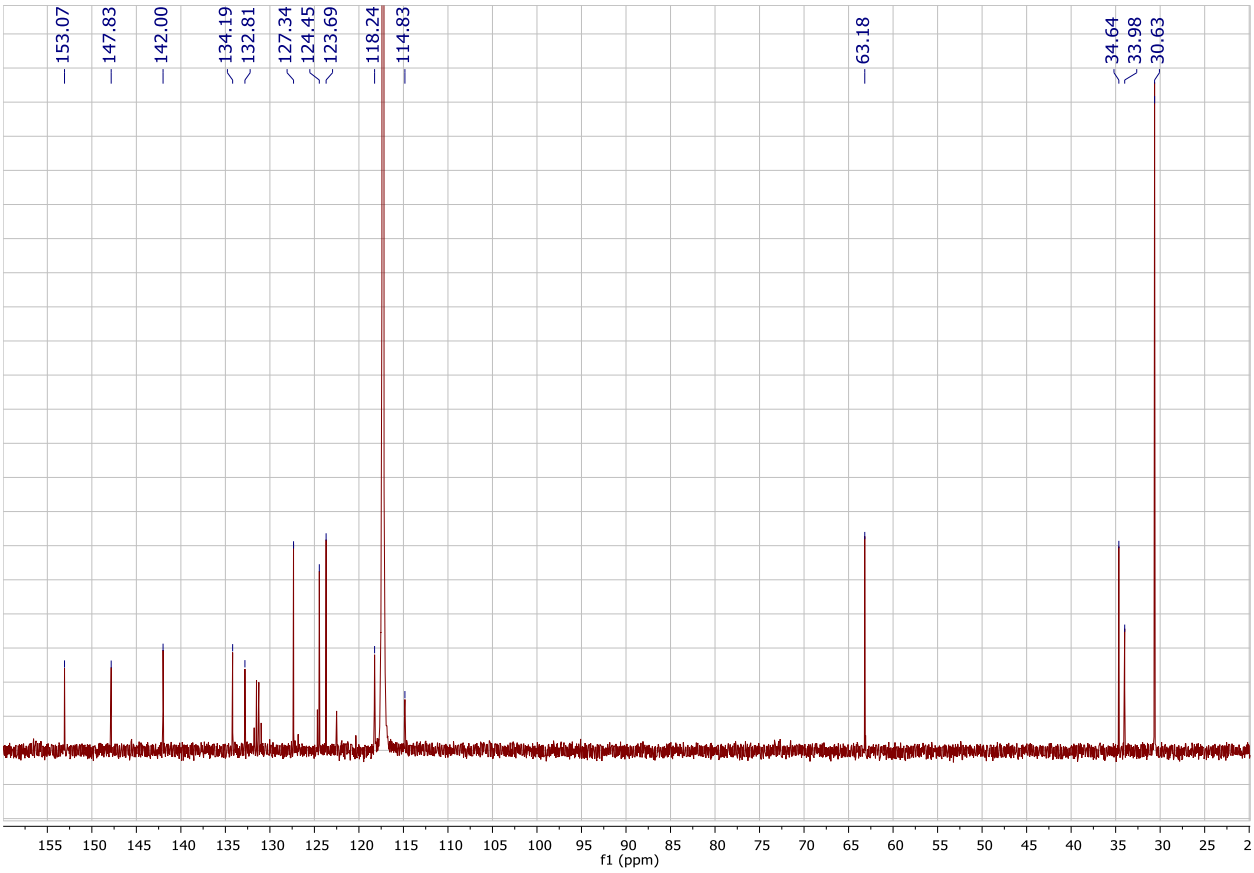
153.07
147.83
142.00
134.19
132.81
127.34
124.45
123.69
118.24
114.83
63.18
34.64
33.98
30.63
f1 (ppm)

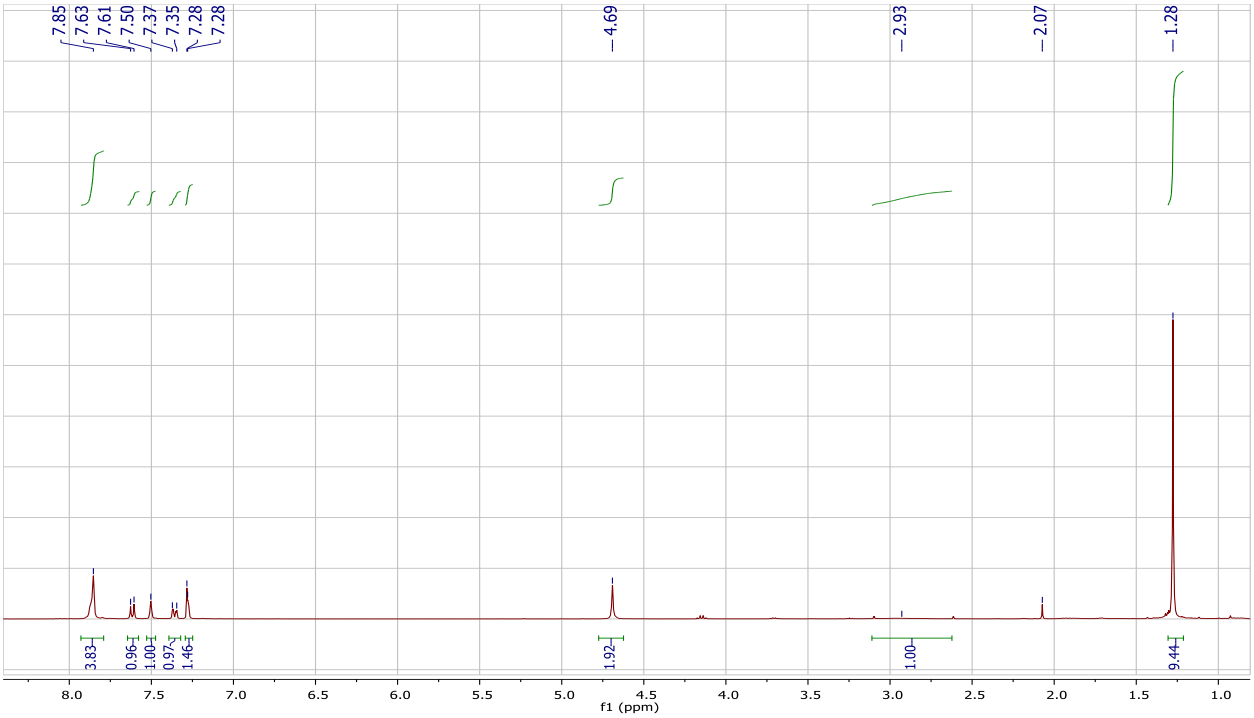
7.85
7.63
7.61
7.50
7.37
7.35
7.28
7.28
4.69
2.93
2.07
1.28
3.83
0.96
1.00
0.97
1.46
1.92
1.00
9.44
f1 (ppm)

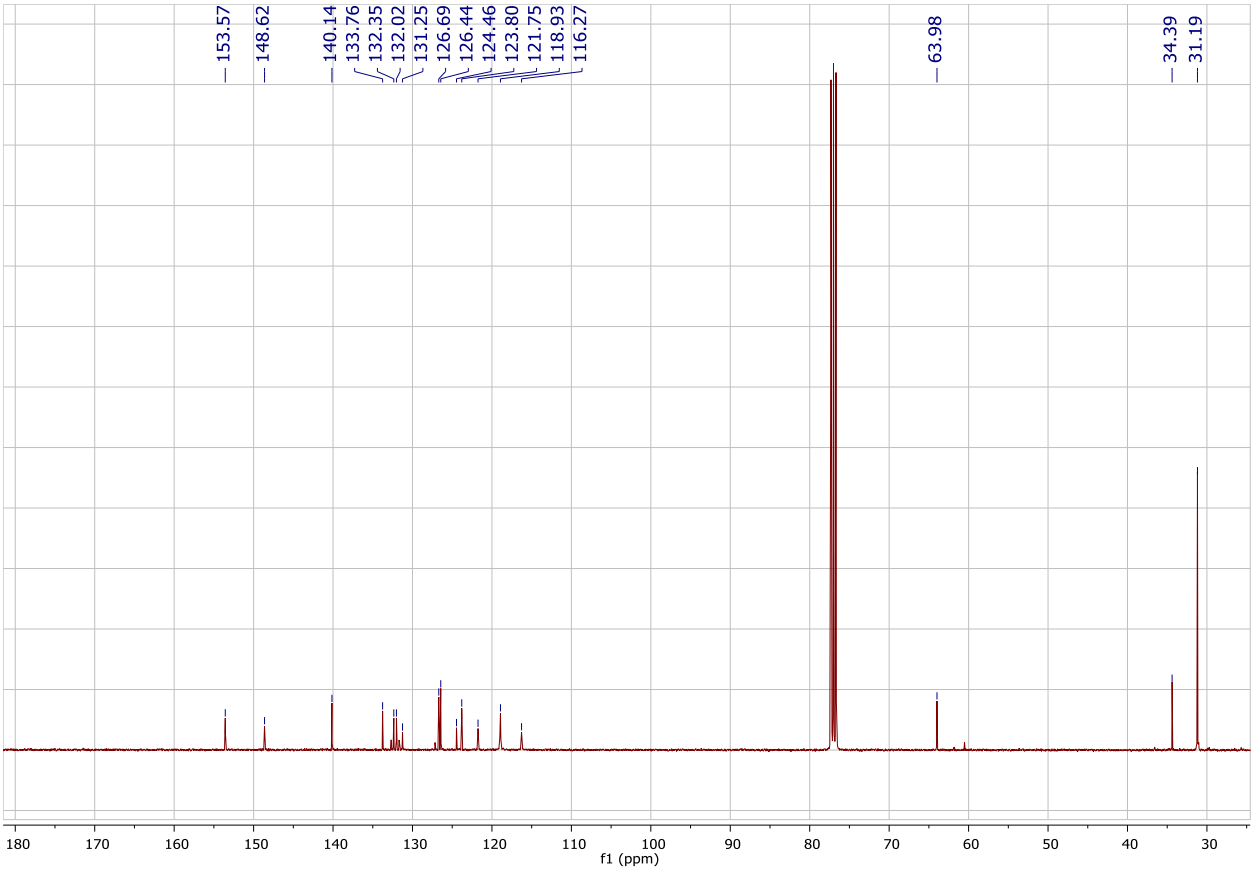
153.57
148.62
140.14
133.76
132.35
132.02
131.25
126.69
126.44
124.46
123.80
121.75
118.93
116.27
63.98
34.39
31.19
f1 (ppm)

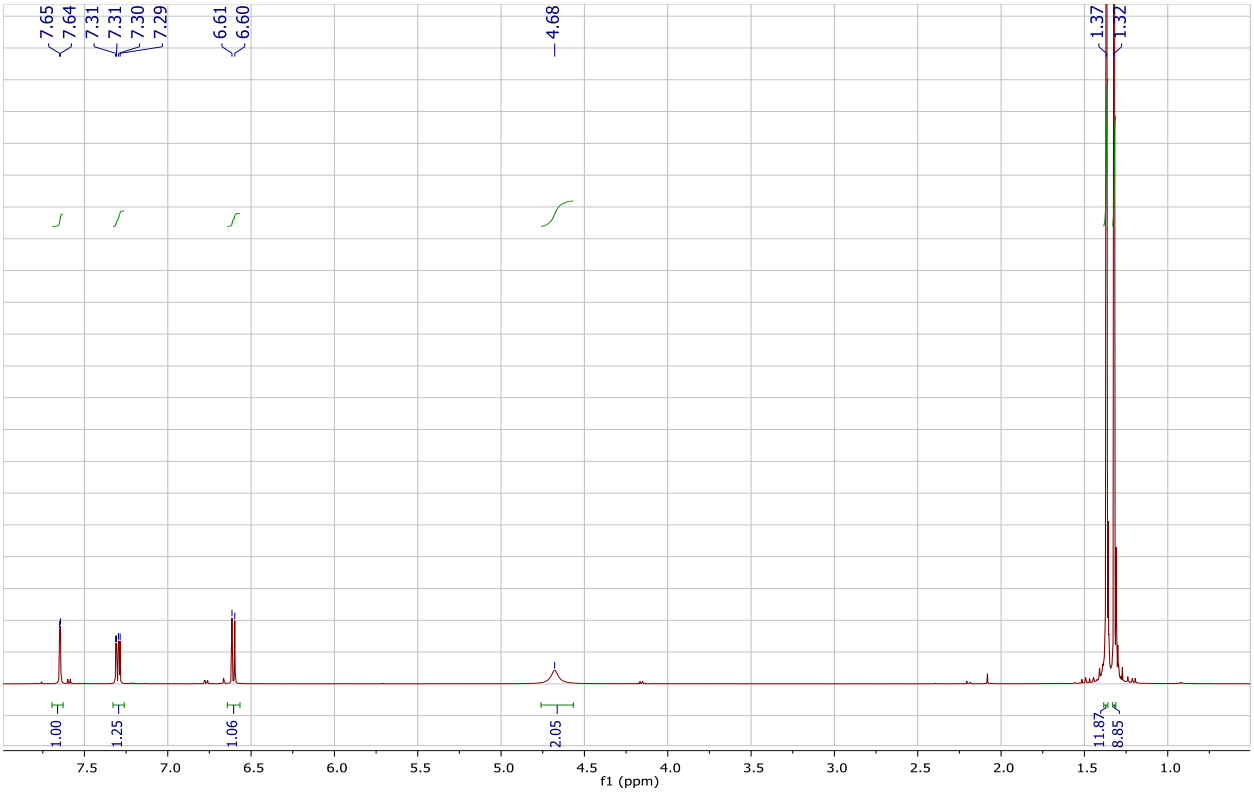
7.65
7.64
7.31
7.31
7.30
7.29
6.61
6.60
4.68
1.37
1.32
1.00
1.25
1.06
2.05
11.87
8.85
f1 (ppm)

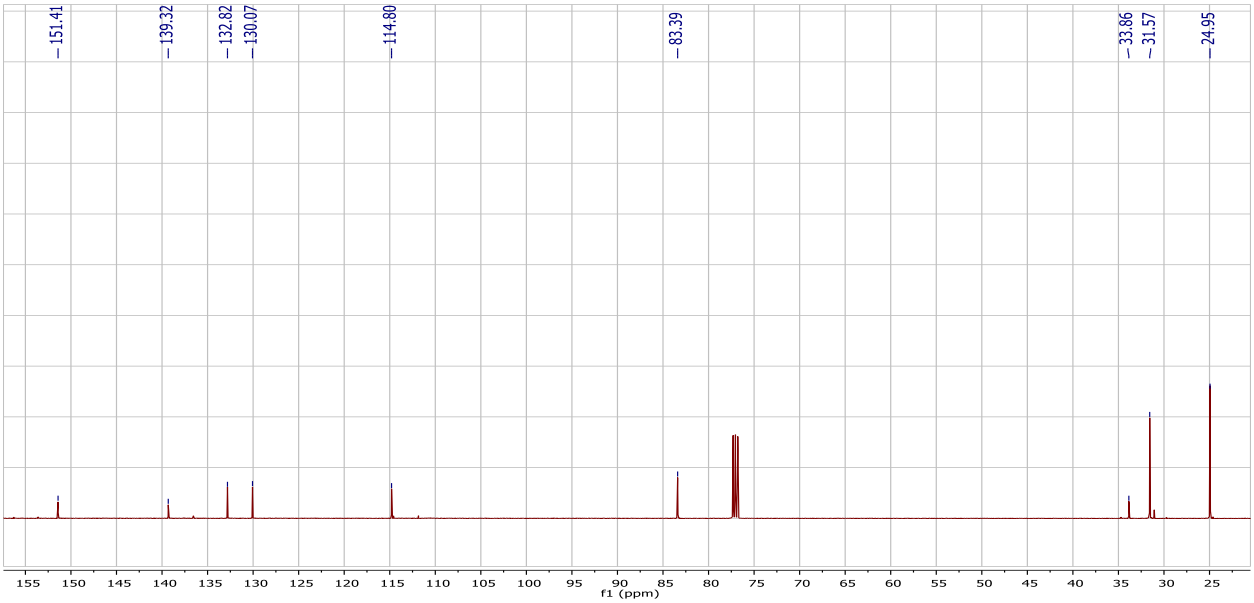
151.41
139.32
132.82
130.07
114.80
83.39
33.86
31.57
24.95
f1 (ppm)

128

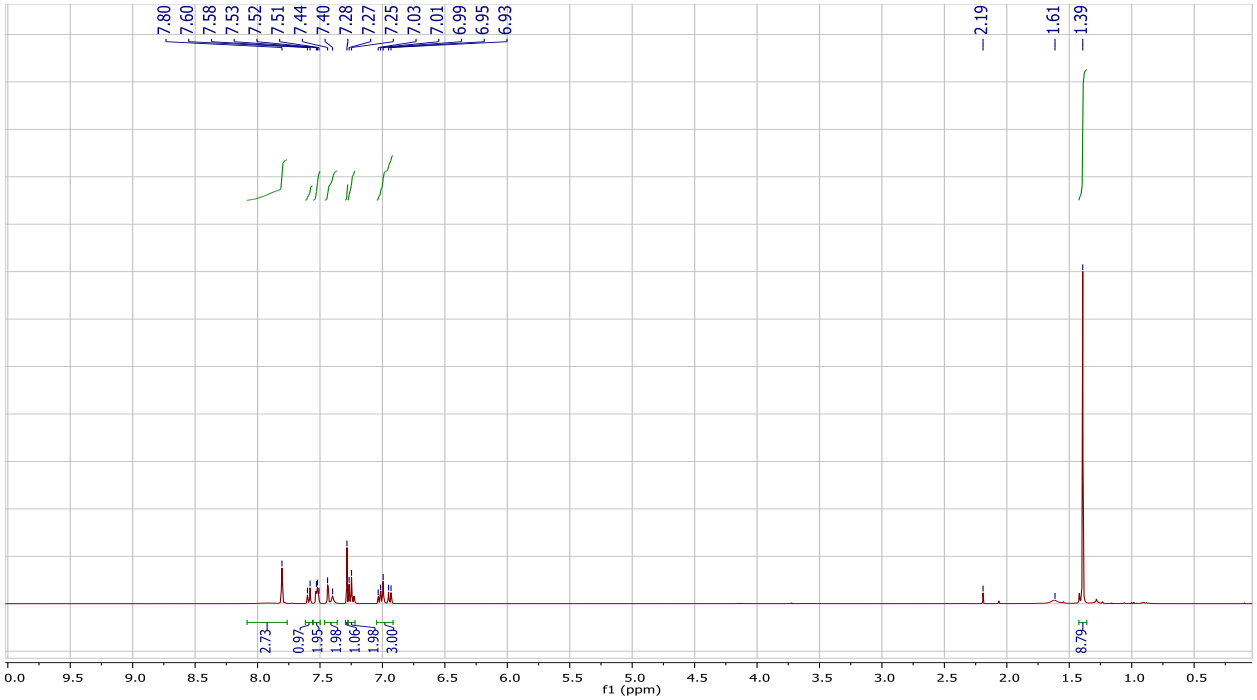
7.80
7.60
7.58
7.53
7.52
7.51
7.44
7.40
7.28
7.27
7.25
7.03
7.01
6.99
6.95
6.93
2.19
1.61
1.39
2.73
0.97
1.95
1.98
1.06
1.98
3.00
8.79
f1 (ppm)

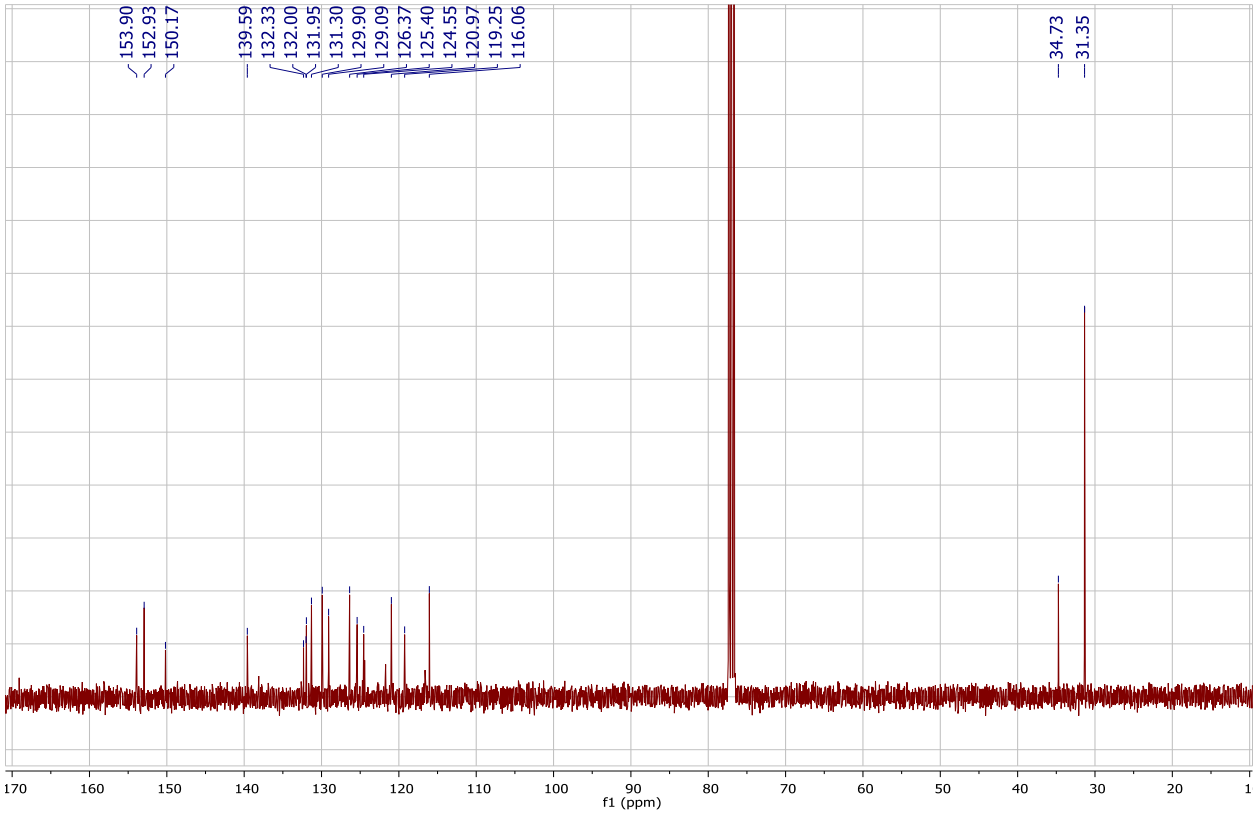
153.90
152.93
150.17
139.59
132.33
132.00
131.95
131.30
129.90
129.09
126.37
125.40
124.55
120.97
119.25
116.06
34.73
31.35
f1 (ppm)

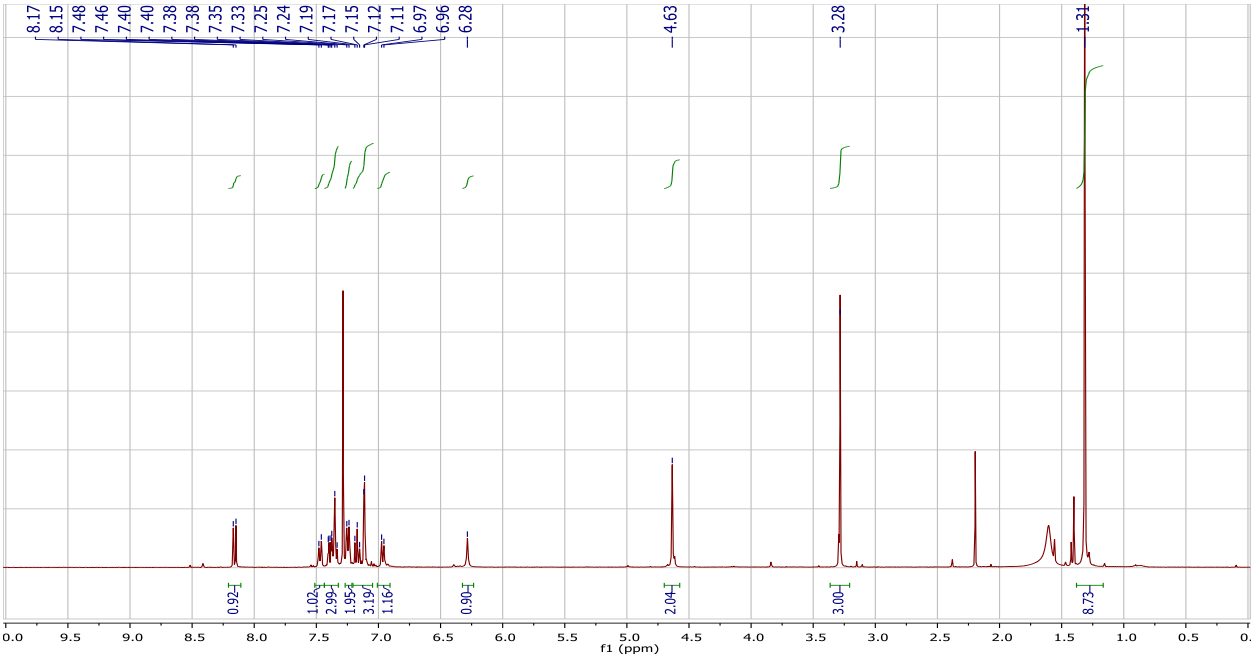
8.17
8.15
7.48
7.46
7.40
7.40
7.38
7.38
7.35
7.33
7.25
7.24
7.19
7.17
7.15
7.12
7.11
6.97
6.96
6.28
4.63
3.28
1.31
0.92
1.02
2.99
1.95
3.19
1.16
0.90
2.04
3.00
8.73
f1 (ppm)

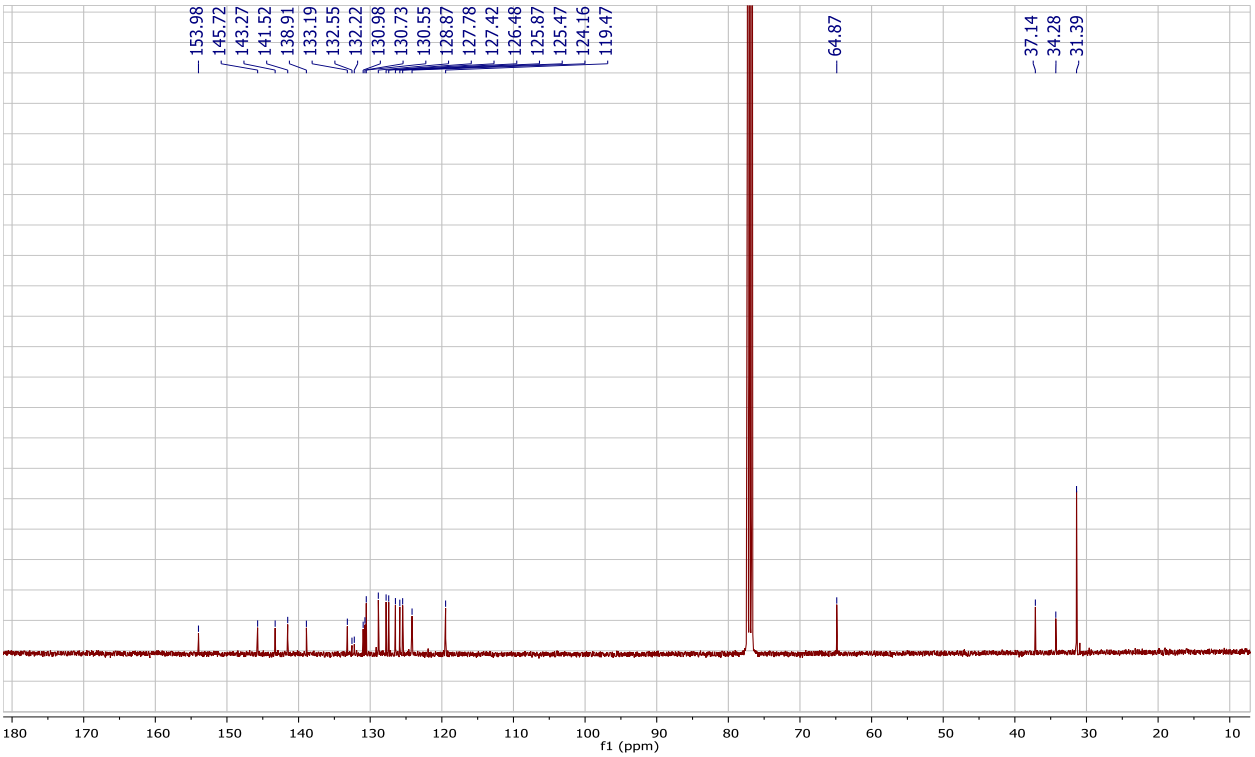
153.98
145.72
143.27
141.52
138.91
133.19
132.55
132.22
130.98
130.73
130.55
128.87
127.78
127.42
126.48
125.87
125.47
124.16
119.47
64.87
37.14
34.28
31.39
f1 (ppm)

135

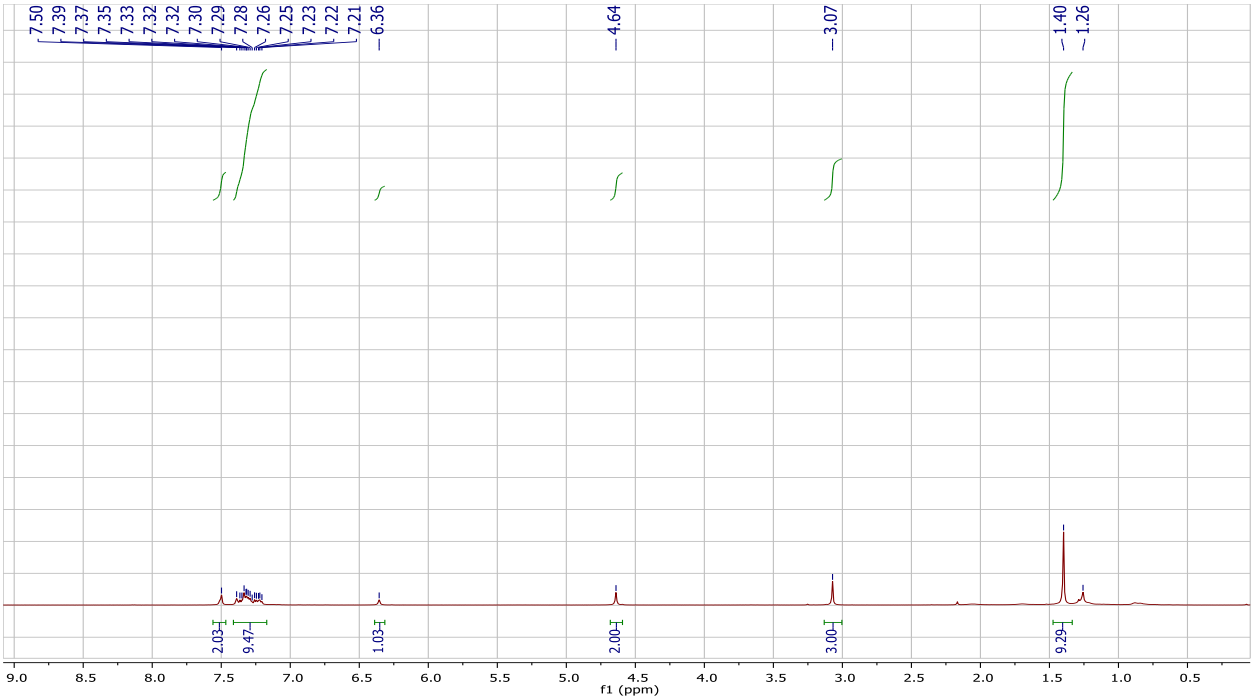
7.50
7.39
7.37
7.35
7.33
7.32
7.32
7.30
7.29
7.28
7.26
7.25
7.23
7.22
7.21
6.36
4.64
3.07
1.40
1.26
2.03
9.47
1.03
2.00
3.00
9.29
f1 (ppm)

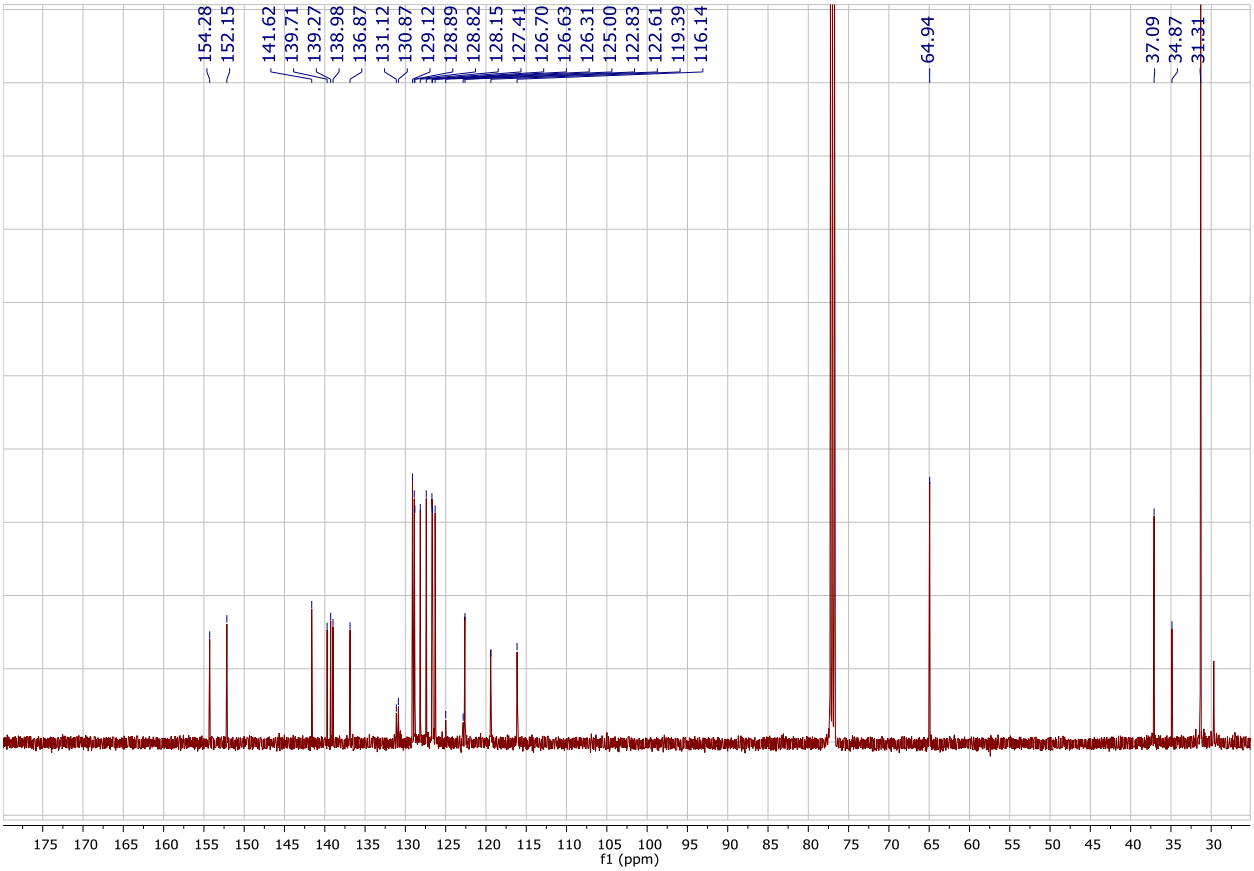
154.28
152.15
141.62
139.71
139.27
138.98
136.87
131.12
130.87
129.12
128.89
128.82
128.15
127.41
126.70
126.63
126.31
125.00
122.83
122.61
119.39
116.14
64.94
37.09
34.87
31.31
f1 (ppm)

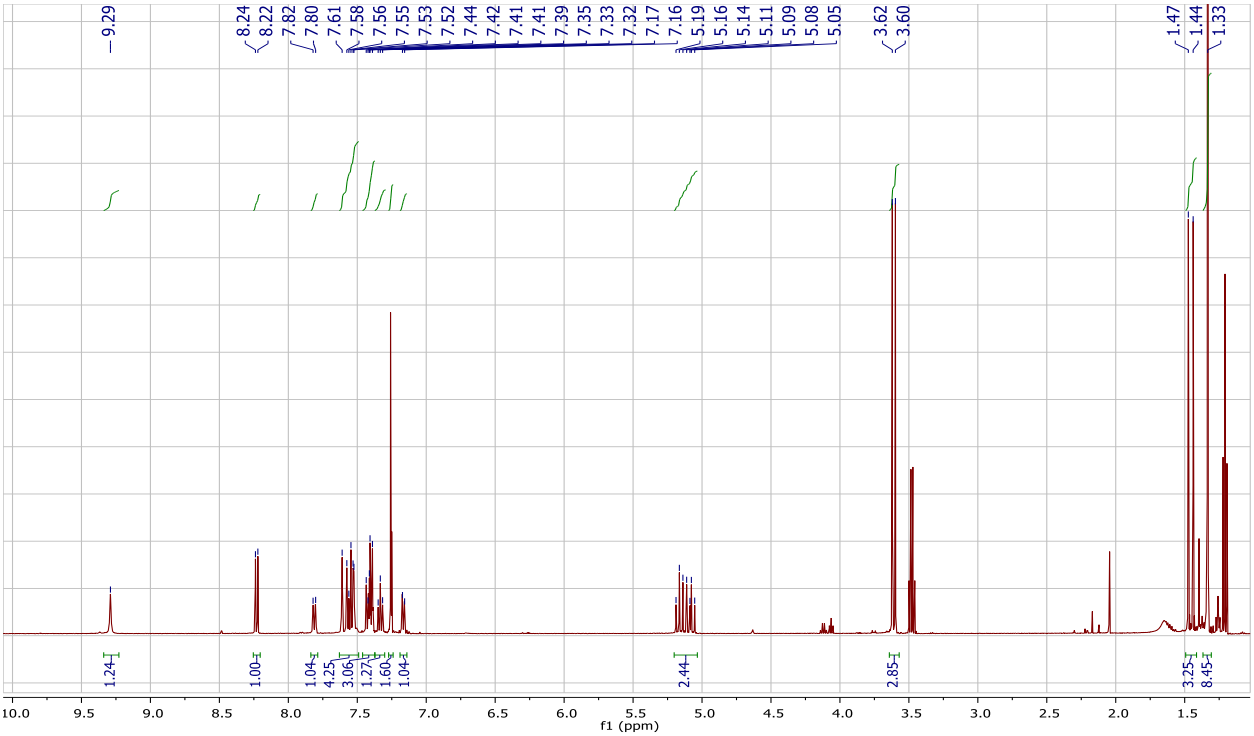
9.29
8.24
8.22
7.82
7.80
7.61
7.58
7.56
7.55
7.53
7.52
7.44
7.42
7.41
7.41
7.39
7.35
7.33
7.32
7.17
7.16
5.19
5.16
5.14
5.11
5.09
5.08
5.05
3.62
3.60
1.47
1.44
1.33
1.24
1.00
1.04
4.25
3.06
1.27
1.60
1.04
2.44
2.85
3.25
8.45
f1 (ppm)

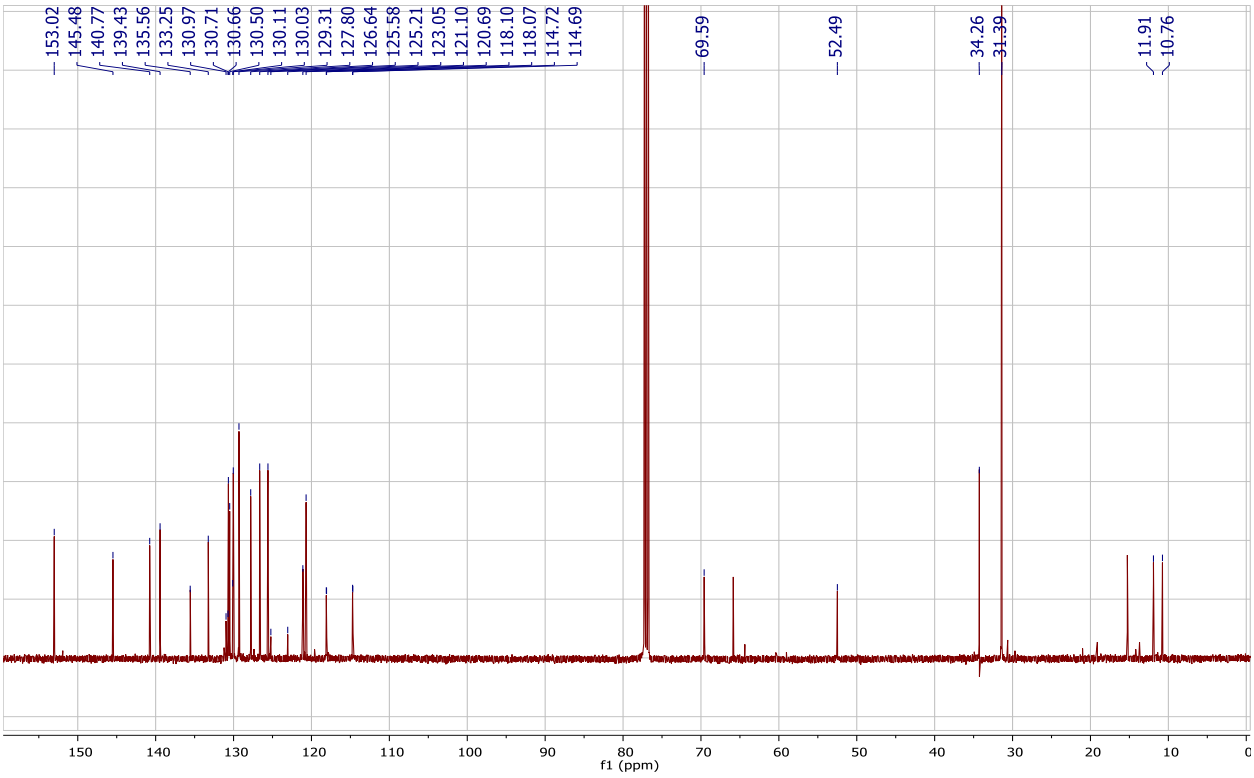
153.02
145.48
140.77
139.43
135.56
133.25
130.97
130.71
130.66
130.50
130.11
130.03
129.31
127.80
126.64
125.58
125.21
123.05
121.10
120.69
118.10
118.07
114.72
114.69
69.59
52.49
34.26
31.39
11.91
10.76
f1 (ppm)

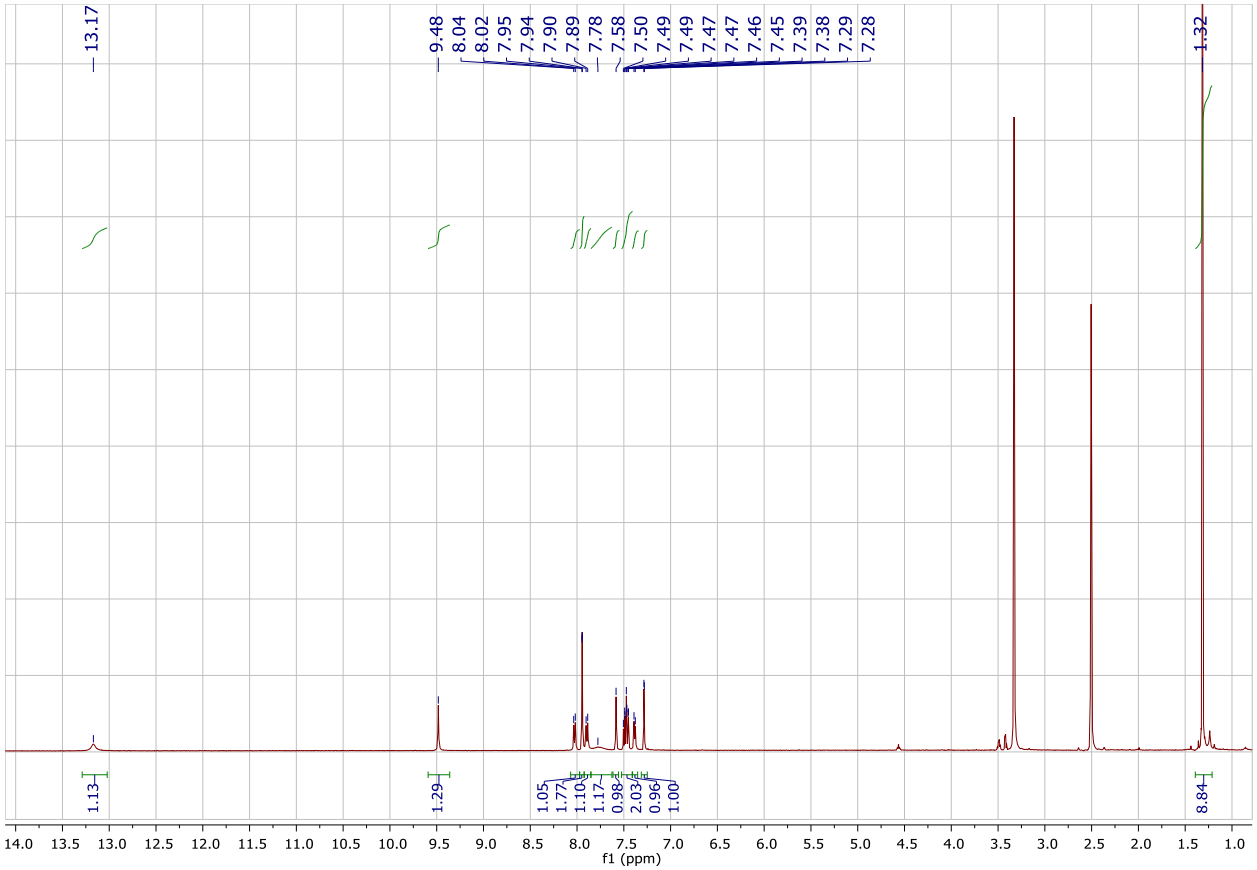
13.17
9.48
8.04
8.02
7.95
7.94
7.90
7.89
7.78
7.58
7.50
7.49
7.49
7.47
7.47
7.46
7.45
7.39
7.38
7.29
7.28
1.32
1.13
1.29
1.05
1.77
1.10
1.17
0.98
2.03
0.96
1.00
8.84
f1 (ppm)

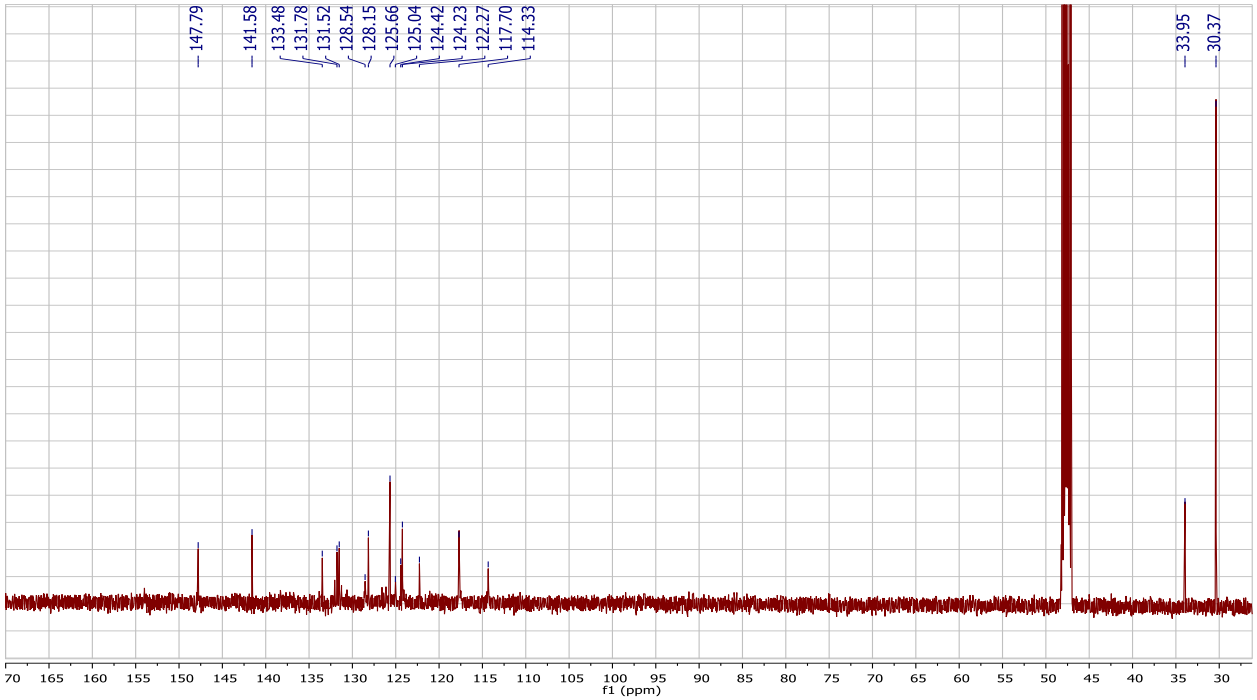
147.79
141.58
133.48
131.78
131.52
128.54
128.15
125.66
125.04
124.42
124.23
122.27
117.70
114.33
33.95
30.37
f1 (ppm)

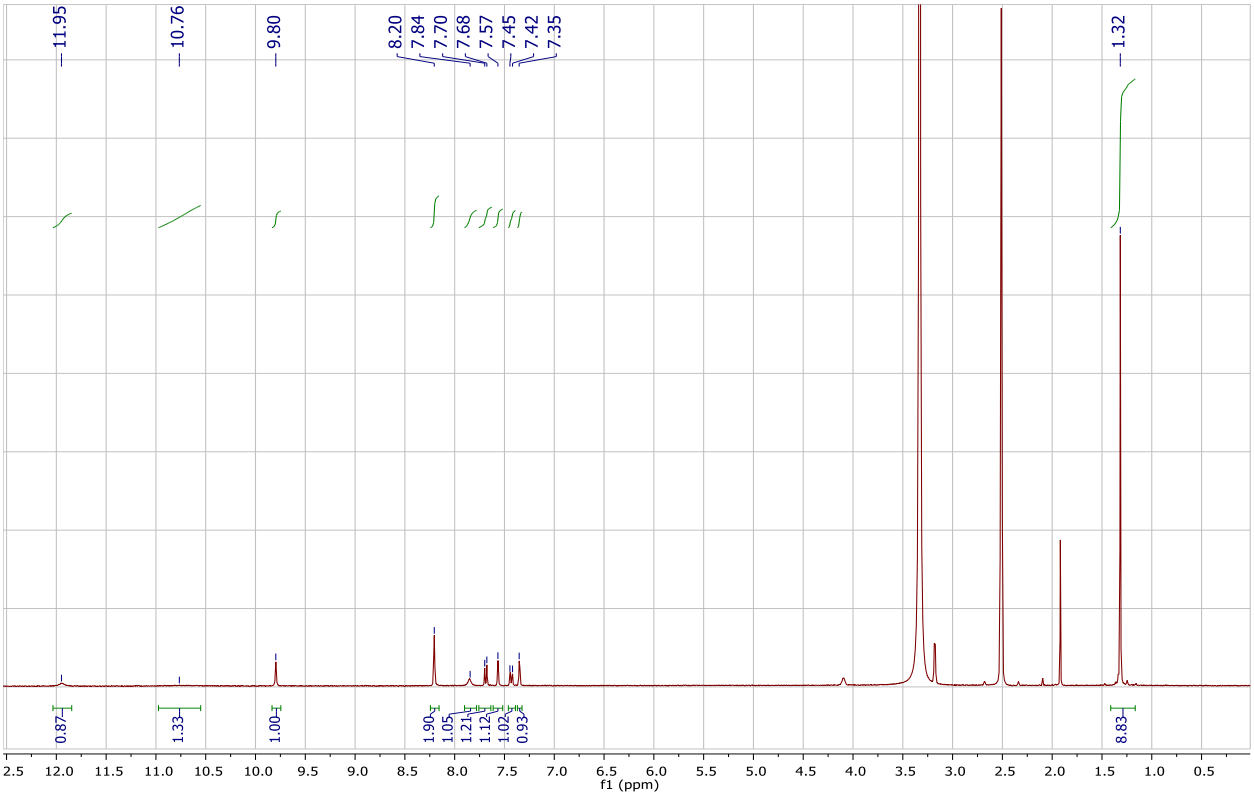
11.95
10.76
9.80
8.20
7.84
7.70
7.68
7.57
7.45
7.42
7.35
1.32
0.87
1.33
1.00
1.90
1.05
1.21
1.12
1.02
0.93
8.83
f1 (ppm)

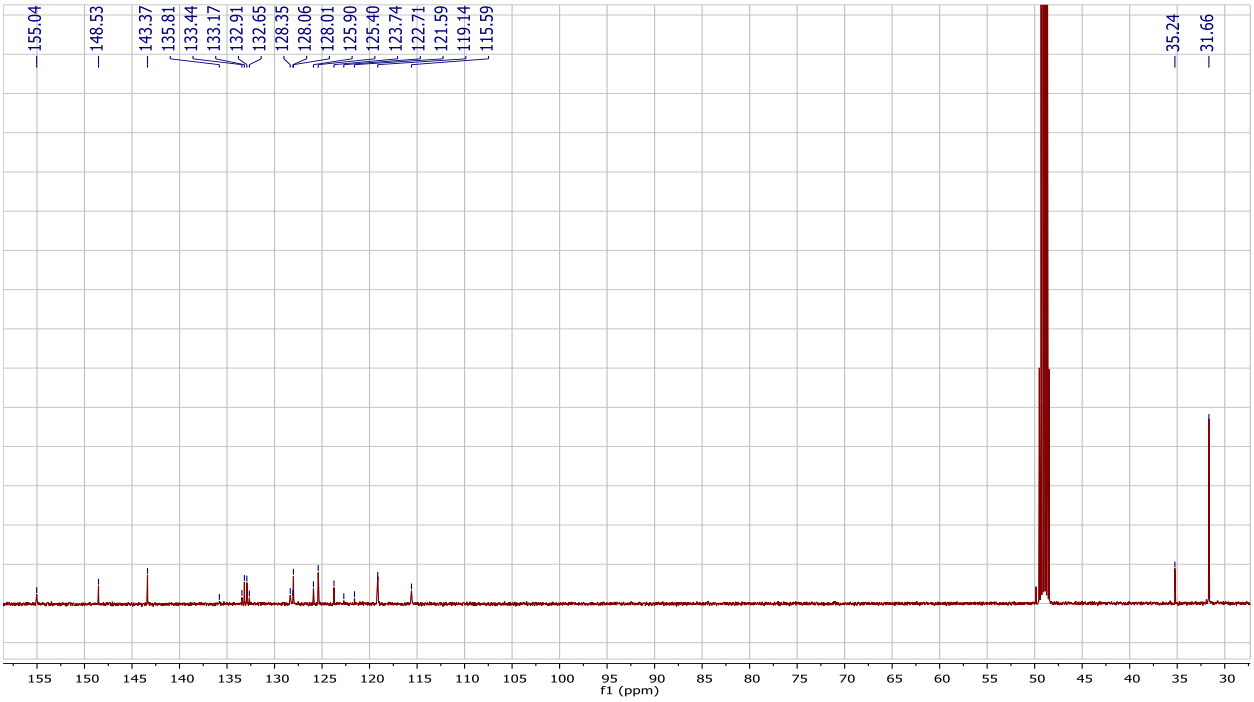
155.04
148.53
143.37
135.81
133.44
133.17
132.91
132.65
128.35
128.06
128.01
125.90
125.40
123.74
122.71
121.59
119.14
115.59
35.24
31.66
f1 (ppm)

5.6.2 Diels-Alder Project

183

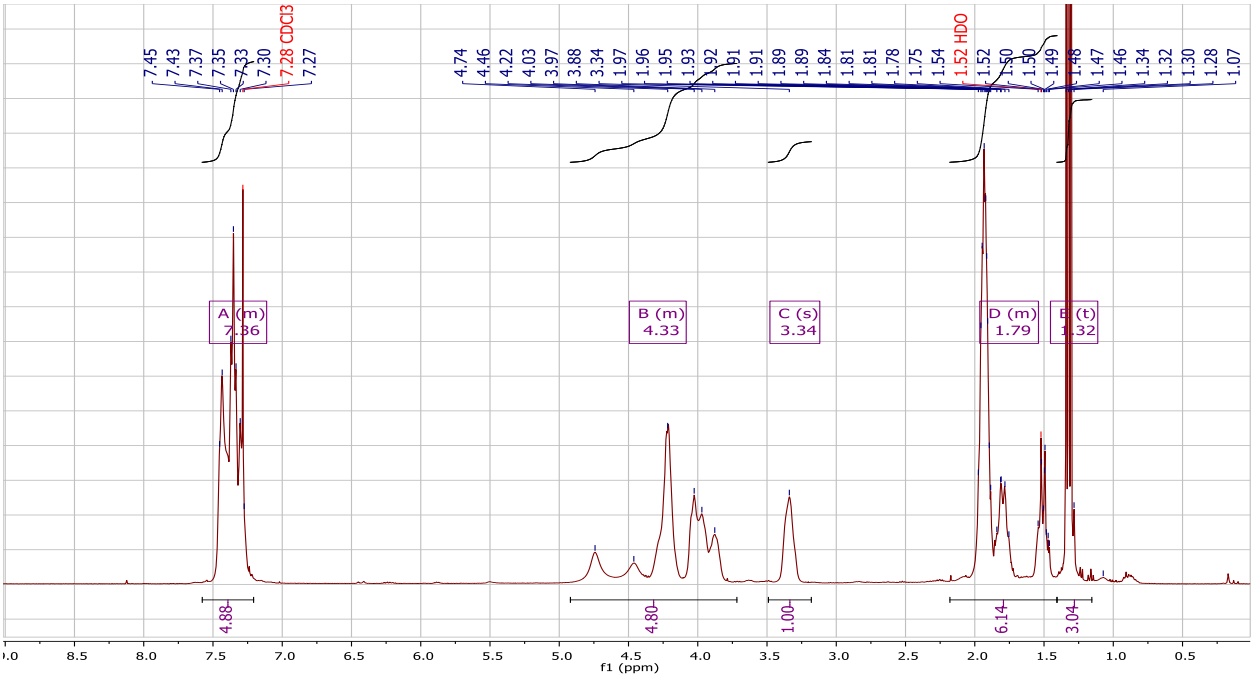

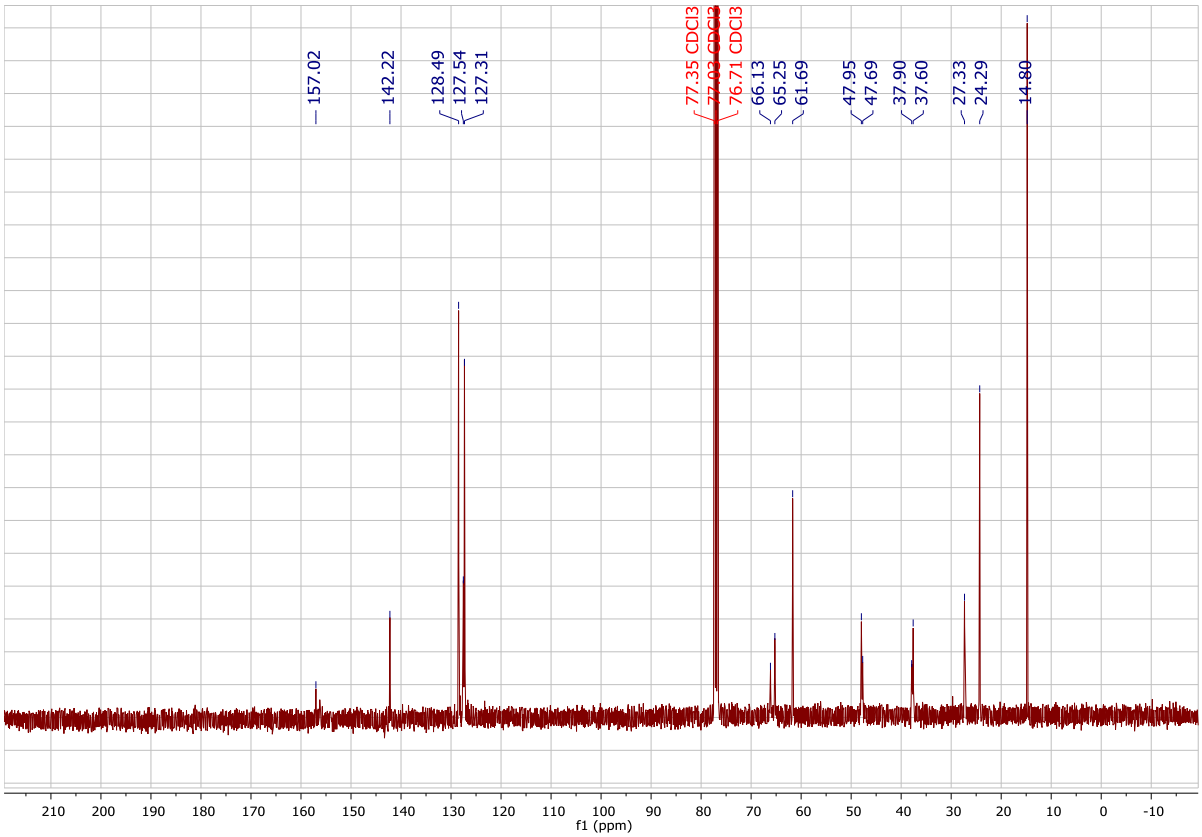

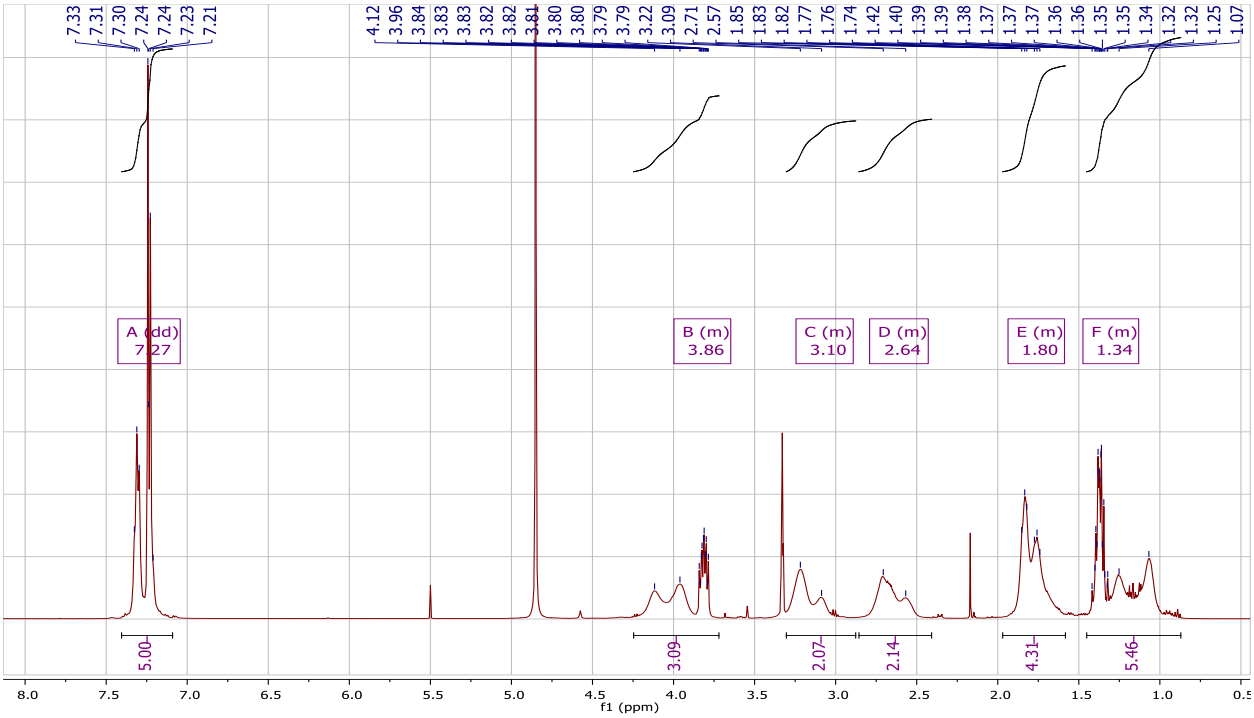
7.33
7.31
7.30
7.24
7.24
7.23
7.21
4.12
3.96
3.84
3.83
3.83
3.82
3.82
3.81
3.80
3.80
3.79
3.79
3.22
3.09
2.71
2.57
1.85
1.83
1.82
1.77
1.76
1.74
1.42
1.40
1.39
1.39
1.38
1.37
1.37
1.37
1.36
1.36
1.35
1.35
1.34
1.32
1.32
1.25
1.07
A (dd)
7.27
B (m)
3.86
C (m)
3.10
D (m)
2.64
E (m)
1.80
F (m)
1.34
5.00
3.09
2.07
2.14
4.31
5.46
f1 (ppm)

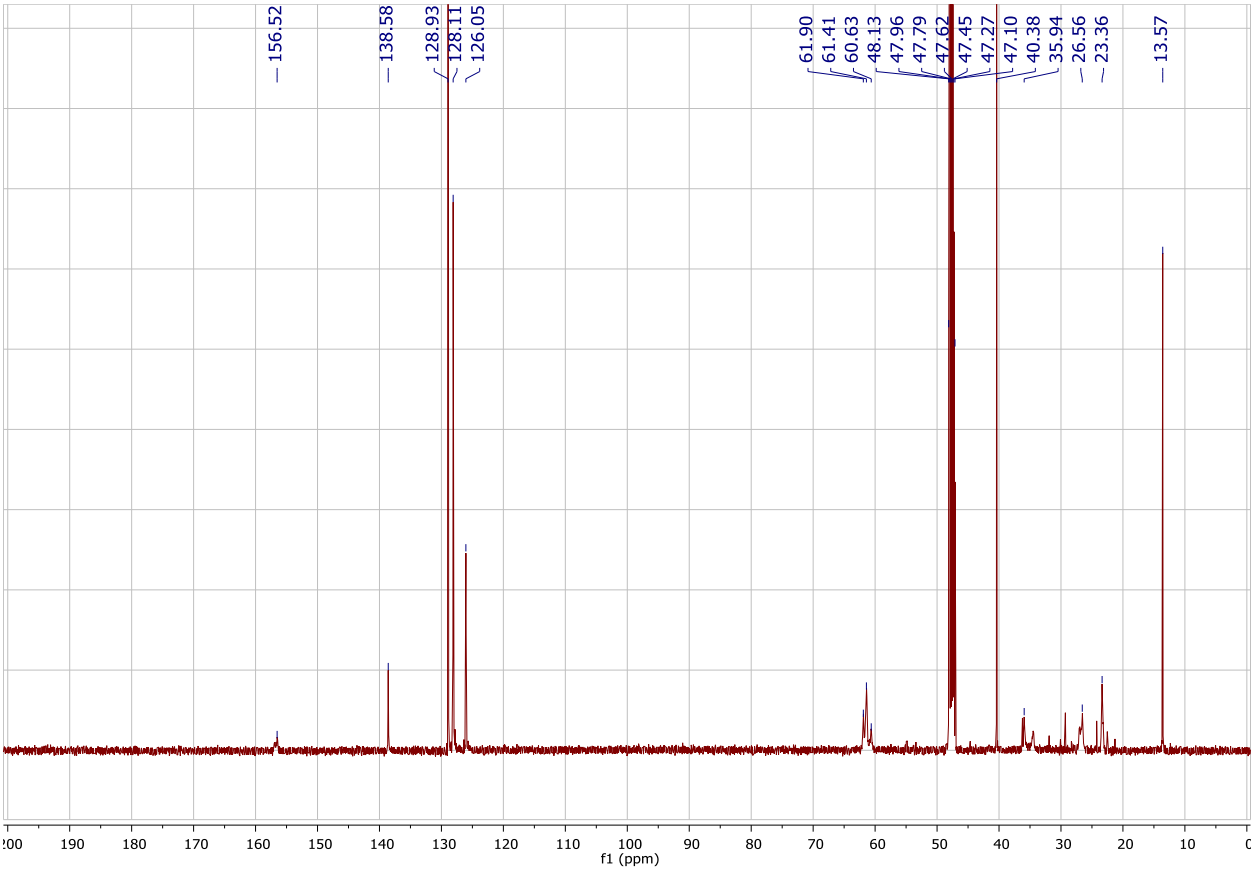
156.52
138.58
128.93
128.11
126.05
61.90
61.41
60.63
48.13
47.96
47.79
47.62
47.45
47.27
47.10
40.38
35.94
26.56
23.36
13.57
f1 (ppm)

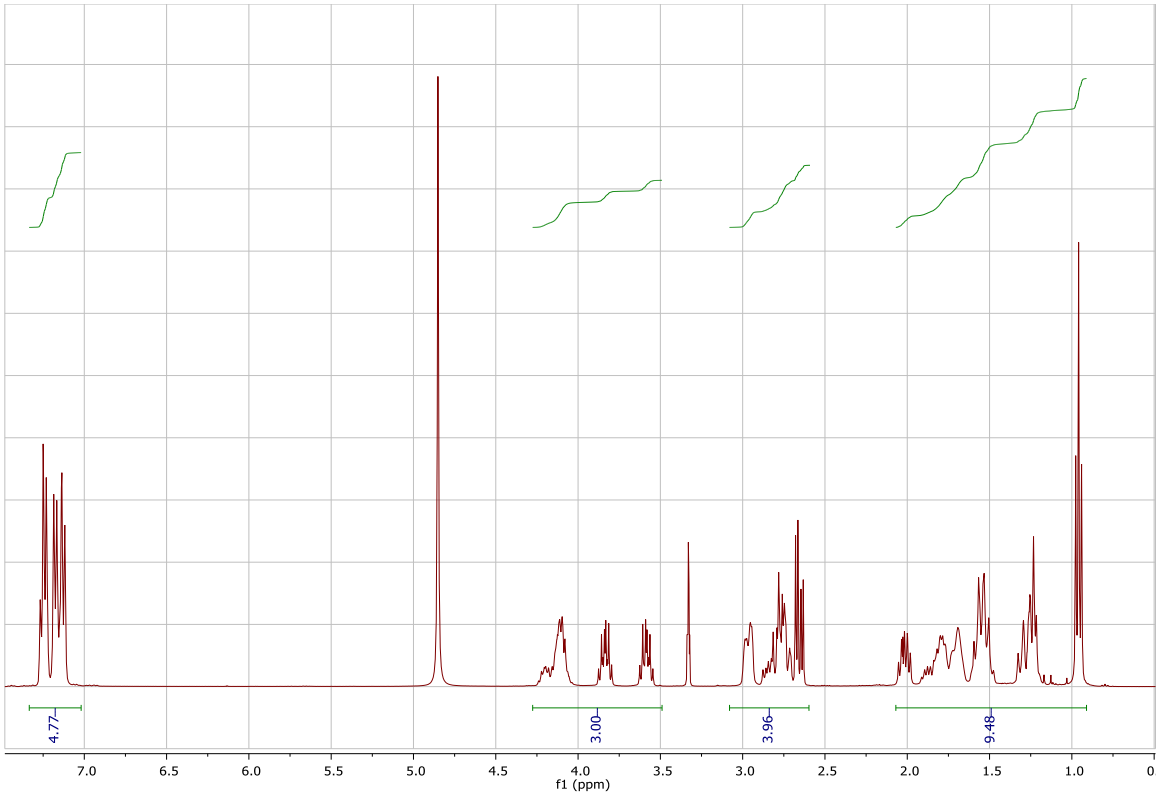
4.77
3.00
3.96
9.48
7.0
6.5
6.0
5.5
5.0
4.5
4.0
3.5
3.0
2.5
2.0
1.5
1.0
0
f1 (ppm)

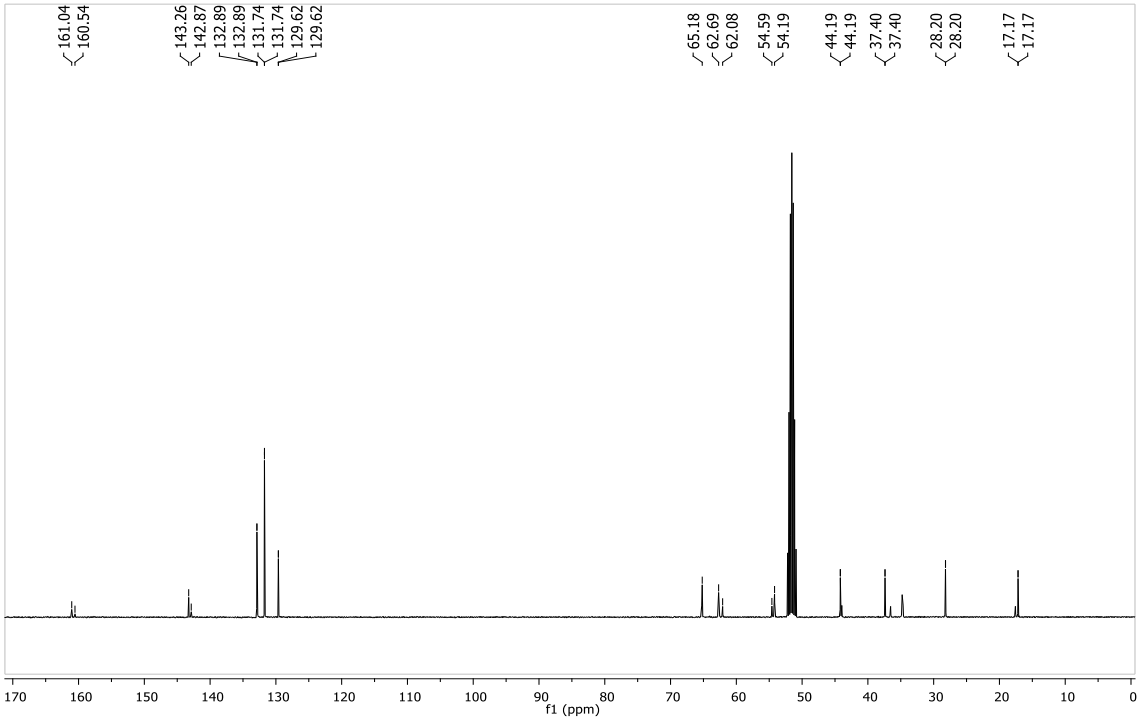
161.04
160.54
143.26
142.87
132.89
132.89
131.74
131.74
129.62
129.62
65.18
62.69
62.08
54.59
54.19
44.19
44.19
37.40
37.40
28.20
28.20
17.17
17.17
170
160
150
140
130
120
110
100
90
80
70
60
50
40
30
20
10
0
f1 (ppm)

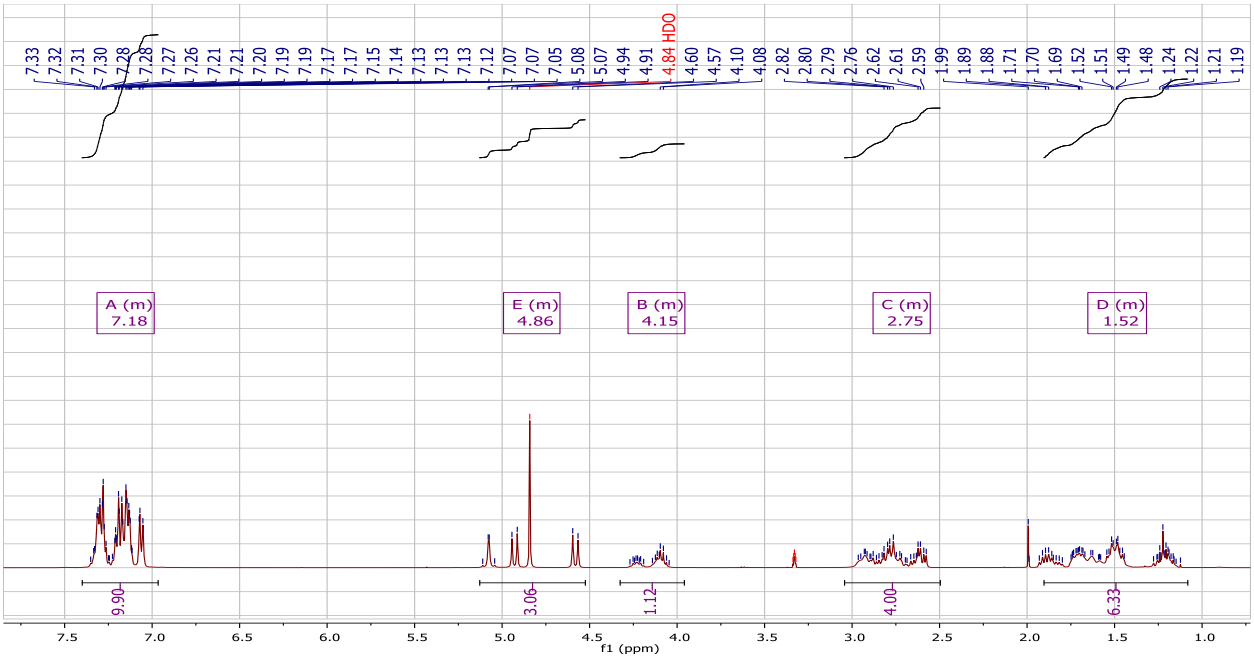
7.33 7.32 7.31 7.30 7.28 7.28 7.27 7.26 7.21 7.21 7.20 7.19 7.19 7.17 7.17 7.15 7.14 7.13 7.13 7.12 7.07 7.07 7.05 5.08 5.07 4.94 4.91 4.84 HDO 4.60 4.57 4.10 4.08 2.82 2.80 2.79 2.76 2.62 2.61 2.59 1.99 1.89 1.88 1.71 1.70 1.69 1.52 1.51 1.49 1.48 1.24 1.22 1.21 1.19
A (m) 7.18
E (m) 4.86
B (m) 4.15
C (m) 2.75
D (m) 1.52
9.90
3.06
1.12
4.00
6.33
f1 (ppm)

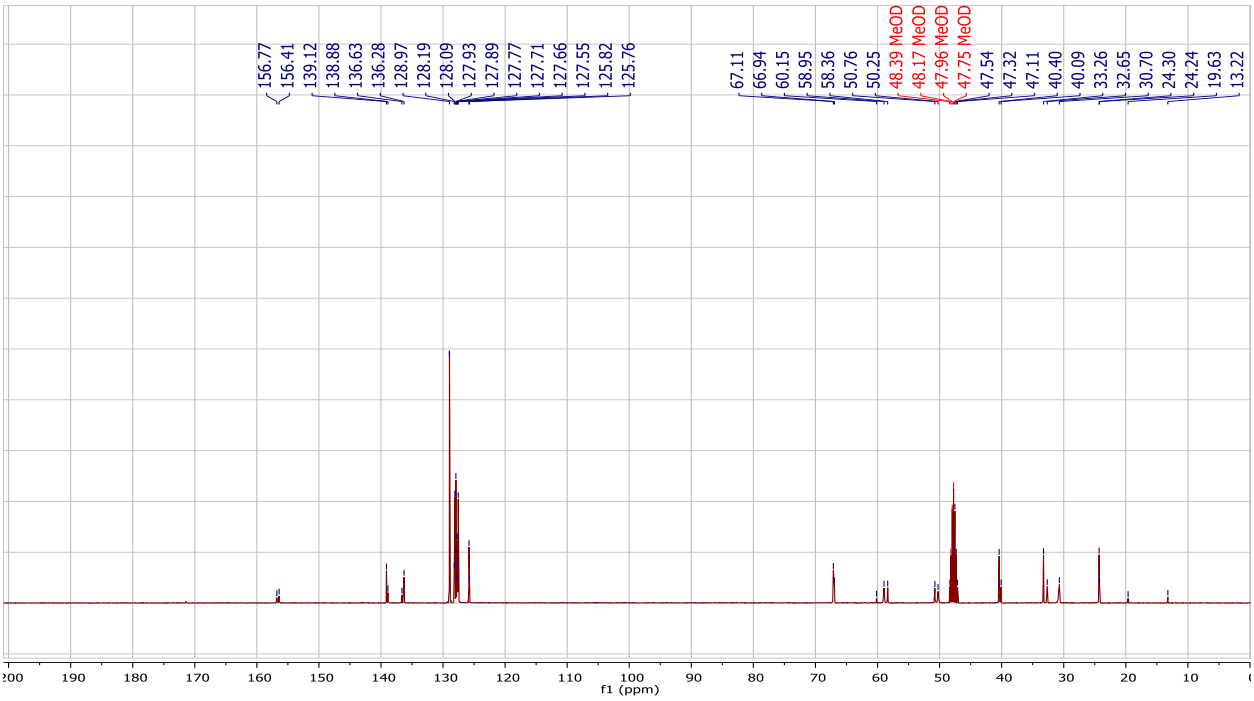
156.77 156.41 139.12 138.88 136.63 136.28 128.97 128.19 128.09 127.93 127.89 127.77 127.71 127.66 127.55 125.82 125.76
67.11 66.94 60.15 58.95 58.36 50.76 50.25 48.39 MeOD 48.17 MeOD 47.96 MeOD 47.75 MeOD 47.54 47.32 47.11 40.40 40.09 33.26 32.65 30.70 24.30 24.24 19.63 13.22
f1 (ppm)

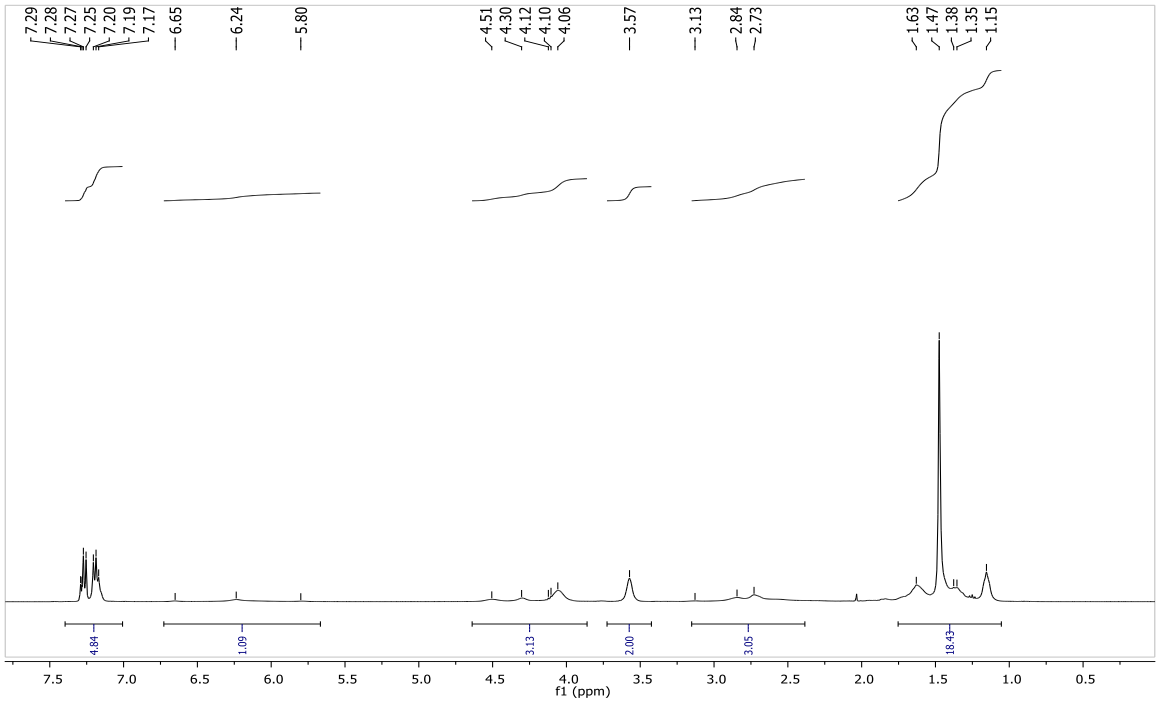
7.29
7.28
7.27
7.25
7.20
7.19
7.17
6.65
6.24
5.80
4.51
4.30
4.12
4.10
4.06
3.57
3.13
2.84
2.73
1.63
1.47
1.38
1.35
1.15
4.84
1.09
3.13
2.00
3.05
18.43
f1 (ppm)

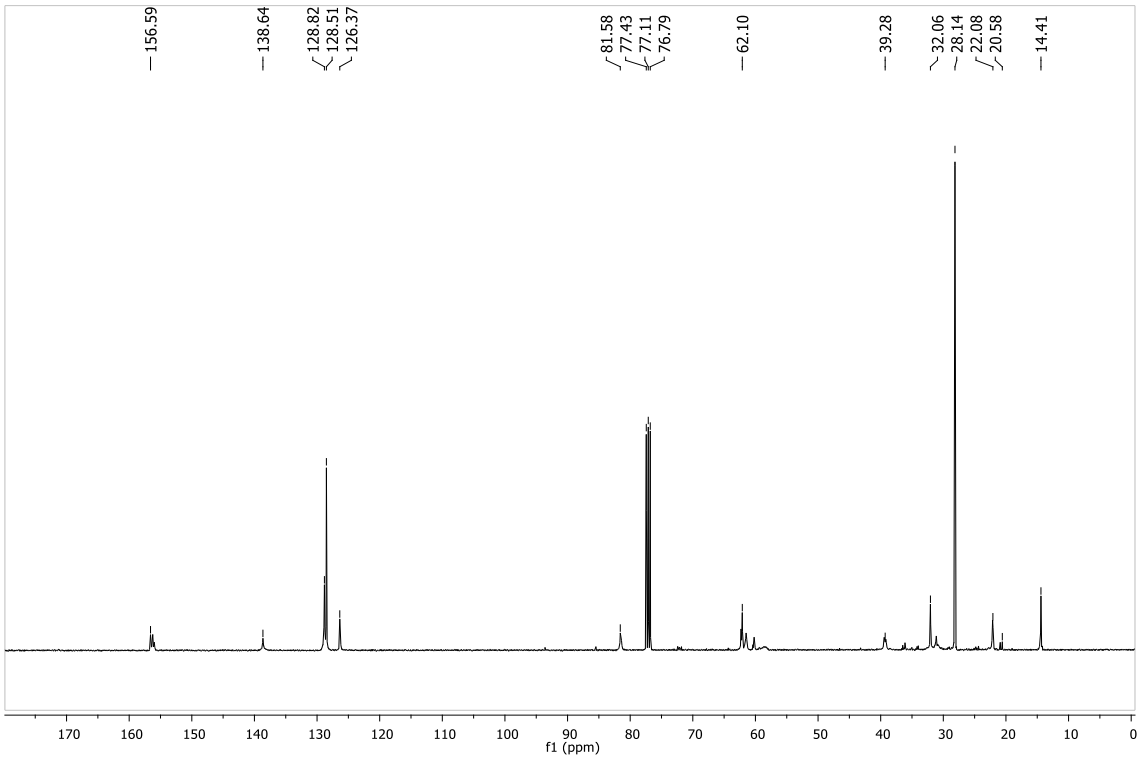
156.59
138.64
128.82
128.51
126.37
81.58
77.43
77.11
76.79
62.10
39.28
32.06
28.14
22.08
20.58
14.41
f1 (ppm)


3.24
4.25
1.00
5.15
3.99
4.8 4.6 4.4 4.2 4.0 3.8 3.6 3.4 3.2 3.0 2.8 2.6 2.4 2.2 2.0 1.8 1.6 1.4 1.2 1.0 0.8 0.6
f1 (ppm)

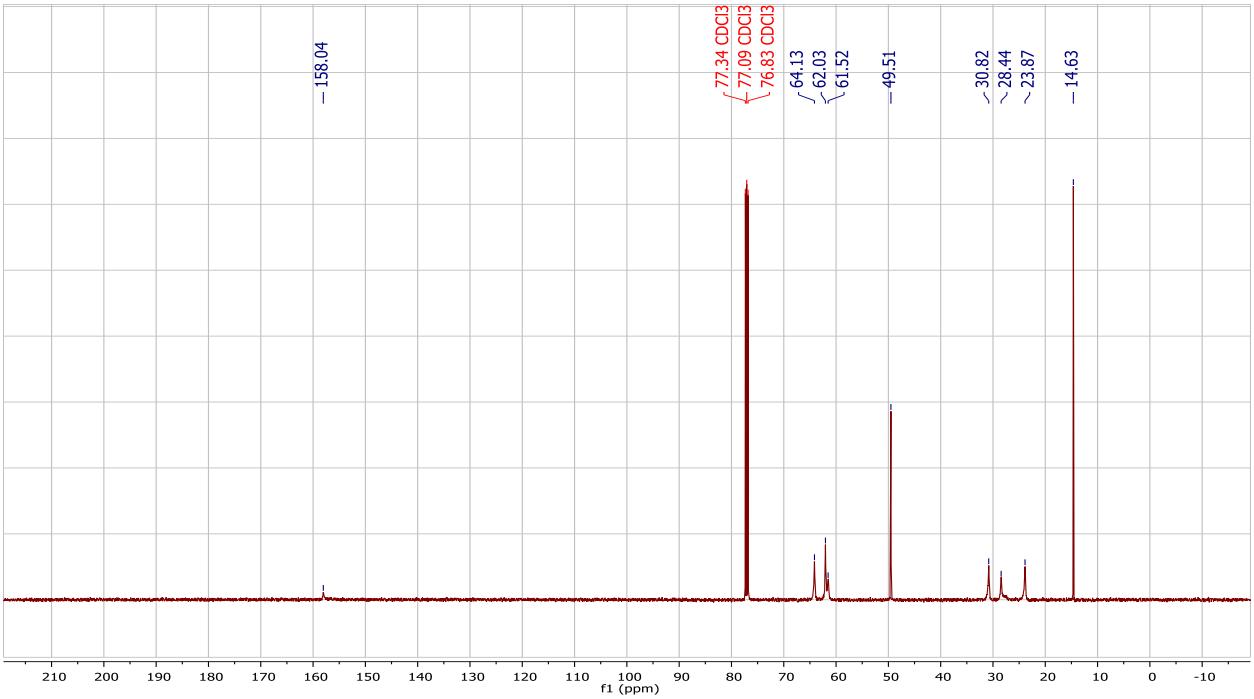
158.04
77.34 CDCl3
77.09 CDCl3
76.83 CDCl3
64.13
62.03
61.52
49.51
30.82
28.44
23.87
14.63
210 200 190 180 170 160 150 140 130 120 110 100 90 80 70 60 50 40 30 20 10 0 -10
f1 (ppm)

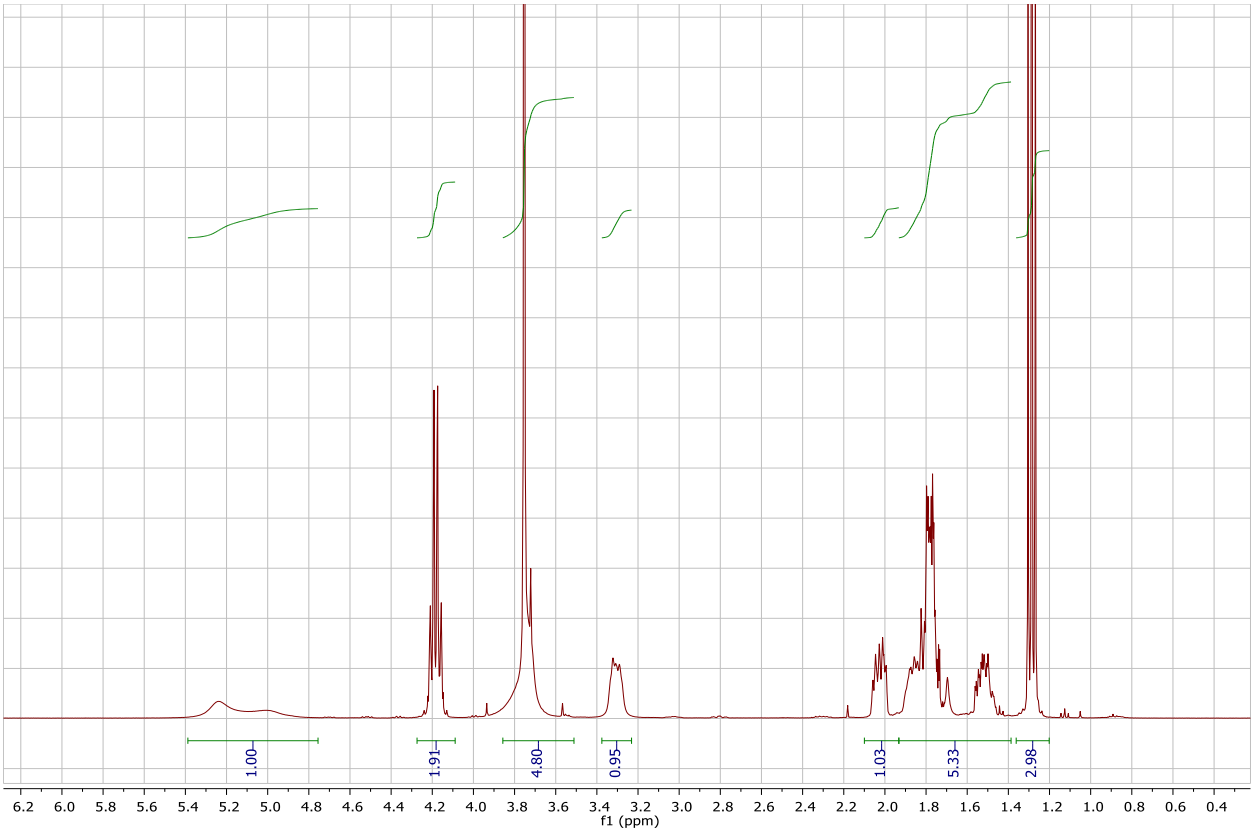
1.00
1.91
4.80
0.95
1.03
5.33
2.98
f1 (ppm)

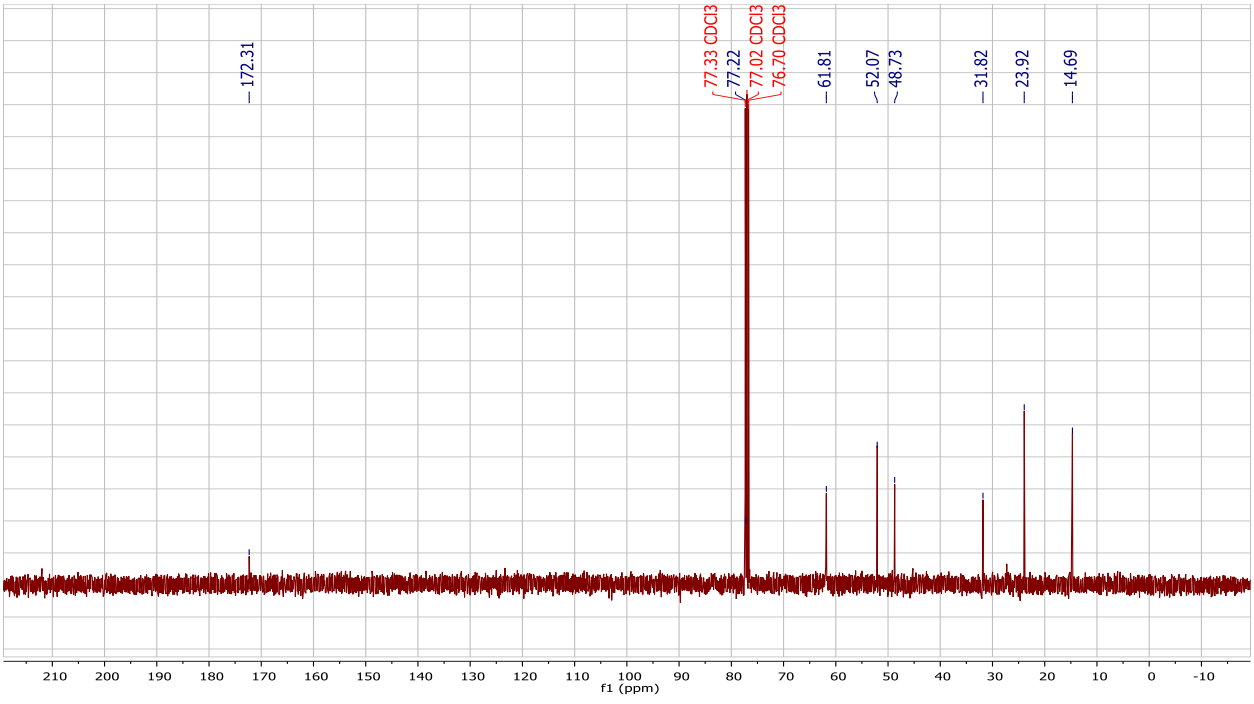
172.31
77.33 CDCl3
77.22
77.02 CDCl3
76.70 CDCl3
61.81
52.07
48.73
31.82
23.92
14.69
f1 (ppm)

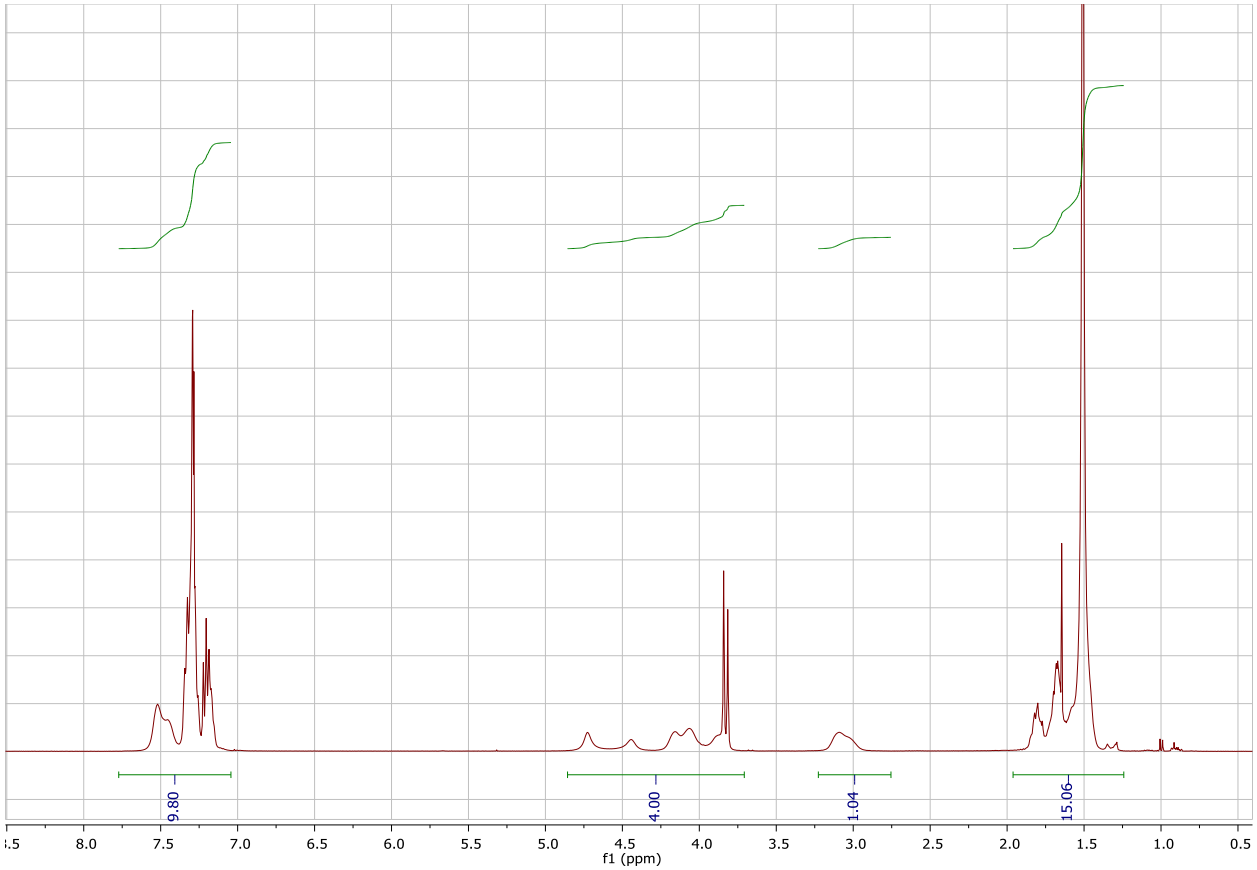
9.80
4.00
1.04
15.06
f1 (ppm)

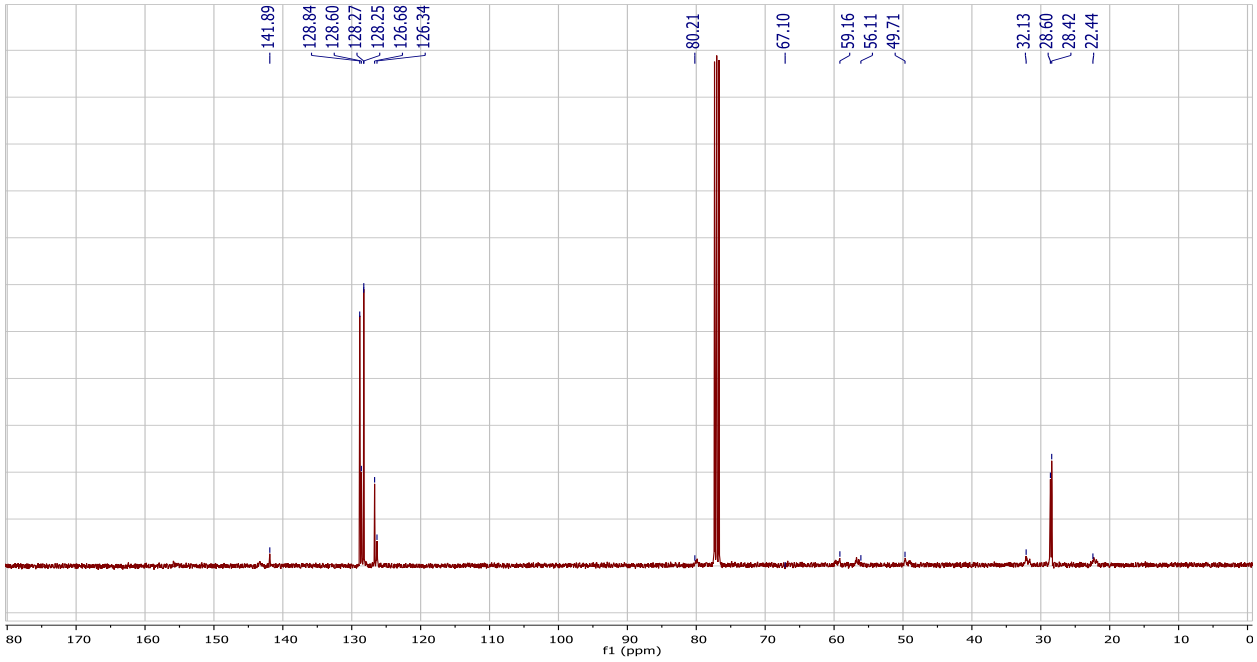
141.89
128.84
128.60
128.27
128.25
126.68
126.34
80.21
67.10
59.16
56.11
49.71
32.13
28.60
28.42
22.44
f1 (ppm)

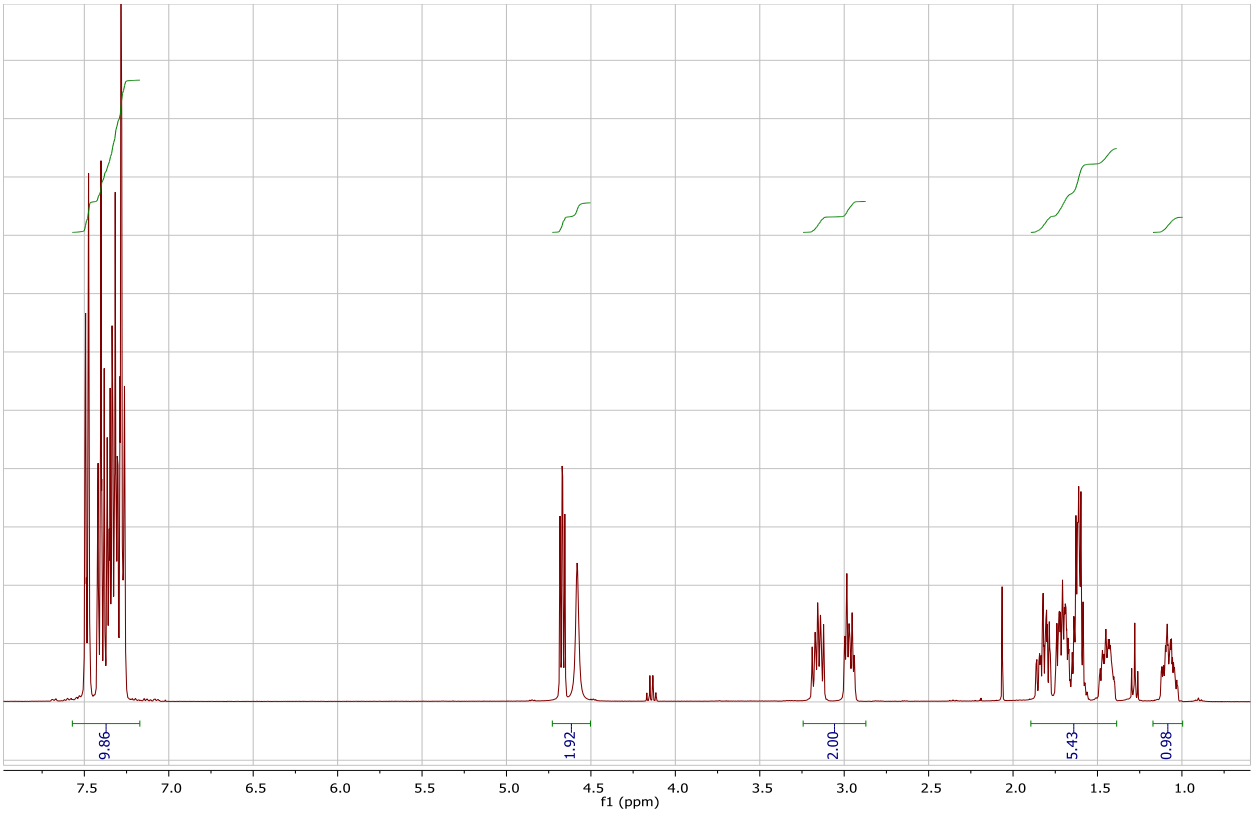
9.86
1.92
2.00
5.43
0.98
7.5
7.0
6.5
6.0
5.5
5.0
4.5
4.0
3.5
3.0
2.5
2.0
1.5
1.0
f1 (ppm)

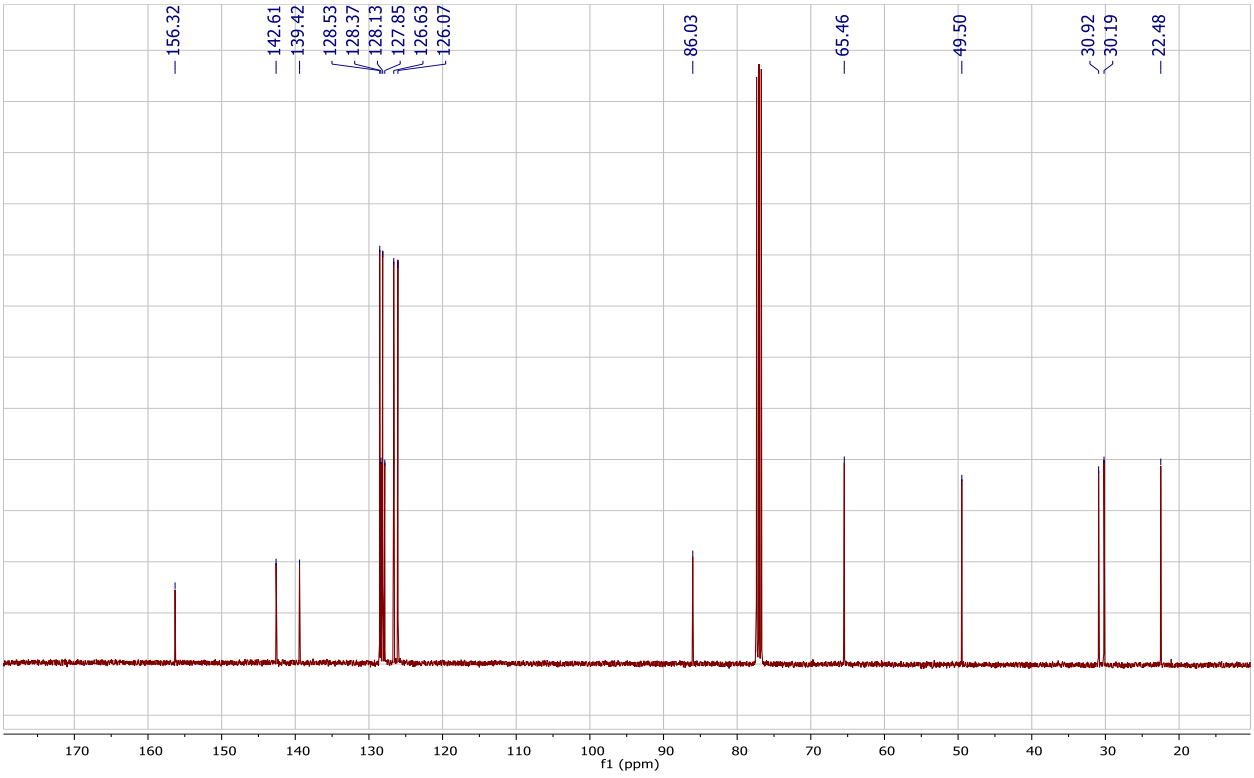
156.32
142.61
139.42
128.53
128.37
128.13
127.85
126.63
126.07
86.03
65.46
49.50
30.92
30.19
22.48
170
160
150
140
130
120
110
100
90
80
70
60
50
40
30
20
f1 (ppm)

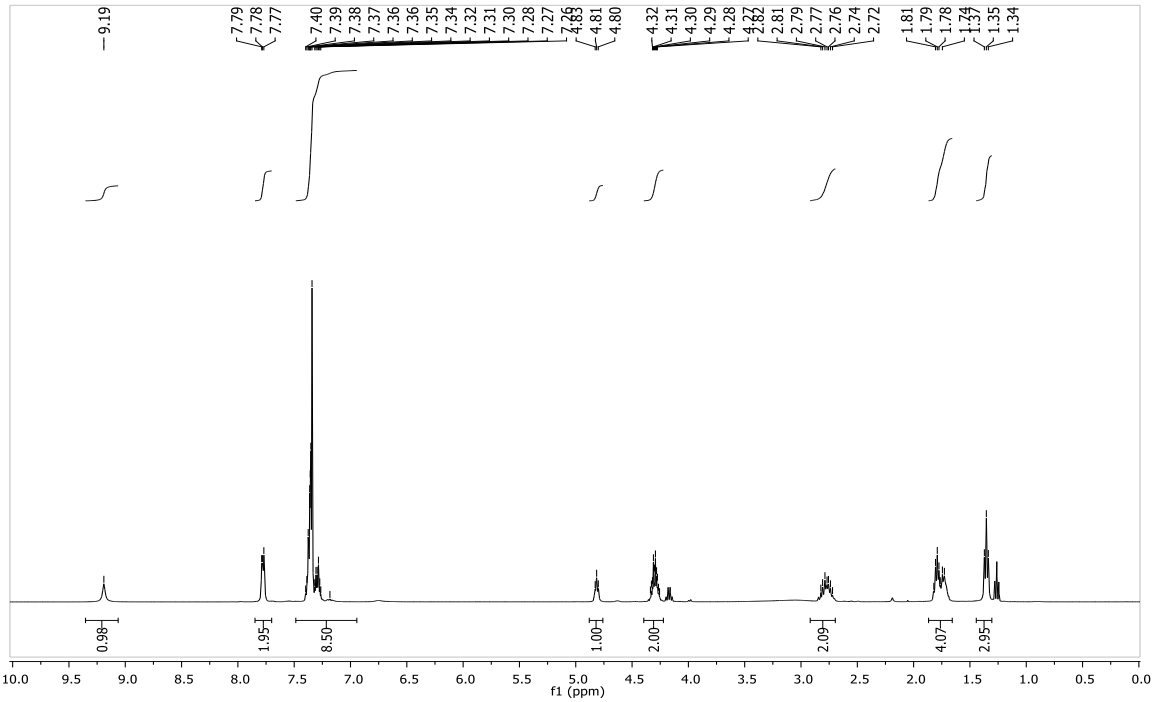
9.19
7.79
7.78
7.77
7.40
7.39
7.38
7.37
7.36
7.36
7.35
7.34
7.32
7.31
7.30
7.28
7.27
7.26
4.83
4.81
4.80
4.32
4.31
4.30
4.29
4.28
4.27
2.82
2.81
2.79
2.77
2.76
2.74
2.72
1.81
1.79
1.78
1.74
1.37
1.35
1.34
0.98
1.95
8.50
1.00
2.00
2.09
4.07
2.95
f1 (ppm)

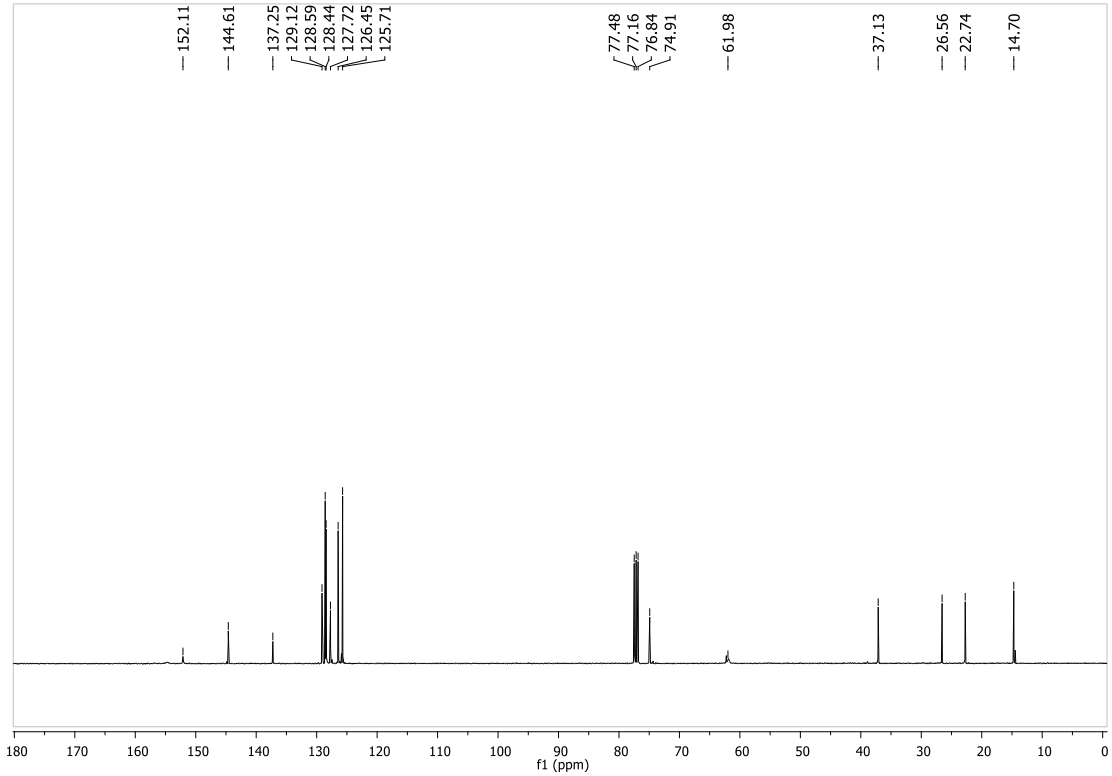
152.11
144.61
137.25
129.12
128.59
128.44
127.72
126.45
125.71
77.48
77.16
76.84
74.91
61.98
37.13
26.56
22.74
14.70
f1 (ppm)

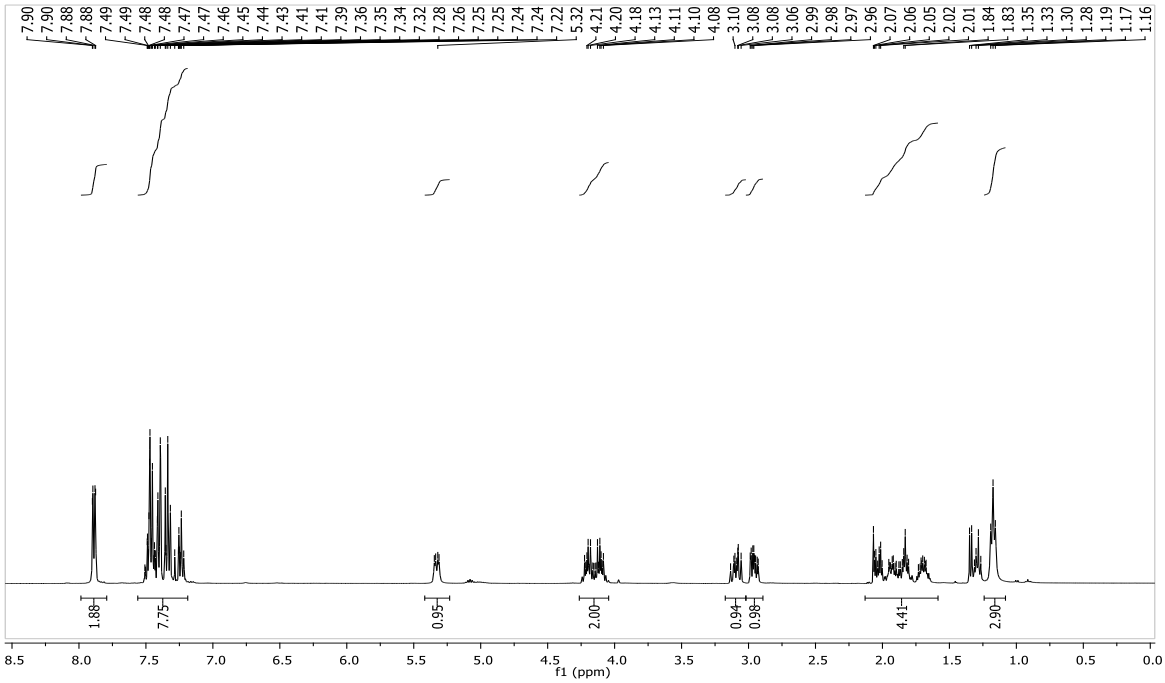
7.90
7.90
7.88
7.88
7.49
7.49
7.48
7.48
7.47
7.47
7.46
7.45
7.44
7.43
7.41
7.41
7.39
7.36
7.35
7.34
7.32
7.28
7.26
7.25
7.25
7.24
7.24
7.22
5.32
4.21
4.20
4.18
4.13
4.11
4.10
4.08
3.10
3.08
3.08
3.06
2.99
2.98
2.97
2.96
2.07
2.06
2.05
2.02
2.01
1.84
1.83
1.35
1.33
1.30
1.28
1.19
1.17
1.16
1.88
7.75
0.95
2.00
0.94
0.98
4.41
2.90
f1 (ppm)

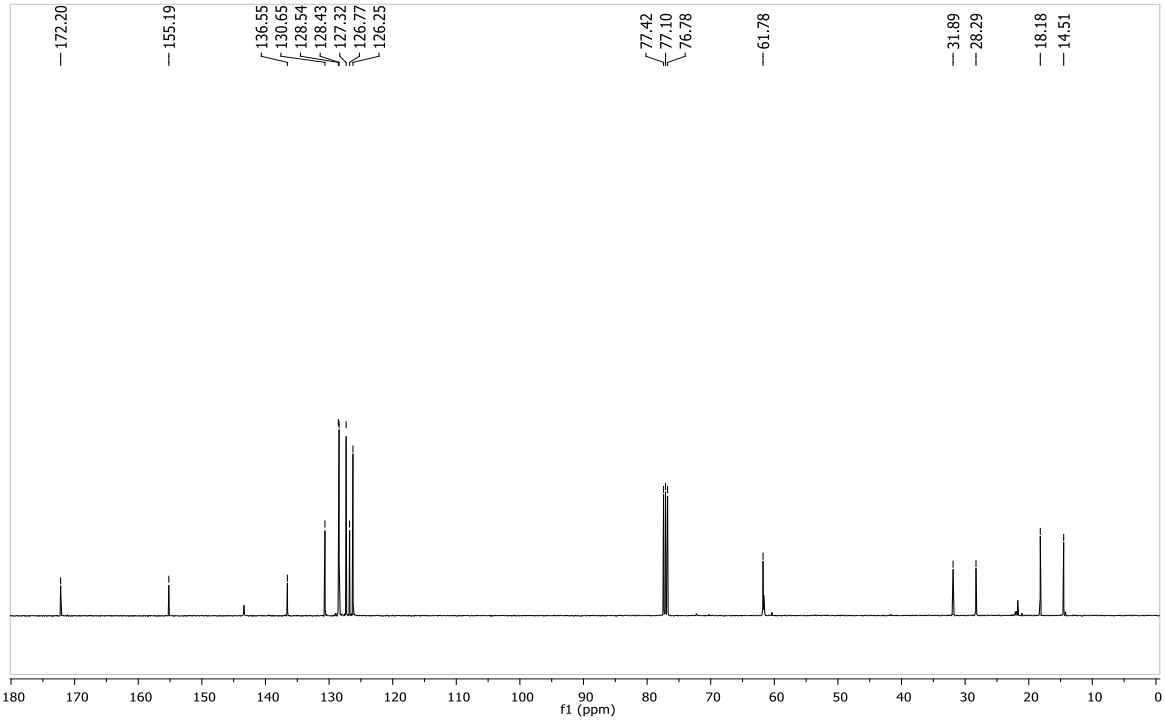
172.20
155.19
136.55
130.65
128.54
128.43
127.32
126.77
126.25
77.42
77.10
76.78
61.78
31.89
28.29
18.18
14.51
f1 (ppm)

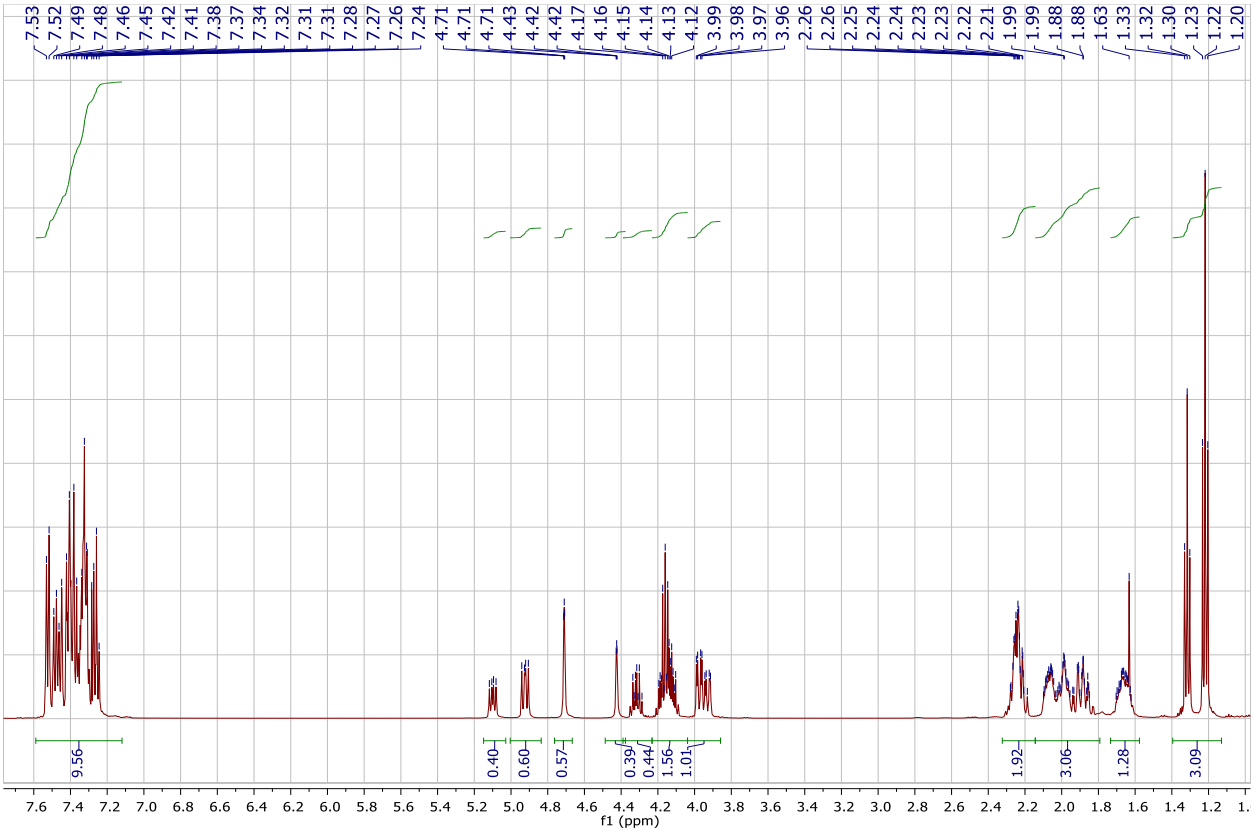
7.53 7.52 7.49 7.48 7.46 7.45 7.42 7.41 7.38 7.37 7.34 7.32 7.31 7.31 7.28 7.27 7.26 7.24
4.71 4.71 4.43 4.42 4.42 4.17 4.16 4.15 4.14 4.13 4.12 3.99 3.98 3.97 3.96
2.26 2.26 2.25 2.24 2.24 2.23 2.23 2.22 2.21 1.99 1.99 1.88 1.88 1.63 1.33 1.32 1.30 1.23 1.22 1.20
9.56 0.40 0.60 0.57 0.39 0.44 1.56 1.01 1.92 3.06 1.28 3.09
f1 (ppm)

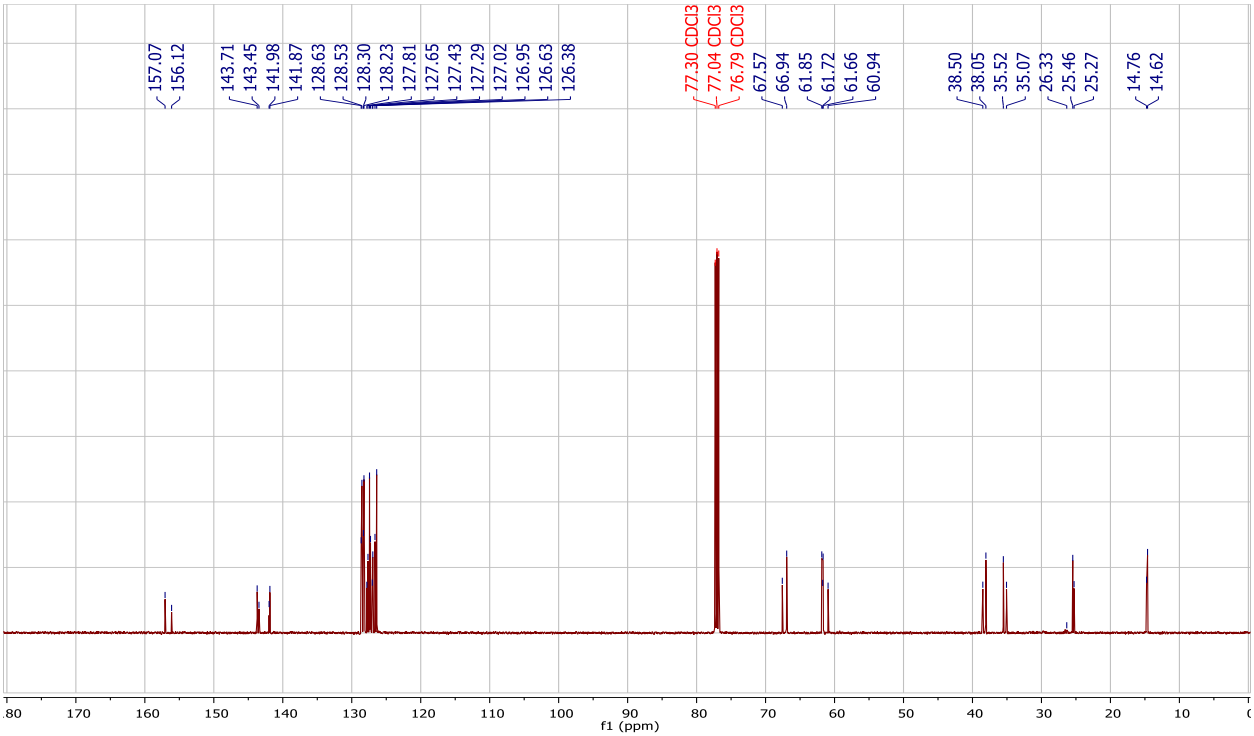
157.07 156.12 143.71 143.45 141.98 141.87 128.63 128.53 128.30 128.23 127.81 127.65 127.43 127.29 127.02 126.95 126.63 126.38
77.30 CDCl3 77.04 CDCl3 76.79 CDCl3
67.57 66.94 61.85 61.72 61.66 60.94
38.50 38.05 35.52 35.07 26.33 25.46 25.27 14.76 14.62
f1 (ppm)

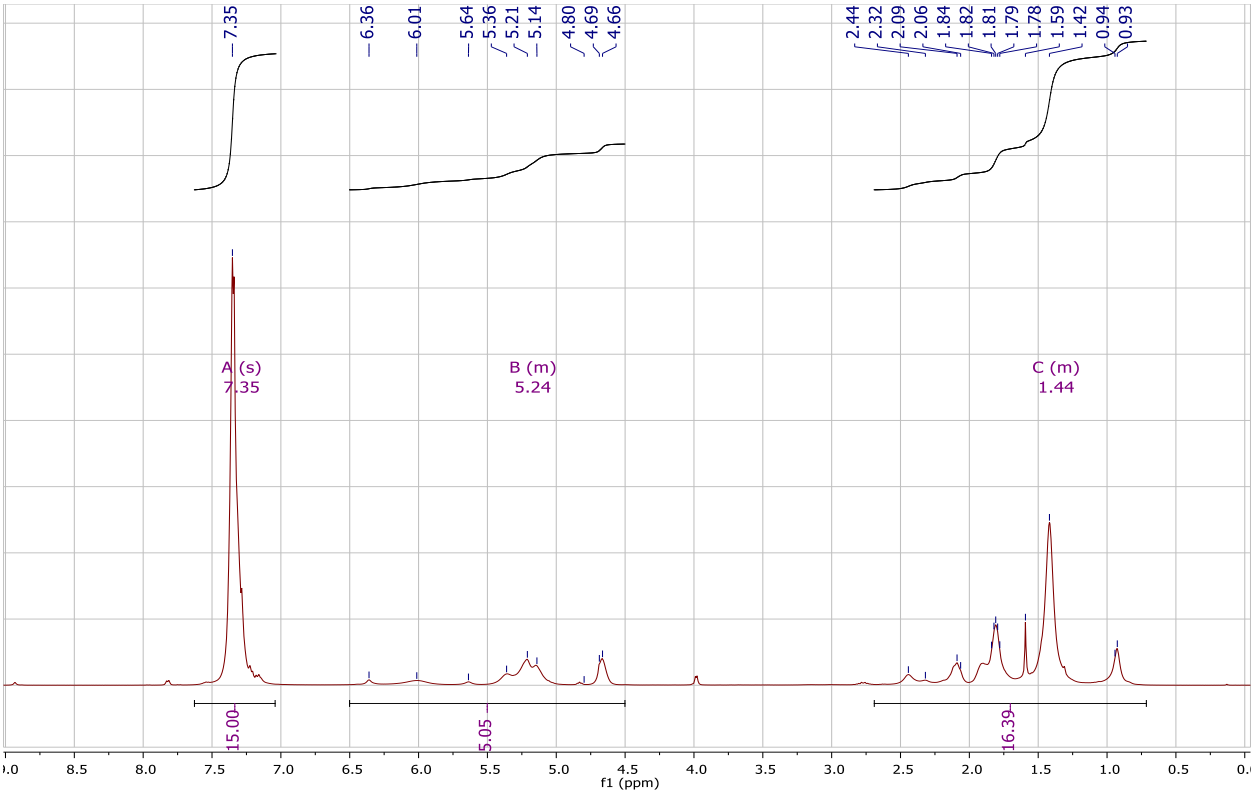
7.35
6.36
6.01
5.64
5.36
5.21
5.14
4.80
4.69
4.66
2.44
2.32
2.09
2.06
1.84
1.82
1.81
1.79
1.78
1.59
1.42
0.94
0.93
A (s)
7.35
B (m)
5.24
C (m)
1.44
15.00
5.05
16.39
f1 (ppm)

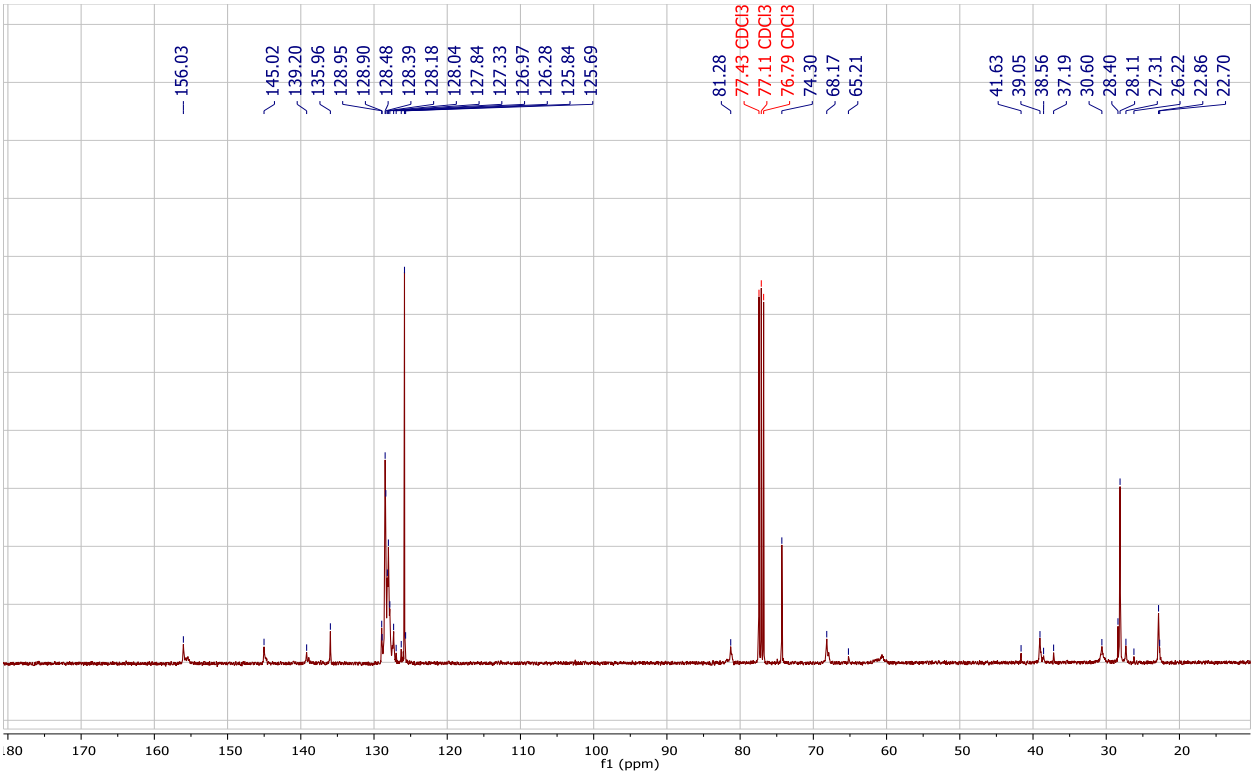
156.03
145.02
139.20
135.96
128.95
128.90
128.48
128.39
128.18
128.04
127.84
127.33
126.97
126.28
125.84
125.69
81.28
77.43 CDCl3
77.11 CDCl3
76.79 CDCl3
74.30
68.17
65.21
41.63
39.05
38.56
37.19
30.60
28.40
28.11
27.31
26.22
22.86
22.70
f1 (ppm)

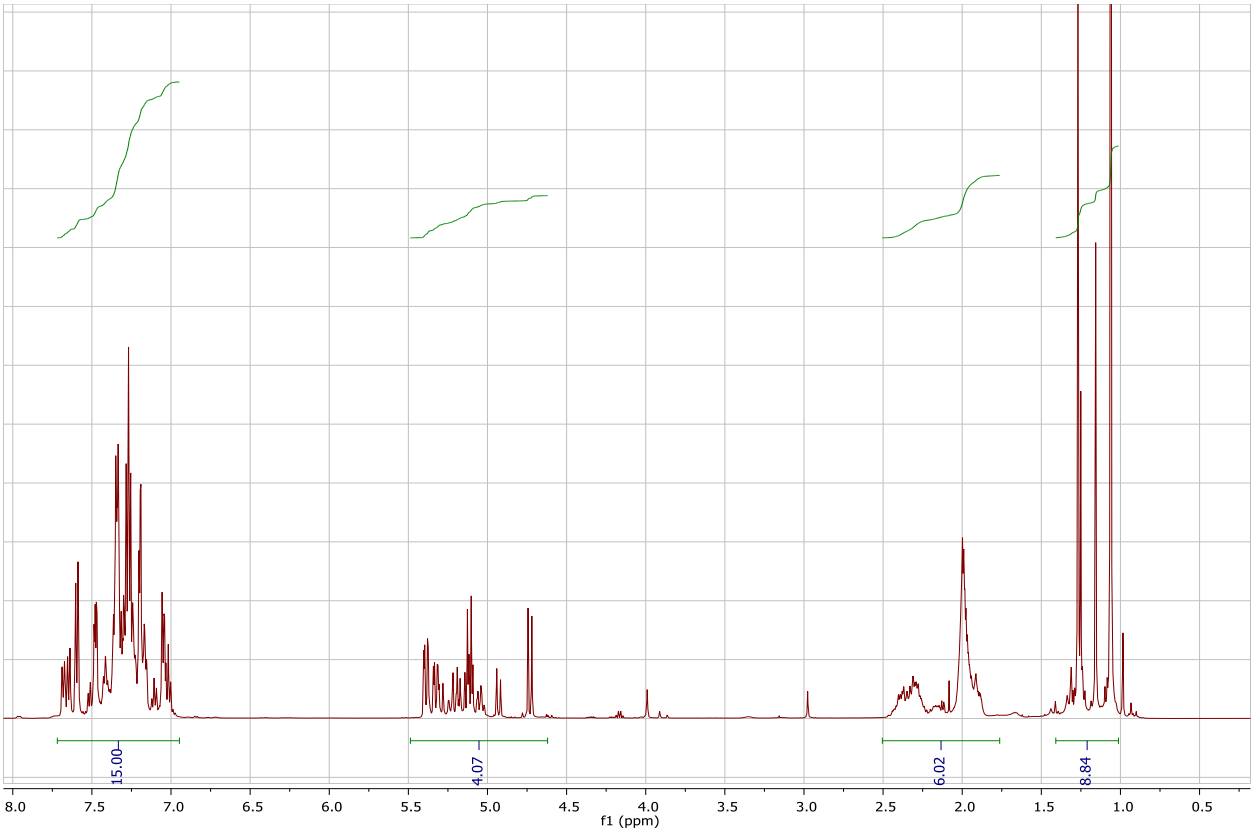
15.00
4.07
6.02
8.84
8.0
7.5
7.0
6.5
6.0
5.5
5.0
4.5
4.0
3.5
3.0
2.5
2.0
1.5
1.0
0.5
f1 (ppm)

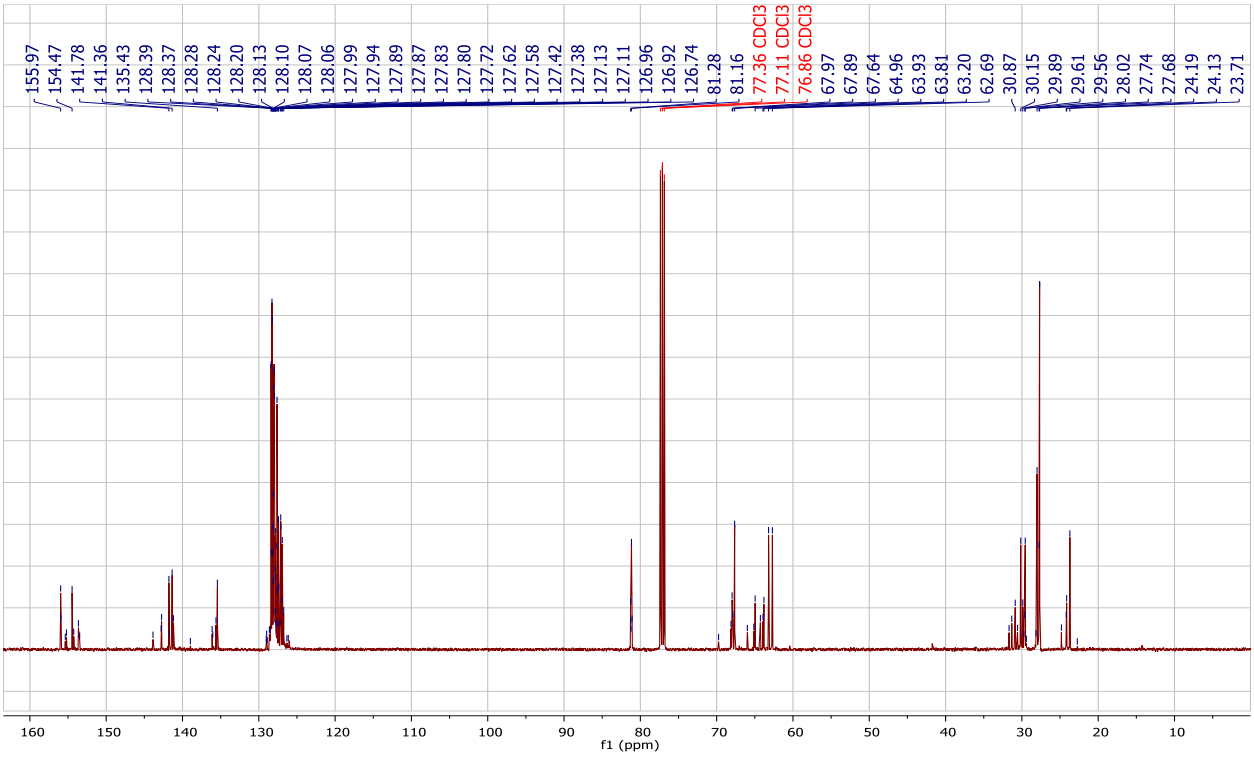
155.97
154.47
141.78
141.36
135.43
128.39
128.37
128.28
128.24
128.20
128.13
128.10
128.07
128.06
127.99
127.94
127.89
127.87
127.83
127.80
127.72
127.62
127.58
127.42
127.38
127.13
127.11
126.96
126.92
126.74
81.28
81.16
77.36 CDCl3
77.11 CDCl3
76.86 CDCl3
67.97
67.89
67.64
64.96
63.93
63.81
63.20
62.69
30.87
30.15
29.89
29.61
29.56
28.02
27.74
27.68
24.19
24.13
23.71
160
150
140
130
120
110
100
90
80
70
60
50
40
30
20
10
f1 (ppm)

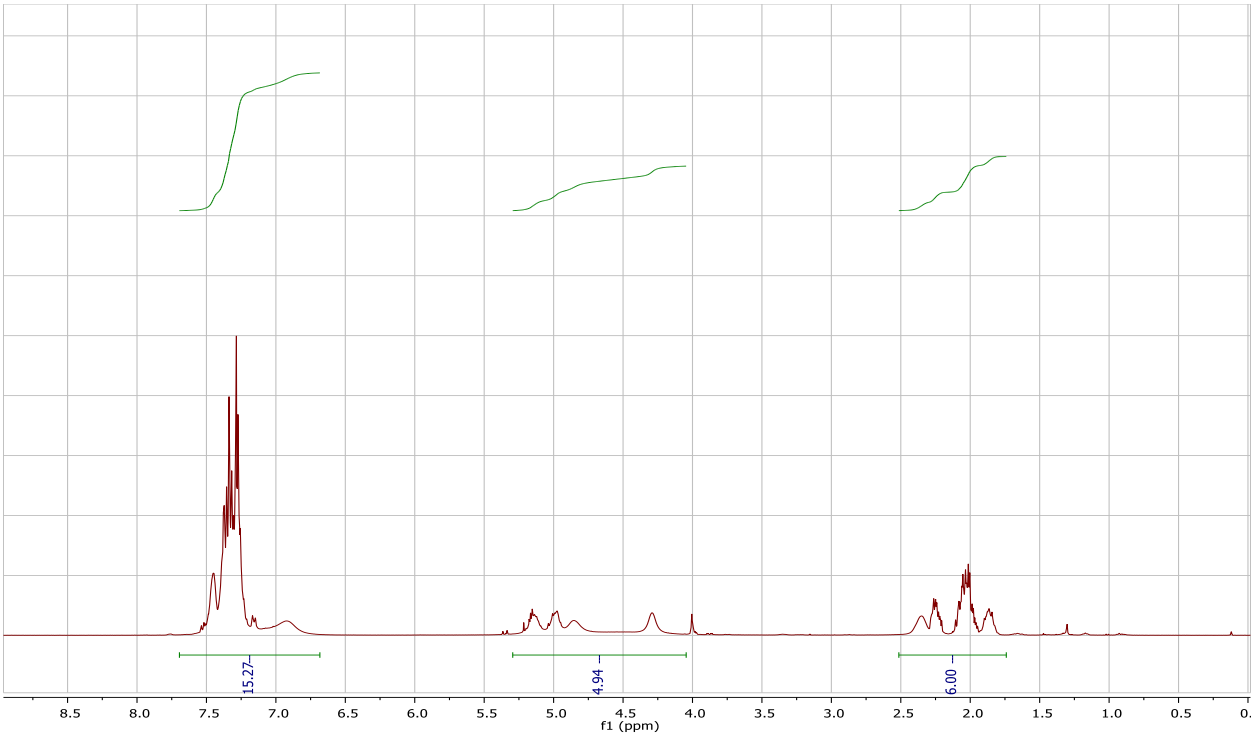
15.27
4.94
6.00
8.5 8.0 7.5 7.0 6.5 6.0 5.5 5.0 4.5 4.0 3.5 3.0 2.5 2.0 1.5 1.0 0.5 0.
f1 (ppm)

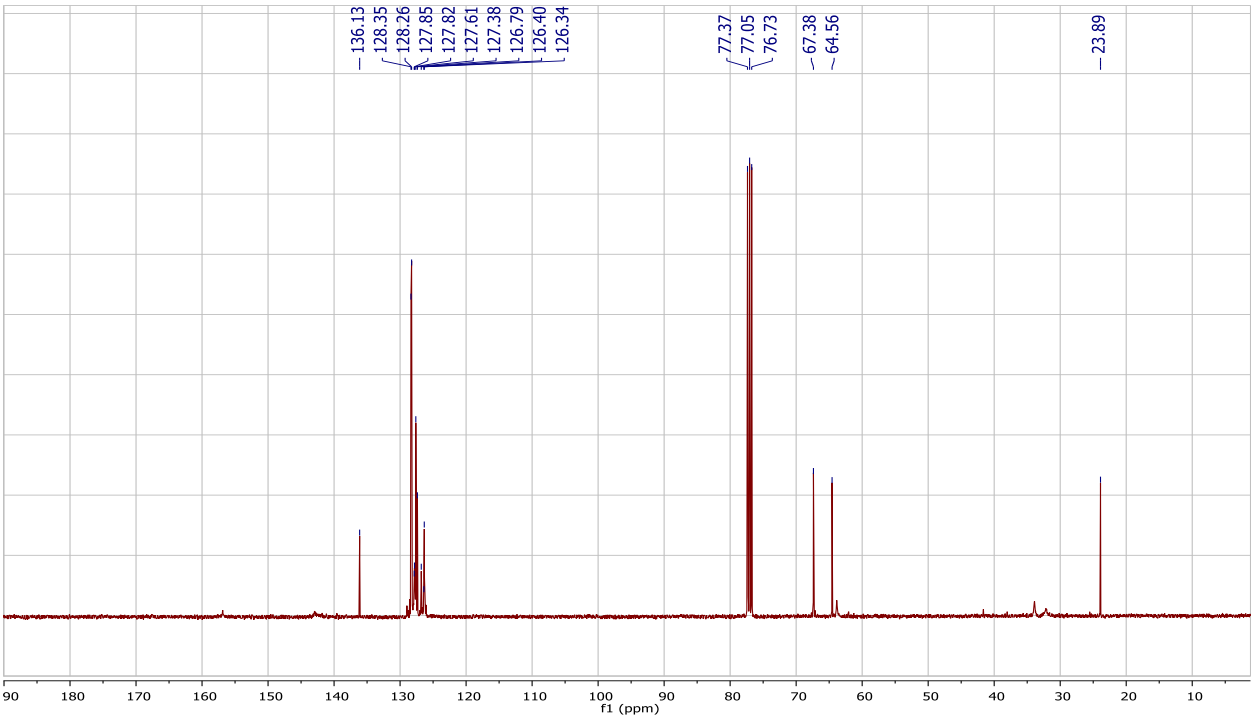
136.13
128.35
128.26
127.85
127.82
127.61
127.38
126.79
126.40
126.34
77.37
77.05
76.73
67.38
64.56
23.89
90 180 170 160 150 140 130 120 110 100 90 80 70 60 50 40 30 20 10
f1 (ppm)

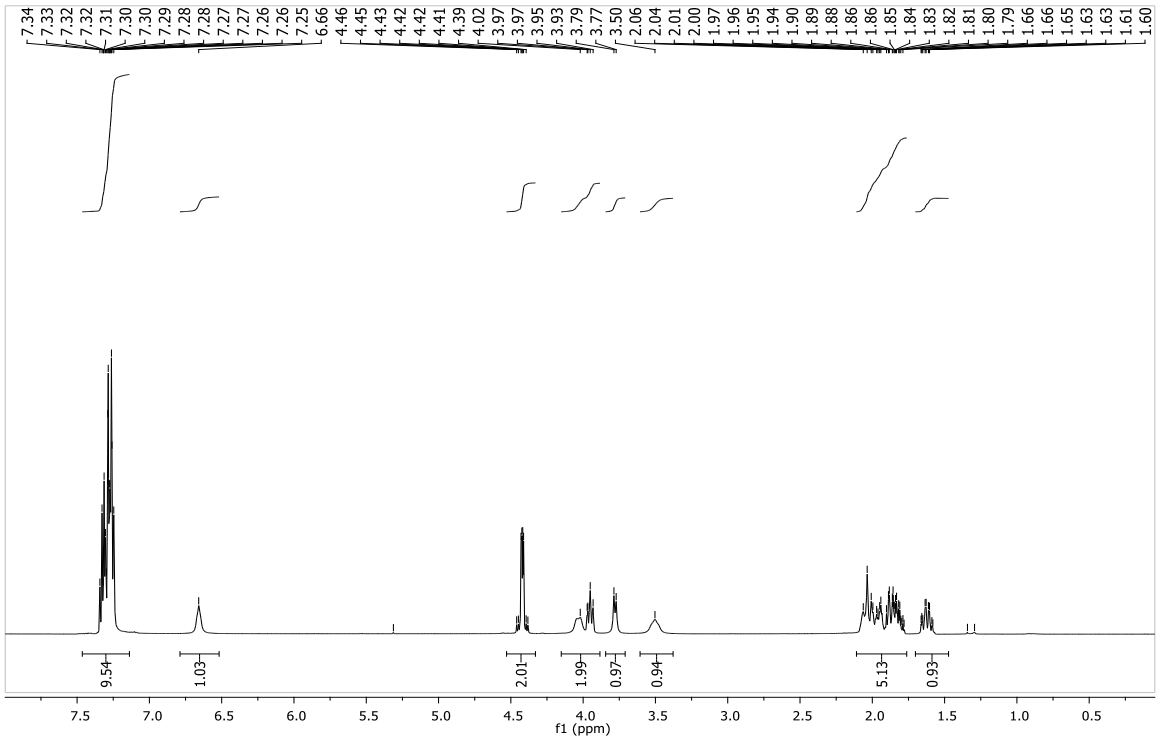
7.34 7.33 7.32 7.32 7.31 7.30 7.30 7.29 7.28 7.28 7.27 7.27 7.26 7.26 7.25 6.66
4.46 4.45 4.43 4.42 4.42 4.41 4.39 4.02 3.97 3.97 3.95 3.93 3.79 3.77 3.50 2.06 2.04 2.01 2.00 1.97 1.96 1.95 1.94 1.90 1.89 1.88 1.86 1.86 1.85 1.84 1.83 1.82 1.81 1.80 1.79 1.66 1.66 1.65 1.63 1.63 1.61 1.60
9.54
1.03
2.01
1.99
0.97
0.94
5.13
0.93
7.5 7.0 6.5 6.0 5.5 5.0 4.5 4.0 3.5 3.0 2.5 2.0 1.5 1.0 0.5
f1 (ppm)

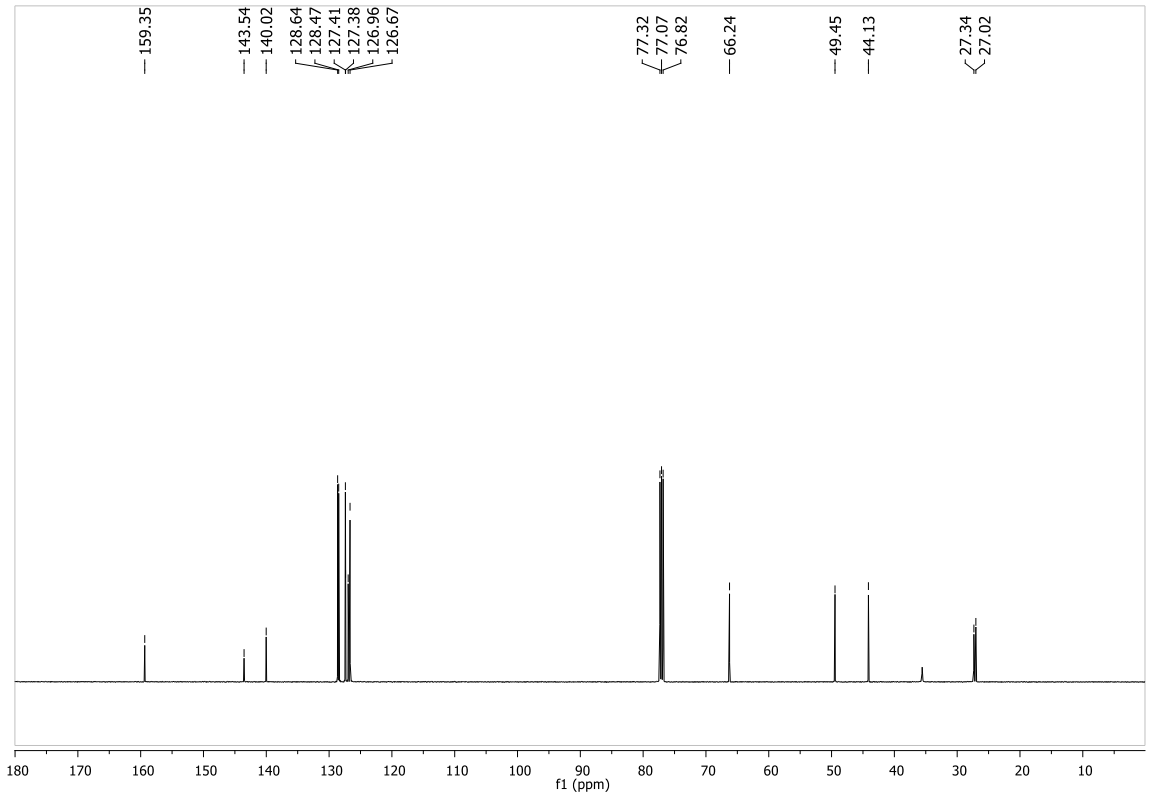
159.35
143.54
140.02
128.64
128.47
127.41
127.38
126.96
126.67
77.32
77.07
76.82
66.24
49.45
44.13
27.34
27.02
180 170 160 150 140 130 120 110 100 90 80 70 60 50 40 30 20 10
f1 (ppm)

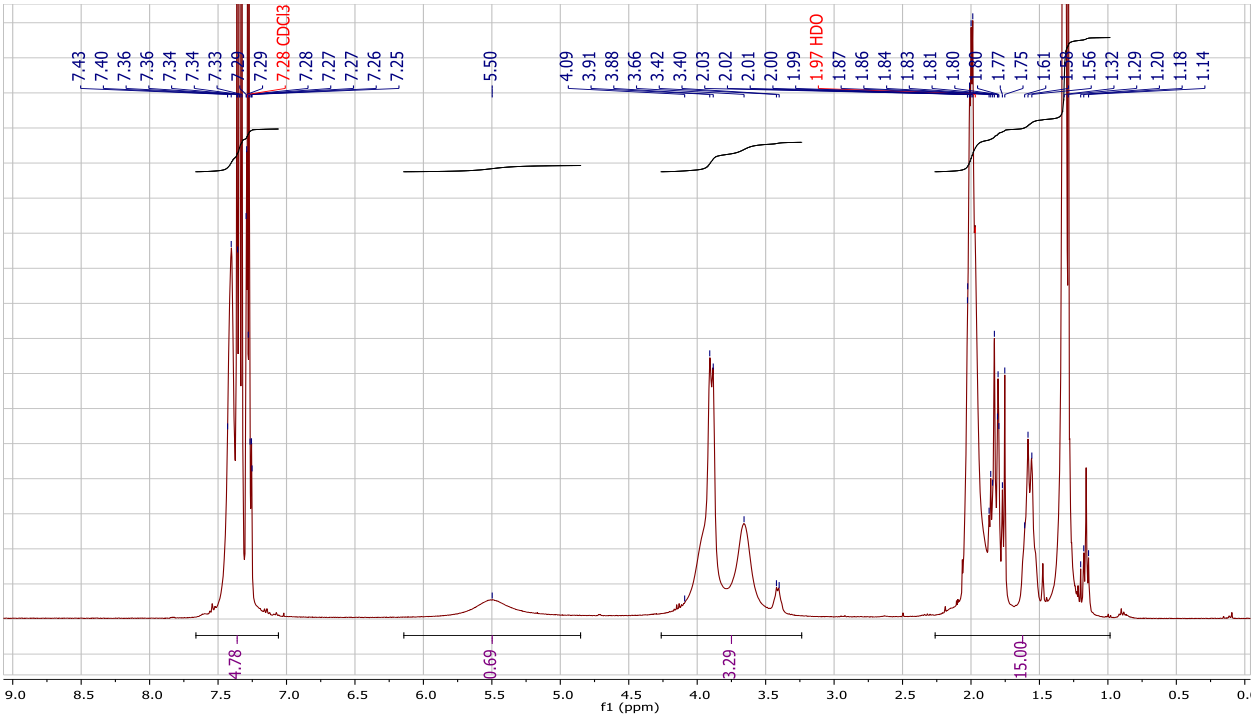
7.43
7.40
7.36
7.36
7.34
7.34
7.33
7.29
7.29
7.28 CDCl3
7.28
7.27
7.27
7.26
7.25
5.50
4.09
3.91
3.88
3.66
3.42
3.40
2.03
2.02
2.01
2.00
1.99
1.97 HDO
1.87
1.86
1.84
1.83
1.81
1.80
1.80
1.77
1.75
1.61
1.56
1.56
1.32
1.29
1.20
1.18
1.14
4.78
0.69
3.29
15.00
f1 (ppm)

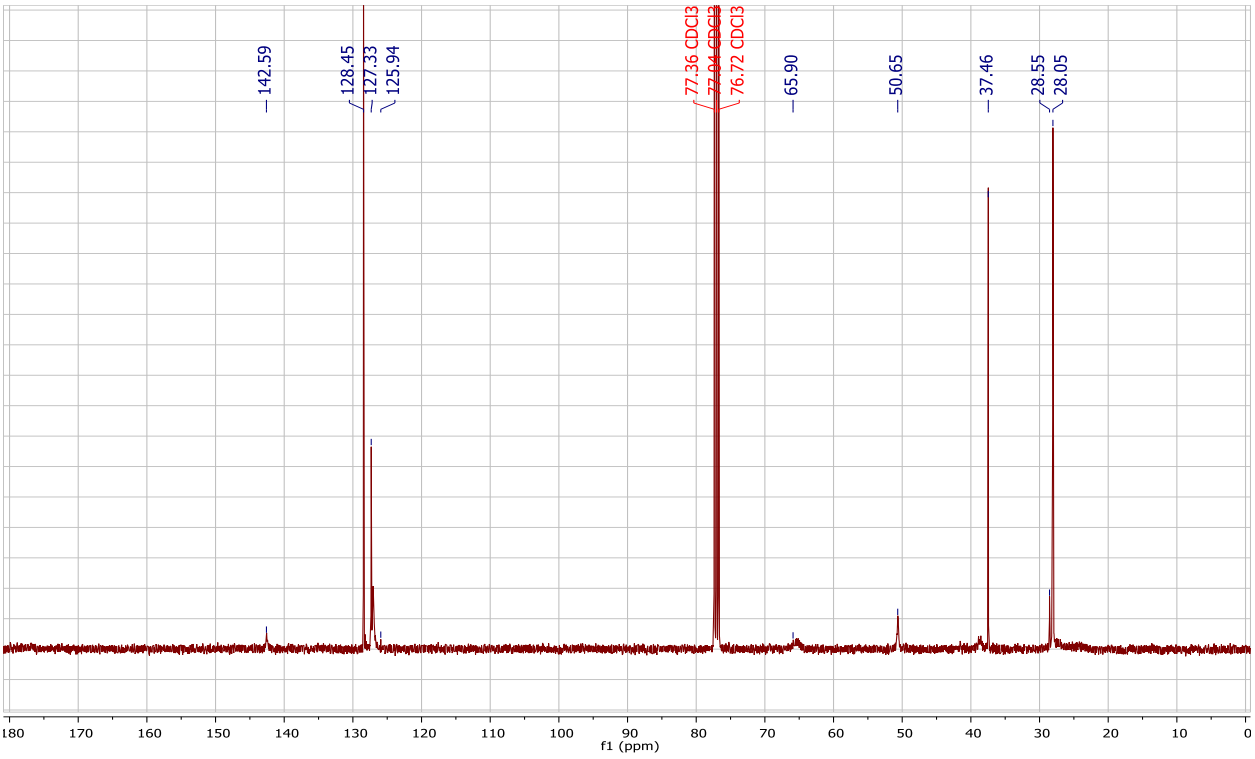
142.59
128.45
127.33
125.94
77.36 CDCl3
77.04 CDCl3
76.72 CDCl3
65.90
50.65
37.46
28.55
28.05
f1 (ppm)

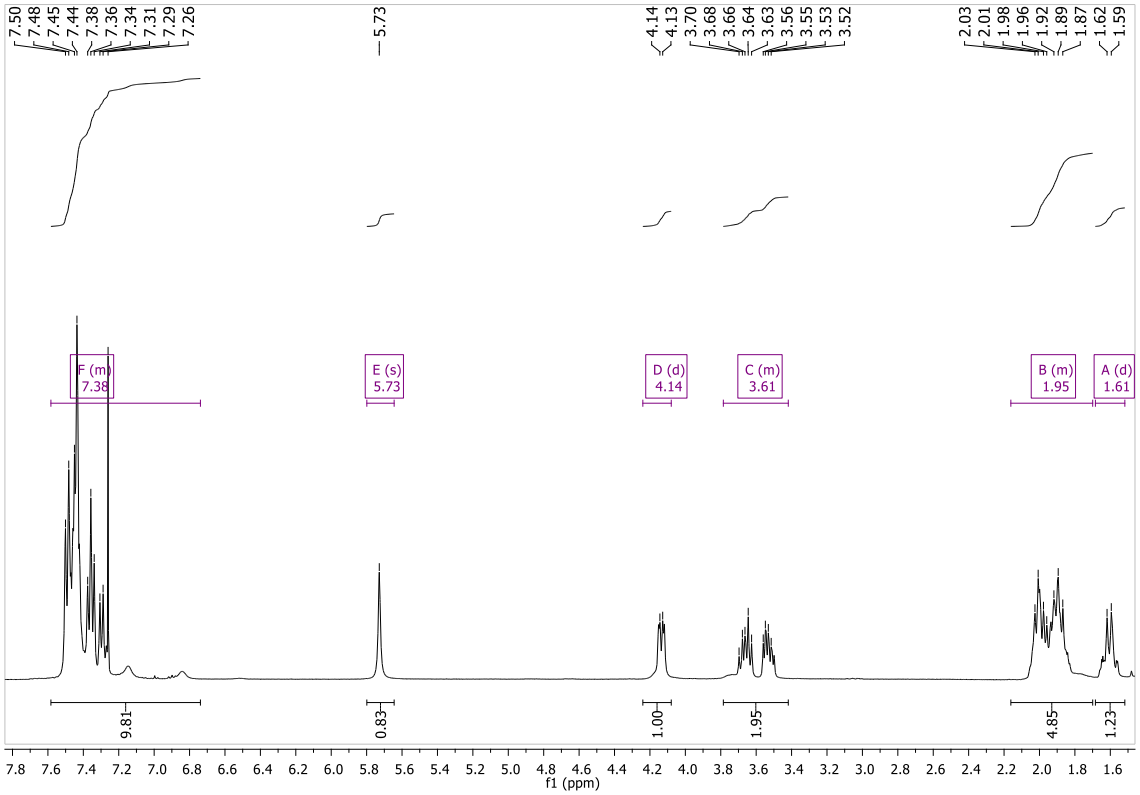
7.50
7.48
7.45
7.44
7.38
7.36
7.34
7.31
7.29
7.26
5.73
4.14
4.13
3.70
3.68
3.66
3.64
3.63
3.56
3.55
3.53
3.52
2.03
2.01
1.98
1.96
1.92
1.89
1.87
1.62
1.59
F (m) 7.38
E (s) 5.73
D (d) 4.14
C (m) 3.61
B (m) 1.95
A (d) 1.61
9.81
0.83
1.00
1.95
4.85
1.23
f1 (ppm)

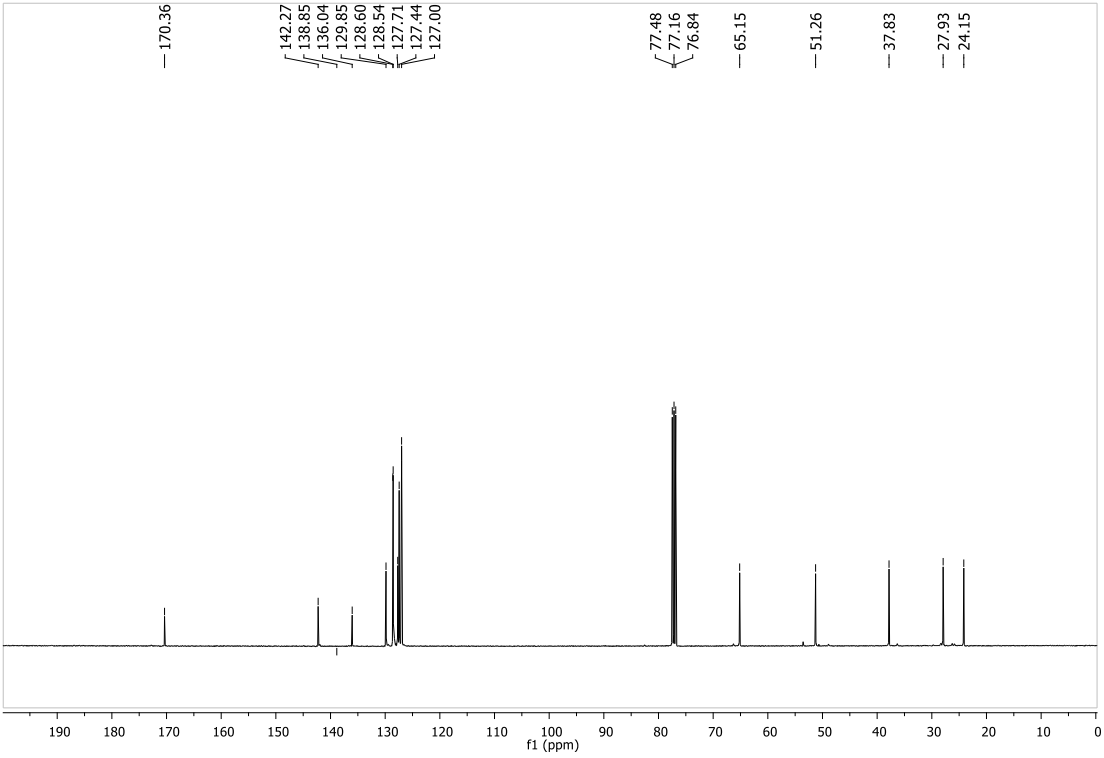
170.36
142.27
138.85
136.04
129.85
128.60
128.54
127.71
127.44
127.00
77.48
77.16
76.84
65.15
51.26
37.83
27.93
24.15
f1 (ppm)

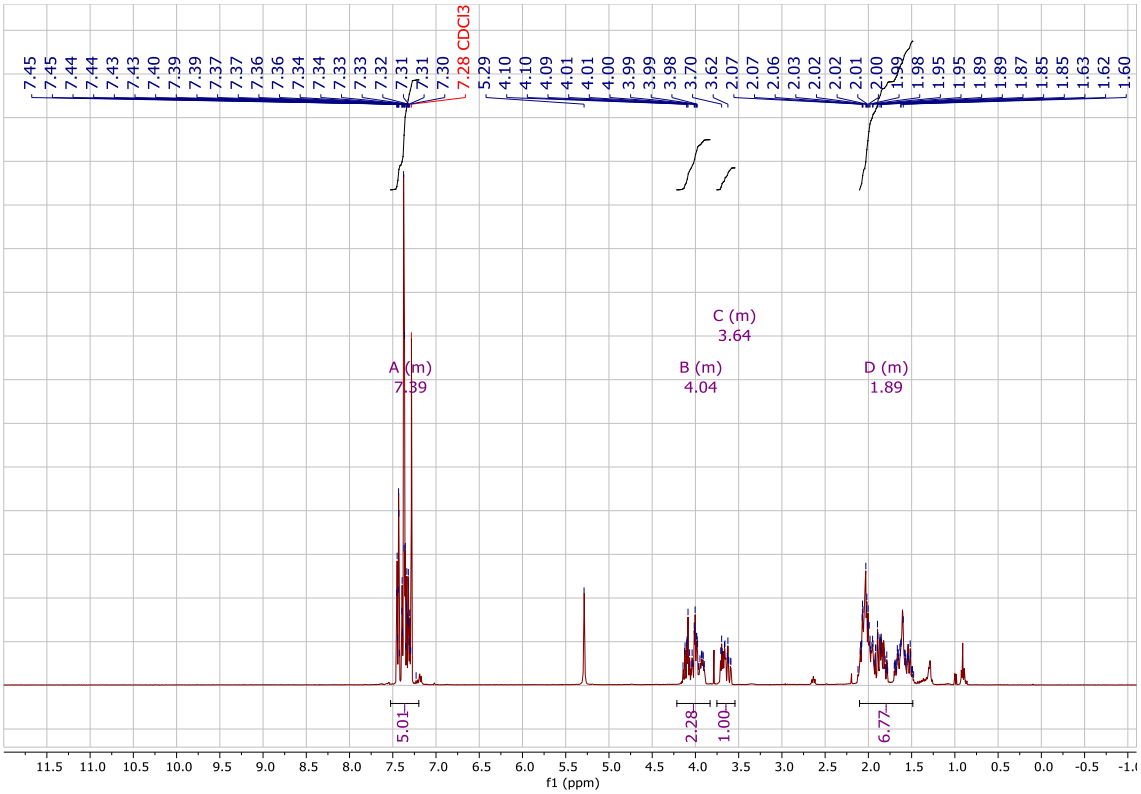
7.45 7.45 7.44 7.44 7.43 7.43 7.40 7.39 7.39 7.37 7.37 7.36 7.36 7.34 7.34 7.33 7.33 7.32 7.31 7.31 7.30 7.28 CDCl3 5.29 4.10 4.10 4.09 4.01 4.01 4.00 3.99 3.99 3.98 3.70 3.62 2.07 2.07 2.06 2.03 2.02 2.02 2.01 2.00 1.99 1.98 1.95 1.95 1.89 1.89 1.87 1.85 1.85 1.63 1.62 1.60
A (m) 7.39
B (m) 4.04
C (m) 3.64
D (m) 1.89
5.01
2.28
1.00
6.77
f1 (ppm)

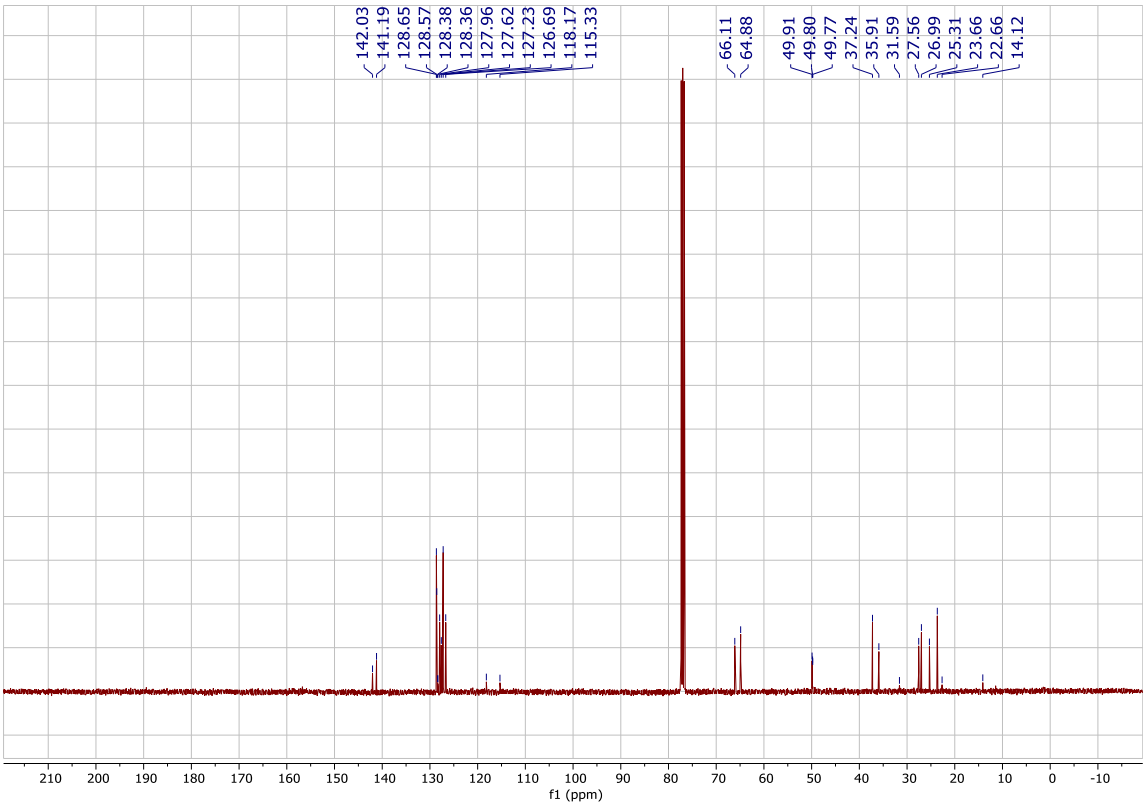
142.03 141.19 128.65 128.57 128.38 128.36 127.96 127.62 127.23 126.69 118.17 115.33
66.11 64.88 49.91 49.80 49.77 37.24 35.91 31.59 27.56 26.99 25.31 23.66 22.66 14.12
f1 (ppm)

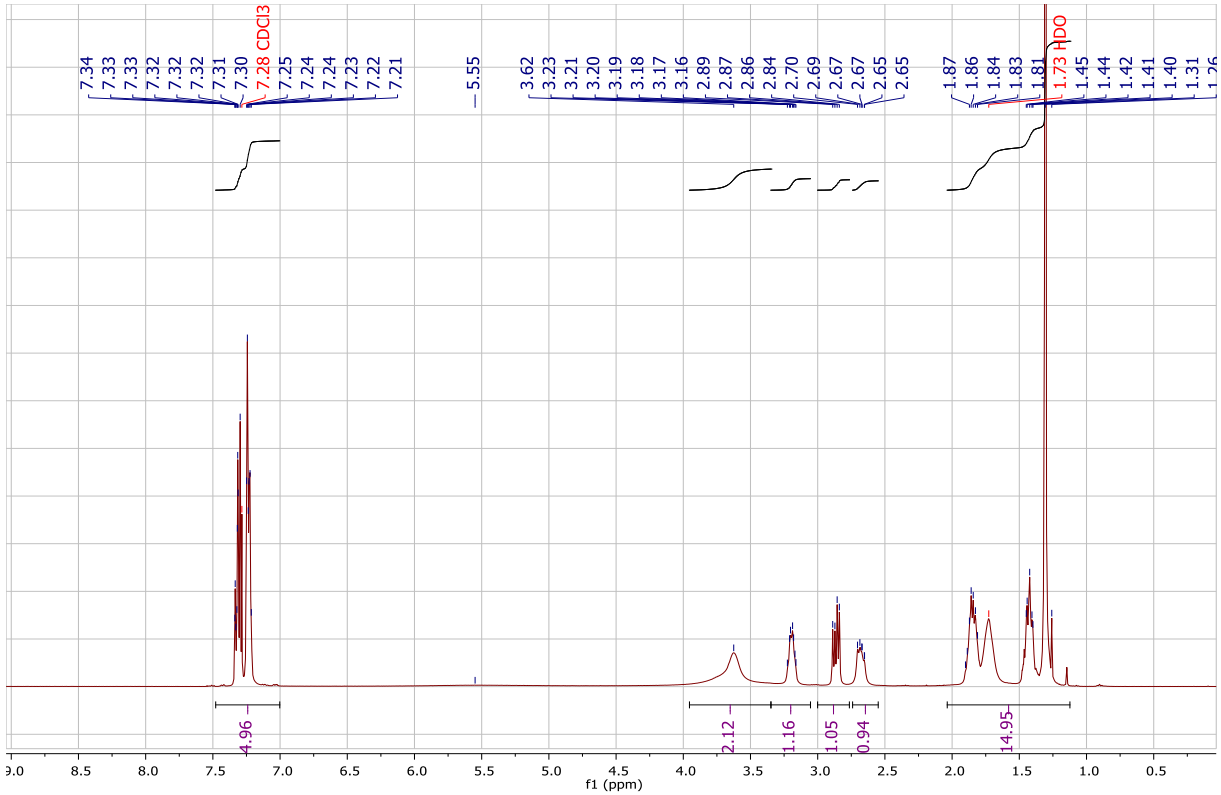
7.34
7.33
7.33
7.32
7.32
7.32
7.31
7.30
7.28 CDCl3
7.25
7.24
7.24
7.23
7.22
7.21
5.55
3.62
3.23
3.21
3.20
3.19
3.18
3.17
3.16
2.89
2.87
2.86
2.84
2.70
2.69
2.67
2.67
2.65
2.65
1.87
1.86
1.84
1.83
1.81
1.73 HDO
1.45
1.44
1.42
1.41
1.40
1.31
4.96
2.12
1.16
1.05
0.94
14.95
f1 (ppm)

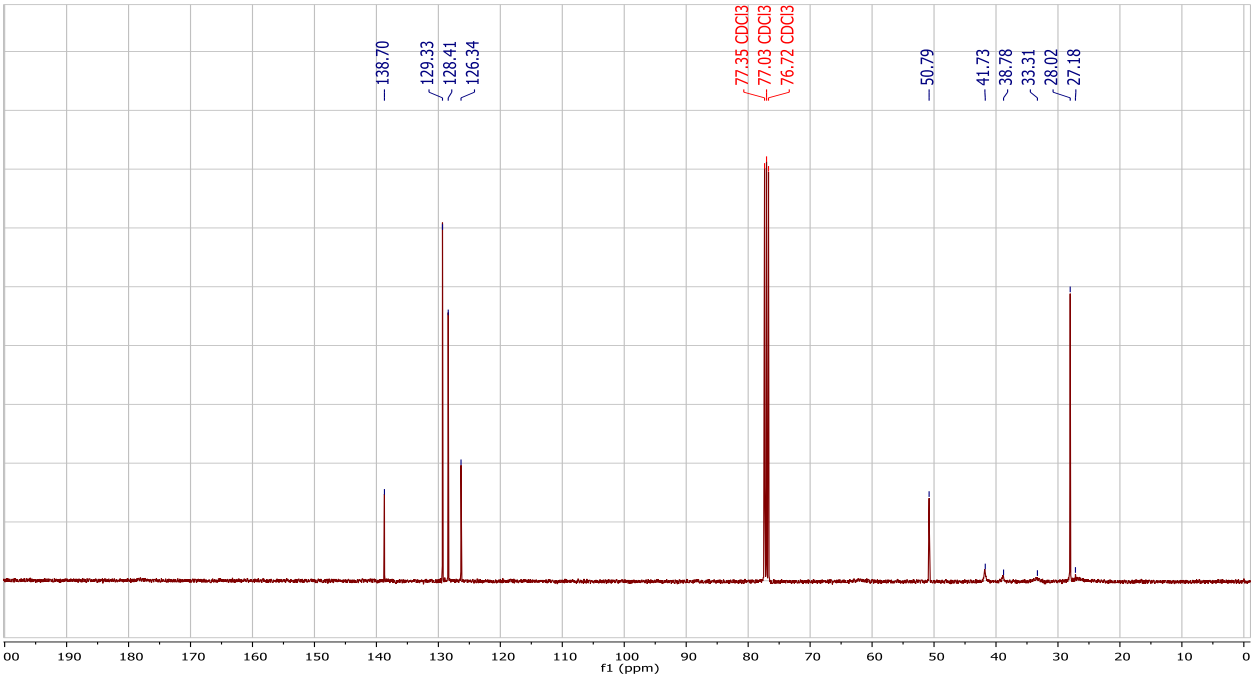
138.70
129.33
128.41
126.34
77.35 CDCl3
77.03 CDCl3
76.72 CDCl3
50.79
41.73
38.78
33.31
28.02
27.18
f1 (ppm)

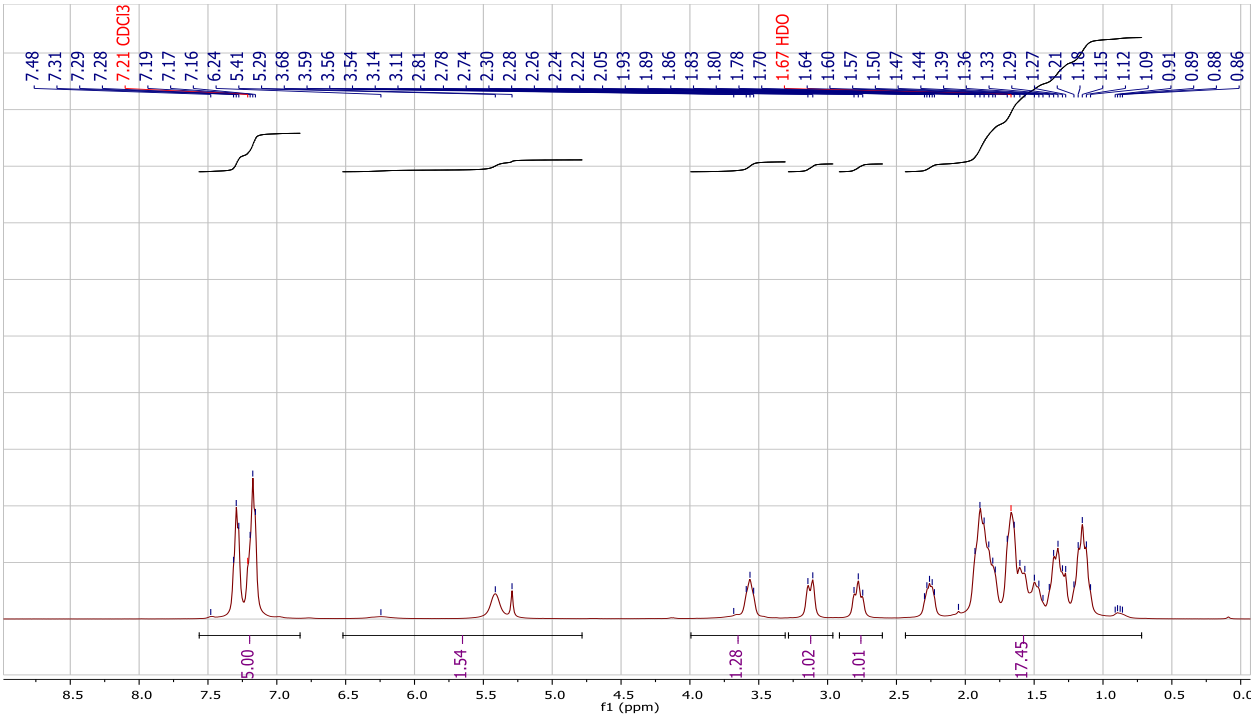
7.48
7.31
7.29
7.28
7.21 CDCl3
7.19
7.17
7.16
6.24
5.41
5.29
3.68
3.59
3.56
3.54
3.14
3.11
2.81
2.78
2.74
2.30
2.28
2.26
2.24
2.22
2.05
1.93
1.89
1.86
1.83
1.80
1.78
1.70
1.67 HDO
1.64
1.60
1.57
1.50
1.47
1.44
1.39
1.36
1.33
1.29
1.27
1.21
1.18
1.15
1.12
1.09
0.91
0.89
0.88
0.86
5.00
1.54
1.28
1.02
1.01
17.45
f1 (ppm)

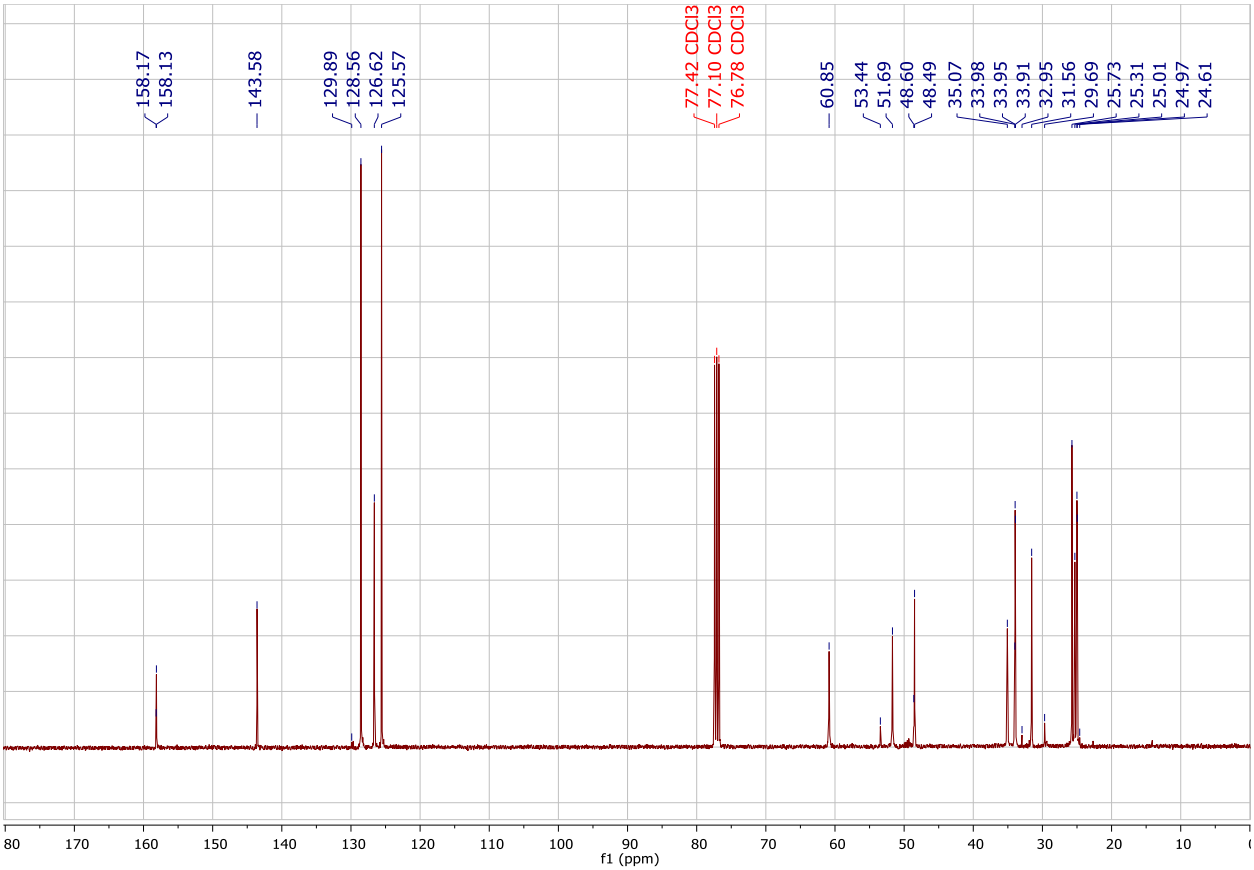
158.17
158.13
143.58
129.89
128.56
126.62
125.57
77.42 CDCl3
77.10 CDCl3
76.78 CDCl3
60.85
53.44
51.69
48.60
48.49
35.07
33.98
33.95
33.91
32.95
31.56
29.69
25.73
25.31
25.01
24.97
24.61
f1 (ppm)


4.90
5.00
6.07
6.47
7.5
7.0
6.5
6.0
5.5
5.0
4.5
4.0
3.5
3.0
2.5
2.0
1.5
1.0
f1 (ppm)

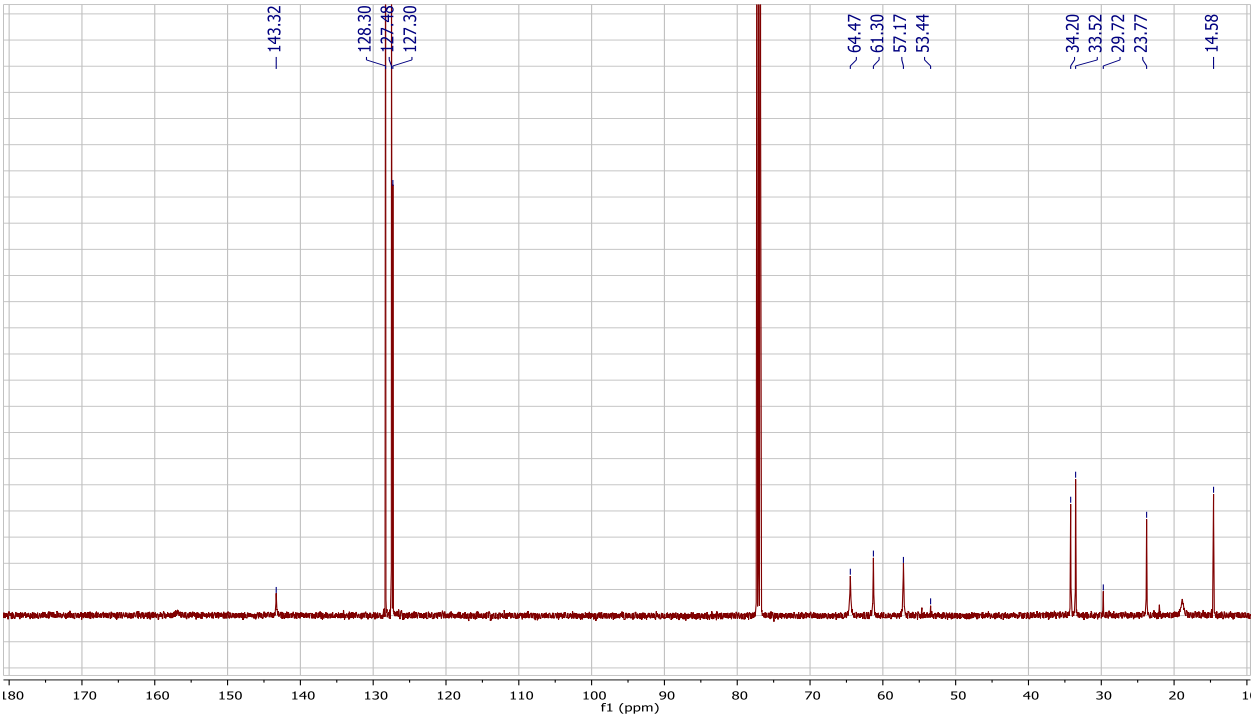
143.32
128.30
127.48
127.30
64.47
61.30
57.17
53.44
34.20
33.52
29.72
23.77
14.58
180
170
160
150
140
130
120
110
100
90
80
70
60
50
40
30
20
f1 (ppm)

281 (at 87 °C)

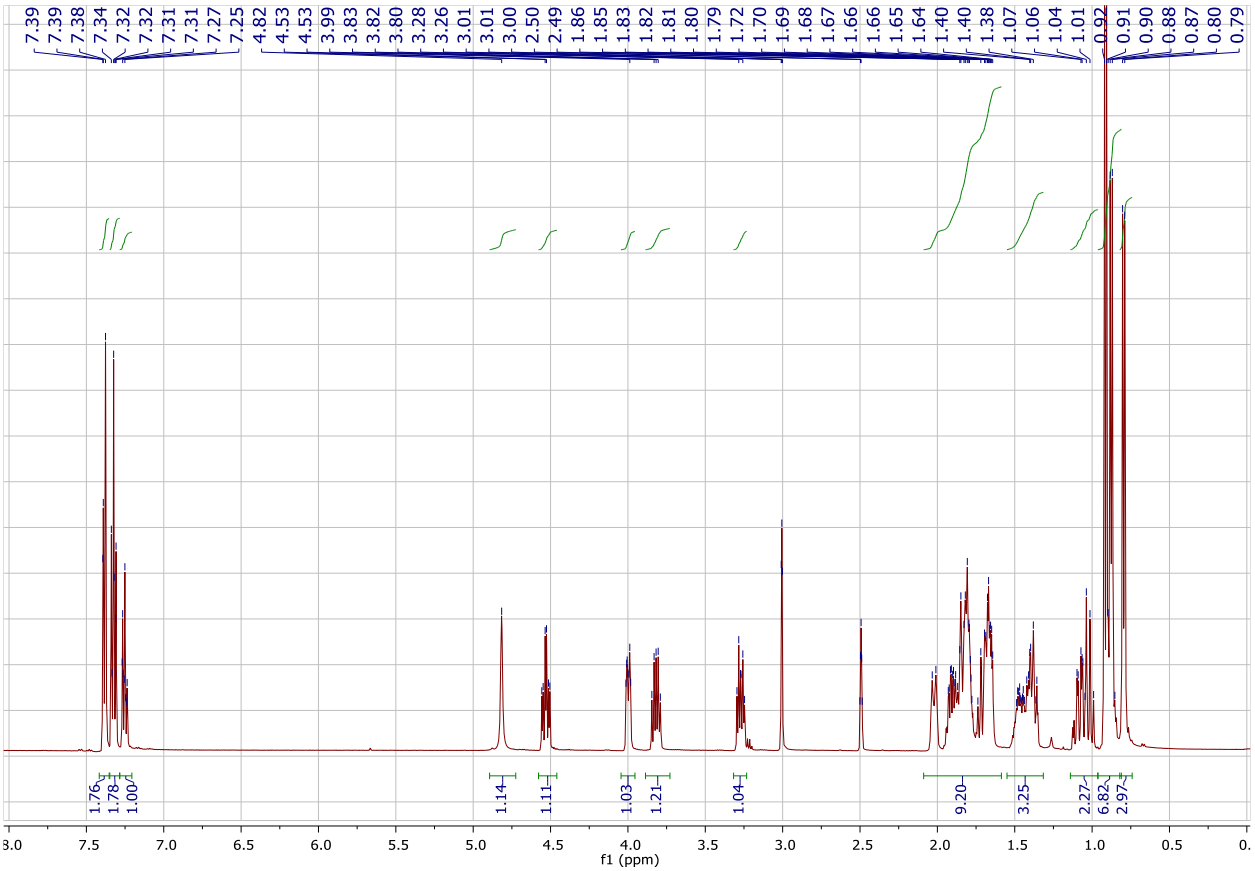
7.39
7.39
7.38
7.34
7.32
7.32
7.31
7.31
7.27
7.25
4.82
4.53
4.53
3.99
3.83
3.82
3.80
3.28
3.26
3.01
3.01
3.00
2.50
2.49
1.86
1.85
1.83
1.82
1.81
1.80
1.79
1.72
1.70
1.69
1.68
1.67
1.66
1.66
1.65
1.64
1.40
1.40
1.38
1.07
1.06
1.04
1.01
0.92
0.91
0.90
0.88
0.87
0.80
0.79
1.76
1.78
1.00
1.14
1.11
1.03
1.21
1.04
9.20
3.25
2.27
6.82
2.97
f1 (ppm)

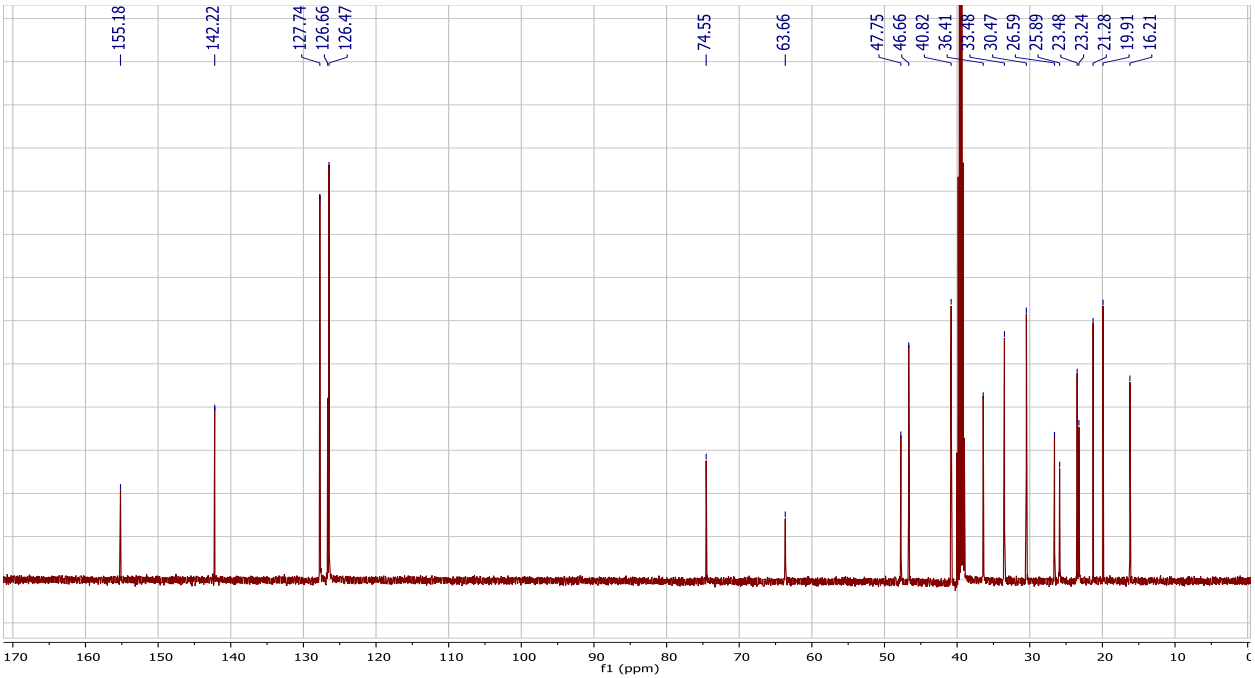
155.18
142.22
127.74
126.66
126.47
74.55
63.66
47.75
46.66
40.82
36.41
33.48
30.47
26.59
25.89
23.48
23.24
21.28
19.91
16.21
f1 (ppm)

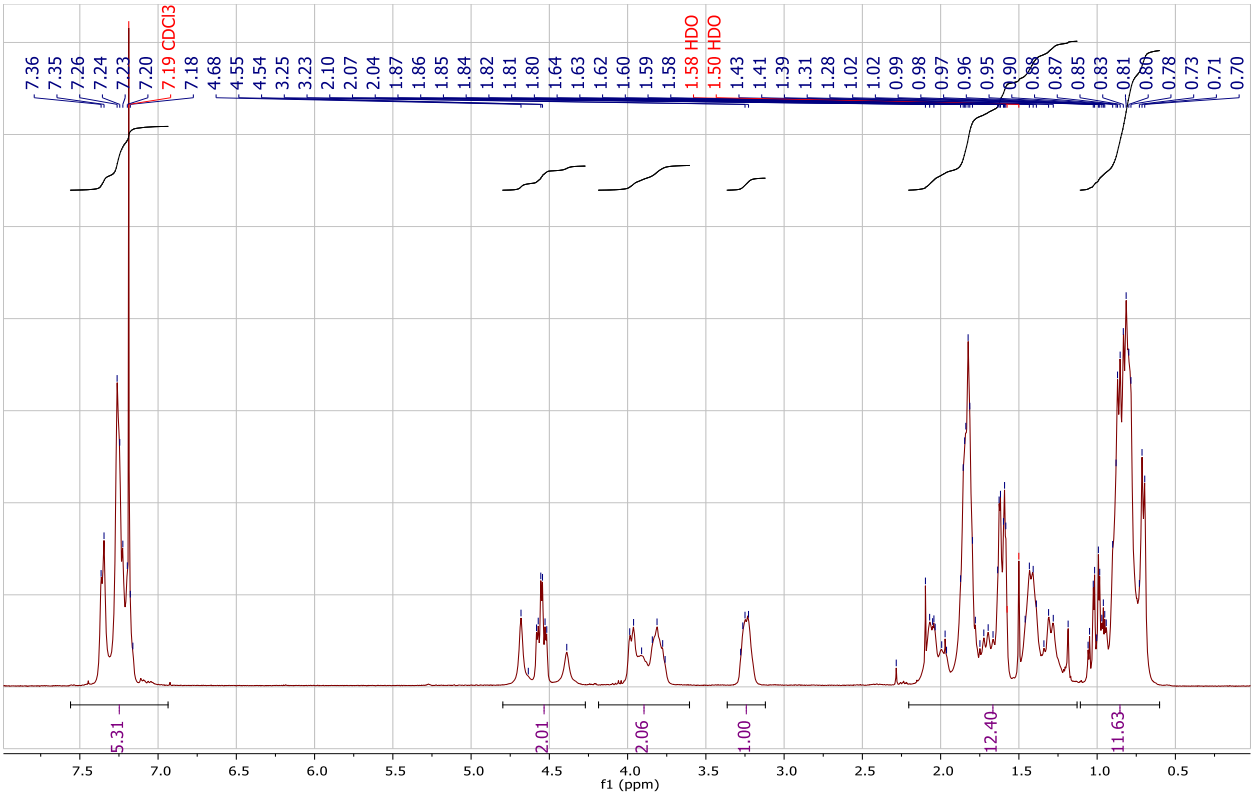
7.36
7.35
7.26
7.24
7.23
7.20
7.19 CDCl3
7.18
4.68
4.55
4.54
3.25
3.23
2.10
2.07
2.04
1.87
1.86
1.85
1.84
1.82
1.81
1.80
1.64
1.63
1.62
1.60
1.59
1.58
1.58 HDO
1.50 HDO
1.43
1.41
1.39
1.31
1.28
1.02
1.02
0.99
0.98
0.97
0.96
0.95
0.90
0.88
0.87
0.85
0.83
0.81
0.80
0.78
0.73
0.71
0.70
5.31
2.01
2.06
1.00
12.40
11.63
f1 (ppm)

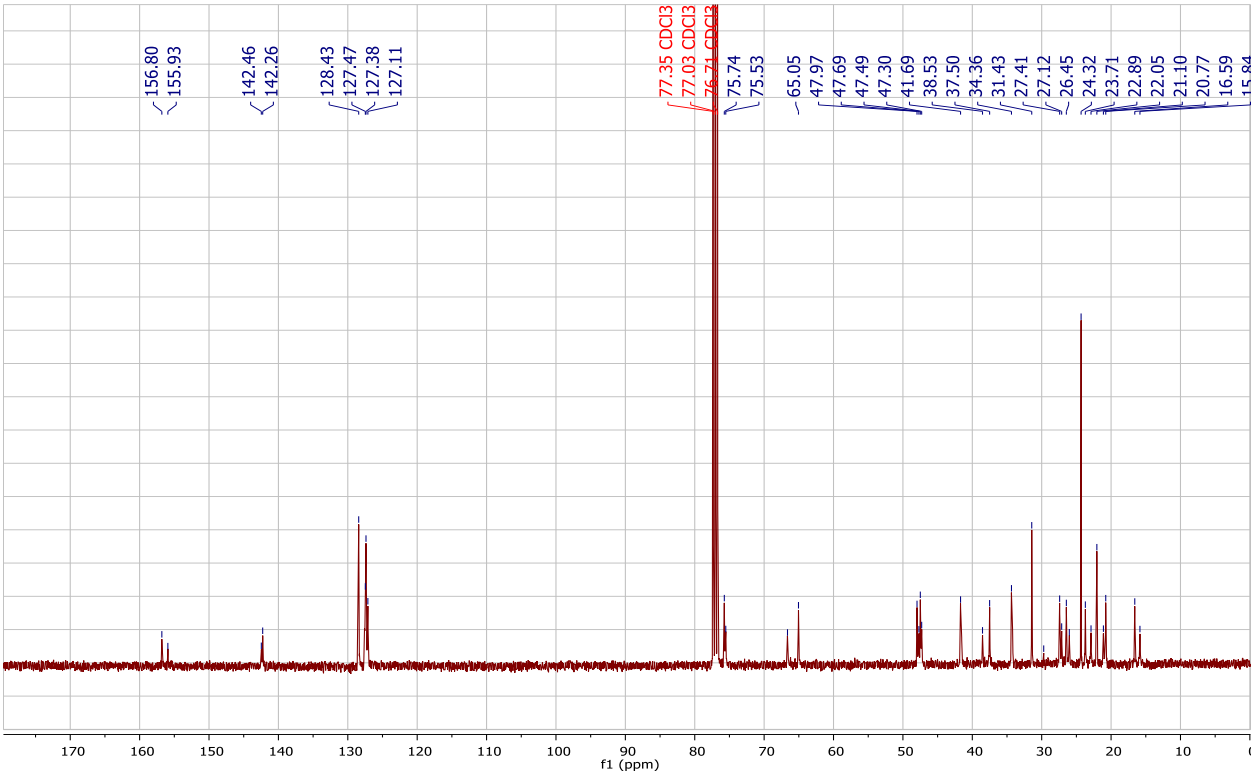
156.80
155.93
142.46
142.26
128.43
127.47
127.38
127.11
77.35 CDCl3
77.03 CDCl3
76.71 CDCl3
75.74
75.53
65.05
47.97
47.69
47.49
47.30
41.69
38.53
37.50
34.36
31.43
27.41
27.12
26.45
24.32
23.71
22.89
22.05
21.10
20.77
16.59
f1 (ppm)

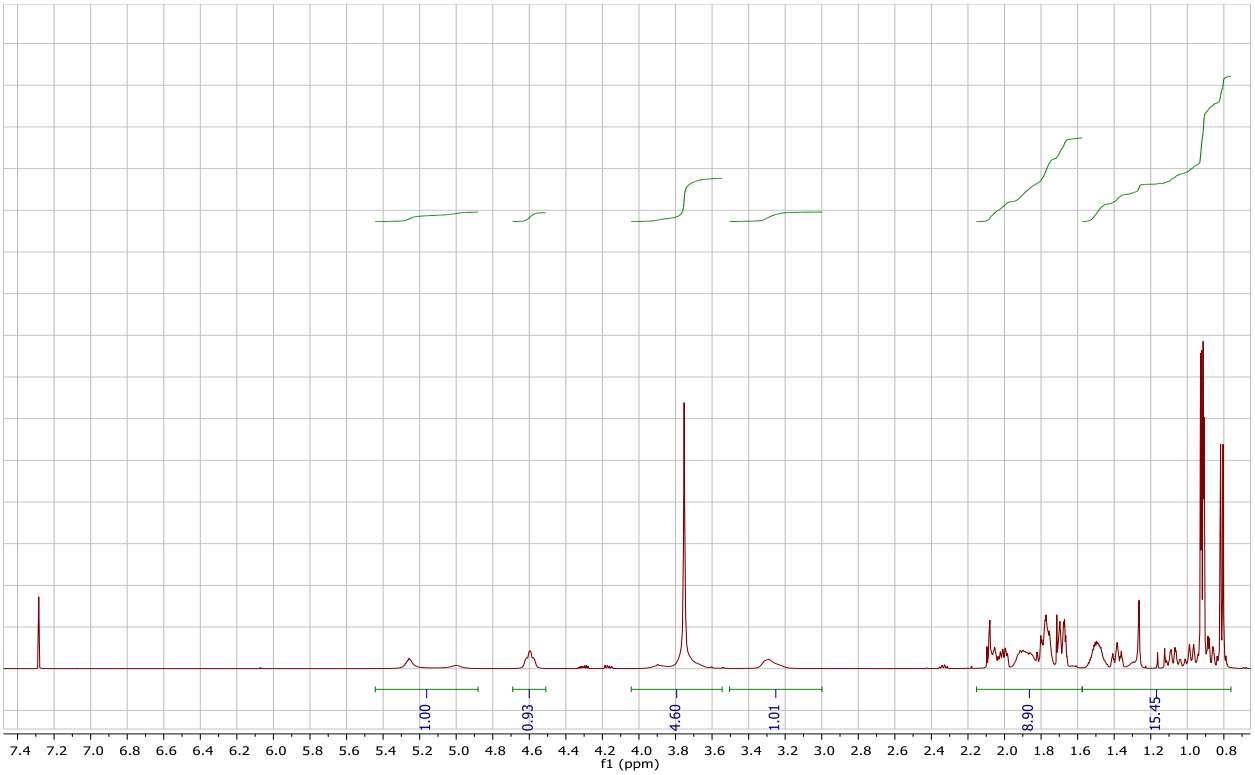
1.00
0.93
4.60
1.01
8.90
15.45
f1 (ppm)

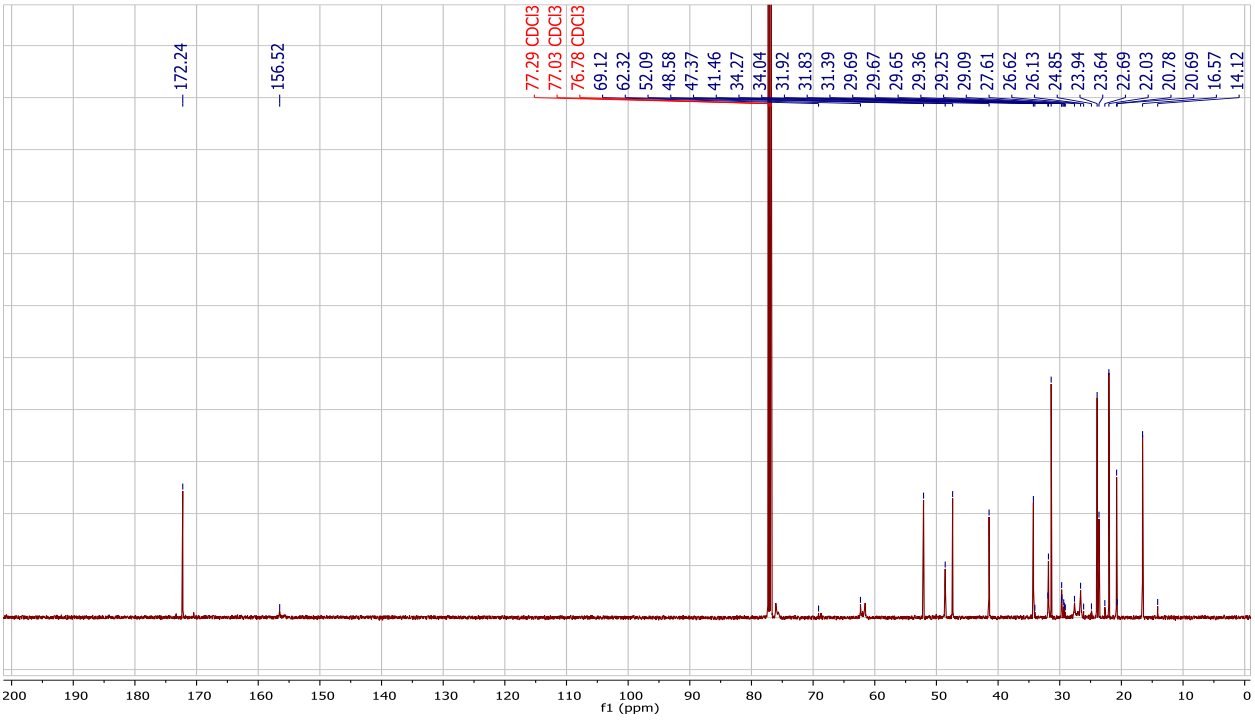
172.24
156.52
77.29 CDCl3
77.03 CDCl3
76.78 CDCl3
69.12
62.32
52.09
48.58
47.37
41.46
34.27
34.04
31.92
31.83
31.39
29.69
29.67
29.65
29.36
29.25
29.09
27.61
26.62
26.13
24.85
23.94
23.64
22.69
22.03
20.78
20.69
16.57
14.12
f1 (ppm)

Diels-Alder Products

157

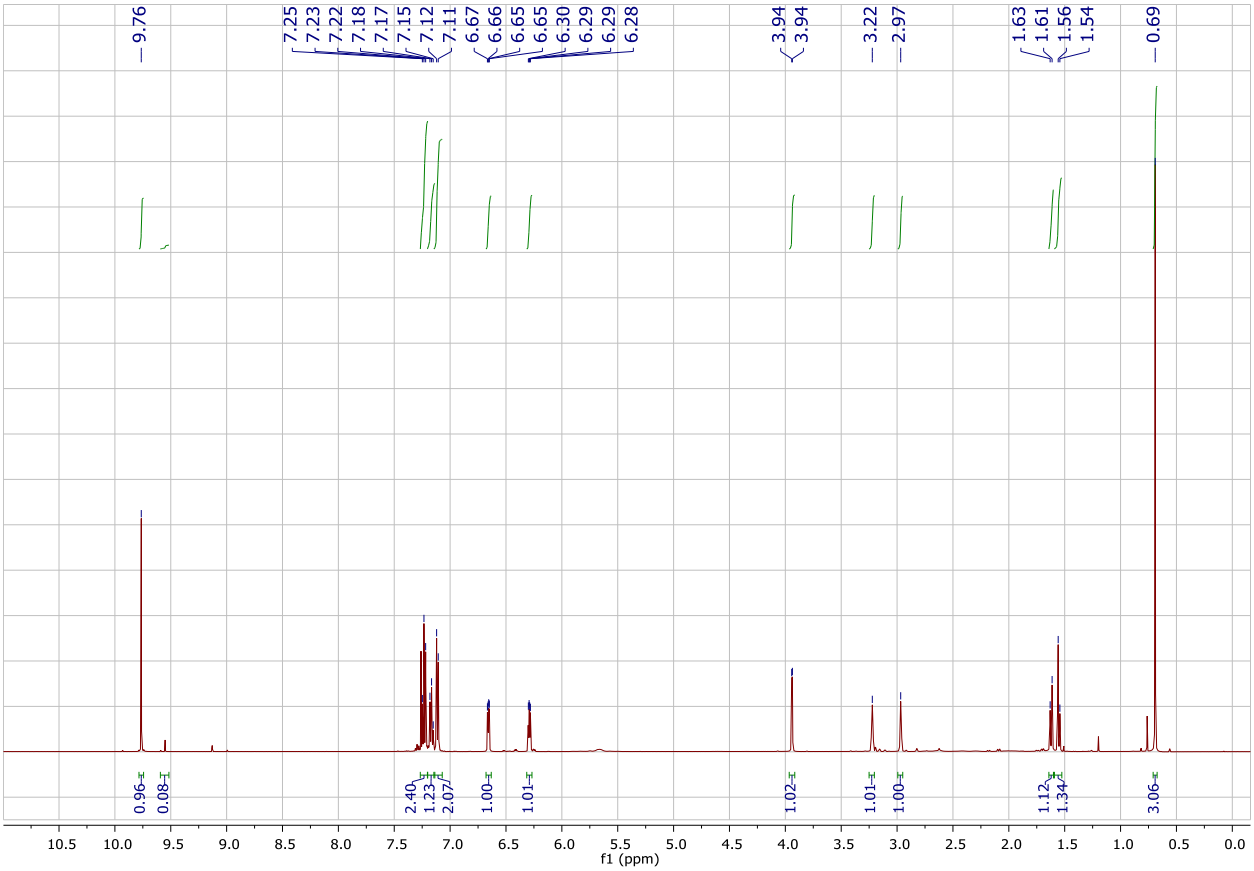

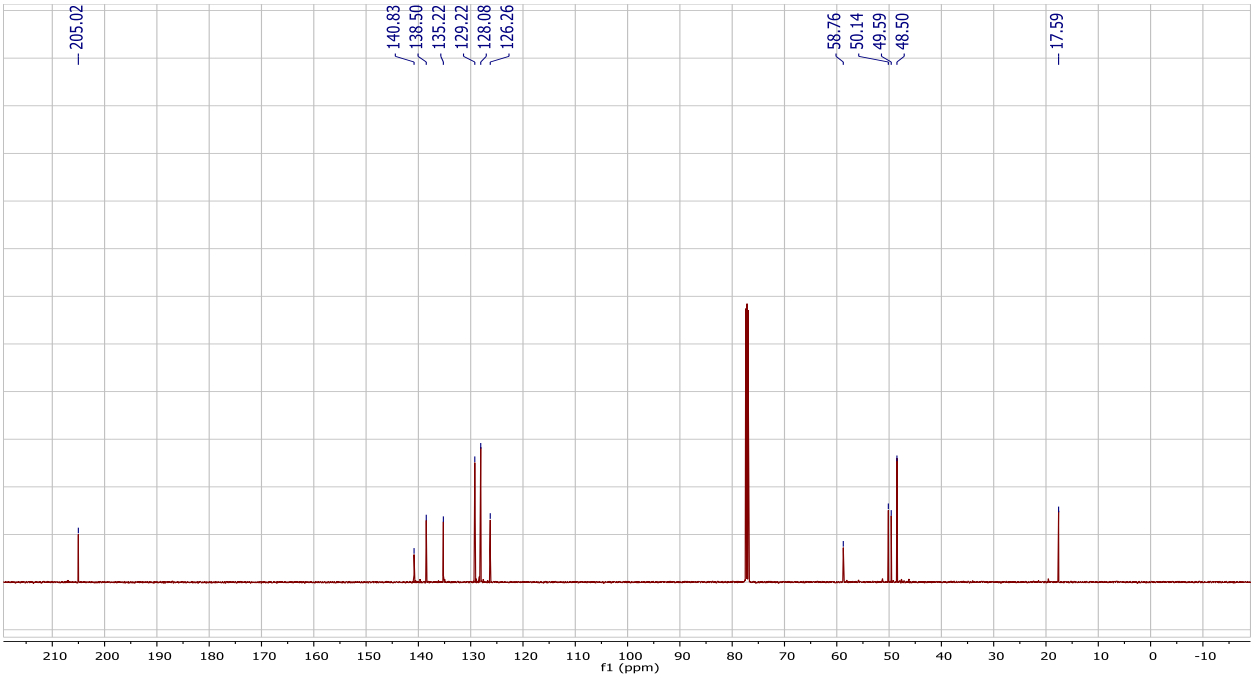

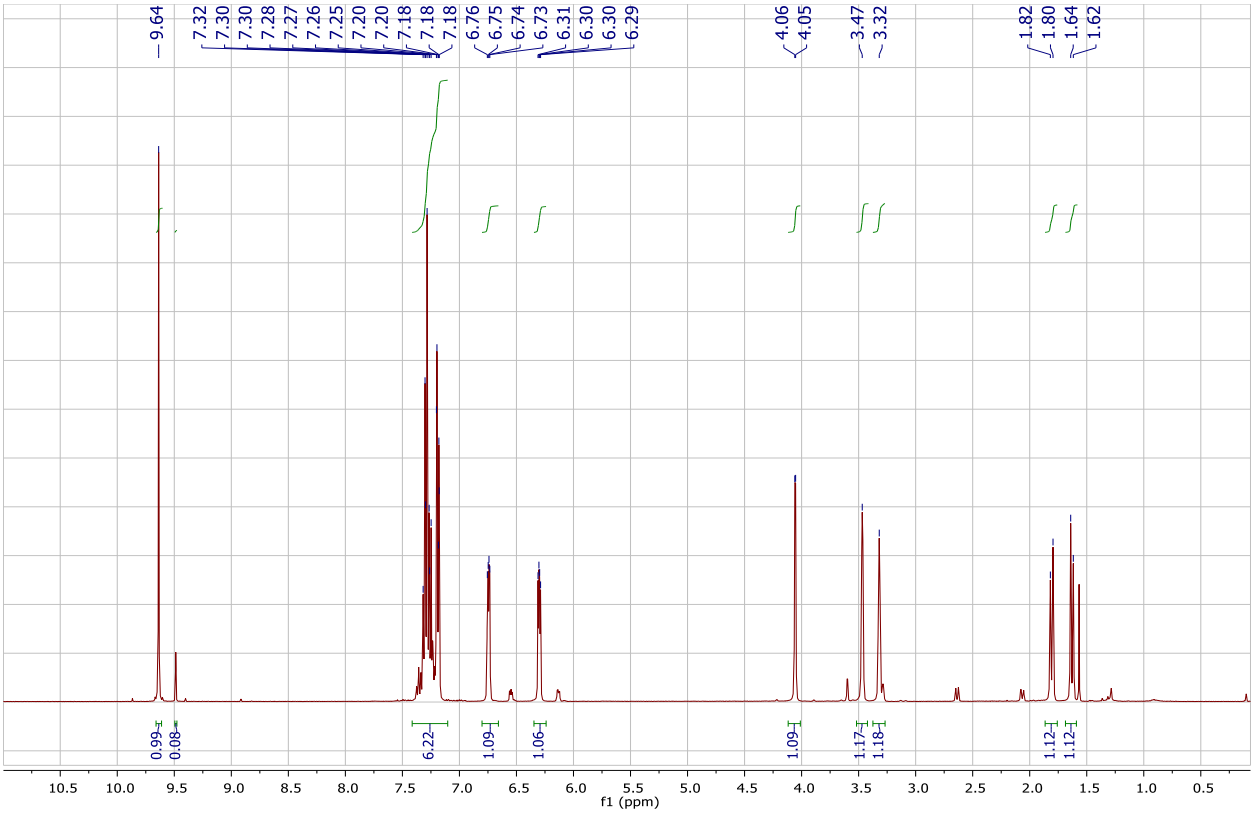
9.64
7.32
7.30
7.30
7.28
7.27
7.26
7.25
7.20
7.20
7.18
7.18
7.18
6.76
6.75
6.74
6.73
6.31
6.30
6.30
6.29
4.06
4.05
3.47
3.32
1.82
1.80
1.64
1.62
0.99
0.08
6.22
1.09
1.06
1.09
1.17
1.18
1.12
1.12
f1 (ppm)

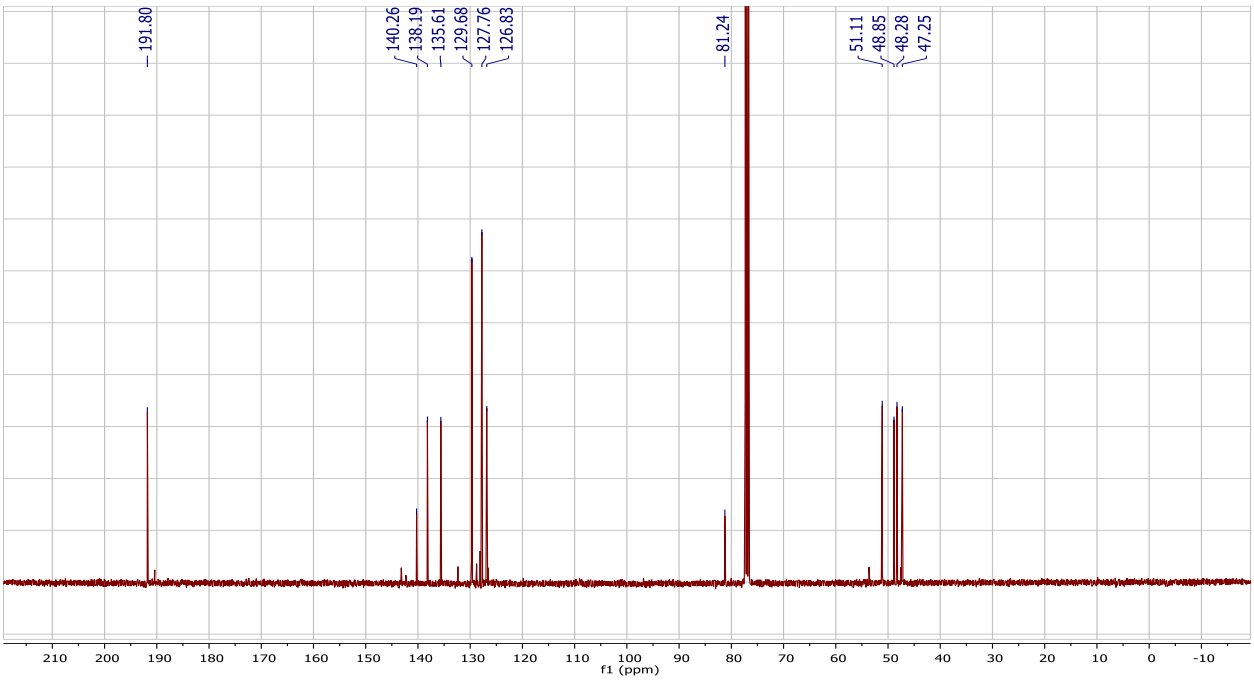
191.80
140.26
138.19
135.61
129.68
127.76
126.83
81.24
51.11
48.85
48.28
47.25
f1 (ppm)

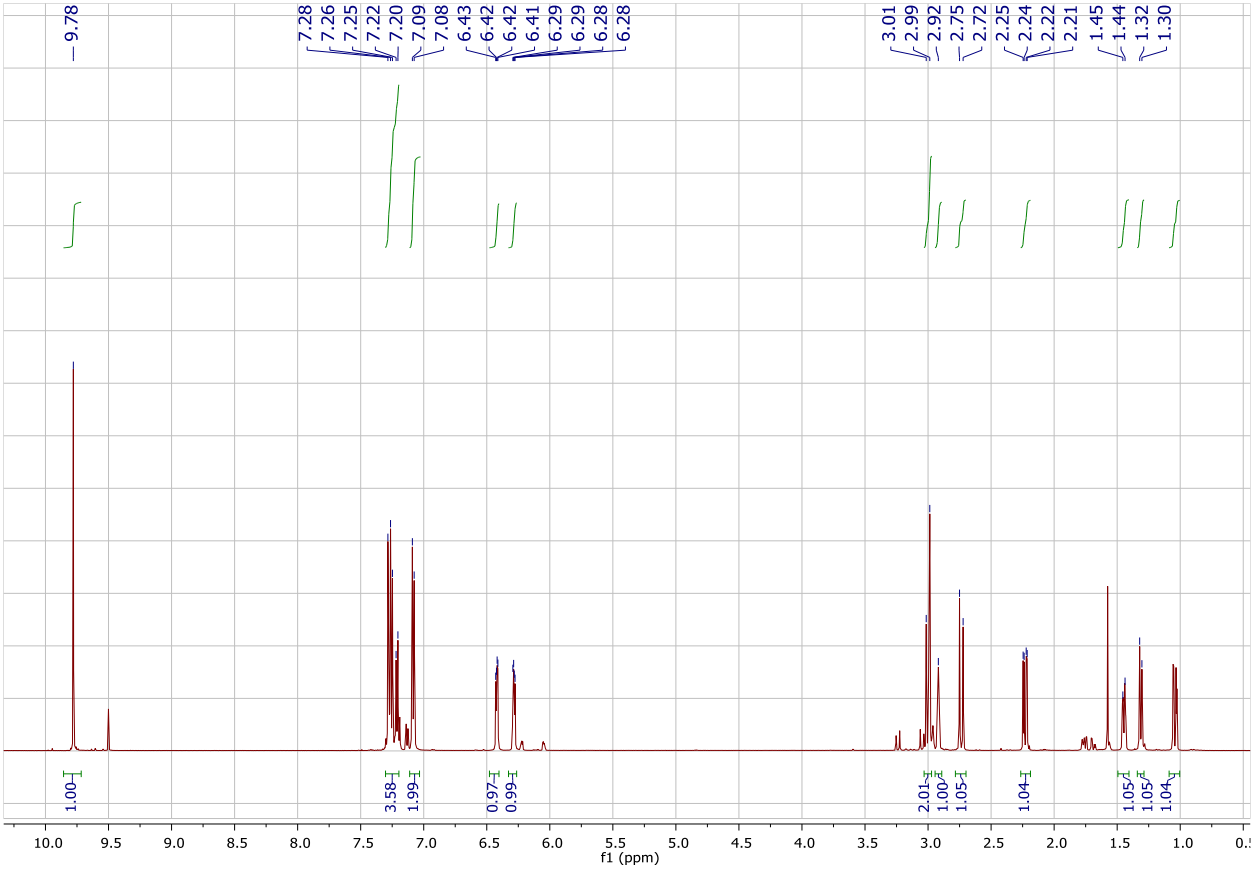
9.78
7.28
7.26
7.25
7.22
7.20
7.09
7.08
6.43
6.42
6.42
6.41
6.29
6.29
6.28
6.28
3.01
2.99
2.92
2.75
2.72
2.25
2.24
2.22
2.21
1.45
1.44
1.32
1.30
1.00
3.58
1.99
0.97
0.99
2.01
1.00
1.05
1.04
1.05
1.05
1.04
f1 (ppm)

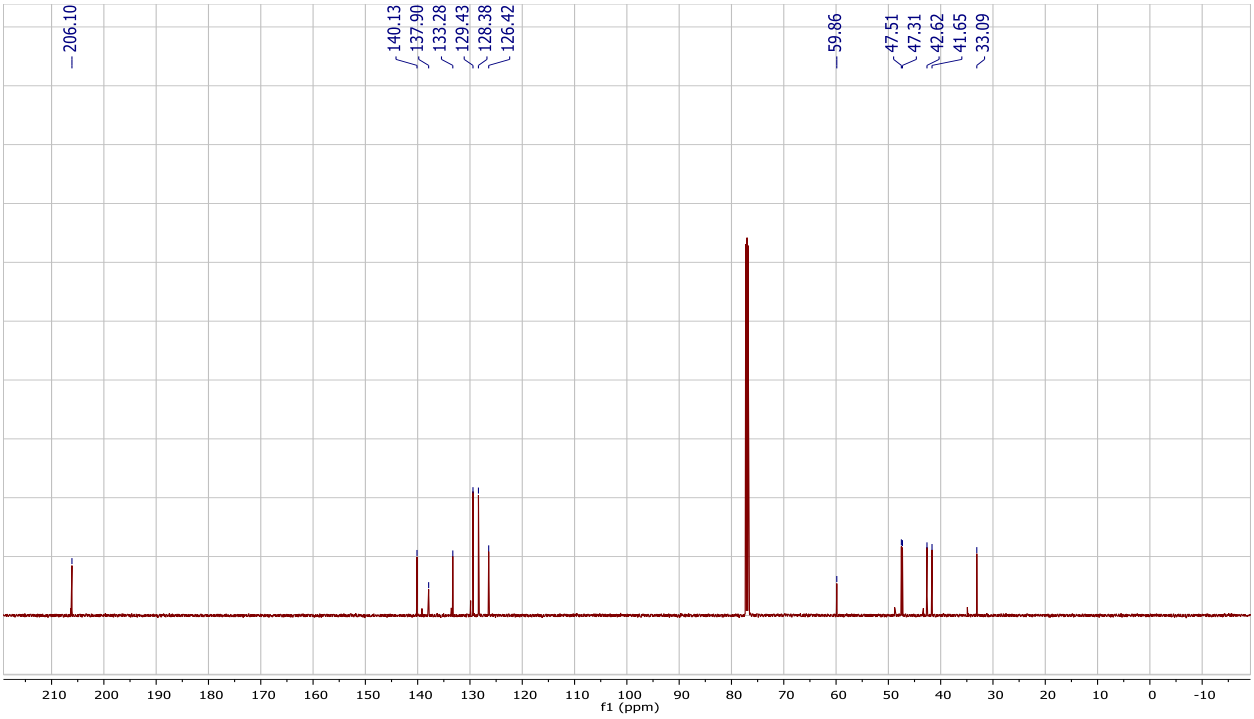
206.10
140.13
137.90
133.28
129.43
128.38
126.42
59.86
47.51
47.31
42.62
41.65
33.09
f1 (ppm)

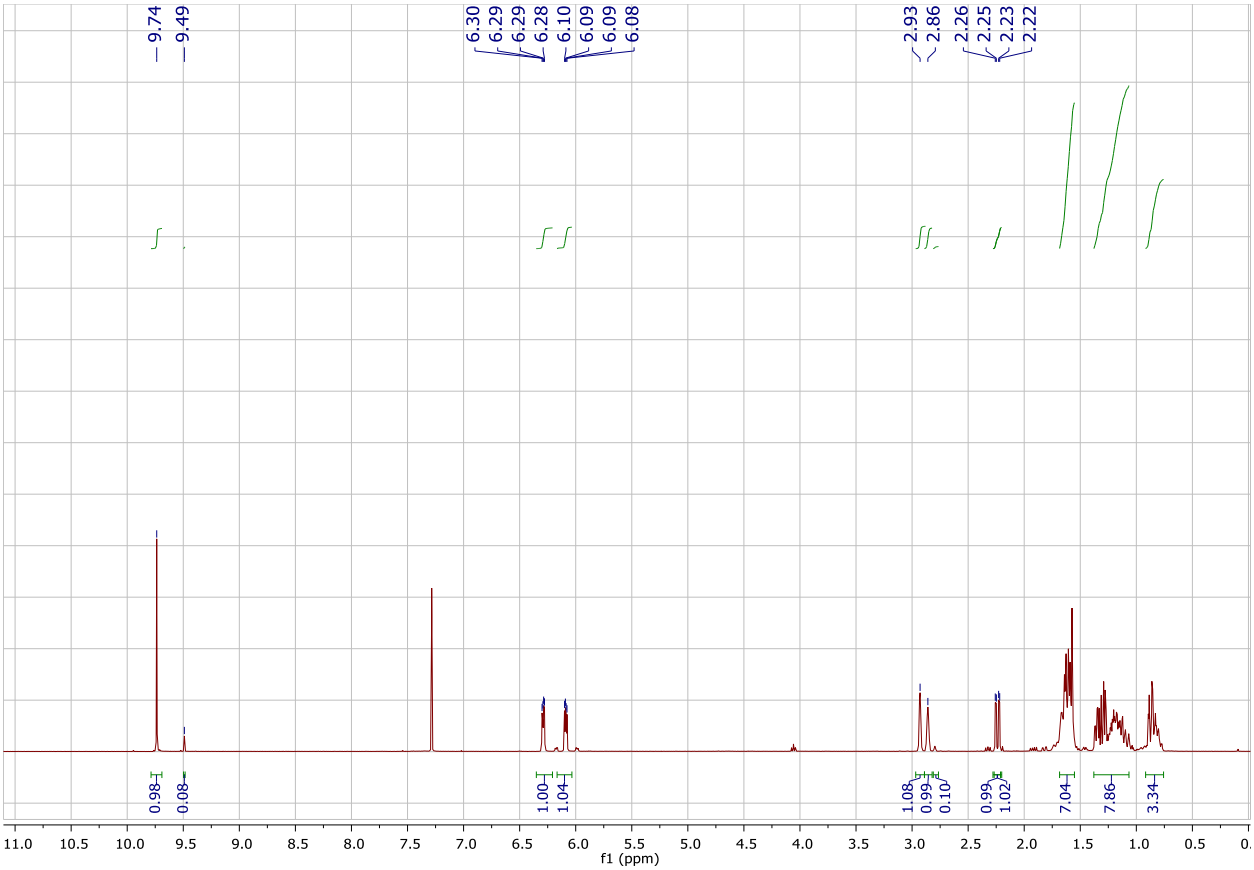
9.74
9.49
6.30
6.29
6.29
6.28
6.10
6.09
6.09
6.08
2.93
2.86
2.26
2.25
2.23
2.22
0.98
0.08
1.00
1.04
1.08
0.99
0.10
0.99
1.02
7.04
7.86
3.34
f1 (ppm)

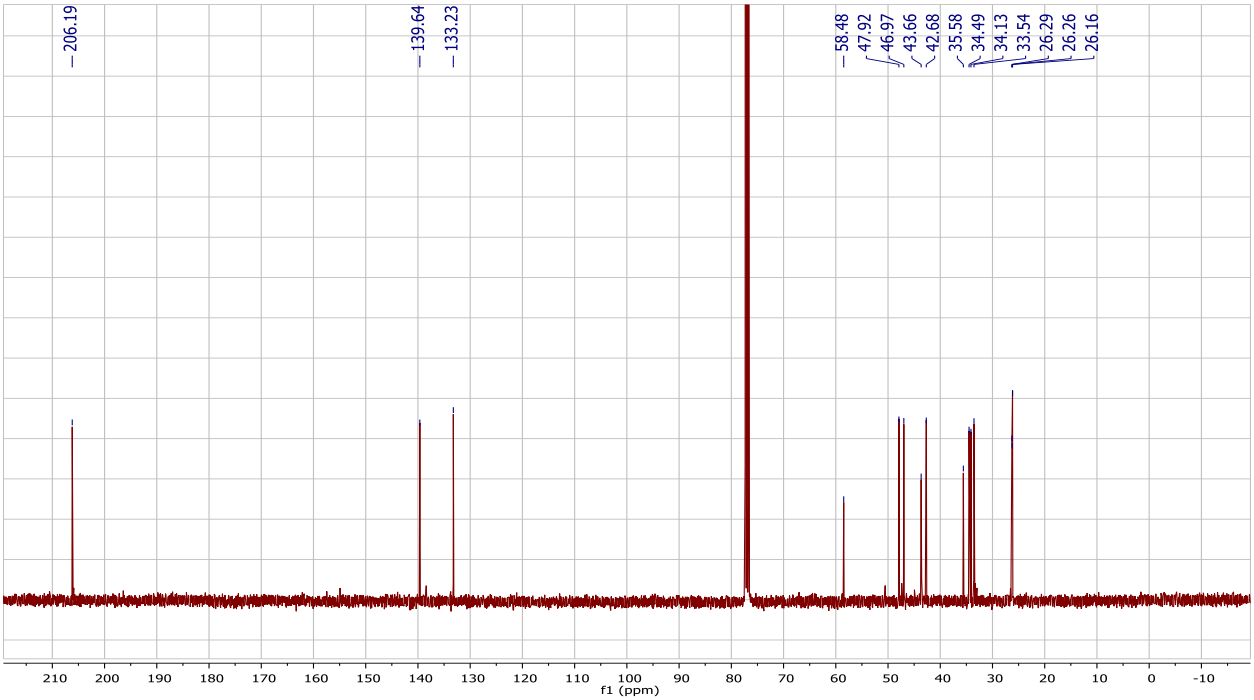
206.19
139.64
133.23
58.48
47.92
46.97
43.66
42.68
35.58
34.49
34.13
33.54
26.29
26.26
26.16
f1 (ppm)